Effects of Microstructure and Strain Ageing on Toughness of Nuclear PWR Reactor Weld Metals.

By

Victoria Jane Farron.

Volume II

A thesis submitted to the Faculty of Engineering of the University of Birmingham for the degree of Doctor of Philosophy.

School of Metallurgy and Materials.

The University of Birmingham.

Edgbaston,

Birmingham.

B15 2TT.

2009.

Table 2. 1 - Summary of weld metal inclusion characteristics. The data is compiled from various sources.

Type of Weld	Size Distribution*				Chemical Composition	
	$V_v \times 10^{-3}$	d_v	$N_v \times 10^{7}$	S_v	Constituent elements	Reported phases
C-Mn steel weld metals	3-8	0.3-0.6	1-10	10-50	Si, Mn, O, S, (traces of Al, Ti and Cu)	SiO_2, $MnOSiO_2$, MnS, (Cu_xS)
Low-alloy steel weld metals	2-6	0.3-0.7	10-40	10-40	Al, Ti, Si, Mn, O, S, N, (Cu)	$MnOAl_2O_3$, γ-Al_2O_3, TiN, $MnOSiO_2$, SiO_2, α-MnS, β-MnS, (Cu_xS)

* V_v: Volume fraction; d_v: arithmetic mean (3-D) particle diameter (μm); N_v: number of particles per unit of volume (mm^{-3}); S_v: total particle surface area per unit volume (mm^2 per mm^3)

Figure 2. 1 - Map showing locations of Nuclear Reactor sites throughout the world. [238]

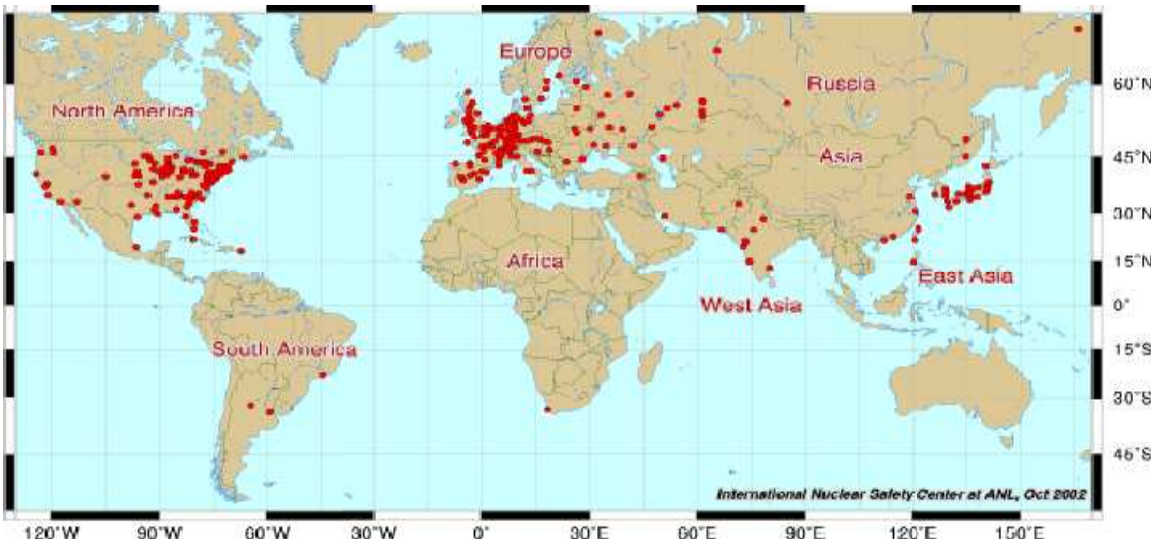

Figure 2. 2 - Schematic diagram of a Pressurized Water Reactor Power Station (a) Overall view, (b) Expanded view of the containment building. [239]

(a)

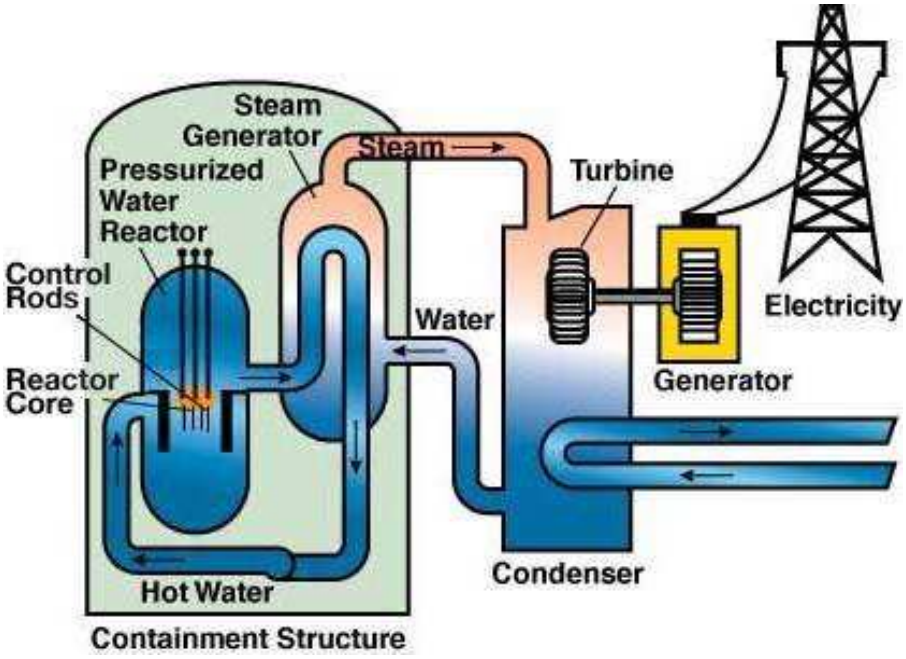

(b)

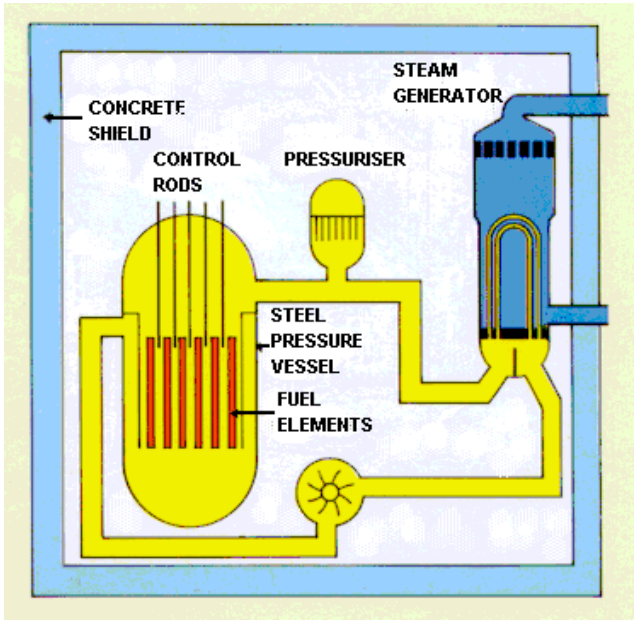

Figure 2. 3 - Schematic diagram of a Pressurized Reactor Core. [239]

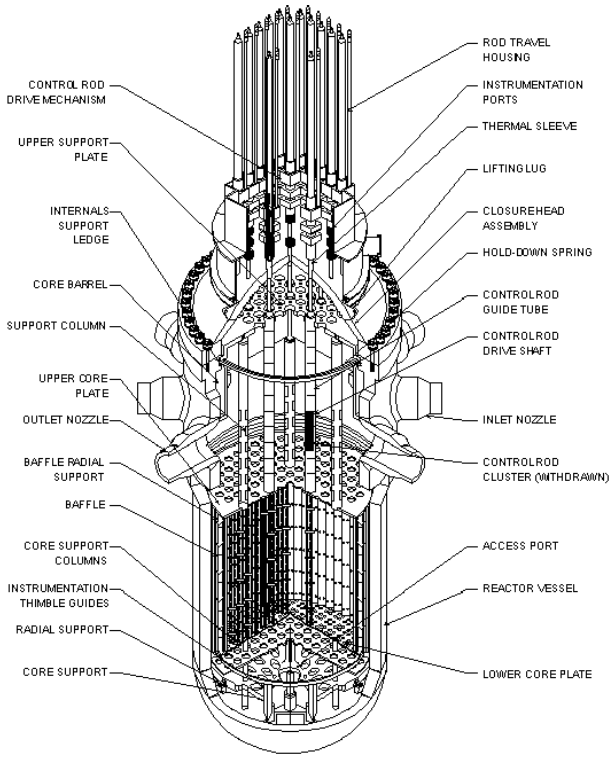

Figure 2. 4 - Photograph showing Sizewell B, Suffolk, the United Kingdom's only PWR. [239]

Figure 2. 5 - Effect of irradiation on the Charpy impact energy transition curve.

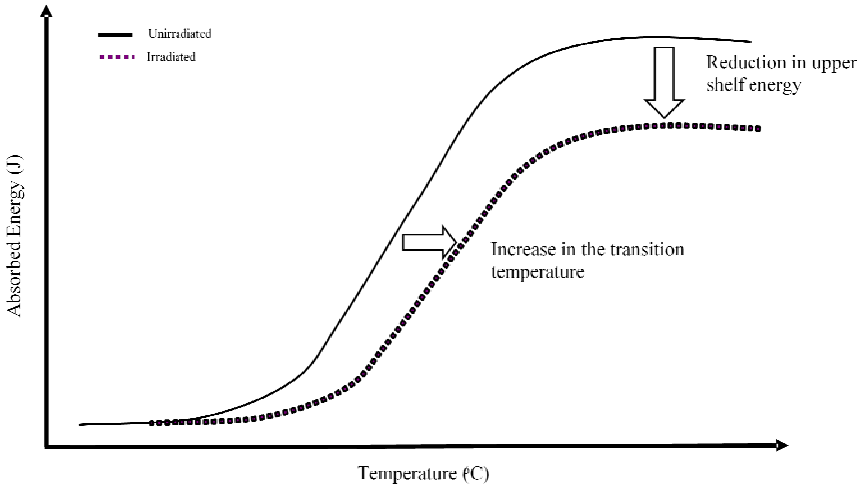

Figure 2. 6 - Failure of Liberty Ships in service during the Second World War (1939 - 1945). [240]

Figure 2. 7 - Precipitation shifts for low Ni PWR submerged - arc welds deduced by comparing the total measured shifts and the model predictions for matrix shift. [20]

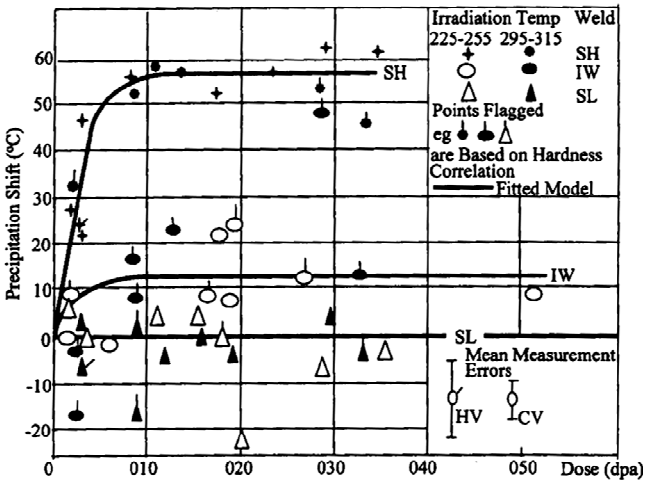

Figure 2. 8 - Slip plans intersecting planes (110). [41]

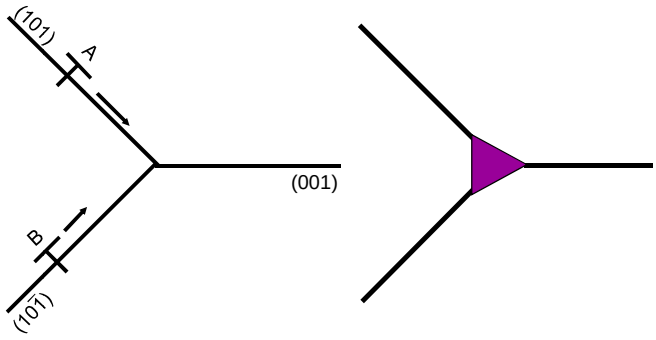

Figure 2. 9 - Force acting on a dislocation line, locate near Cottrell slip. [41]

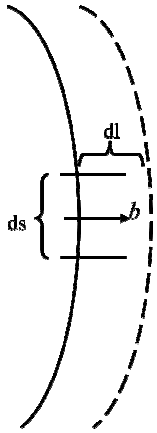

Figure 2. 10 - Typical variation of strength and ductility after cold-working. [40]

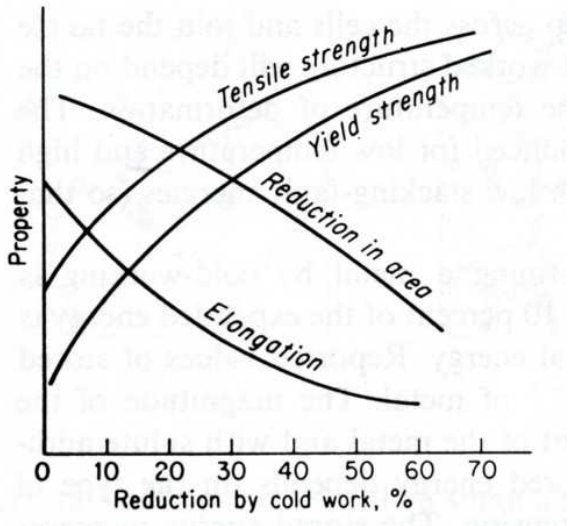

Figure 2. 11 - Engineering stress strain curves, obtained at room temperature from polycrystalline metals tested at room temperature, showing the Bauschinger effect. [51]

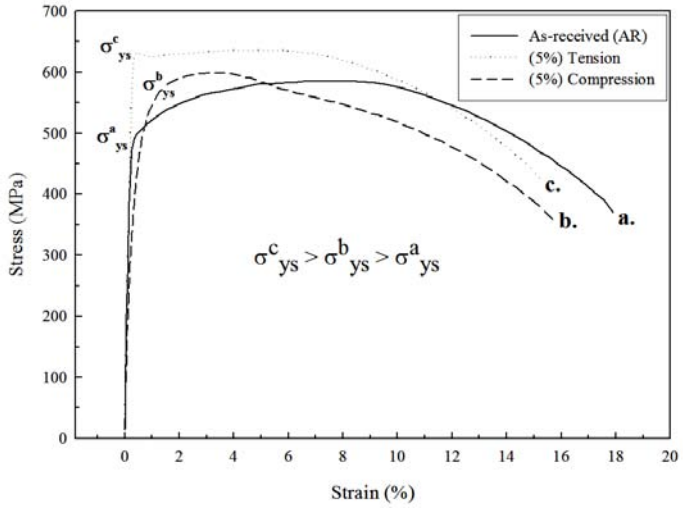

Figure 2. 12 - Effect of prestraining and thermal ageing on Charpy Impact transition curves. [15]

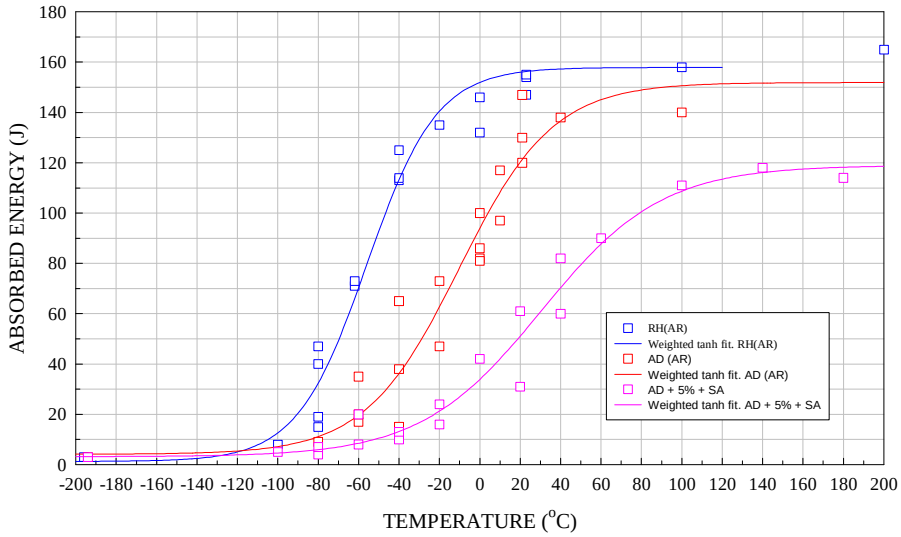

Figure 2. 13 - Effect of temperature of stress - strain curves for A533B steel. [30]

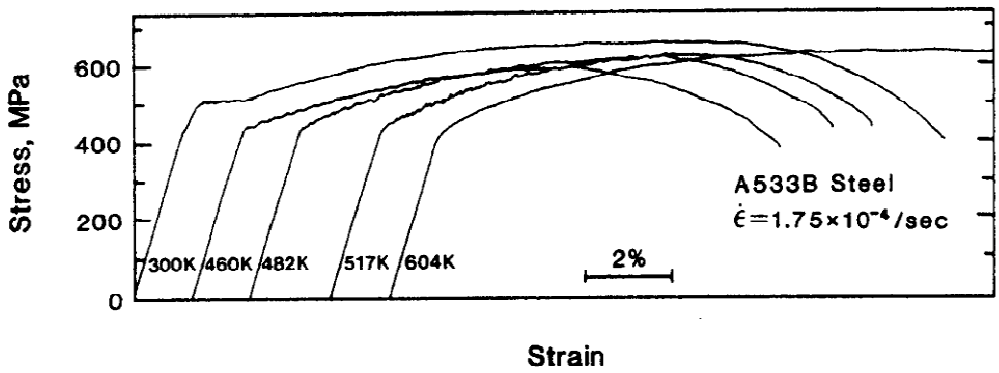

Figure 2. 14 - Effects of dynamic strain ageing of fracture toughness of A533B (a) subsized Charpy specimens obtained by three-pointing bending; and (b) elastic-plastic fracture of precracked Charpy specimens. [30]

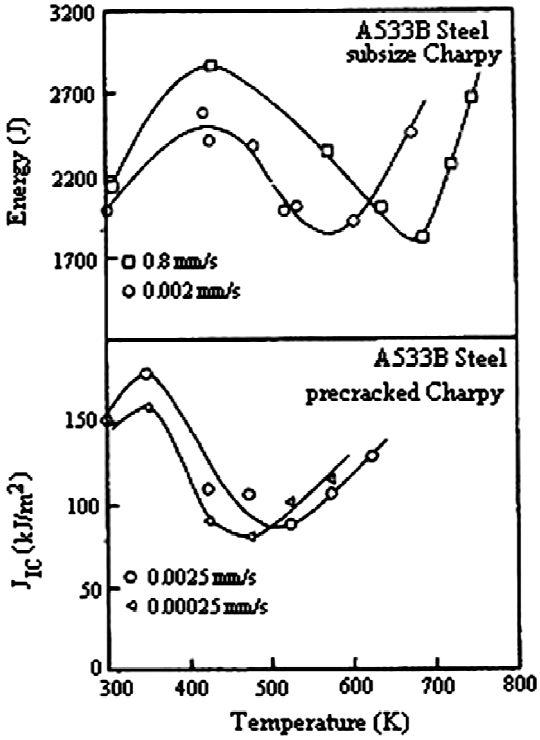

Figure 2. 15 - (a) Illustration of the submerged - arc welding process; (b) Photography of the submerged - arc welding process. [241]

(a) **(b)**

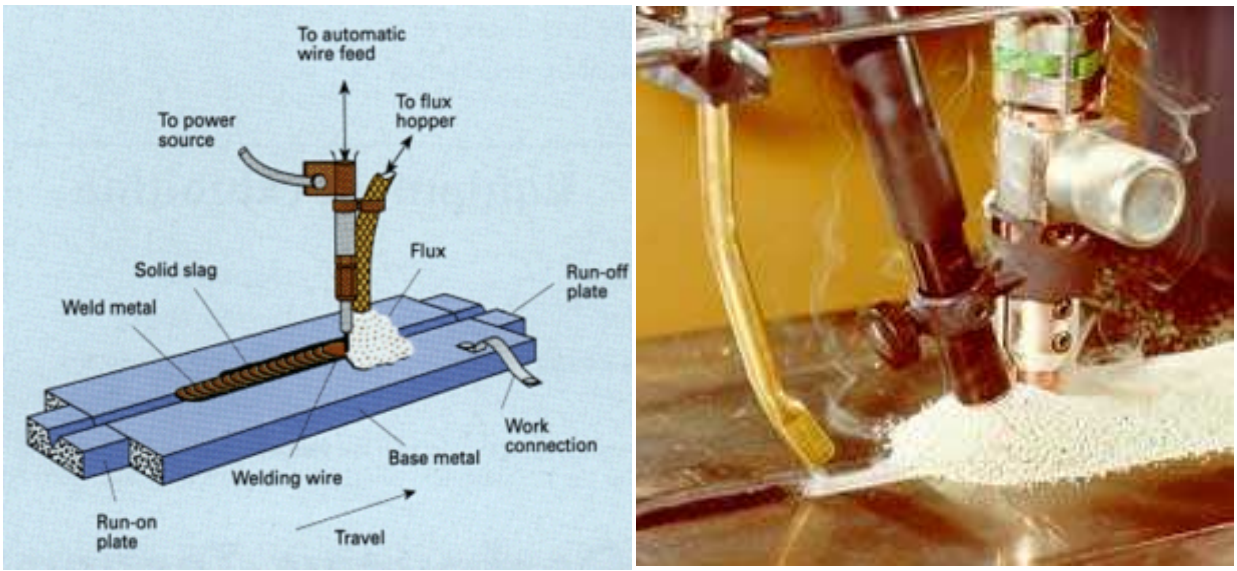

Figure 2. 16 - Illustration of submerged - arc welding process using AC or DC current. [241]

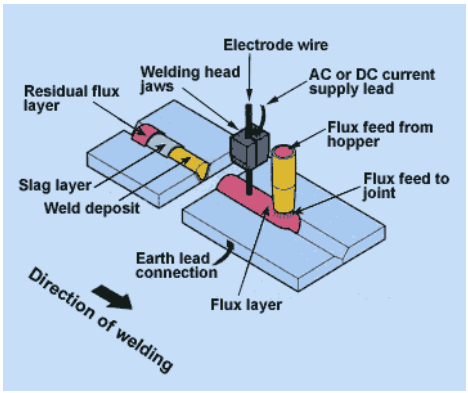

Figure 2. 17 - Graph showing the rate of deposition compared to the welding current and the wire diameter. [241]

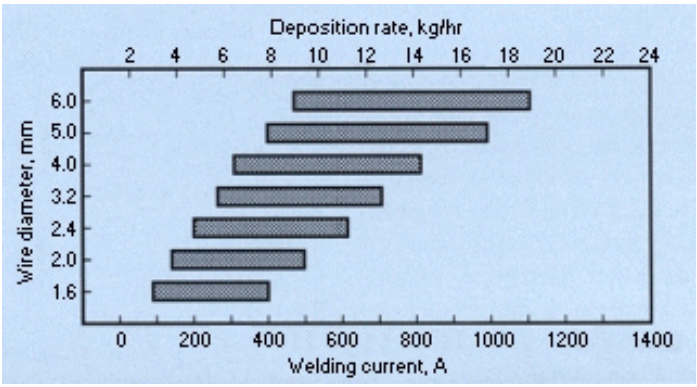

Figure 2. 18 - Schematic diagram of layered structure of inclusion

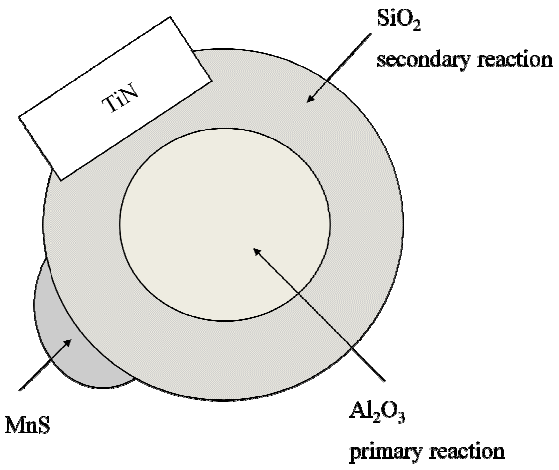

Figure 2. 19 - Deoxidation equilibria in liquid steel at 1660°C. [80]

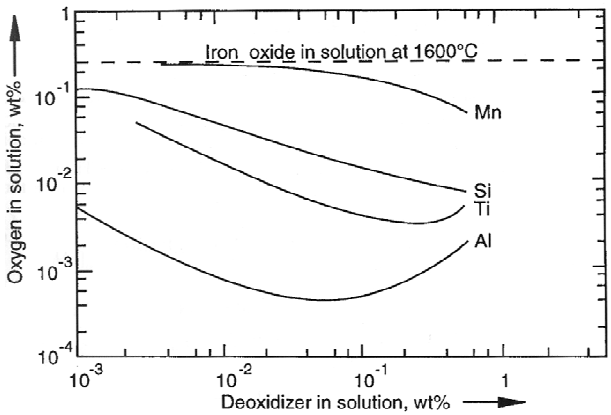

Figure 2. 20 - Illustration of epitaxial growth of columnar grains at the fusion boundary from partly melted base metal grains. [78]

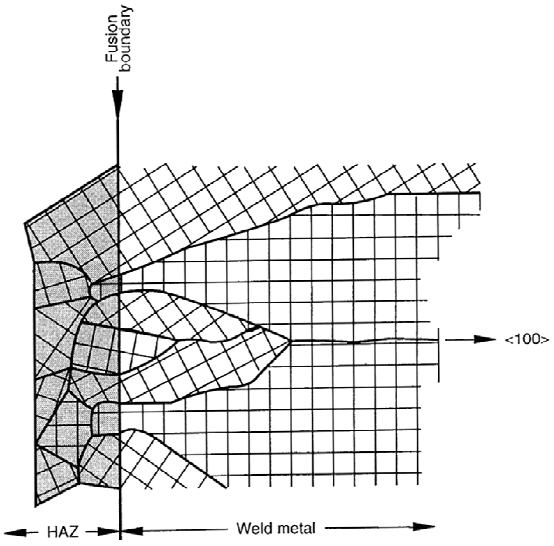

Figure 2. 21 - Schematic representation to the cellular substructure. Schematic section is normal to the columnar grain growth direction.

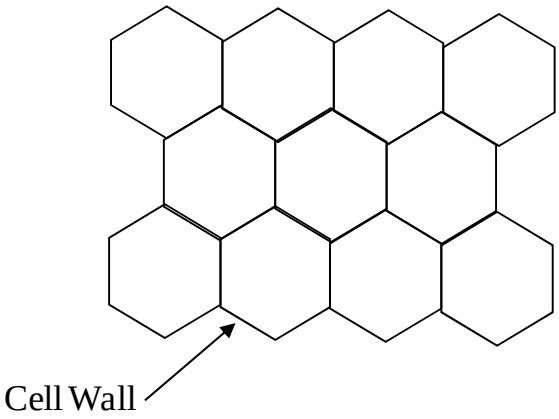

Figure 2. 22 - Comparison of different welding conditions to obtain columnar grain structures. (a) Elliptical weld pool (low welding speed and n3 values); (b) Tear shaped weld pool (high weld speed and n3 values). Arrows showing the direction of the maximum temperature gradient in the weld pool. [242]

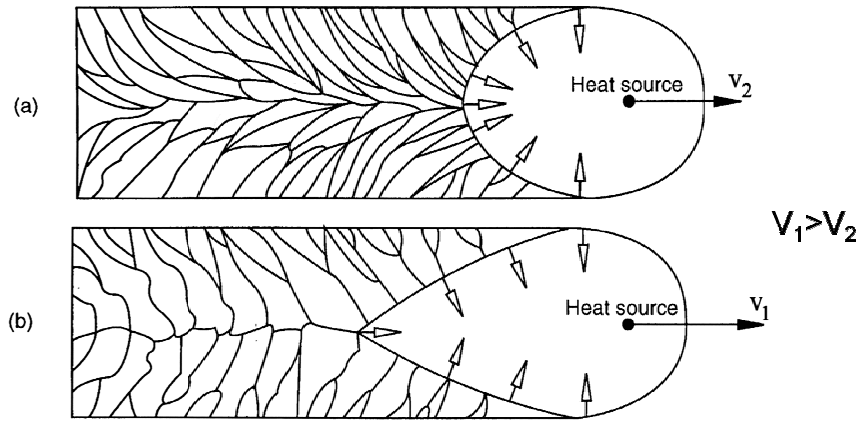

Figure 2. 23a - Metastable Fe - Fe3C system, [92], Figure 2.23b - Schematic of pertectic phase diagram.

(a) (b)

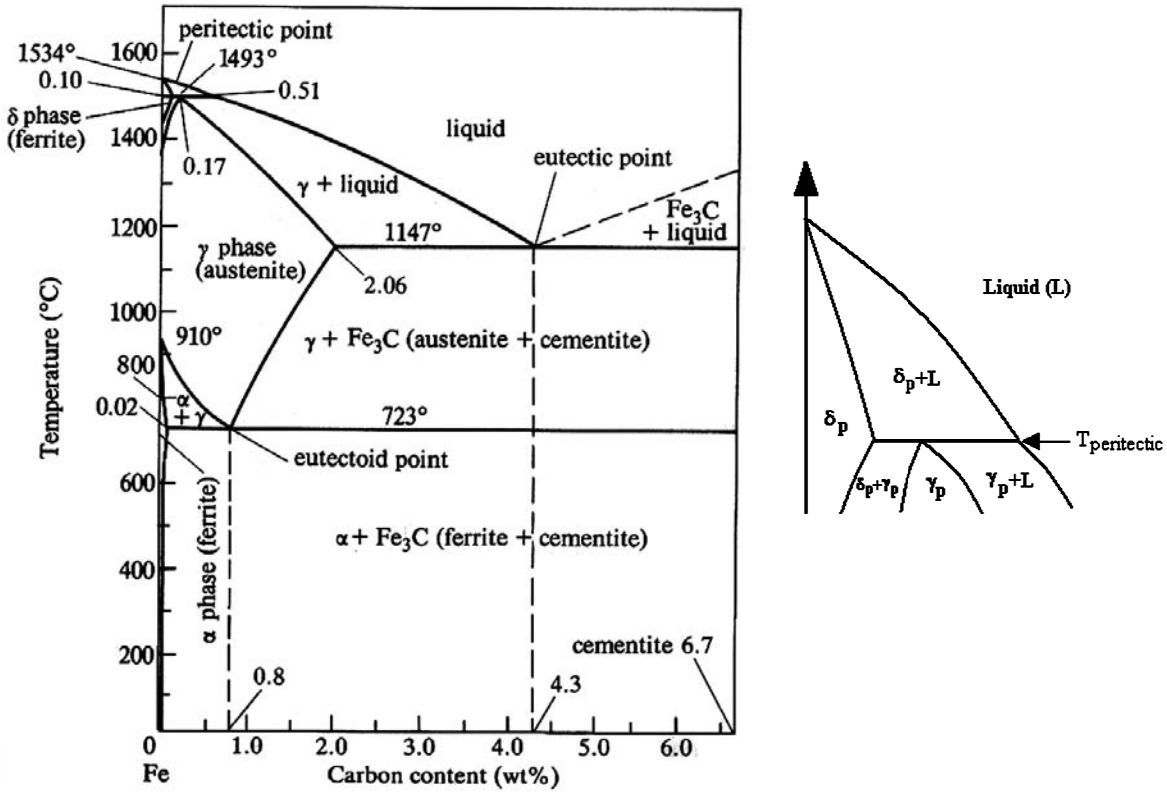

Figure 2. 24 - Illustration representing formation of pearlite, upper and lower bainite. [93]

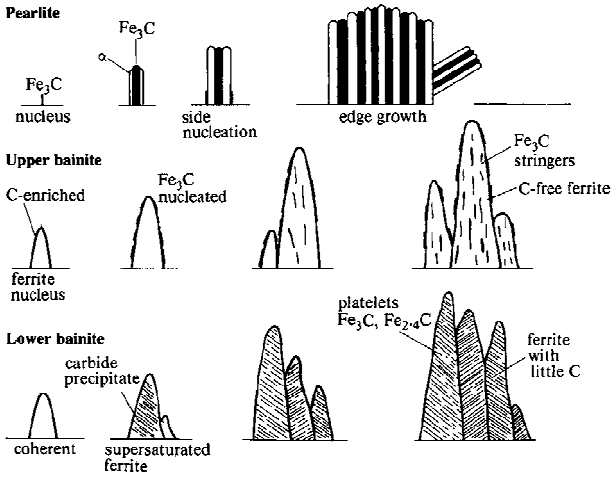

Figure 2. 25 - Illustration for a weld deposit showing the relationship of acicular ferrite-phase compared with other constituents. [126]

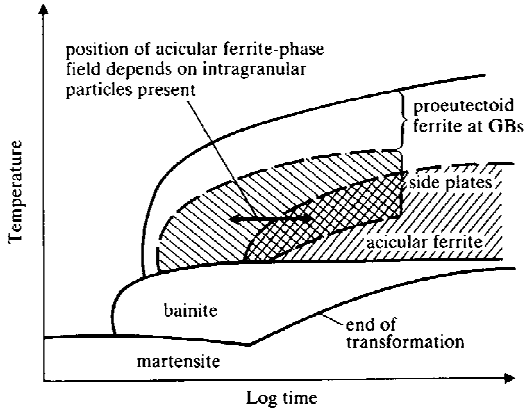

Figure 2. 26 - Solidification of primary delta ferrite with subsequent growth of austenite along the primary δ-phase boundary.

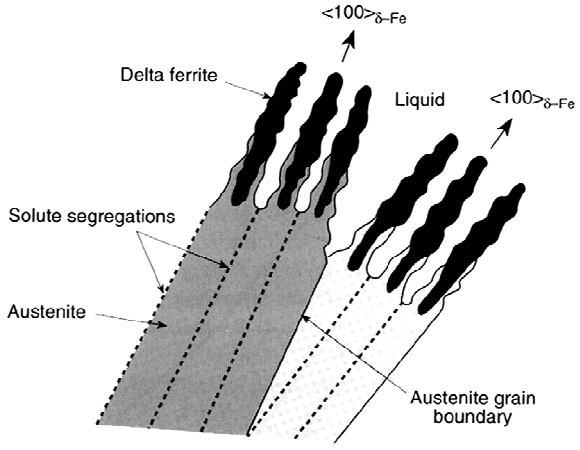

Figure 2. 27 - Austenite to ferrite transformation mechanisms.

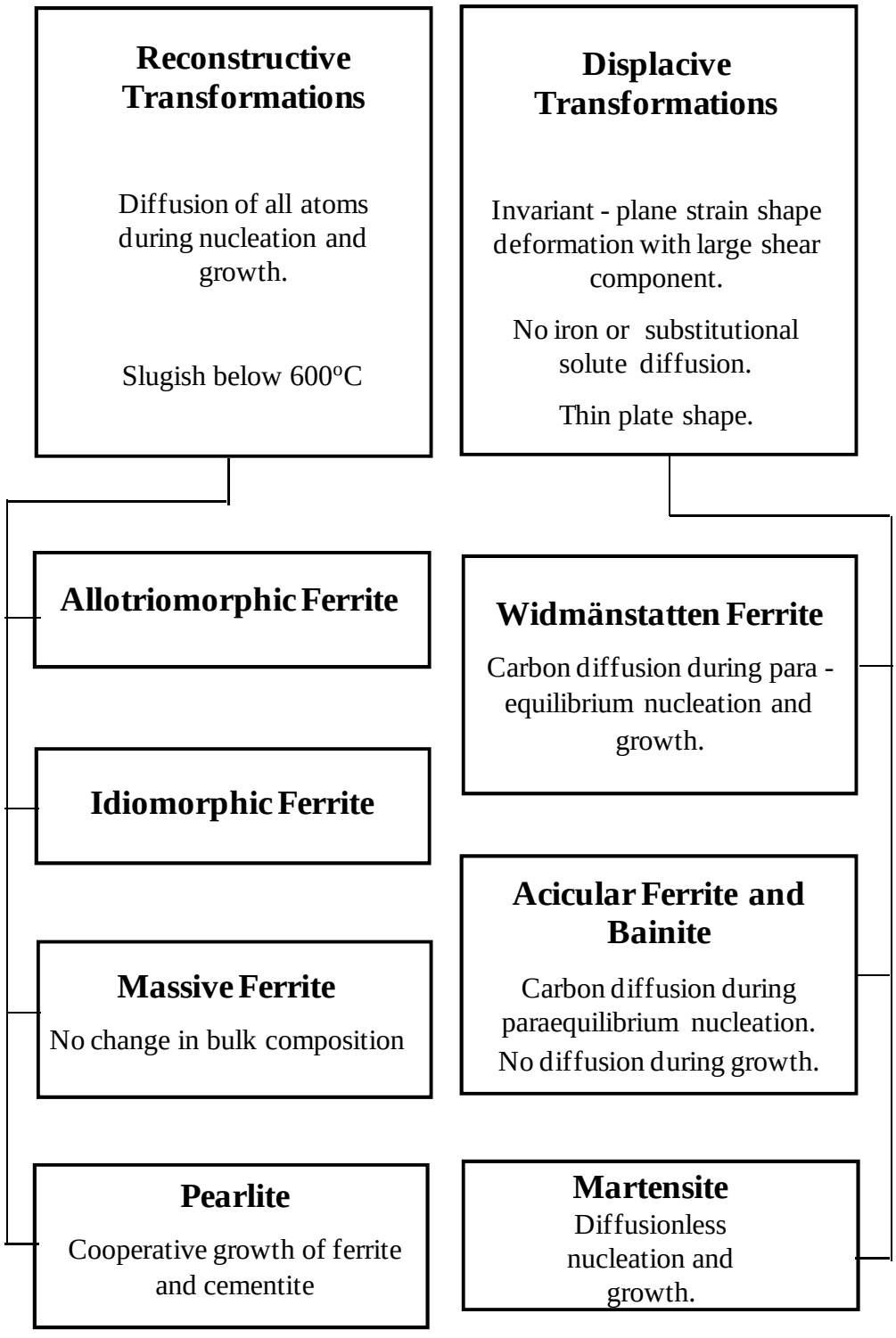

Figure 2. 28 - Schematic diagram showing the development of microstructure of C-Mn weld metals.

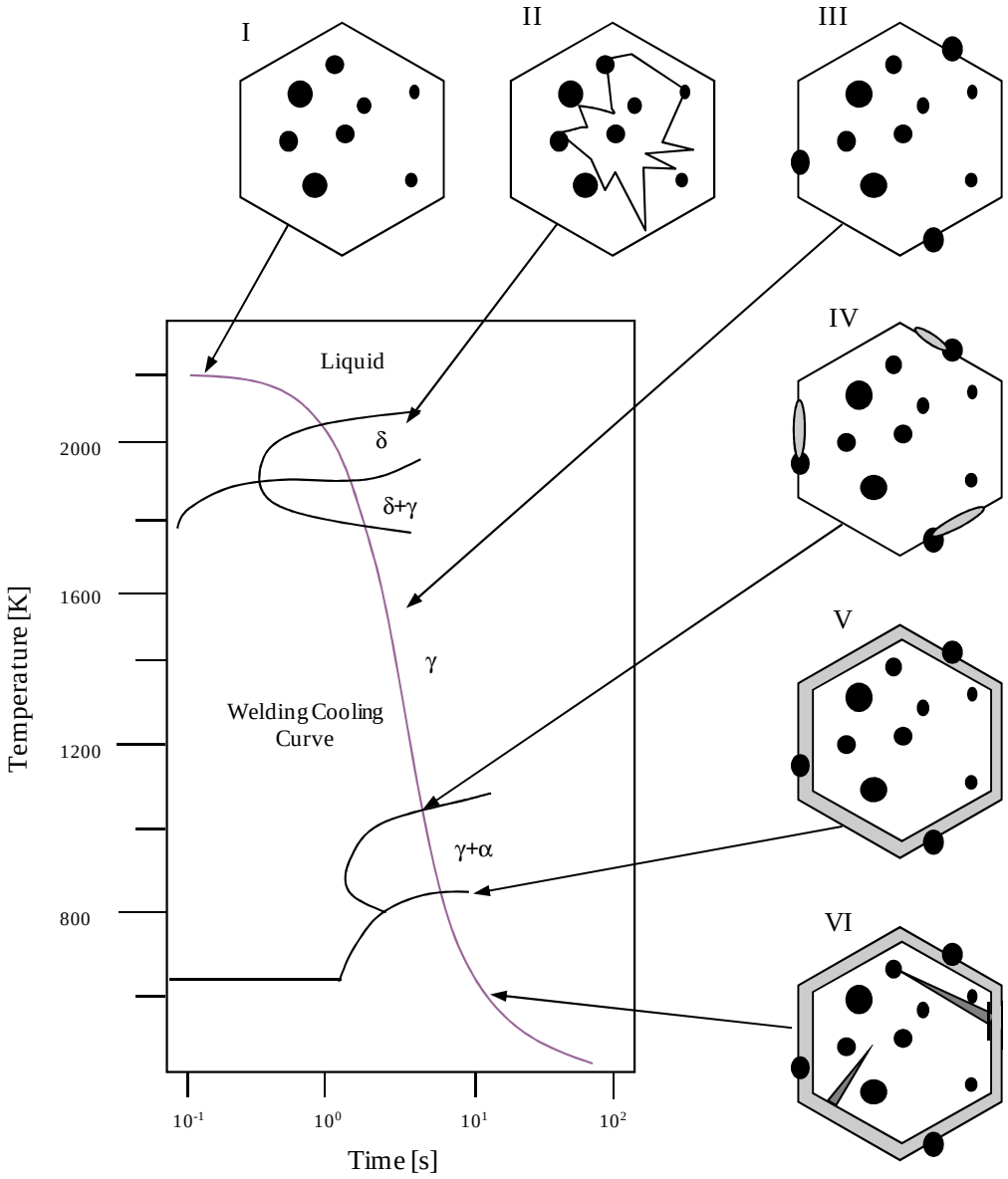

I - Inclusion Formation.

II - Weld pool solidification to δ ferrite.

III - Fully austenitic structure.

IV - Nucleation of allotriomorphic ferrite.

V - Growth of allotriomorphic ferrite along austenite grain boundaries.

VI - Widmanstätten ferrite formation.

VII - Acicular ferrite formation.

Figure 2. 29 - Schematic diagram of mechanisms of transition from acicular ferrite to bainite.

Effect of inclusion density for same austenite grain size.

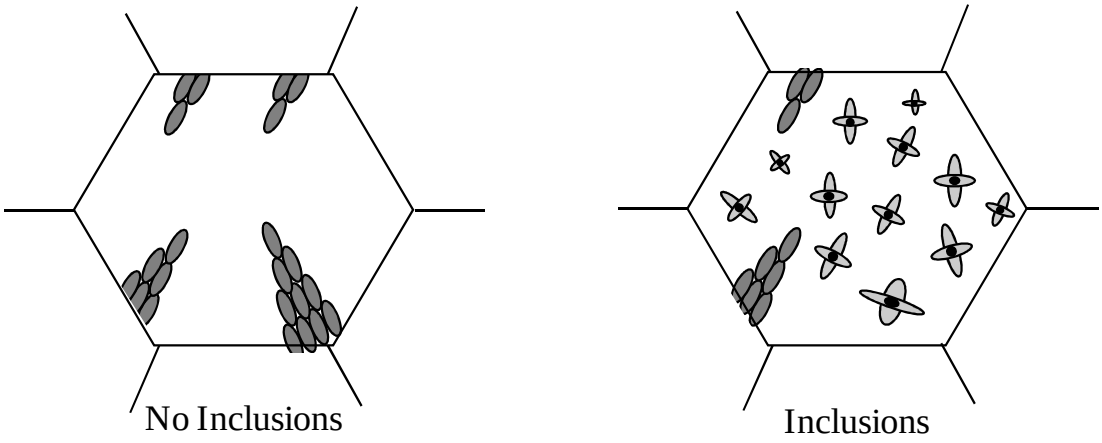

Effect of austenite grain boundary (nucleation site) density

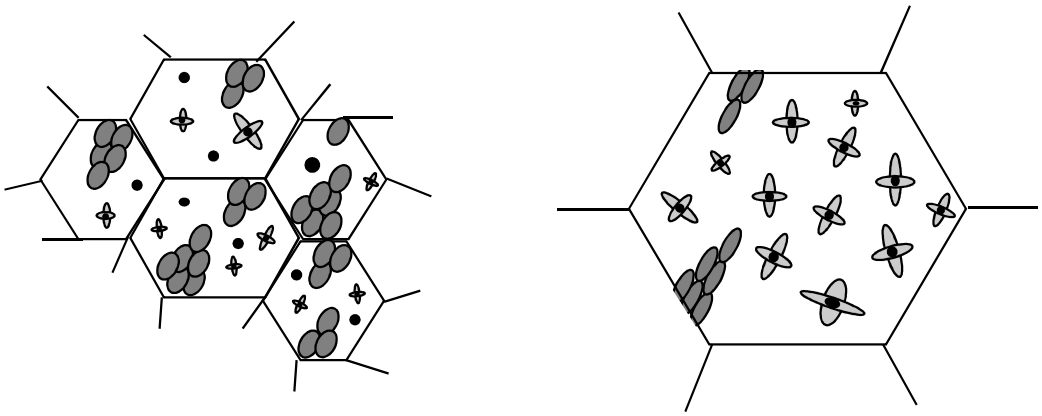

Effect of prior transformation to allotriomorphic ferrite for same austenite grain size

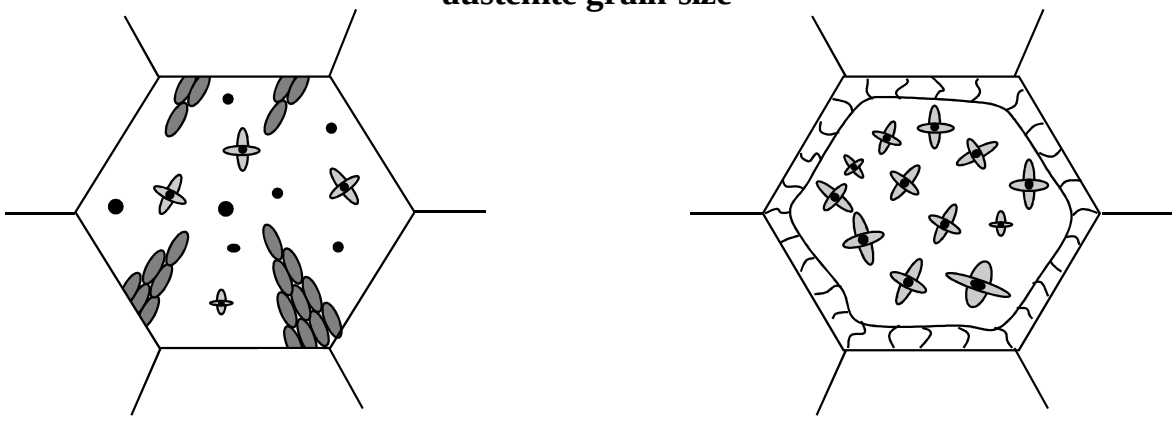

Figure 2. 30 - Primary delta ferrite solidification with subsequent heterogeneous nucleation of austenite at inclusions.

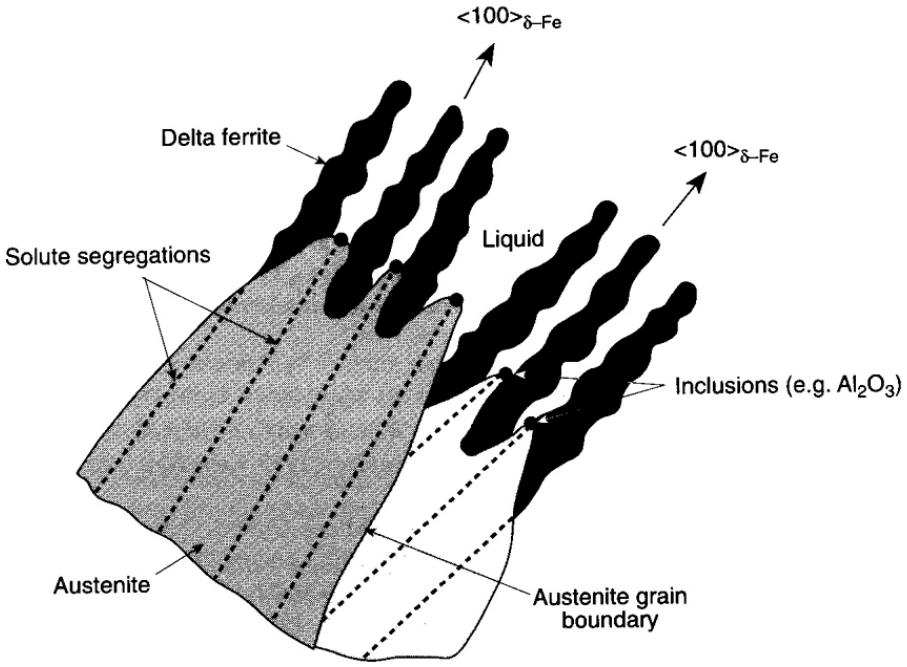

Figure 2. 31 - Nucleation potency of ferrite for differing inclusion types. [78]

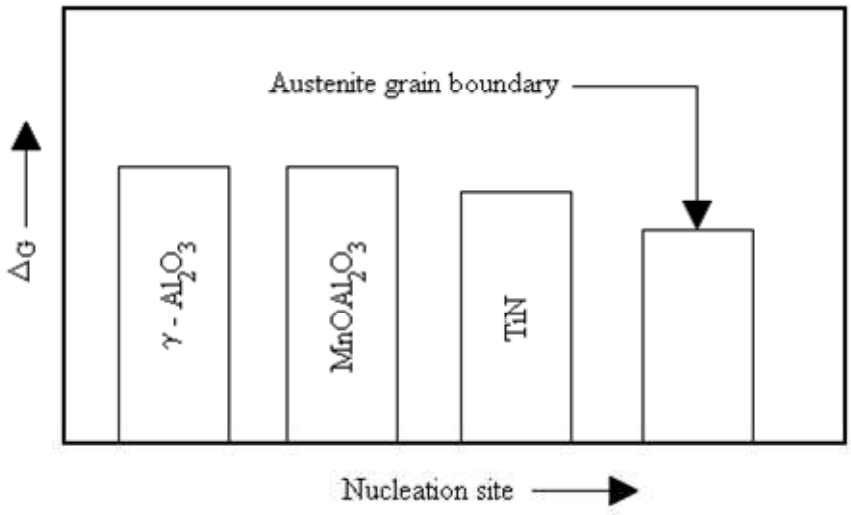

Figure 2. 32 - Illustrations of various welds; (a) Single pass weld; (b) Fusion weld - multipass; (c) high magnification showing As-deposited (AD) and Reheated (RH) microstructures.

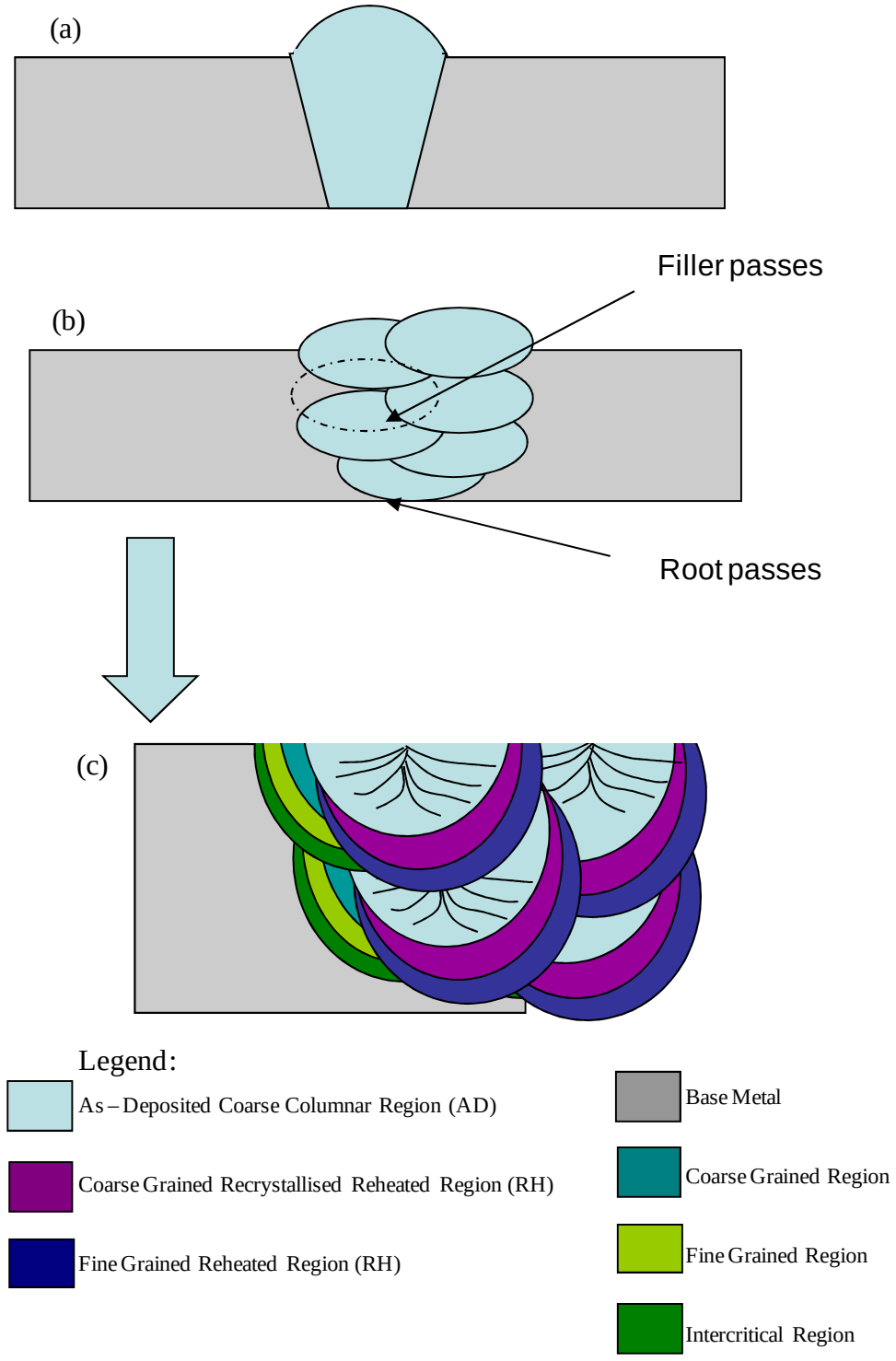

Figure 3. 1 - Central through - thickness in an infinite plate of unit thickness loaded by uniform tensile stress - Griffith's Crack. [163]

Infinite plate: 2a << W

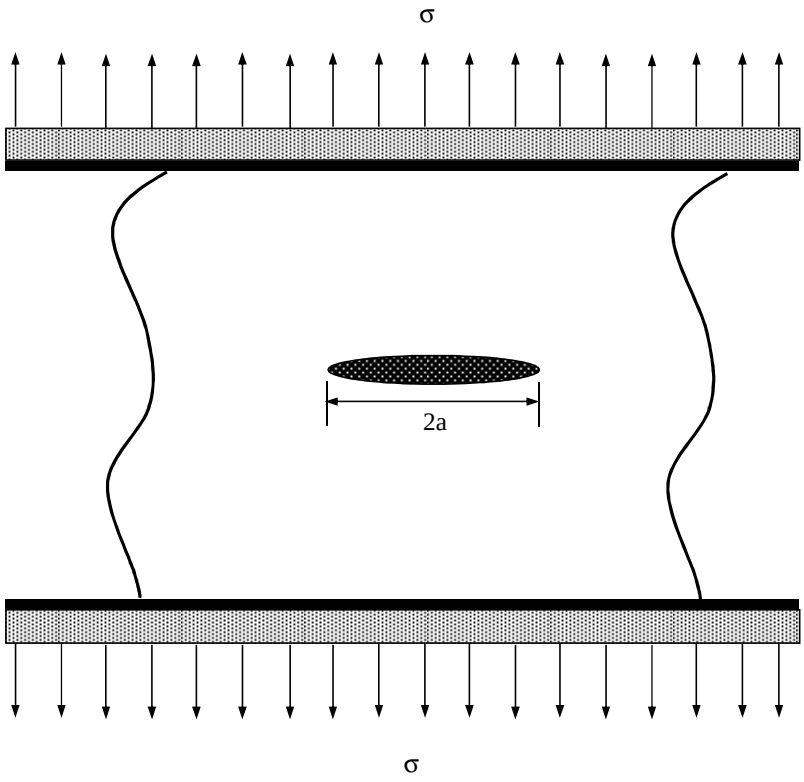

Figure 3. 2 - Griffith theory of brittle fracture. [163]

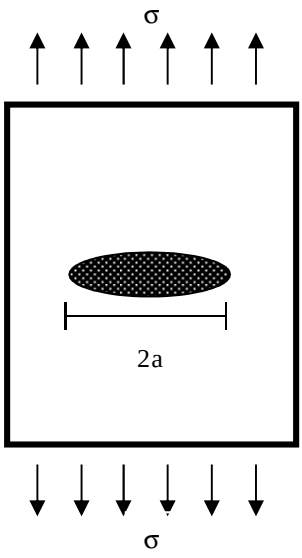

Griffith Crack Model

$$\sigma = \left[\frac{2E\gamma_s}{(1-\upsilon^2)\pi\alpha} \right]^{\frac{1}{2}}$$

Plane strain condition.

$$\sigma = \left(\frac{2E\gamma_s}{\pi\alpha} \right)^{\frac{1}{2}}$$

Plane stress condition.

Figure 3. 3 - Three loading modes. [243]

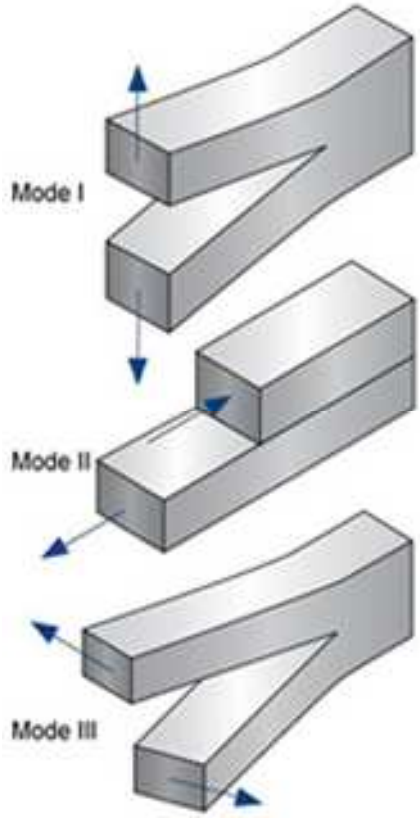

Figure 3. 4 - Biaxially loaded infinite plate containing a crack.

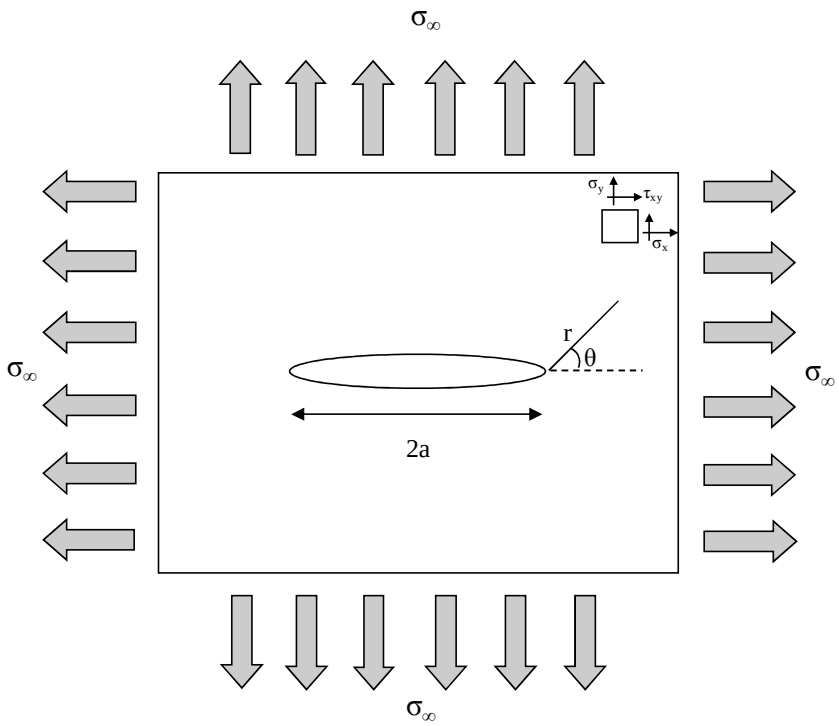

Figure 3. 5 - Single Edge notched bend (SEN) fracture toughness testpieces.

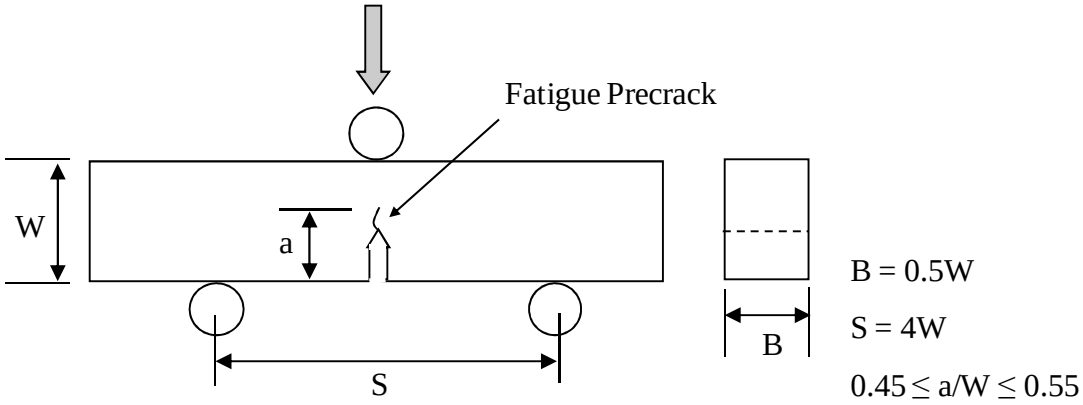

Figure 3. 6 - Compact tension (CT) fracture toughness testpiece.

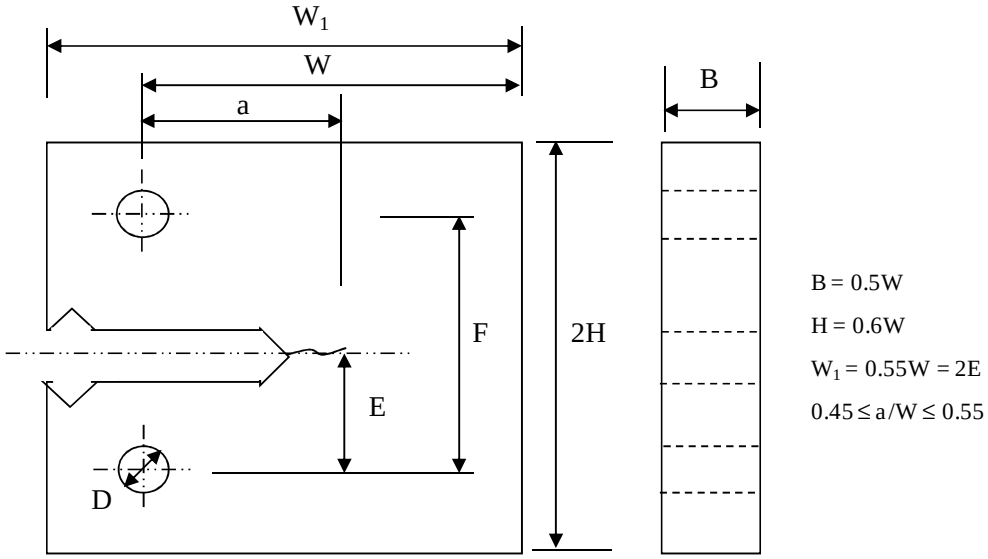

Figure 3. 7 - Standard CTS testpieces (upto 305 mm thick) for a low-alloy structural material steel A533B; variation K_{IC} with temperature. [160]

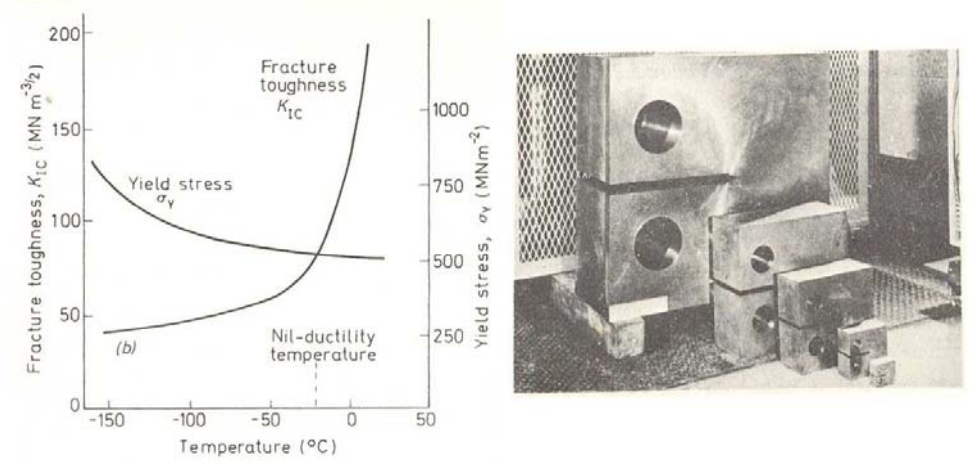

Figure 3. 8 - Wells' estimation of CTOD. [166, 167]

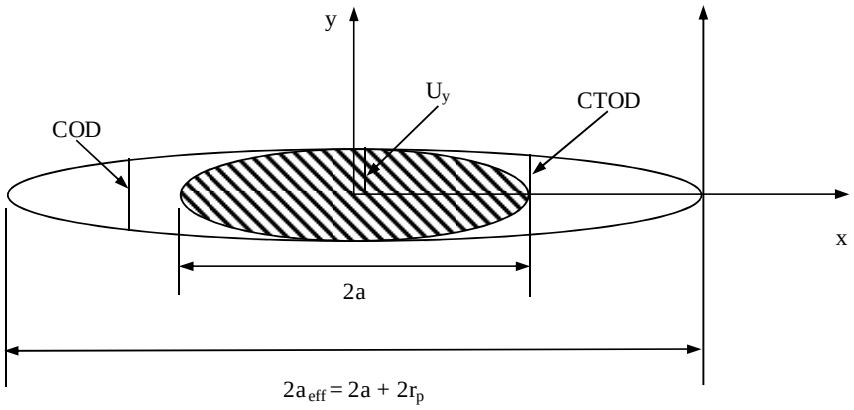

Figure 3. 9 - Model of Crack - tip opening displacement. [40]

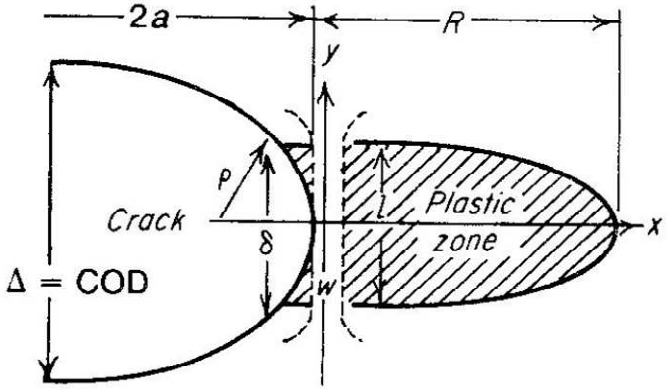

Figure 3. 10 - Schematic representation of Dugdales strip yield model. [244]

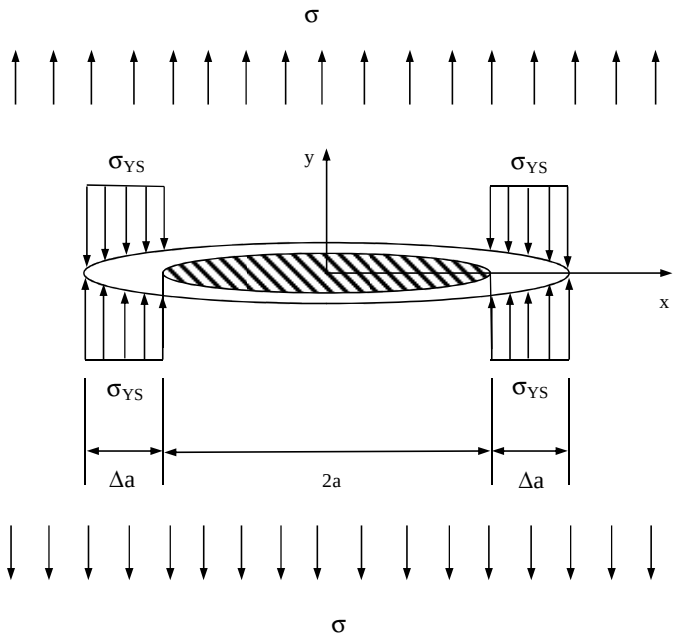

Figure 3. 11 - Definition of CTOD. [245]

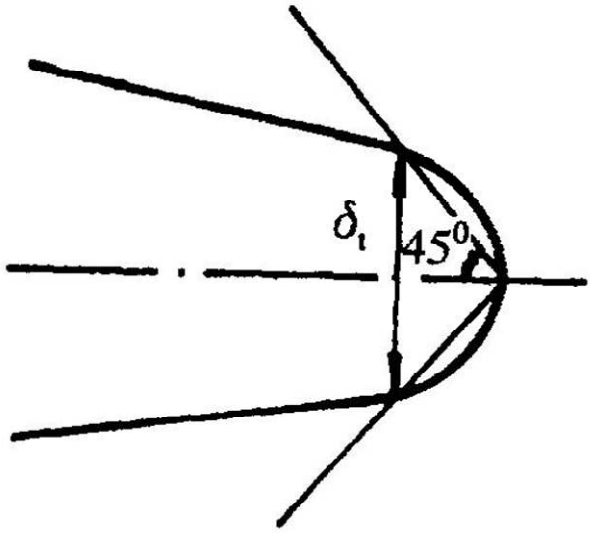

Figure 3. 12 - COD variations with crack growth in three and four point bending specimens. [171]

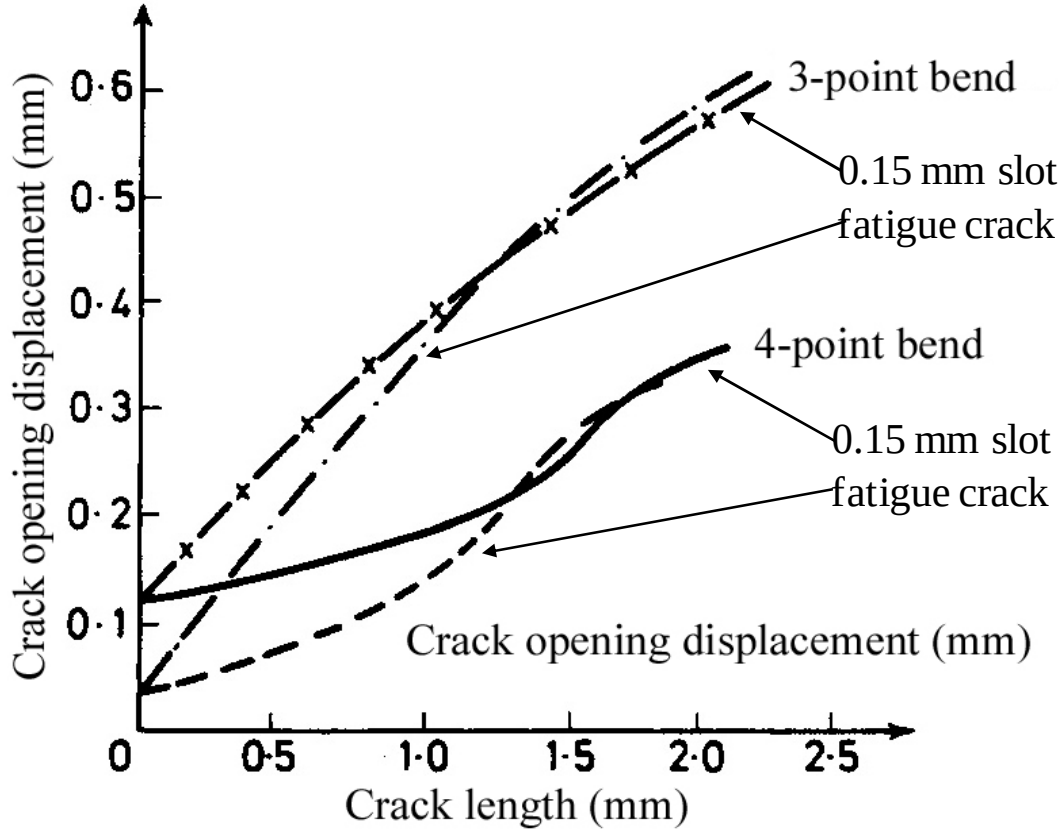

Figure 3. 13 - Effect of specimen thickness on COD. [144]

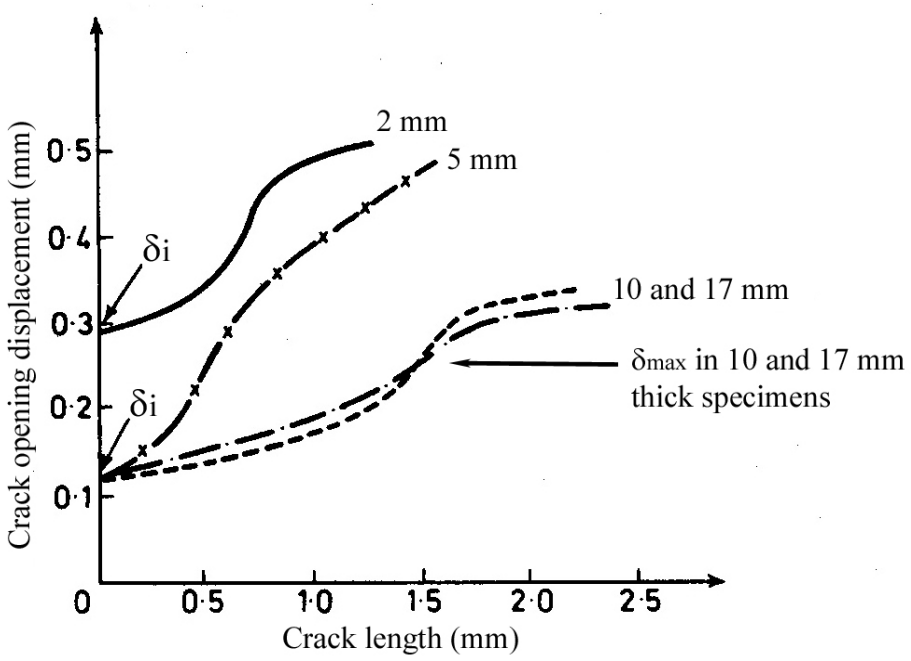

Figure 3. 14 - Effect of specimen geometry measured in the transition region on COD values. [172]

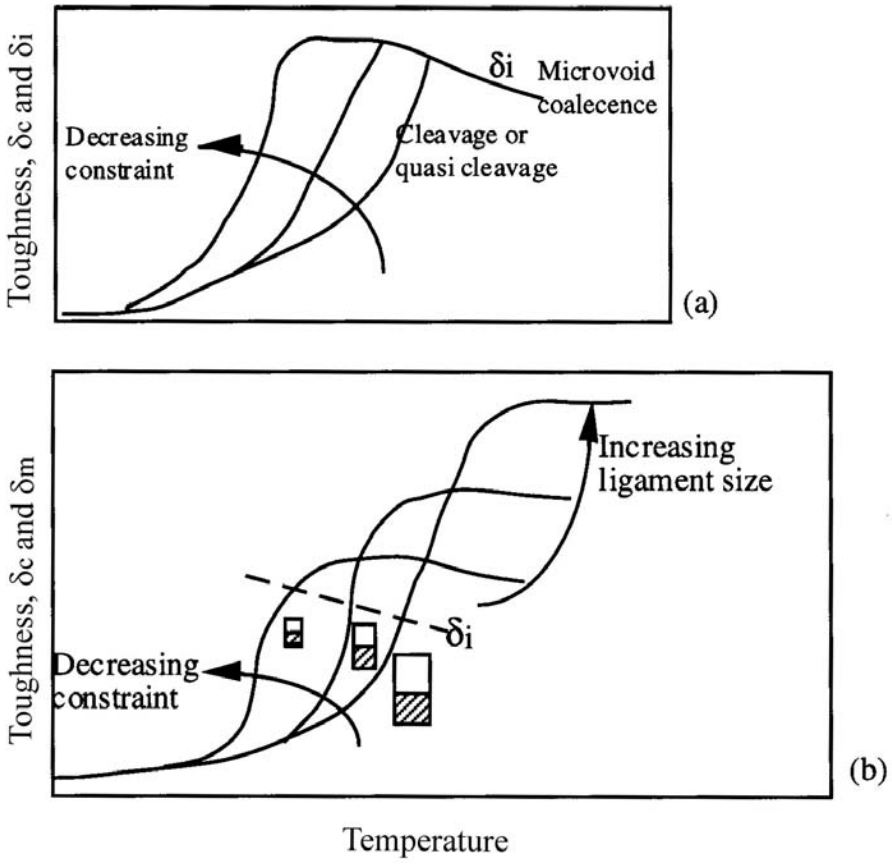

Figure 3. 15 - Variation of yield and fracture stress with grain size in mild steel -196°C. [174]

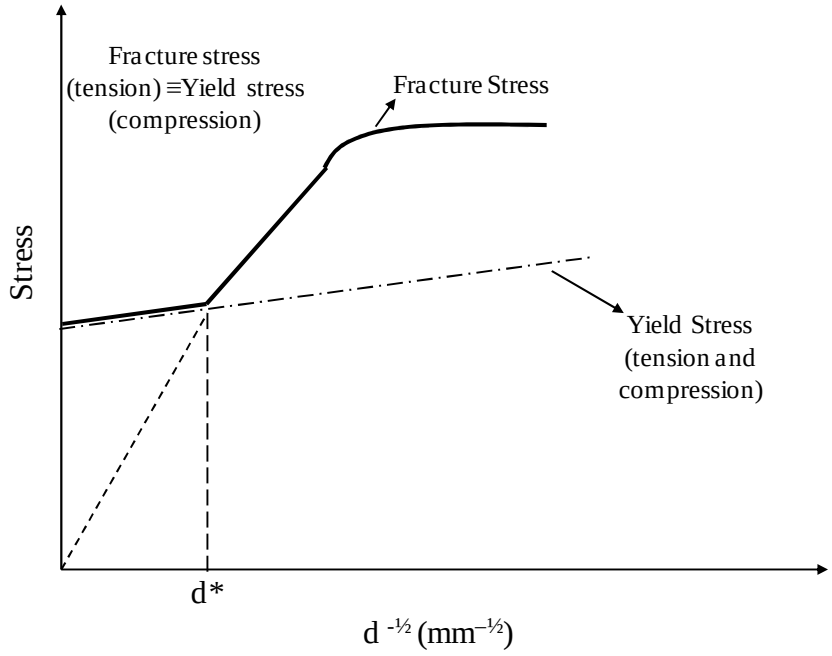

Figure 3. 16 - Crack nucleation due to slip band pile-up at grain boundary.

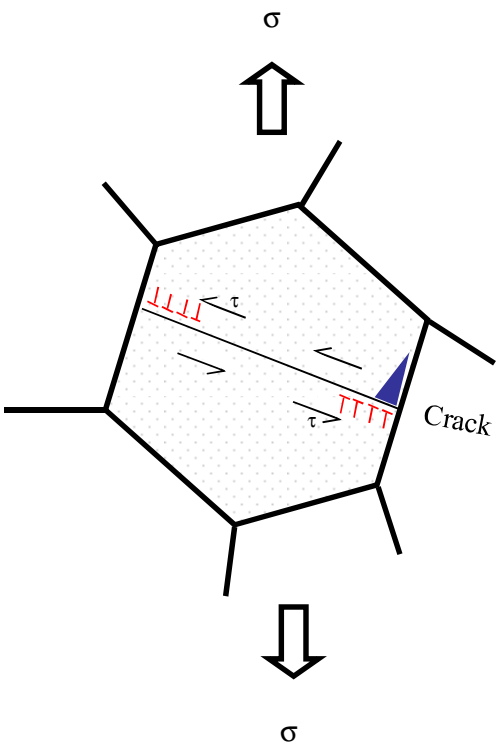

Figure 3. 17 - Stroh's model for cleavage fracture. [176, 177]

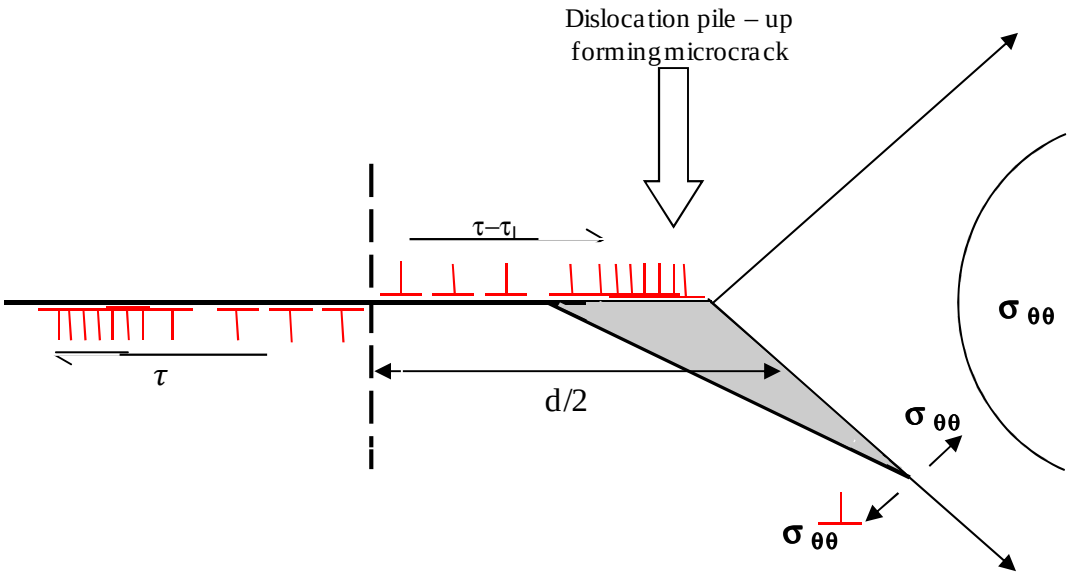

Figure 3. 18 - Orowan's critical tensile stress criterion for brittle fracture. [147, 179]

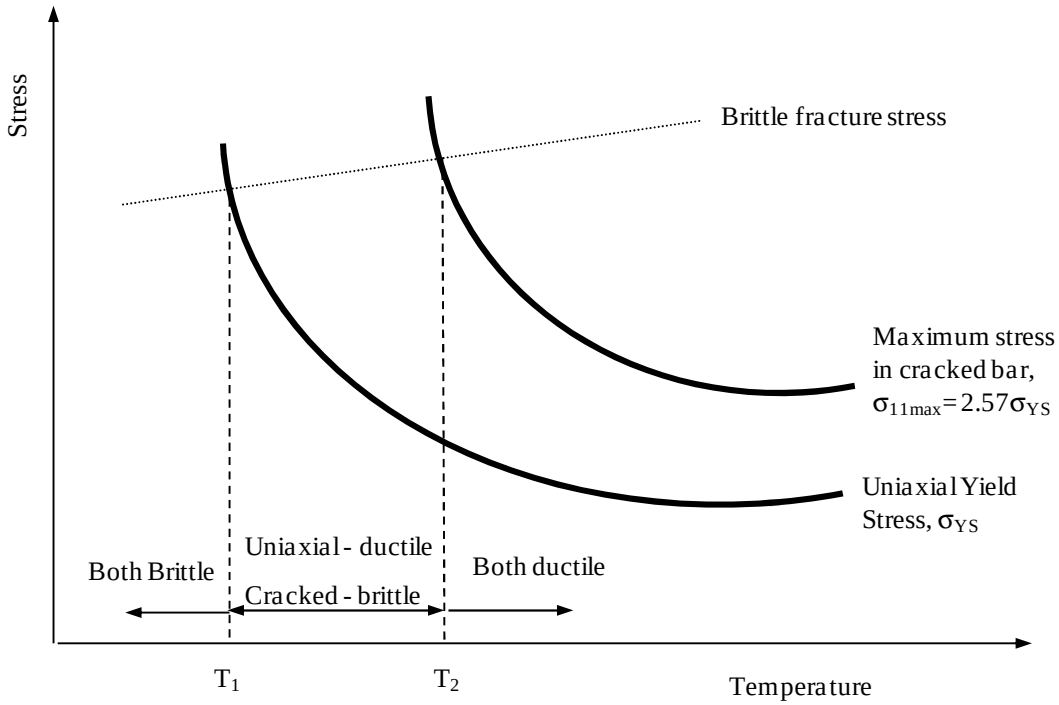

Figure 3. 19 - Cottrell's model for cleavage fracture. [41]

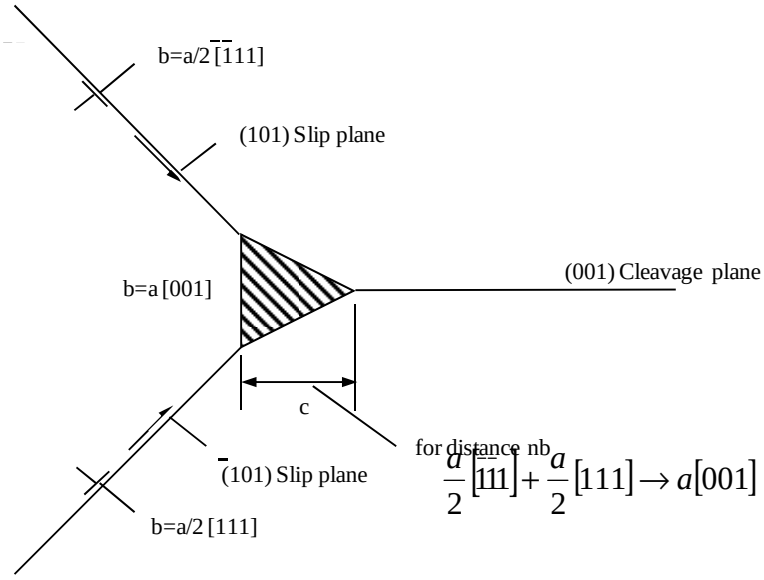

Figure 3. 20 - Smiths model of microcrack formation in grain boundary carbide film. [190]

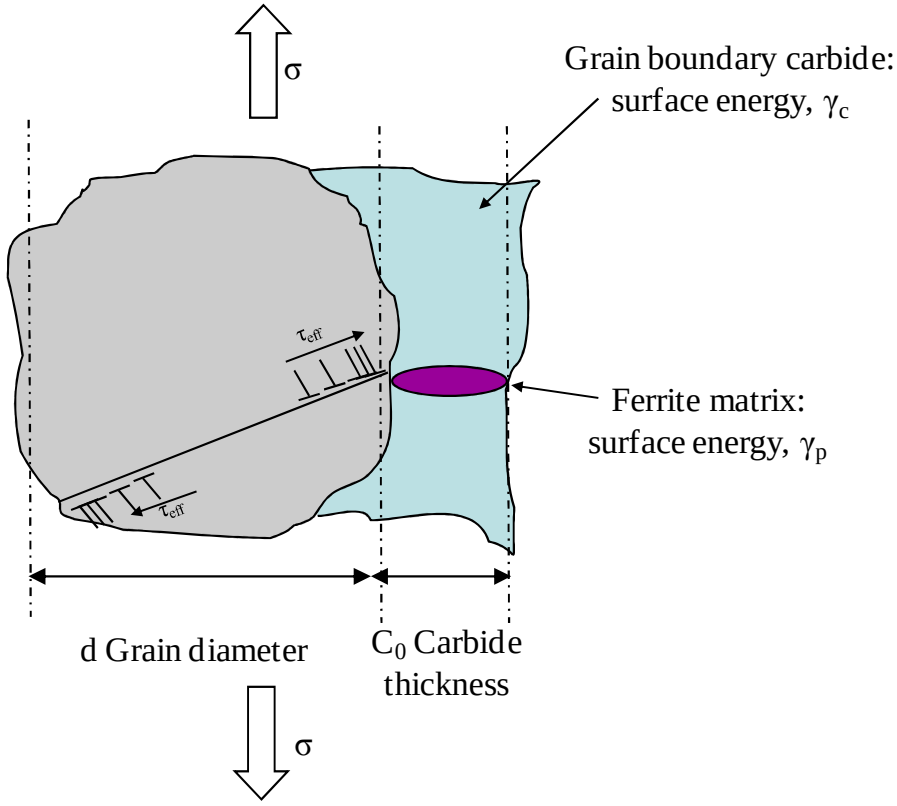

Figure 3. 21 - Variation in stress intensification with applied load. [163]

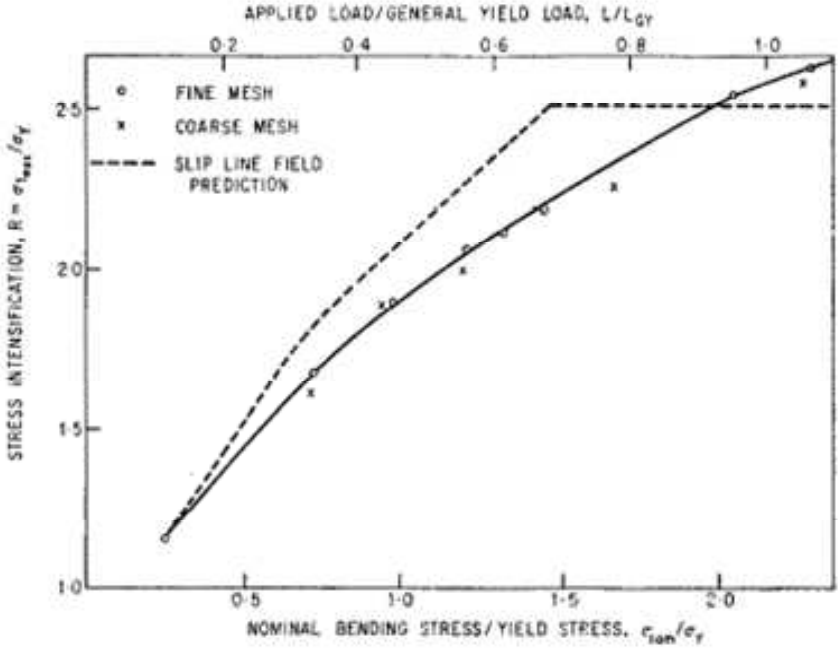

Figure 3. 22 - Variation of maximum principal tensile stress below the notch root at various loads. [163]

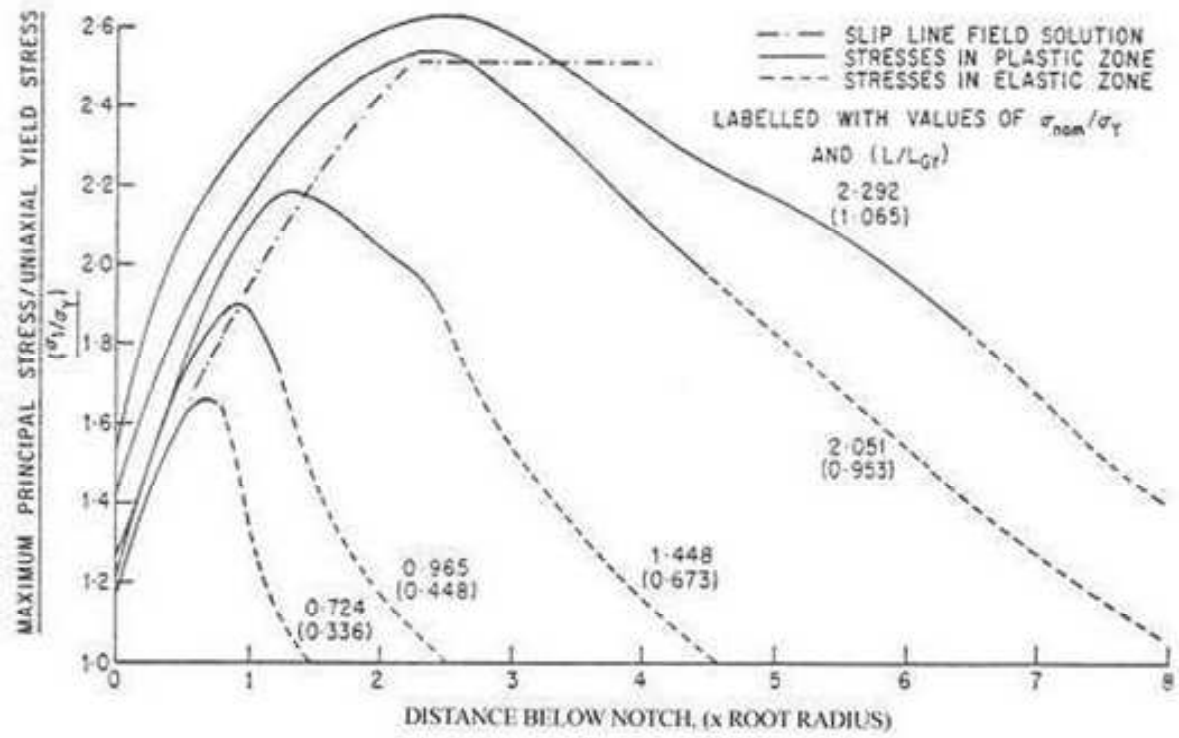

Figure 3. 23 - Propagation of crack in ductile fracture. [113]

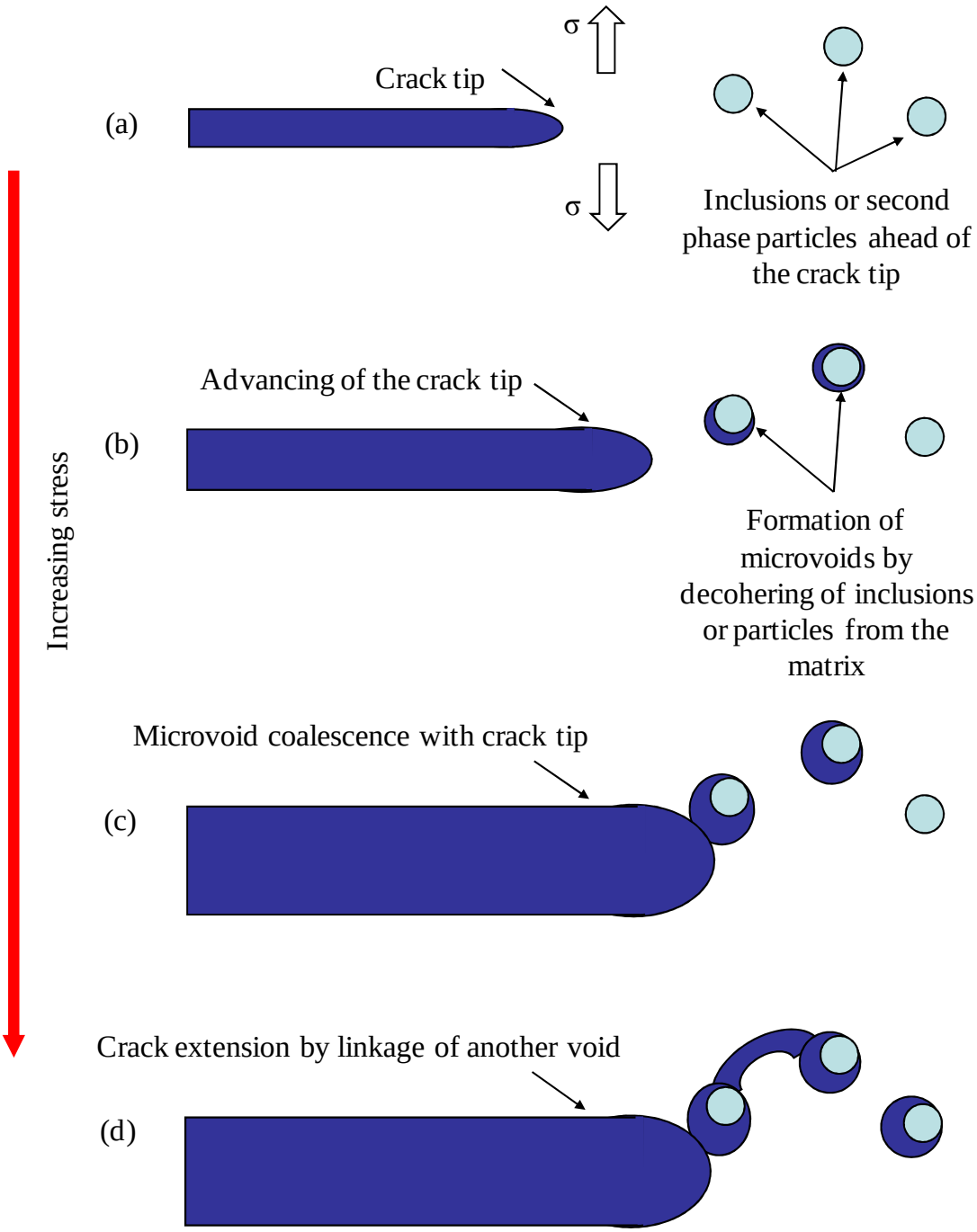

Figure 3. 24 - Representation of a critical fracture event; (a) at low temperature, the critical fracture stress is attained at the second grain boundary ahead of the crack tip, (b) at higher temperatures; high stress intensification is required as the yield stress is lower. [144]

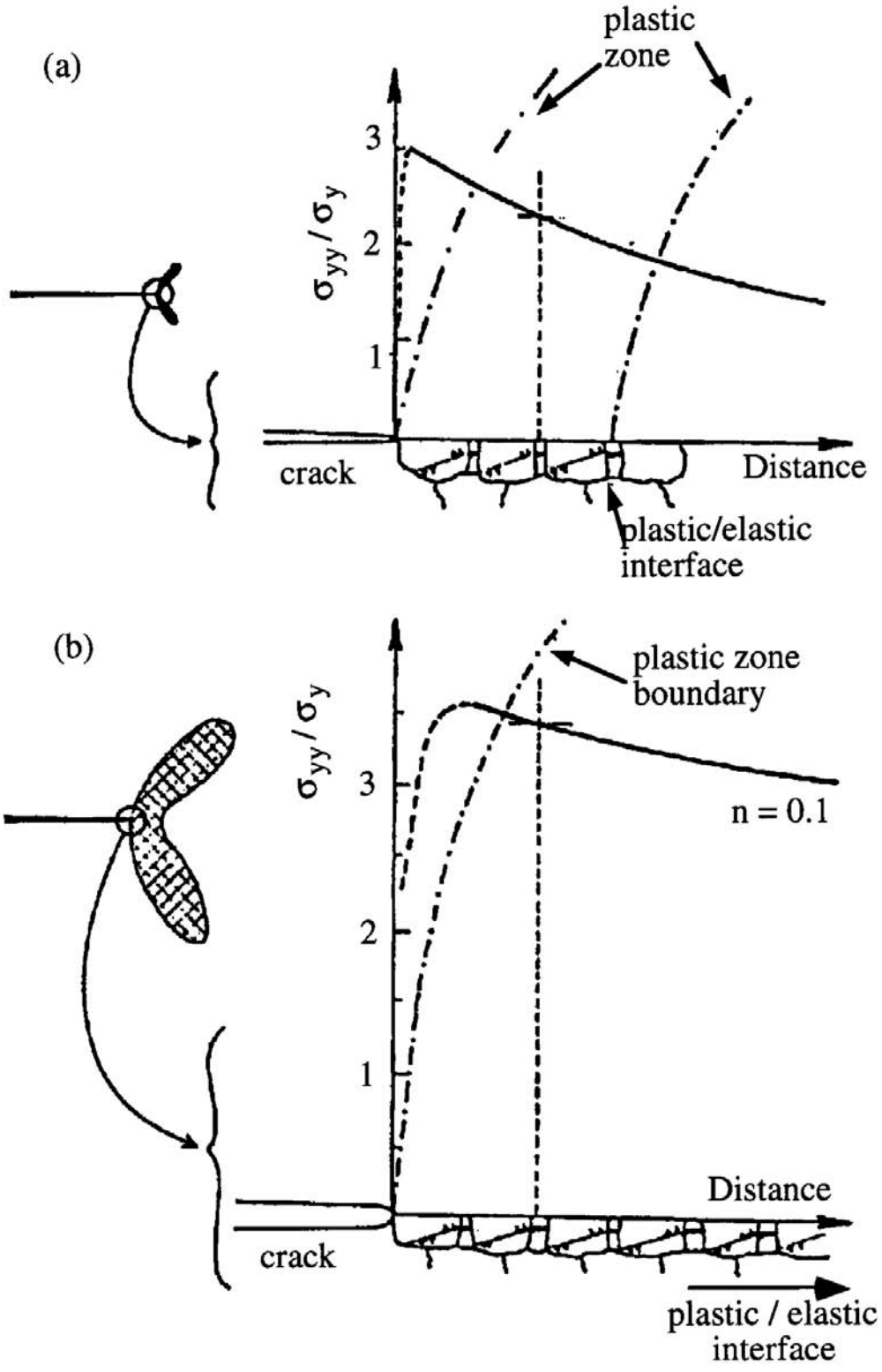

Figure 3.25 - The grain size, d, dependence of characteristic distance, X_0, in Mild Steel. [158]

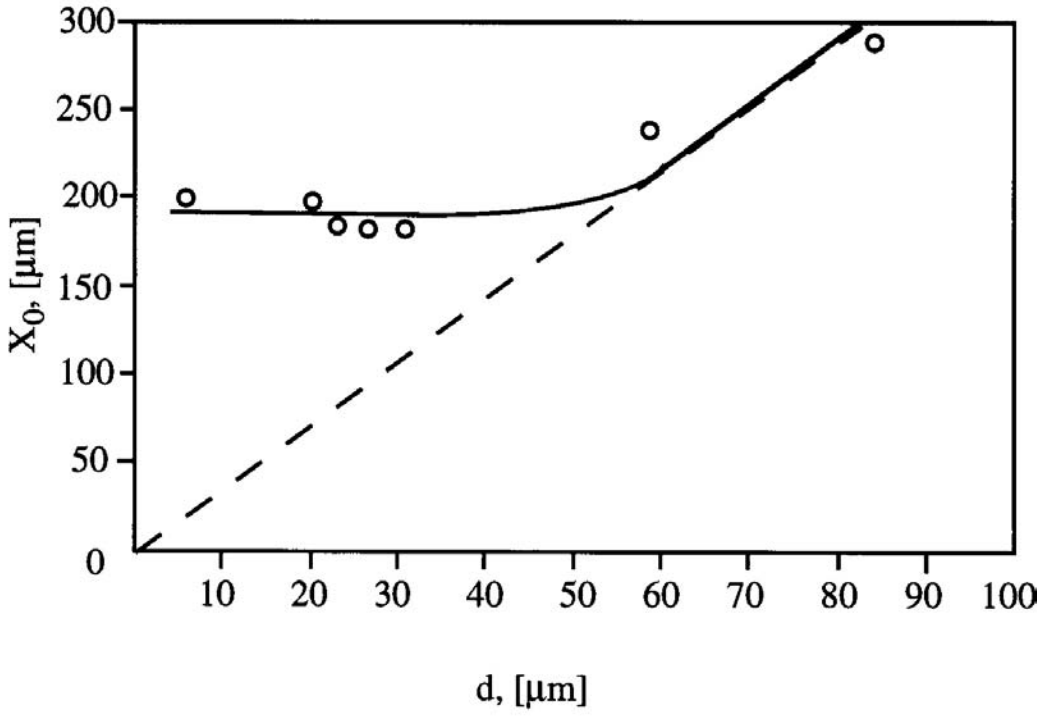

Figure 3. 26 - Grain boundary fracture with and without microvoid coalescence.

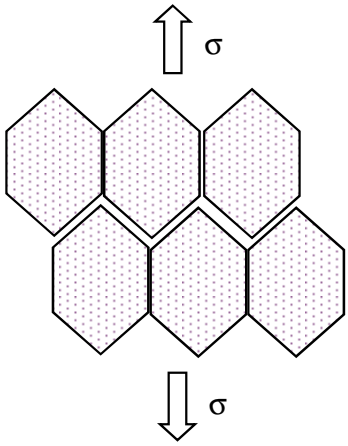

(a) Intergranular fracture without microvoid coalescence.

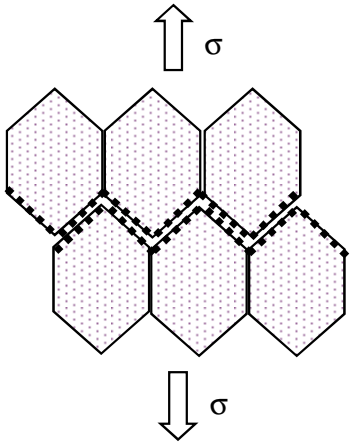

(b) Intergranular fracture with microvoid coalescence.

Table 4. 1 - ESAB weld metal (A533B Class 1) average chemical composition (% by weight)

.

ESAB Weld Average Chemical Composition							
C	**Si**	**Mn**	**P**	**S**	**Cr**	**Mo**	**Ni**
0.029	0.34	1.33	0.009	0.008	0.05	0.47	0.82
Cu	**Nb**	**Pb**	**Sn**	**Ti**	**V**	**W**	**Zr**
0.29	<0.005	-	-	<0.005	0.005	-	-
Al	**As**	**B**	**Co**	**Ca**	**Ce**	**Sb**	**N**
0.021	-	0.0005	-	-	-	-	0.011

Table 4. 2 - Welding parameters used to manufacture ESAB weld.

Parameters used by ESAB			
Heat Input (kJ/mm)	**Flux**	**Filler Wire**	**Current (Amps)**
-	OK 10.47	OK 13.4	525
Arc Voltage (Volts)	**Polarity**	**Preheat Temperature (^{o}C)**	**Travel Speed (mm/min)**
030	d.c. + ve	None	380

Table 4. 3 - Post weld heat treatment procedure.

ESAB Weld Stress Relief Heat Treatment	
1	Load into cool furnace
2	Heat to 610^{o}C at a rate of 100^{o}C/min maximum
3	Hold at 610^{o}C for 7 hours
4	Cool at rate of 100^{o}C/min maximum

Table 4. 4 - Tensile Test Matrix.

	Weld N°1			Weld N°2			
Microstructure	Single	Mixed	Mixed Transverse	Single	Mixed	Mixed Transverse	SA
Orientation	Longitudinal	Longitudinal	Transverse	Longitudinal	Longitudinal	Transverse	Longitudinal
Gauge Diameter	3	8	3	3	5	3	3
Gauge Length	15	40	15	15	25	15	15
Number of Specimens	36	15	18	36	17	18	36

Figure 4. 1 - (a) General dimension of the as - received weld plate, (b) Digital imagine of the as-received weld plate.

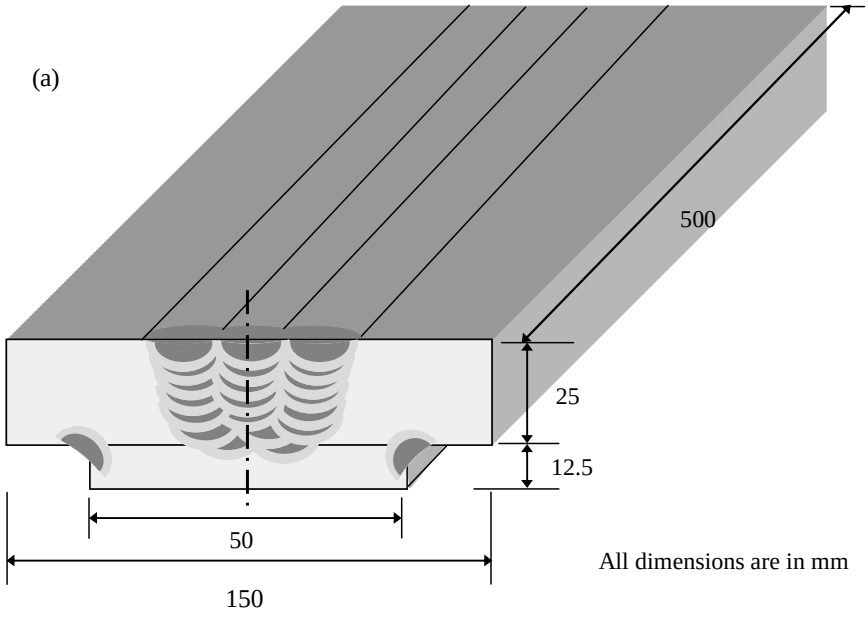

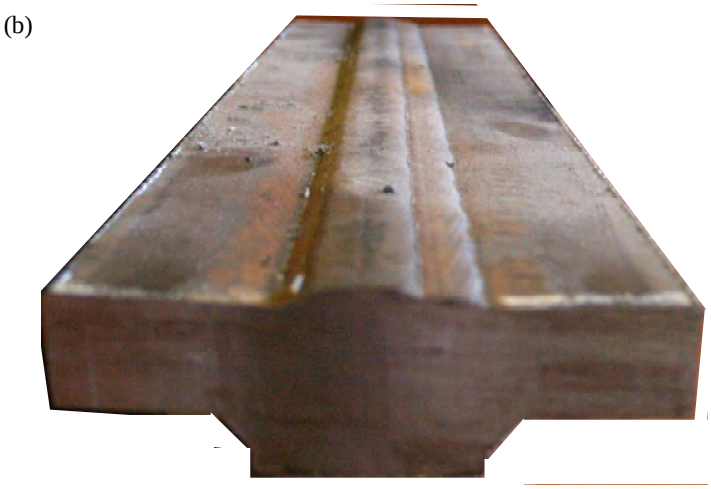

Figure 4. 2 - Macrograph showing Weld N°1, MnMoNi steel weld metal (ESAB A533B Class 1) cross - section showing weld microstructure.

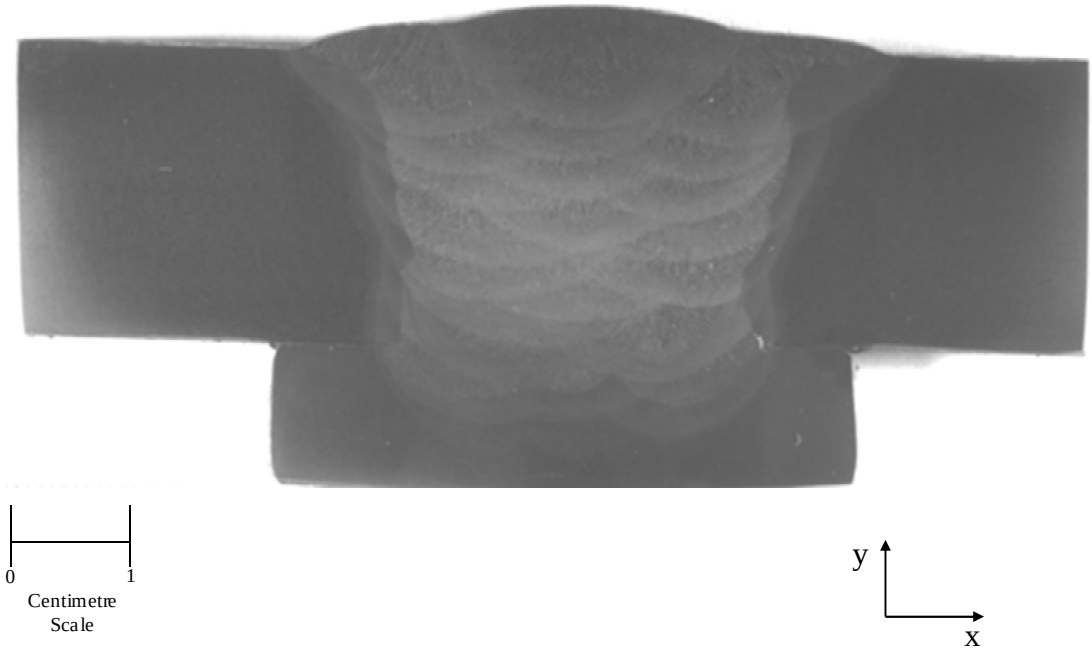

Figure 4. 3 - Macrograph showing Weld N°2, MnMoNi steel weld metal cross - section showing weld microstructure.

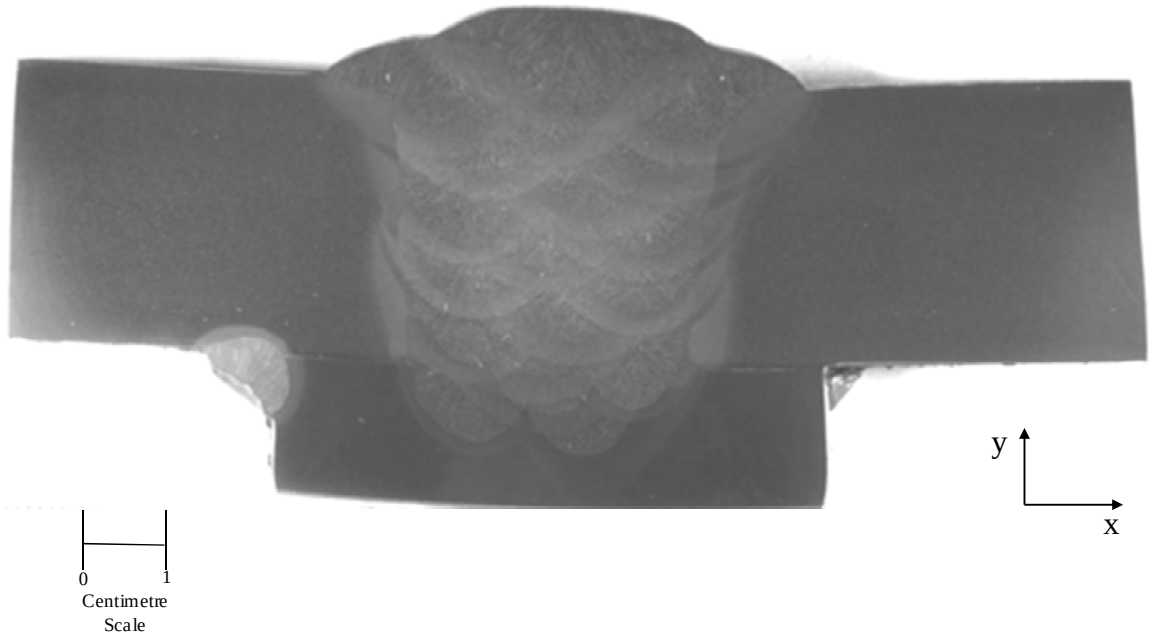

Figure 4. 4 - Macrograph showing low alloy - ferritic steel weld metal (ESAB A533B Class 1) cross - section showing weld microstructure.

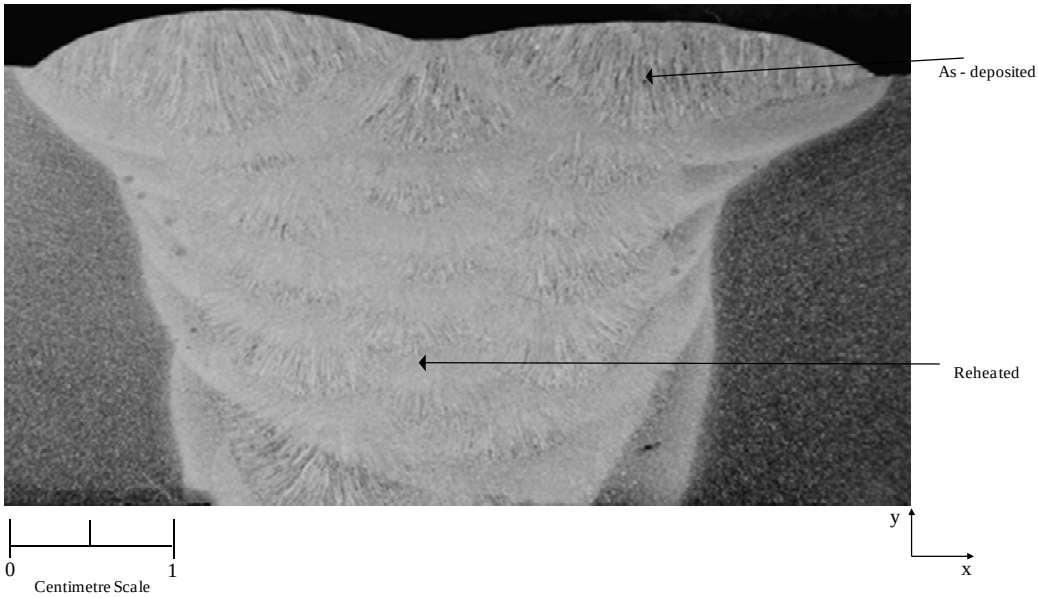

Figure 4. 5 - Schematic diagram of the prestraining arrangement for the specimen.

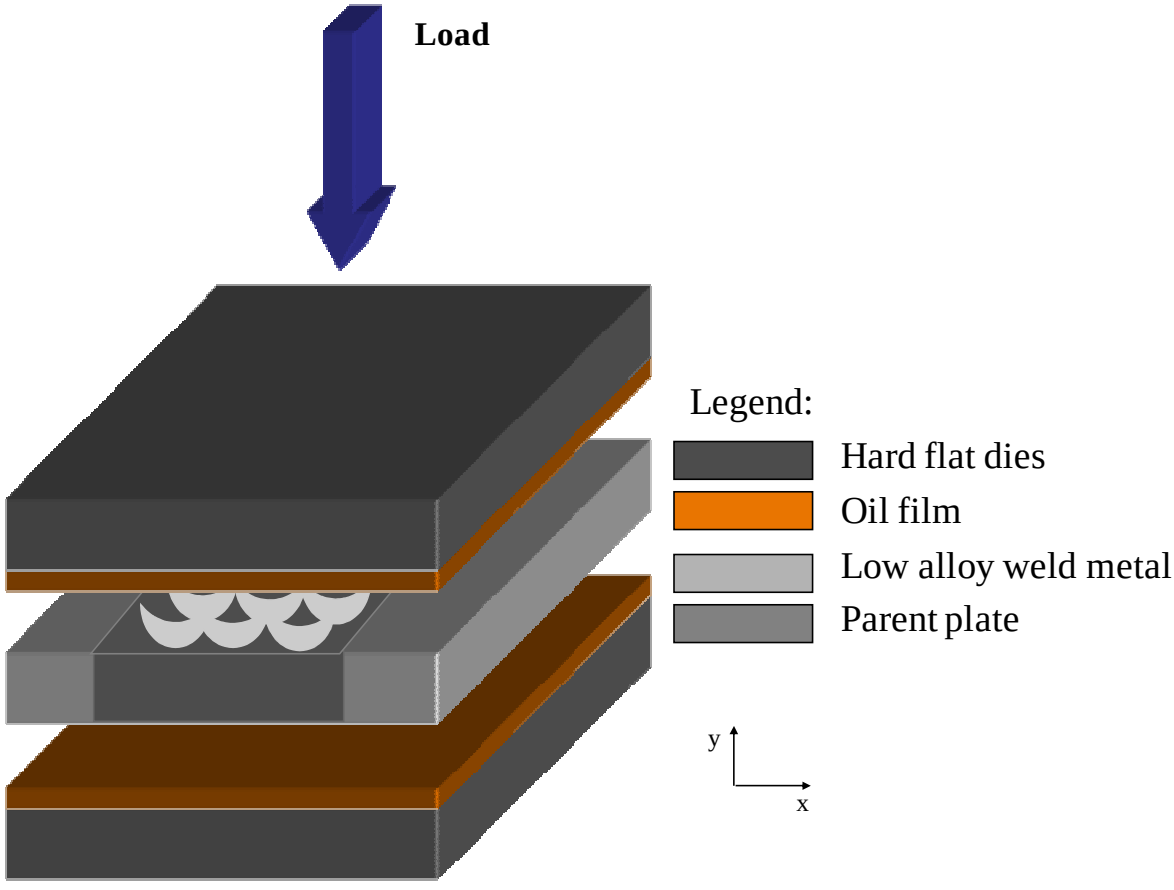

Figure 4. 6 - (a) Dimensions of samples removed from bulk material; (b) Specimen dimensions.

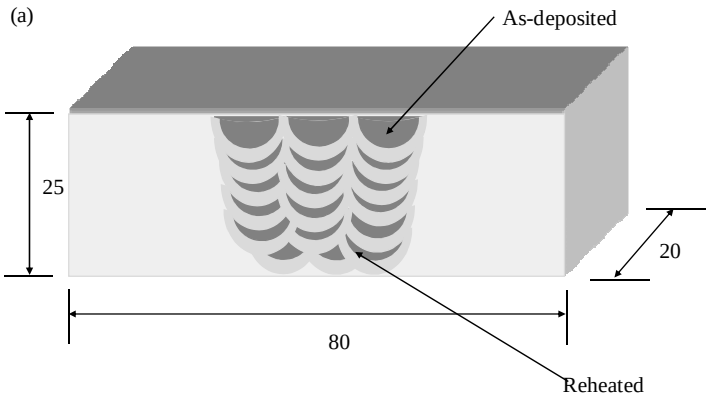

All dimensions are in mm

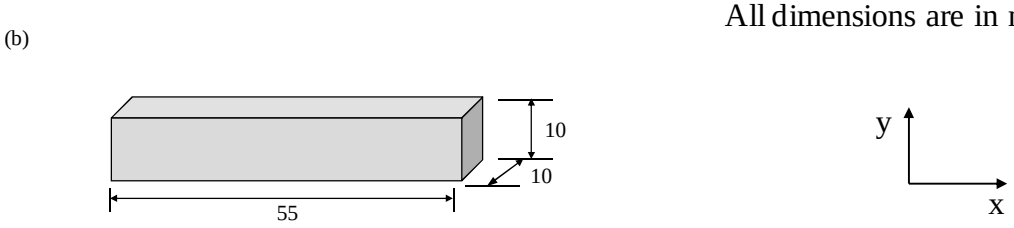

Figure 4. 7 - Schematic diagram of a weld trace locations for the microhardness testing.

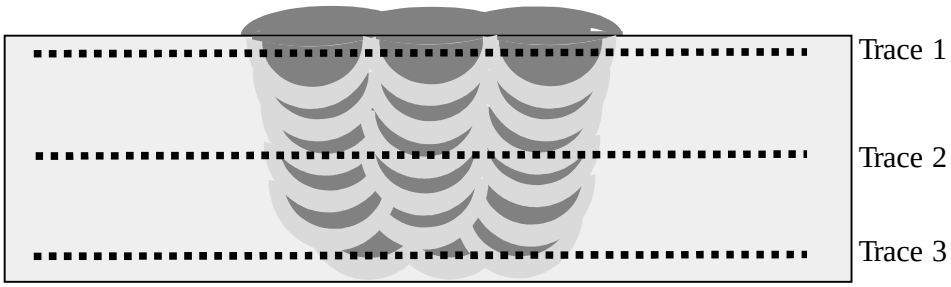

Figure 4. 8 - Schematic diagram of a weld trace locations for microhardness testing.

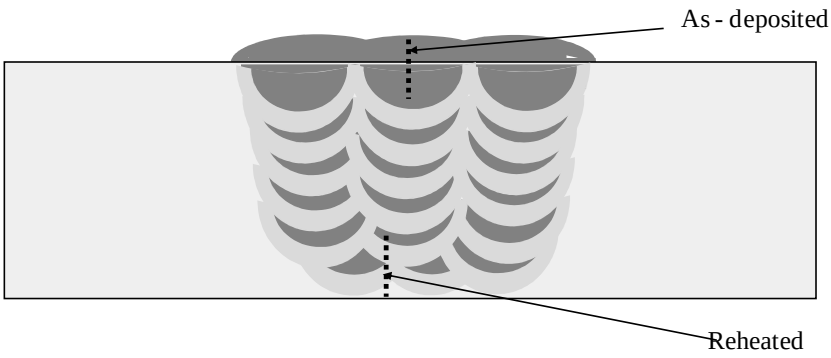

Figure 4. 9 - Schematic of the tensile test specimen geometry; (a) 3mm diameter gauge, (b) 5mm diameter gauge, (c) 8mm diameter gauge.

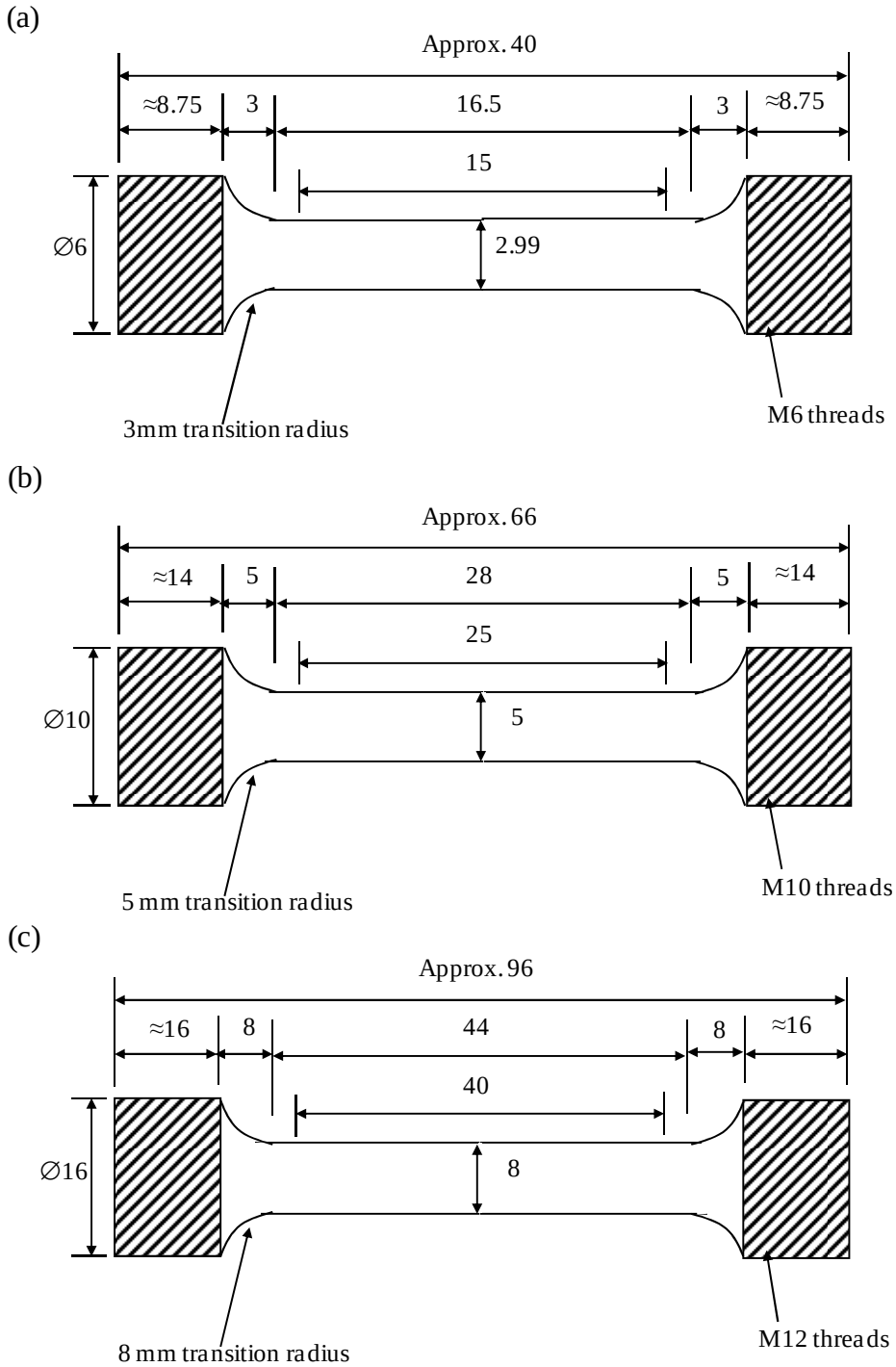

Figure 4. 10 - Schematic diagram detailing the location of the tensile blanks in respect to the weld microstructure; (a) single microstructure longitudinal, (b) mixed microstructure longitudinal, (c) mixed microstructure transverse direction.

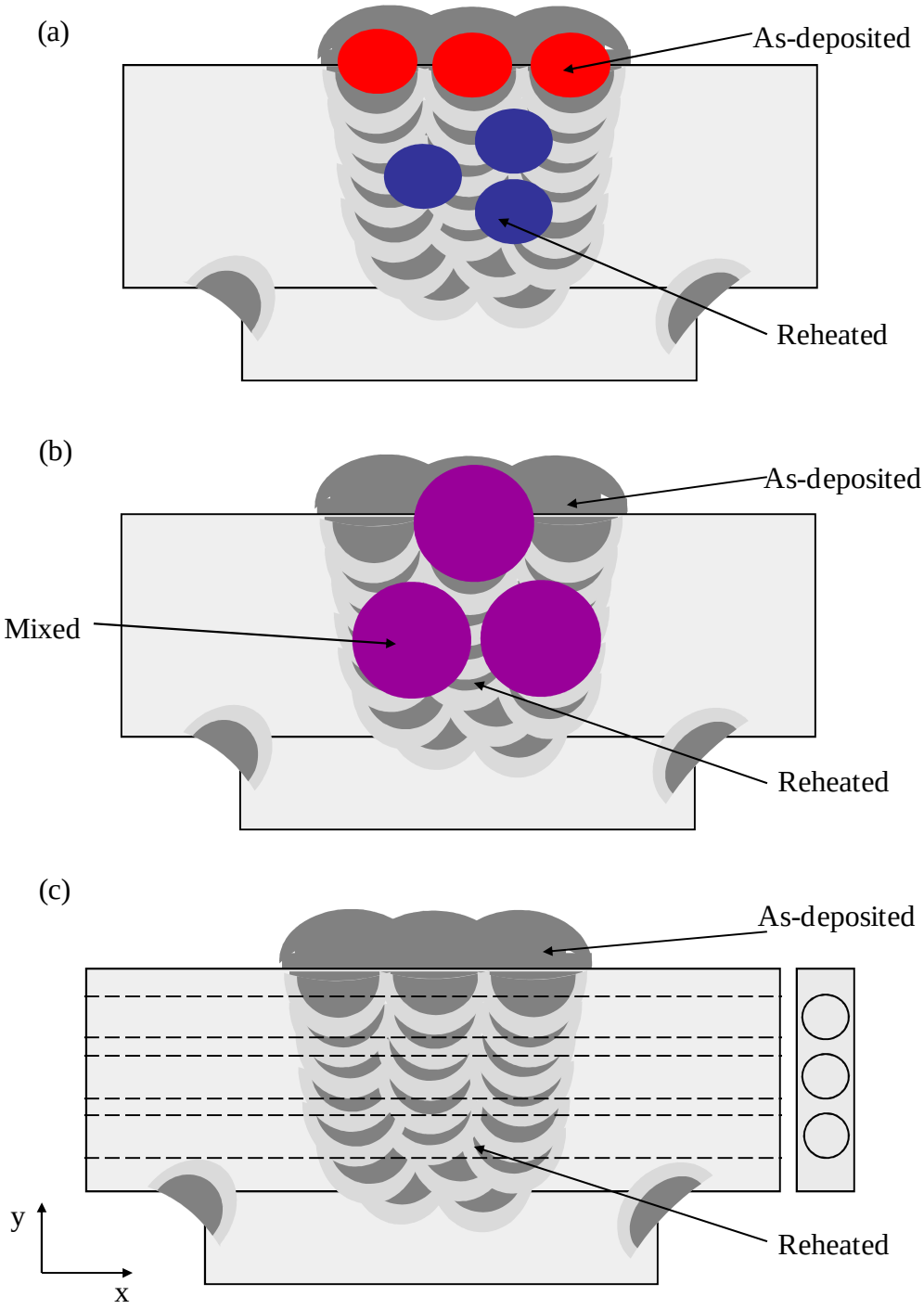

Figure 4. 11 - Unbroken tensile specimens, ranging from: 8mm diameter (top), 5mm diameter (middle) and 3mm diameter (bottom).

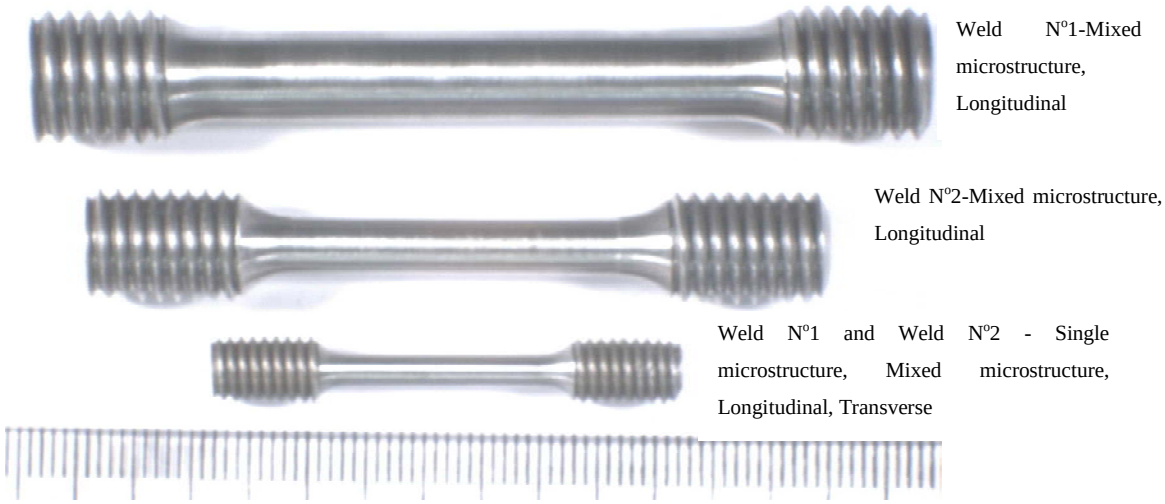

Figure 4. 12 - (a) Locations of the Charpy specimens for related microstructures, (b) Charpy specimen dimensions, (c) Charpy notch profile.

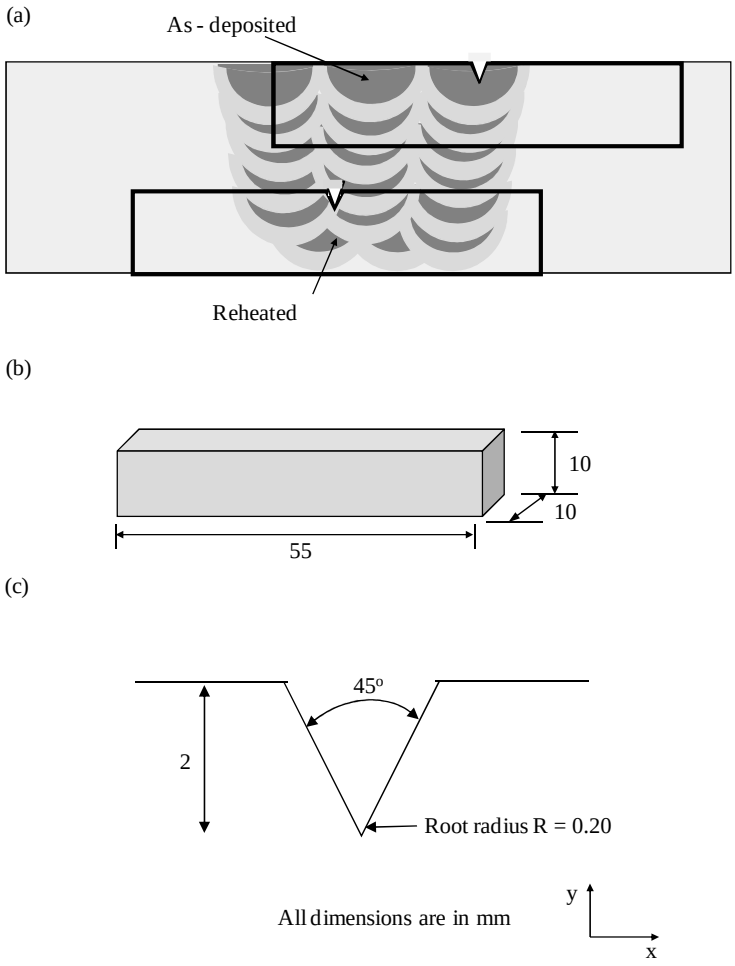

Figure 4. 13 - Schematic representation of Charpy Impact testing configuration.

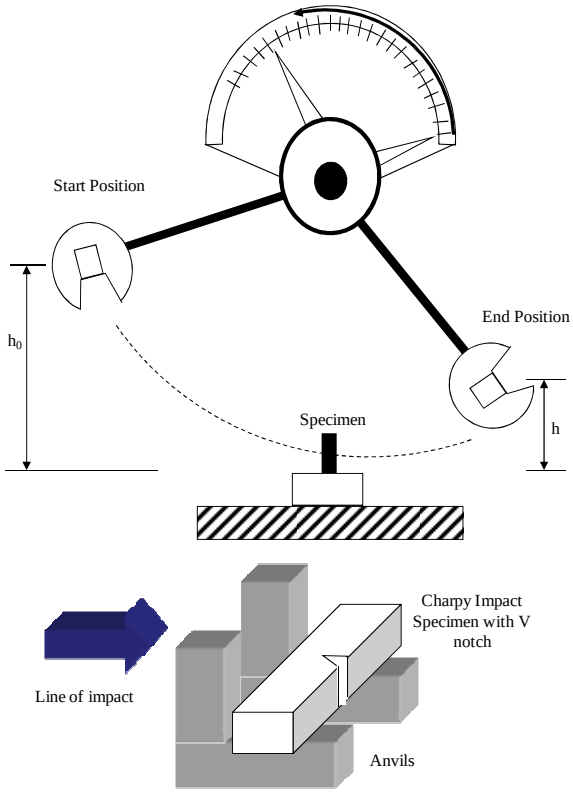

Figure 4. 14 - Fracture surface of Charpy Impact specimens at lower shelf, upper shelf temperatures and temperatures in the transition region.

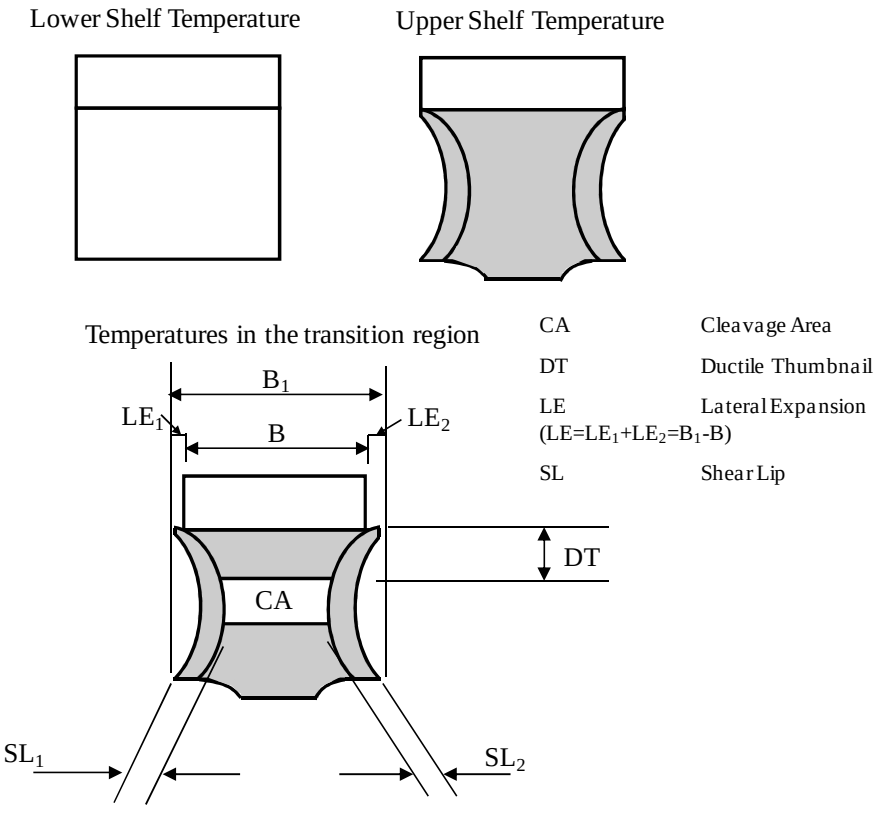

Figure 4. 15 - (a) Locations of the Blunt Notch specimens for related microstructures, (b) Blunt Notch specimen dimensions and notch profile for Charpy sized specimens, (c) Blunt Notch specimen dimensions and notch profile for Traditional sized specimens.

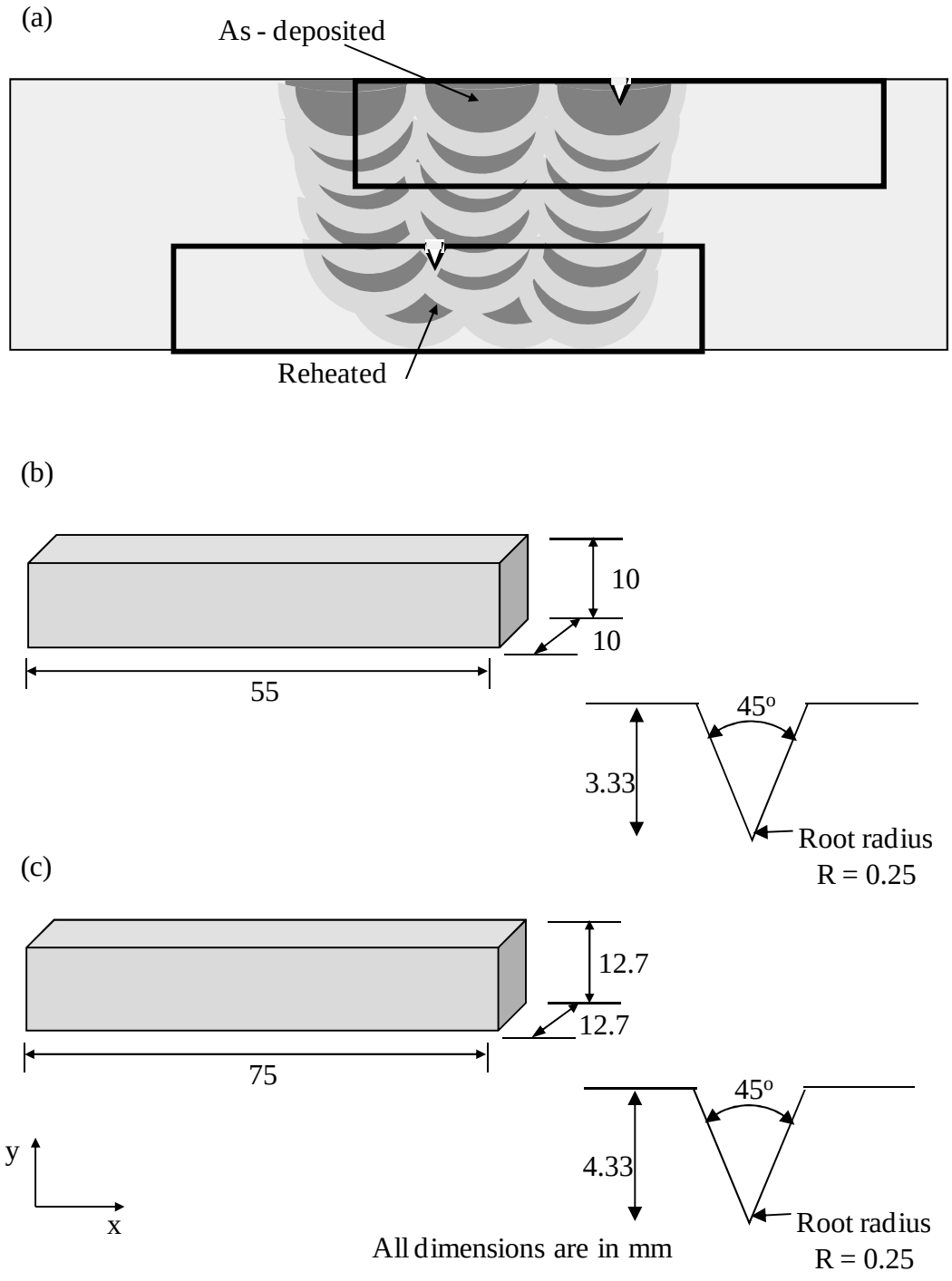

Figure 4. 16 - Four point bend testing arrangement for Blunt Notch tests.

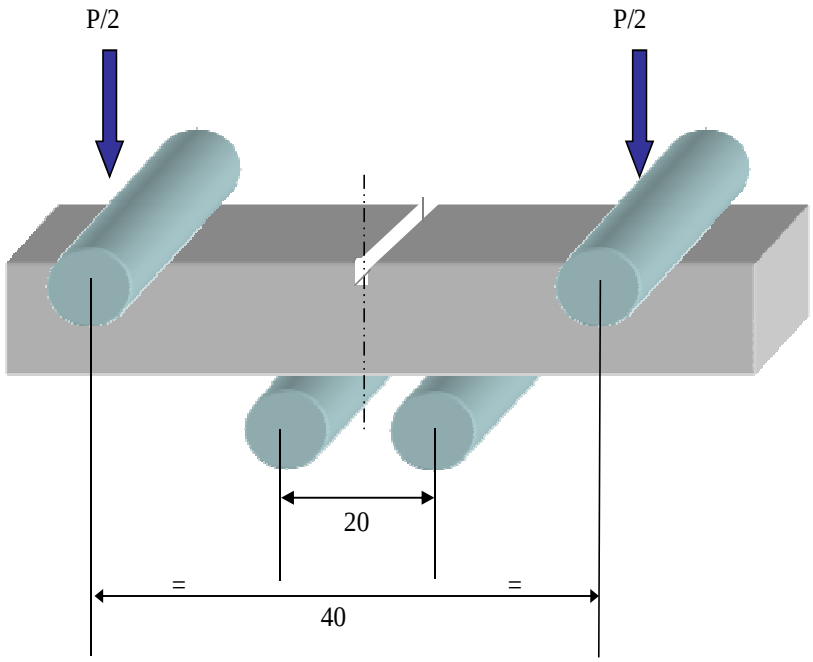

Where P is the applied load. All dimensions are in mm

Figure 4. 17 - Locations of CTOD specimen sampling in relation to the microstructural condition.

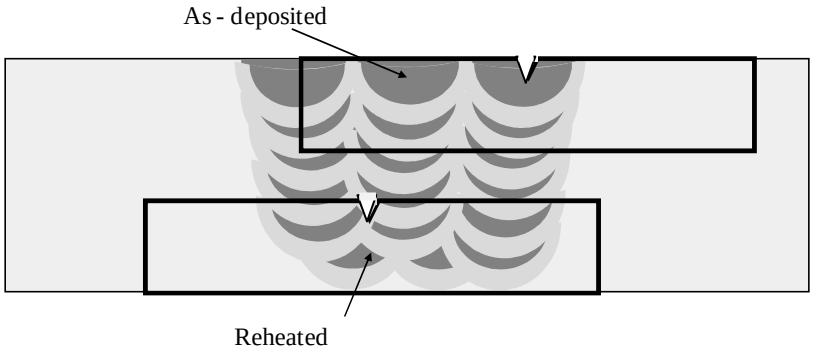

Figure 4. 18 - Notch profile with external knife edges and fatigue-crack.

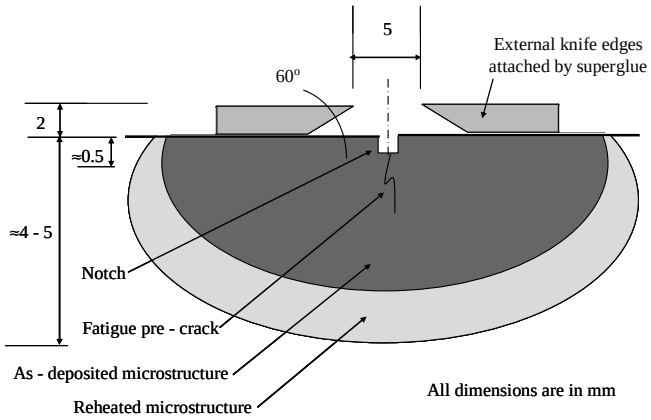

Figure 4. 19 - Crack-tip opening displacement testing arrangement.

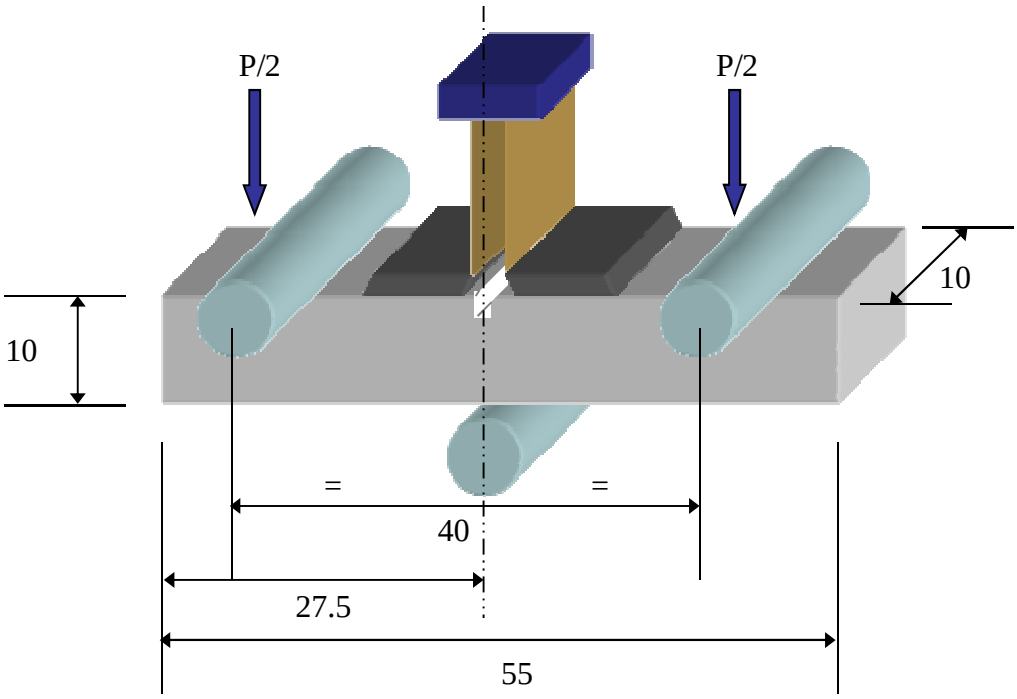

Where P is the applied load. All dimensions are in mm

Figure 4. 20 - Original crack growth and stable crack growth measurement scheme.

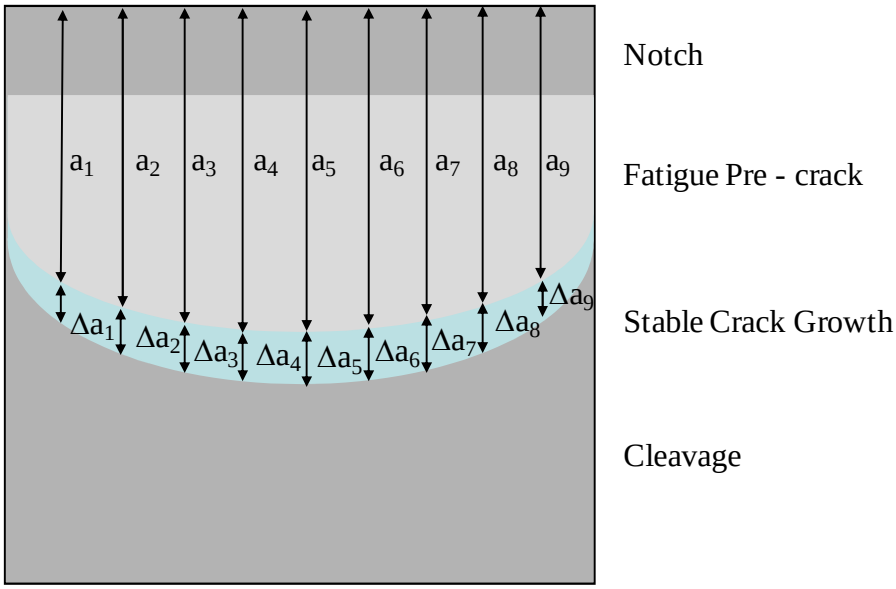

Table 5.1 - Microstructural parameters for Weld N^{o}2 for the parent plate and reheated microstructures.

	Number of Counts		Ferretmin / micron	Ferretmax / micron	Ferretratio / micron	Dcircle/ micron	Area/ micron^2
Parent Plate	14	**Average**	10.51	32.60	0.33	16.18	210.10
		Standard Deviation	2.56	8.43	0.12	2.49	63.10
Parent Plate 2	19	**Average**	9.40	37.99	0.26	16.71	225.84
		Standard Deviation	3.47	9.21	0.12	2.95	76.62
Parent Plate 3	17	**Average**	9.84	39.36	0.29	17.28	235.49
		Standard Deviation	2.32	15.20	0.14	2.22	57.09
Parent Plate 4	20	**Average**	9.44	40.11	0.25	17.32	237.46
		Standard Deviation	1.90	9.07	0.09	1.61	44.35
Parent Plate 5	17	**Average**	10.57	43.45	0.27	19.08	289.45
		Standard Deviation	2.31	11.67	0.14	2.20	68.90
Average	**87**		**9.86**	**38.77**	**0.28**	**17.29**	**239.67**
Coarse RH	12	**Average**	6.84	14.18	0.49	8.90	65.86
		Standard Deviation	2.28	3.28	0.11	2.25	30.58
Coarse RH 2	17	**Average**	10.58	19.77	0.56	12.58	128.54
		Standard Deviation	2.32	5.98	0.14	2.39	48.48
Coarse RH 3	17	**Average**	11.04	19.25	0.58	13.27	143.55
		Standard Deviation	2.73	3.94	0.11	2.64	66.56
Coarse RH 4	17	**Average**	11.38	19.91	0.58	13.16	140.62
		Standard Deviation	2.88	3.94	0.13	2.50	56.57
Coarse RH 5	17	**Average**	12.50	19.78	0.64	13.89	152.40
		Standard Deviation	1.80	3.64	0.11	1.63	38.39
Average	**80**		**10.47**	**18.58**	**0.60**	**12.36**	**126.39**
Fine RH	18	**Average**	5.44	10.22	0.56	6.74	37.10
		Standard Deviation	1.20	2.78	0.16	1.41	15.33
Fine RH 2	17	**Average**	8.50	15.51	0.58	10.16	83.08
		Standard Deviation	1.85	4.13	0.17	1.63	26.54
Fine RH 3	17	**Average**	8.55	13.09	0.66	9.34	70.46
		Standard Deviation	2.22	2.71	0.13	1.65	24.18
Fine RH 4	17	**Average**	9.84	15.38	0.66	10.82	93.23
		Standard Deviation	2.27	2.45	0.17	1.36	23.34
Fine RH 5	18	**Average**	9.15	15.36	0.60	10.50	89.27
		Standard Deviation	2.11	3.14	0.11	1.90	32.64
Fine RH 6	17	**Average**	10.62	16.09	0.64	11.87	113.45
		Standard Deviation	2.35	2.42	0.10	1.97	37.90
Average	**104**		**10.**	**14.28**	**0.62**	**9.90**	**81.10**

Table 5.2 - Microstructural parameters of the weld metal inclusions.

Microstructural Condition	d_a (μm)	N_a ($x10^4/mm^2$)	d_v (μm)	N_v ($x10^7/mm^3$)	S_v ($x10^2/mm$)	V_v (%)	λ_v (μm)
ADAR	0.53	4.97	0.85	6.53	14.82	2.10	0.30
RHAR	0.48	5.10	0.75	7.24	12.80	1.60	0.29
AD5%SA	0.59	2.94	0.92	4.41	11.74	1.80	0.34
RH5%SA	0.45	3.56	0.79	6.00	11.77	1.55	0.30
Mean Value	0.51	4.14	0.83	6.05	12.78	1.76	0.31

Table 5.3 - Major and minor constituents of the weld metal inclusions (as taken from EDX spectra).

Microstructural Condition	Inclusion Diameter, d_a (μm)	Constituents	
		Major	Minor
ADAR	$d_a \leq 3$	Fe, Mn, Co	Cr, Al, Ti, Cu, Ni
	$d_a \leq 2$	Fe, Mn, Co	Cr, Al, Ti, Cu, Ni
	$d_a \leq 1$	Fe, Mn, Co	Cr, Al, Ti, Cu, Ni
RHAR	$d_a \leq 3$	Fe, Mn, Cc	Si, Al, Cu, Ni, Ti, C, N
	$d_a \leq 2$	Fe, Cr	Ni, Cr, Ti, O
	$d_a \leq 1$	Al, Fe, Mn	Ni, Ti, Cu, C, Al, Si N
AD5%SA	$d_a \leq 3$	Mn, Fe	Cu, O C, Ti Cr, Ni, Mo
	$d_a \leq 2$	Mn, Fe	C, Cr, O, N, Cu, Al, Si Ni
	$d_a \leq 1$	Mn, Fe	C, Cr, N, Cu, Al, Si Ni
RH5%SA	$d_a \leq 3$	Mn, Fe	C, O, Cr, Ti, Ni, Cu, Mo, Al, Cu
	$d_a \leq 2$	Mn, Fe	C, Cr, N, Cu, Al, O, Ni, Cu
	$d_a \leq 1$	Mn, Fe	C, N, O Ti, Al, Cu, Co, Ni, Ti, Cr

Table 5.4 - ESAB Weld chemical composition as supplied for Weld N°1 by ESAB; elements that are highlighted are used as baseline for Glow Discharge Spectrometry (GDS).

ESAB Weld Average Chemical Composition							
C	**Si**	**Mn**	**P**	**S**	**Cr**	**Mo**	**Ni**
0.029	0.34	1.33	0.009	0.008	0.05	0.47	0.82
Cu	**Nb**	**Pb**	**Sn**	**Ti**	**V**	**W**	**Zr**
0.29	<0.005	-	-	<0.005	0.005	-	-
Al	**As**	**B**	**Co**	**Ca**	**Ce**	**Sb**	**N**
0.021	-	0.0005	-	-	-	-	0.011

Table 5.5 - Results from GDS analysis for Weld N°1 for the parent plate, heat affected zone and weld material.

	Average Chemical Composition (wt%)					
Weld N°1 Parent Plate	**Fe**	**N**	**C**	**Cr**	**Ni**	
	99.22	0	0.09	0	0.01	
	Al	**Mo**	**Mn**	**Si**	**Co**	**Cu**
	0	0.02	0.51	0.16	0	0.16
Weld N° 1 Heat Affected Zone	**Fe**	**N**	**C**	**Cr**	**Ni**	
	97.33	0	0.89	0	0	
	Al	**Mo**	**Mn**	**Si**	**Co**	**Cu**
	0	0.01	0.48	0.15	0	0.08
Weld N° 1 Weld Material	**Fe**	**N**	**C**	**Cr**	**Ni**	
	96.80	0	0.02	0	0.93	
	Al	**Mo**	**Mn**	**Si**	**Co**	**Cu**
	0	0.51	1.41	0.33	0	0.11

Table 5.6 - Results from GDS analysis for Weld N°2 for the parent plate, heat affected zone and weld material.

	Average Chemical Composition (wt%)					
Weld N° 2 Parent Plate	**Fe**	**N**	**C**	**Cr**	**Ni**	
	99.03	0	0.09	0	0.01	
	Al	**Mo**	**Mn**	**Si**	**Co**	**Cu**
	0	0.02	0.51	0.16	0	0.18
Weld N° 2 Heat Affected Zone	**Fe**	**N**	**C**	**Cr**	**Ni**	
	96.99	0	0.89	0	0.01	
	Al	**Mo**	**Mn**	**Si**	**Co**	**Cu**
	0	0.01	0.48	0.15	0	0.05
Weld N° 2 Weld Material	**Fe**	**N**	**C**	**Cr**	**Ni**	
	96.82	0	0.02	0	0.93	
	Al	**Mo**	**Mn**	**Si**	**Co**	**Cu**
	0	0.50	1.39	0.35	0	0.07

Table 5.7 - Summary of macrohardness values for both Weld N°1 and N°2 for both weld metal conditions for profile Lines 1, 2 and 3.

	Lower H_v	Upper H_v	Mean H_v	Standard Deviation	Number of Counts
Weld N° 1 As - Received Condition					
Line 1	133.2	219.6	188.5	30.3	37
Line 2	130.5	208	172.8	28.7	37
Line 3	130.5	190	161.1	21.5	37
Weld N° 1 5%SA Condition					
Line 1	185.1	257.1	227.4	22.7	37
Line 2	173.5	236.8	209.4	19.3	37
Line 3	173.8	223.9	200.1	16.4	37
Weld N° 2 As - Received Condition					
Line 1	159.2	233.6	205.6	23.8	33
Line 2	169	231.3	197.1	21.4	33
Line 3	158.3	225.8	193.7	21.7	29
Weld N° 2 5%SA Condition					
Line 1	197.4	252.7	228.5	19.5	33
Line 2	185.2	231.6	221.7	14.7	33
Line 3	171.7	225.3	197.6	16.2	33

Table 5.8 - Summary of macrohardness values for both Weld N°1 and N°2 for both weld metal conditions for individual microstructures.

	Min H_V	Max H_V	Mean H_V	Standard Deviation	Number of Counts
Weld N° 1 As-Received					
Parent Plate	130.5	158.9	140.44	8.27	40
Reheated	162.3	191	180.7	7.34	25
As-Deposited	191.3	219.6	203.7	8.69	40
Weld N° 1 5%SA					
Parent Plate	173.5	197.5	186.3	6.09	37
Reheated	201.3	220.8	213.17	4.84	26
As-Deposited	221.2	257.1	234.6	10.8	42
Weld N° 2 As-Received					
Parent Plate	158.3	188.4	172.72	8.14	35
Reheated	191.7	214.7	205.46	6.87	33
As-Deposited	216.3	233.6	225.2	4.96	27
Weld 2 N° 5%SA					
Parent Plate	171.7	198.9	187.28	9.22	28
Reheated	200	223.4	210.77	7.3	39
As-Deposited	225.1	252.7	236.99	7.79	32

Table 5.9 - Summary of microhardness values for both Weld N°1 and N°2 for both microstructures AD and RH and in both weld metal conditions, AR and 5%SA.

	Min H_V	Max H_V	Mean H_V	Standard Deviation	Number of Counts
Weld N° 1					
ADAR	221.8	276.8	243.9	11.2	60
RHAR	174.6	233.8	210.6	11.7	60
AD5%SA	230.0	286.6	256.3	12.4	60
RH5%SA	199.9	236.1	220.7	9.2	60
Weld N° 2					
ADAR	240	279.5	261.4	8.7	60
RHAR	202.3	256.8	233.0	12.7	60
AD5%SA	253.4	290.2	275.7	8.6	60
RH5%SA	220.4	265.1	251.4	10.9	60

Figure 5.1 - Weld N°1 - showing the parent plate microstructure (a) SEM image; (b) optical microscope image.

(a) **(b)**

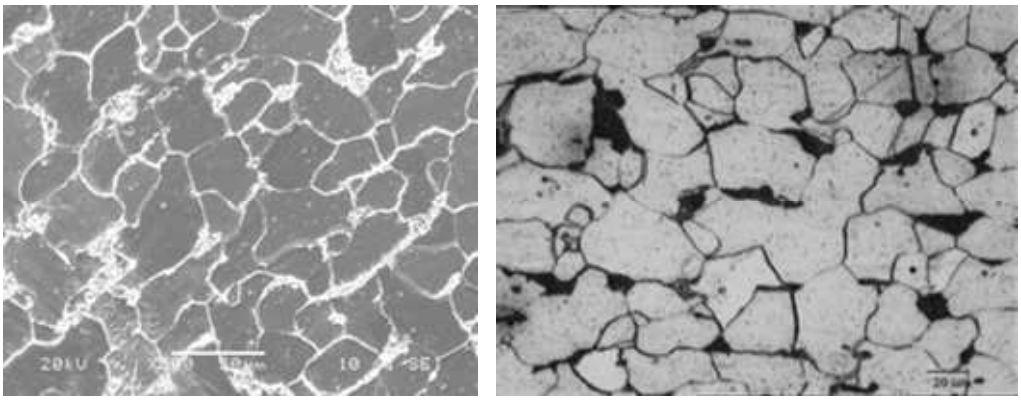

Figure 5.2 - Weld N°1 - showing the as-deposited microstructure (a) SEM image; (b) optical microscope image.

(a) **(b)**

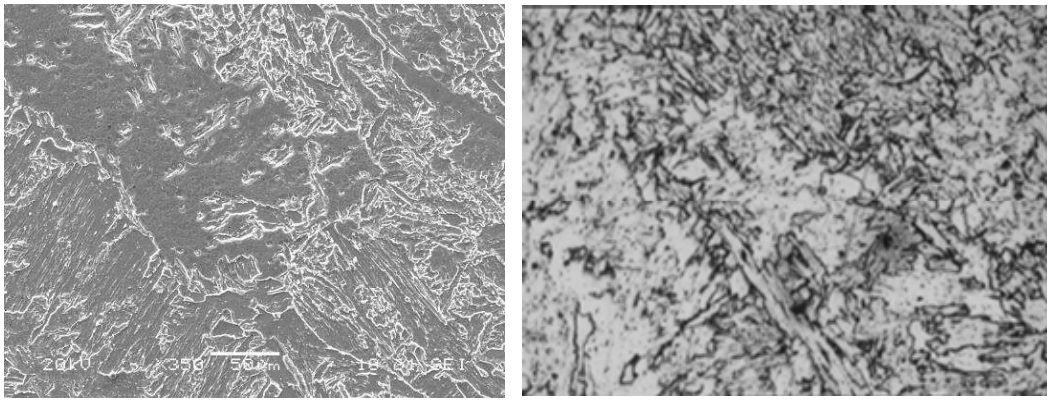

Figure 5.3 - Weld N°1 - showing reheated microstructure (a) SEM image; (b) optical microscope image.

(a) **(b)**

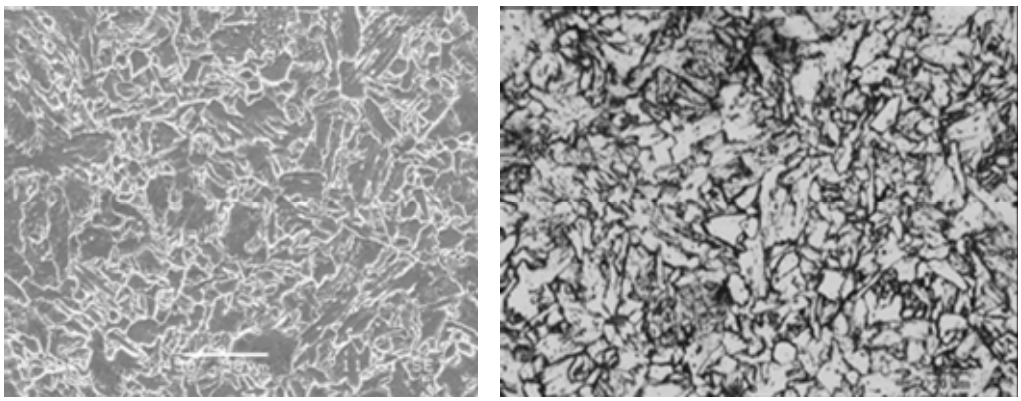

Figure 5.4 - Weld N°1 - showing reheated microstructure located at the bottom of the weld (a) SEM image; (b) optical microscope image.

(a) **(b)**

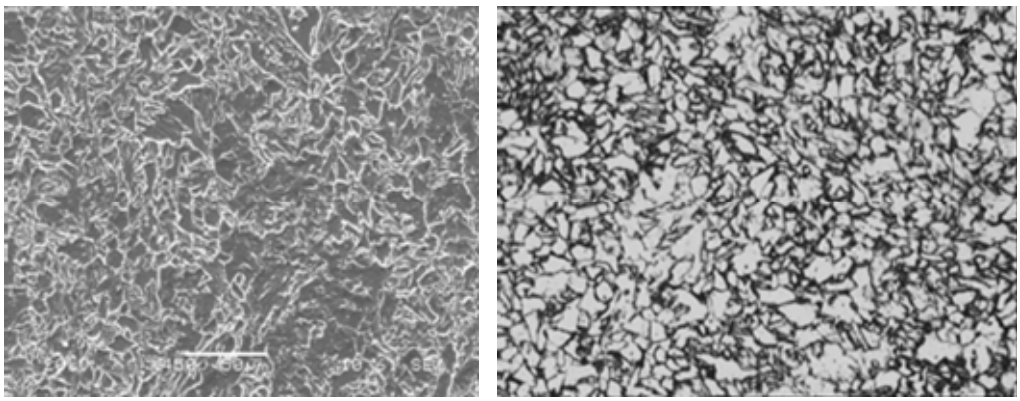

Figure 5.5 - Weld N°2 - showing the parent plate microstructure (a) SEM image; (b) optical microscope image.

(a) **(b)**

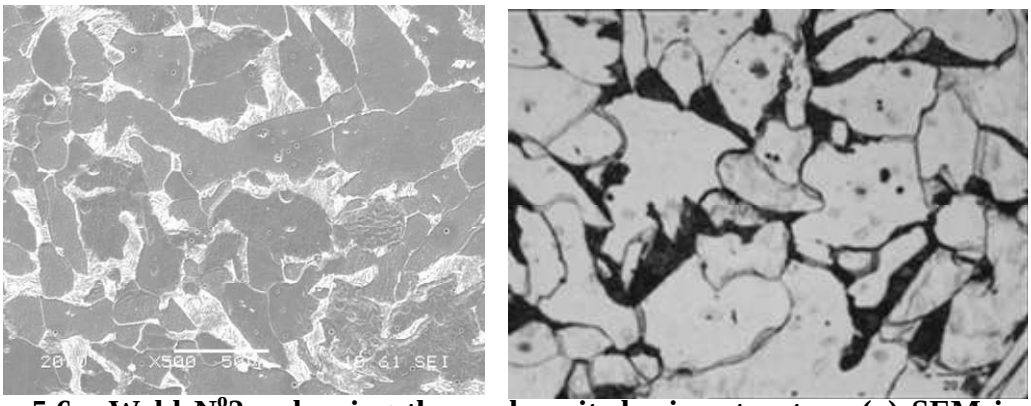

Figure 5.6 - Weld N°2 - showing the as-depsoited microstructure (a) SEM image; (b) optical microscope image.

(a) **(b)**

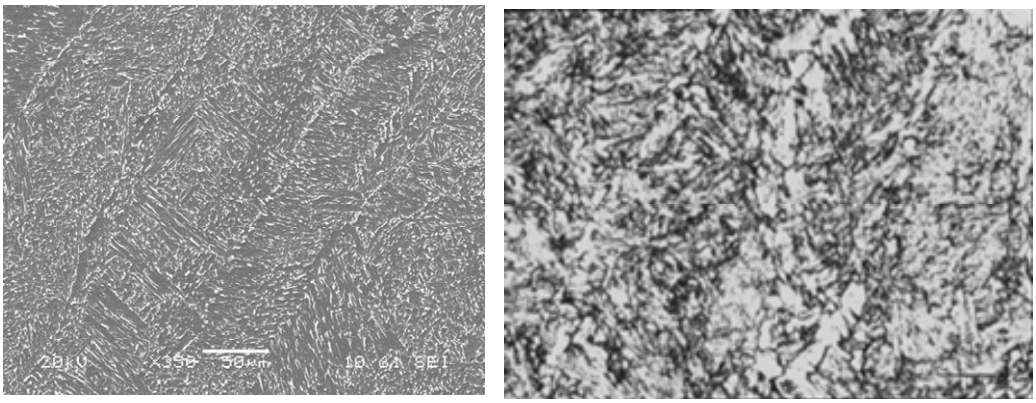

Figure 5.7 - Weld N^{o}2 - showing the reheated microstructure (a) SEM image; (b) optical microscope image.

(a) **(b)**

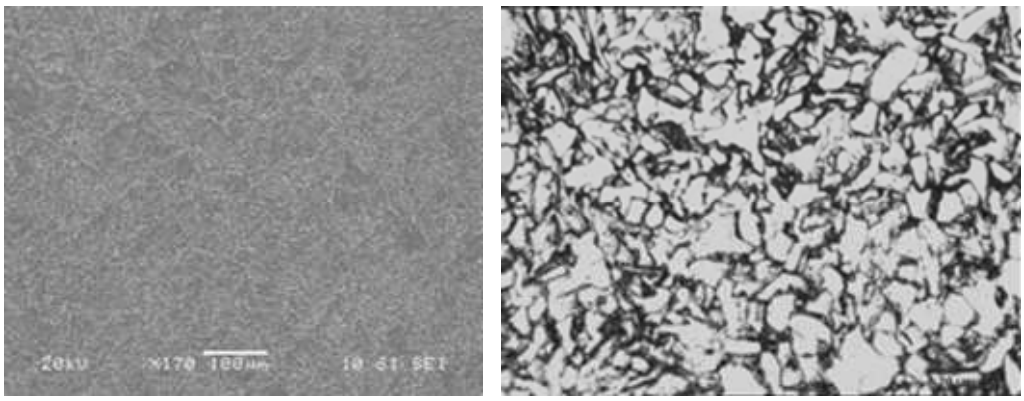

Figure 5.8 - Weld N^{o}2 - showing the reheated microstructure at the top of the weld (a) SEM image; (b) optical microscope image.

(a) **(b)**

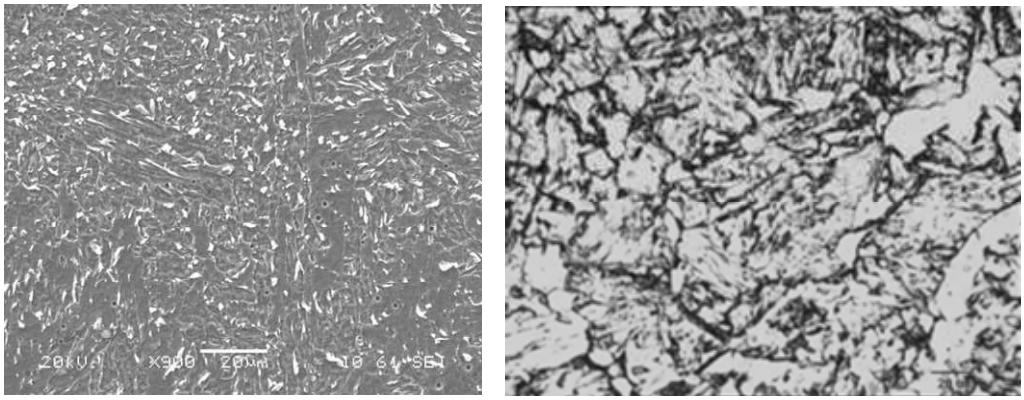

Figure 5.9 - Microstructure of the as - deposited (AD) microstructure; detailing areas of Acicular ferrite, Widmanstätten ferrite and Allotriomorphic ferrite.

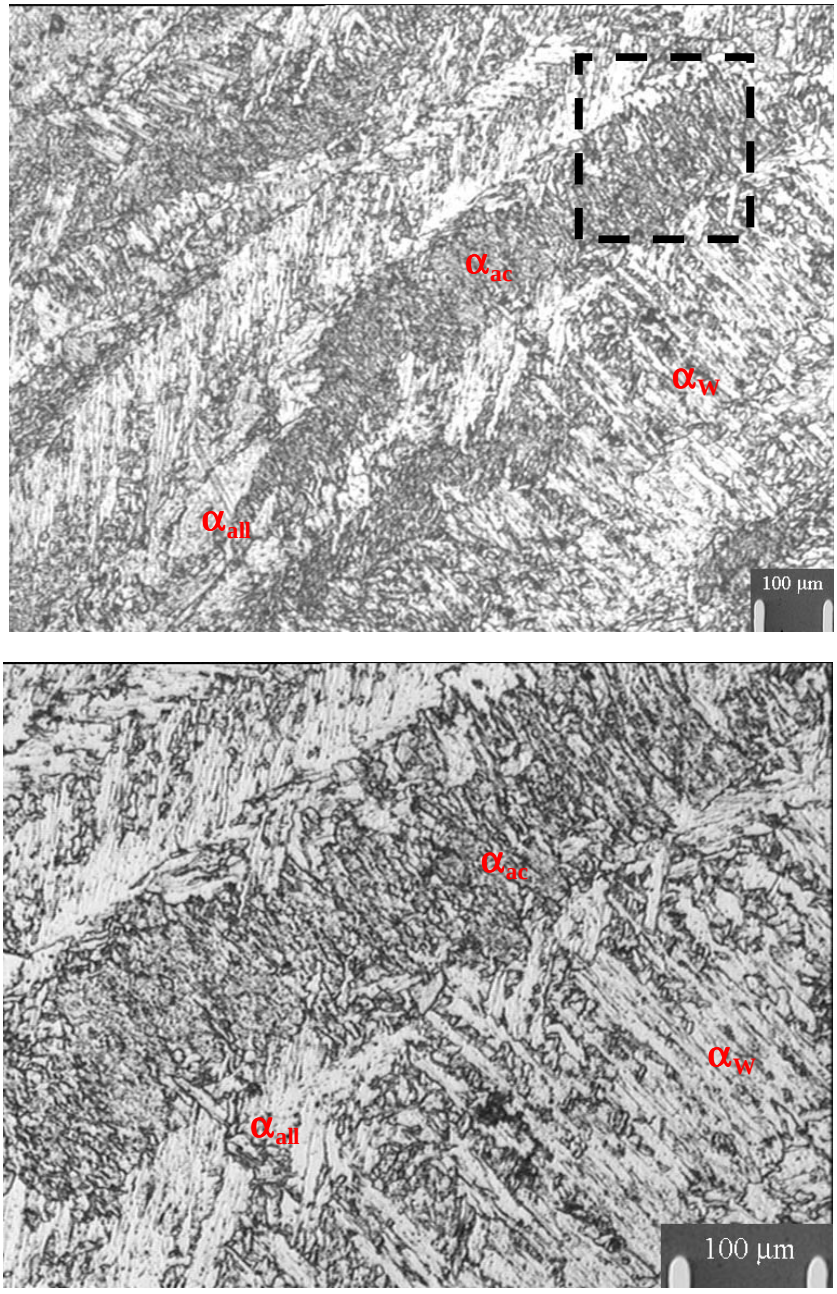

α_{ac} Acicular ferrite
α_{W} Widmanstätten ferrite
α_{all} Allotriomorphic ferrite

Figure 5.10 - Backscatter SEM images of Weld N°2 inclusions for (a) ADAR; (b) RHAR; (c) AD5%SA and (d) RH5%SA.

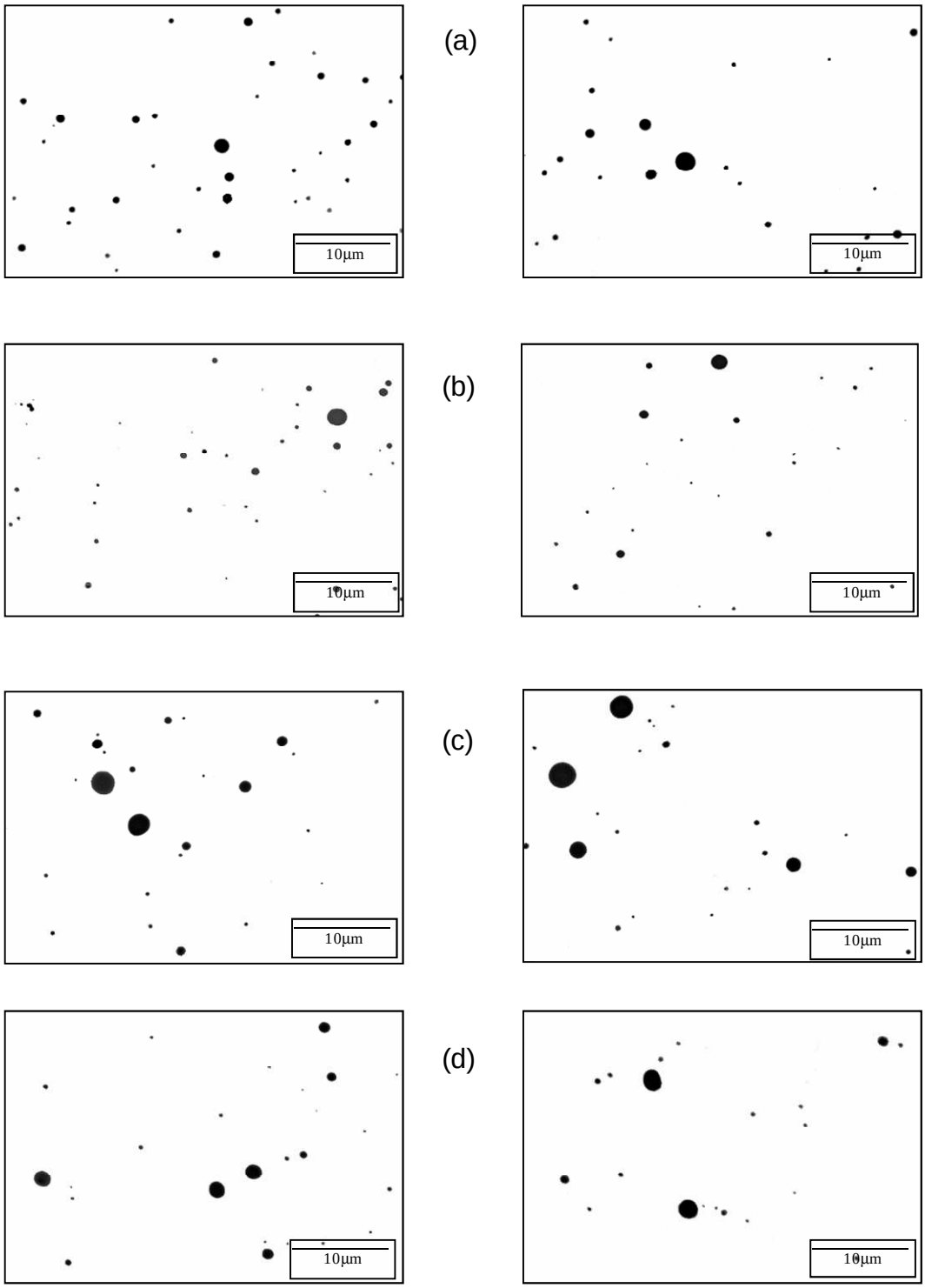

Figure 5.11 -Two - Dimensional weld inclusion size distribution.

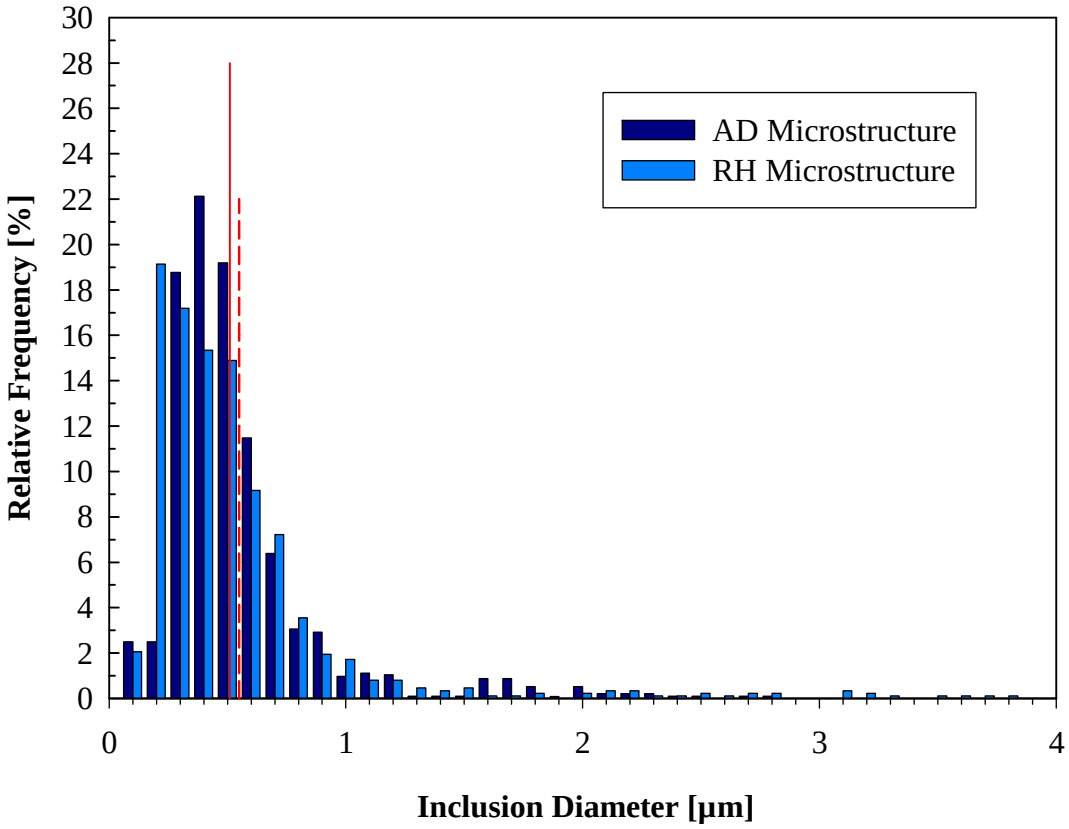

Figure 5.12 - Typical EDX Spectra from inclusion on the fracture surfaces for Weld N^{o}2 AD microstructural condition.

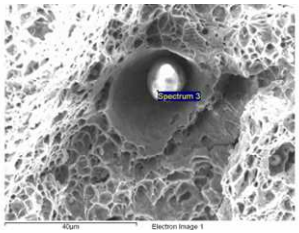

Inclusion diameter <3µm

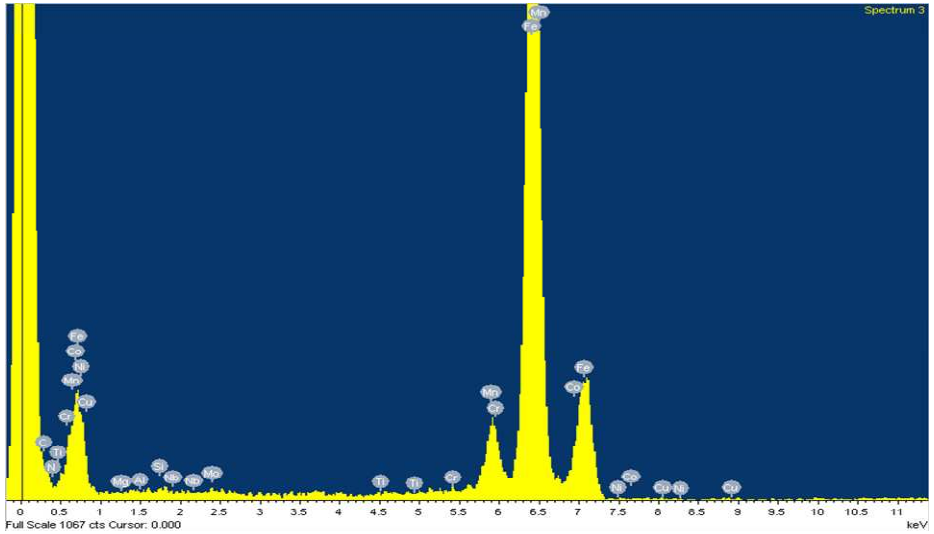

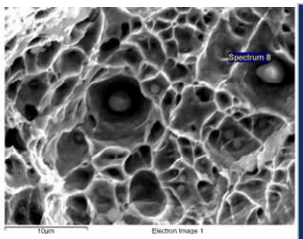

Inclusion diameter <2µm

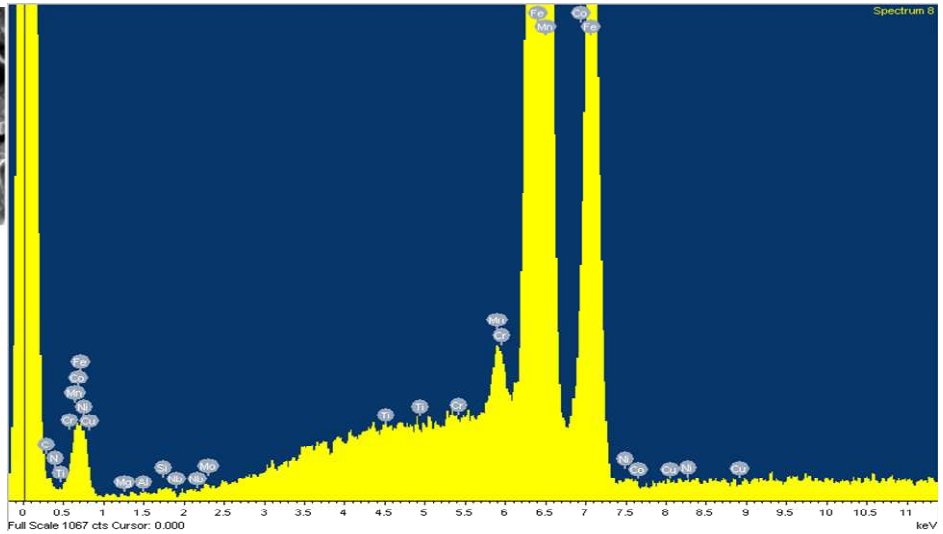

Figure 5.12 - Typical EDX Spectra from inclusion on the fracture surfaces for Weld N^{o}2 AD microstructural condition.

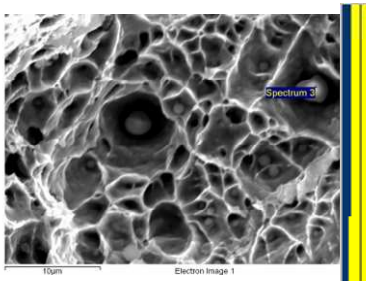

Inclusion diameter <1µm

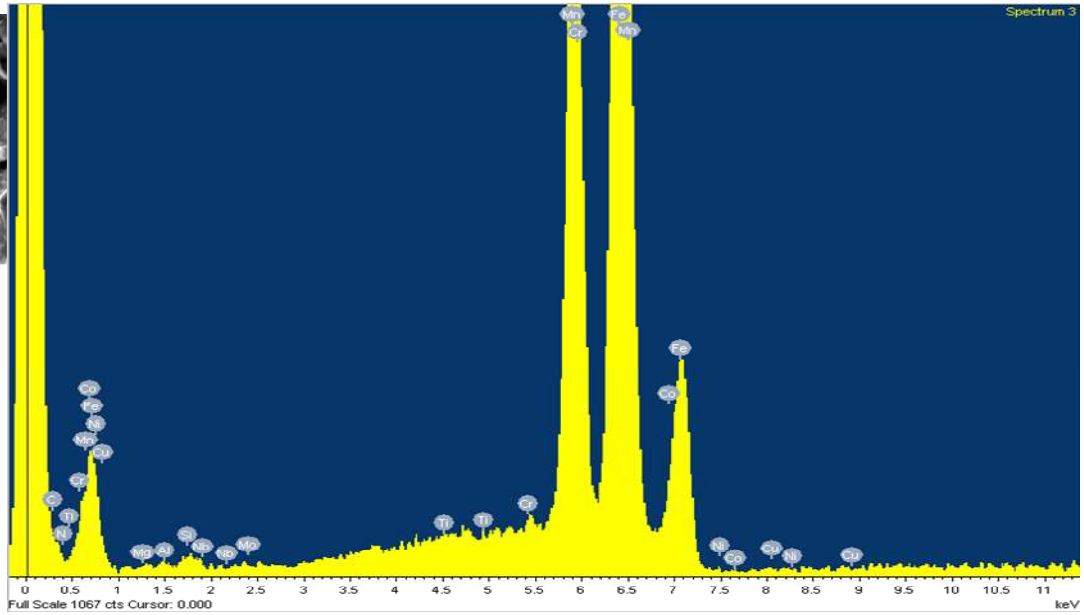

Figure 5.13 - Typical EDX Spectra from inclusion on the fracture surfaces for Weld N°2 RH microstructural condition.

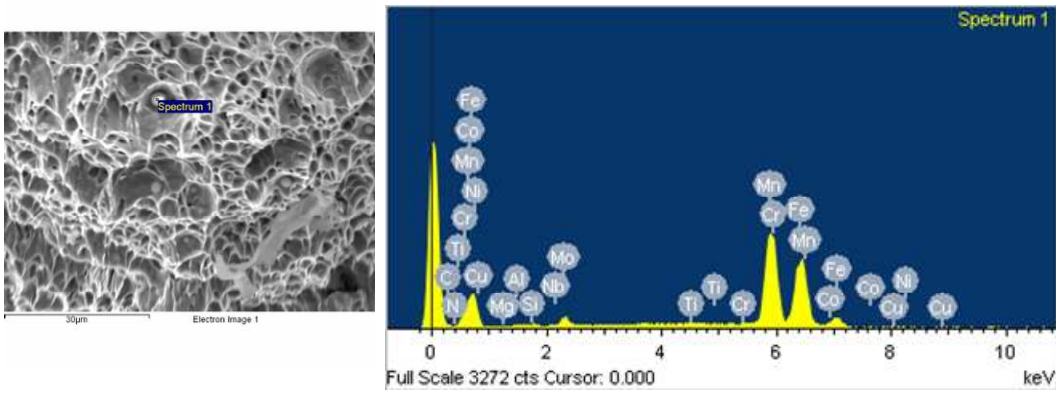

Inclusion diameter <3µm

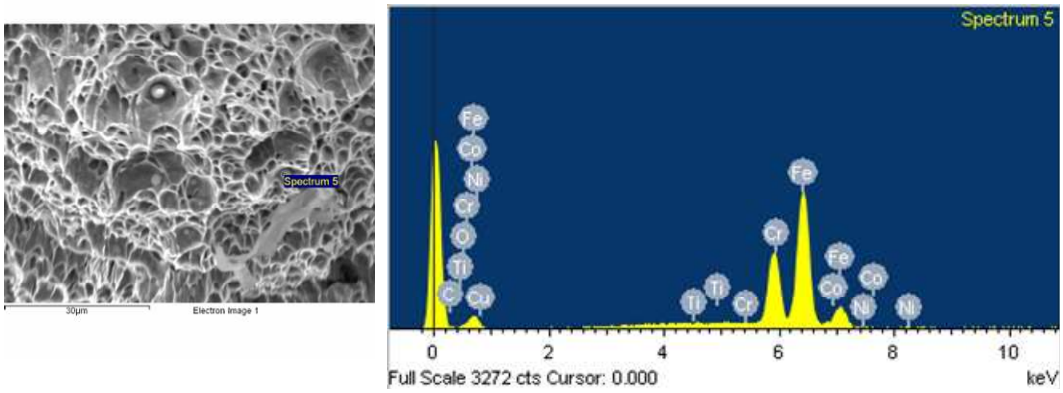

Inclusion diameter <2µm

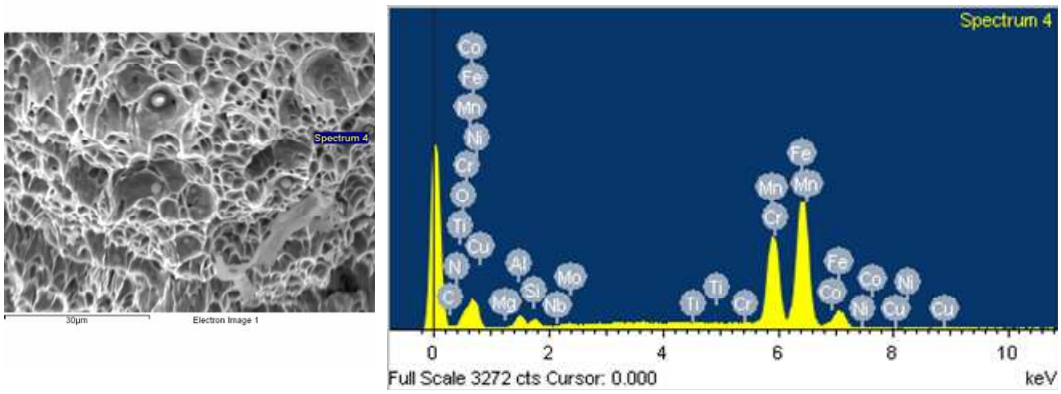

Inclusion diameter <1µm

Figure 5.14 - Typical EDX Spectra from inclusion on the fracture surfaces for Weld N°2 AD5%SA microstructural condition.

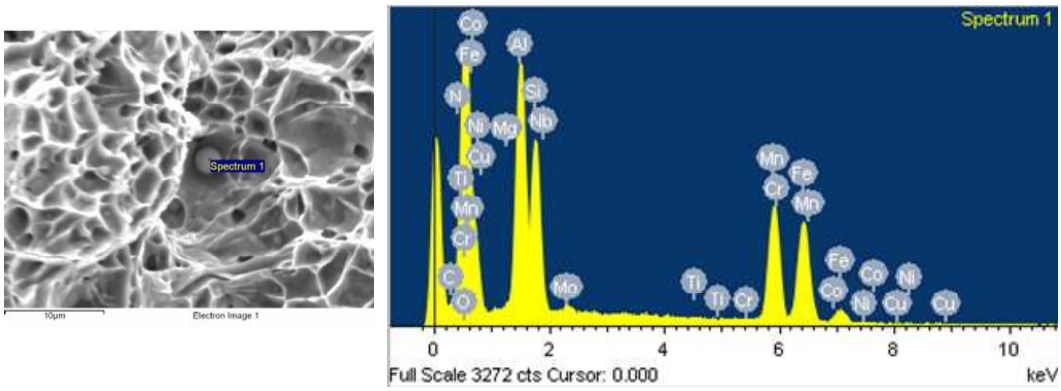

Inclusion diameter <3µm

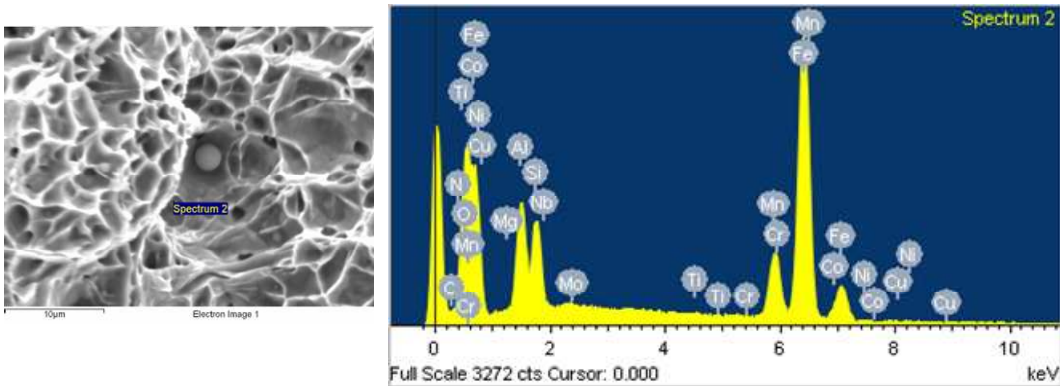

Inclusion diameter <2µm

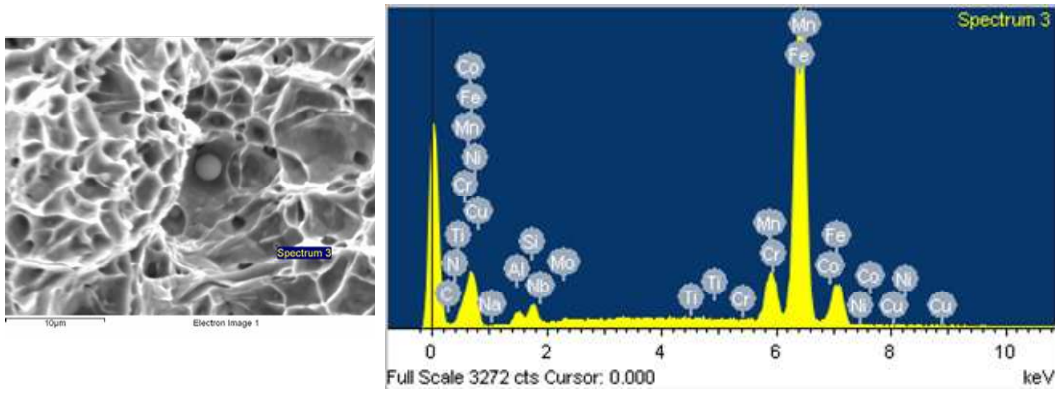

Inclusion diameter <1µm

Figure 5.15 - Typical EDX Spectra from inclusion on the fracture surfaces for Weld N^{o}2 RH5%SA microstructural condition.

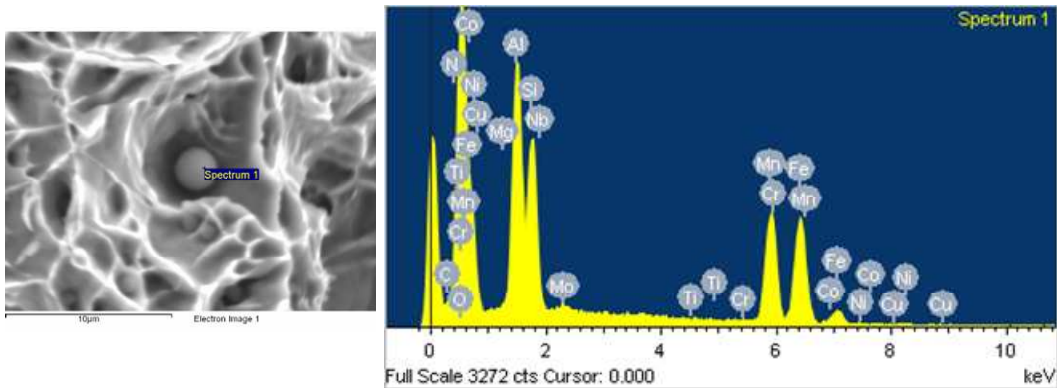

Inclusion diameter <3µm

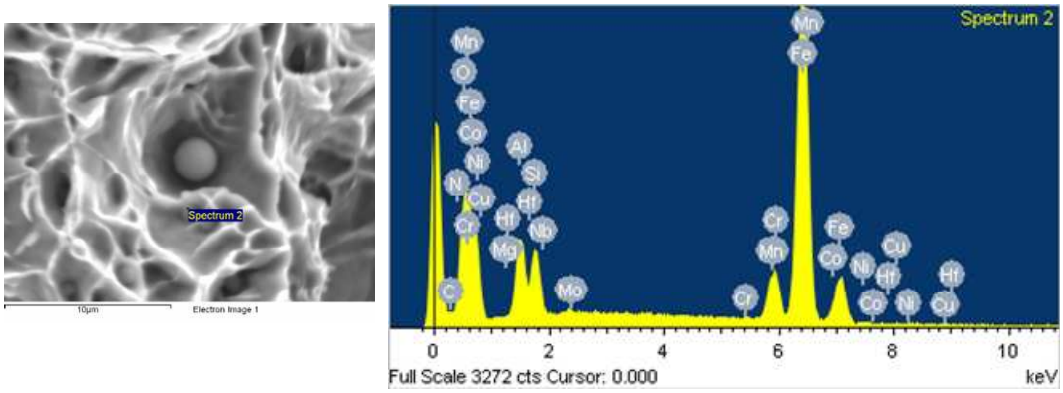

Inclusion diameter <2µm

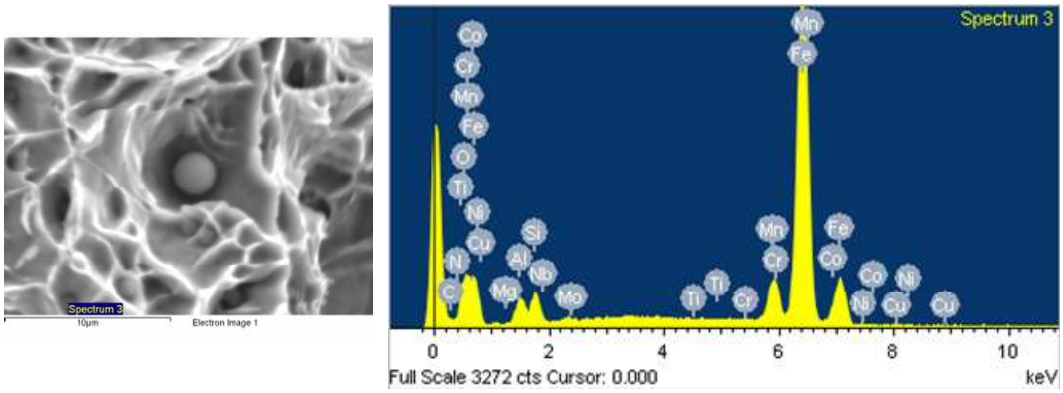

Inclusion diameter <1µm

Figure 5.16 - Glow Discharge Spectroscopy (GDS) for Weld N°1. (a) Parent Plate Material, (b) HAZ (c) Weld Material.

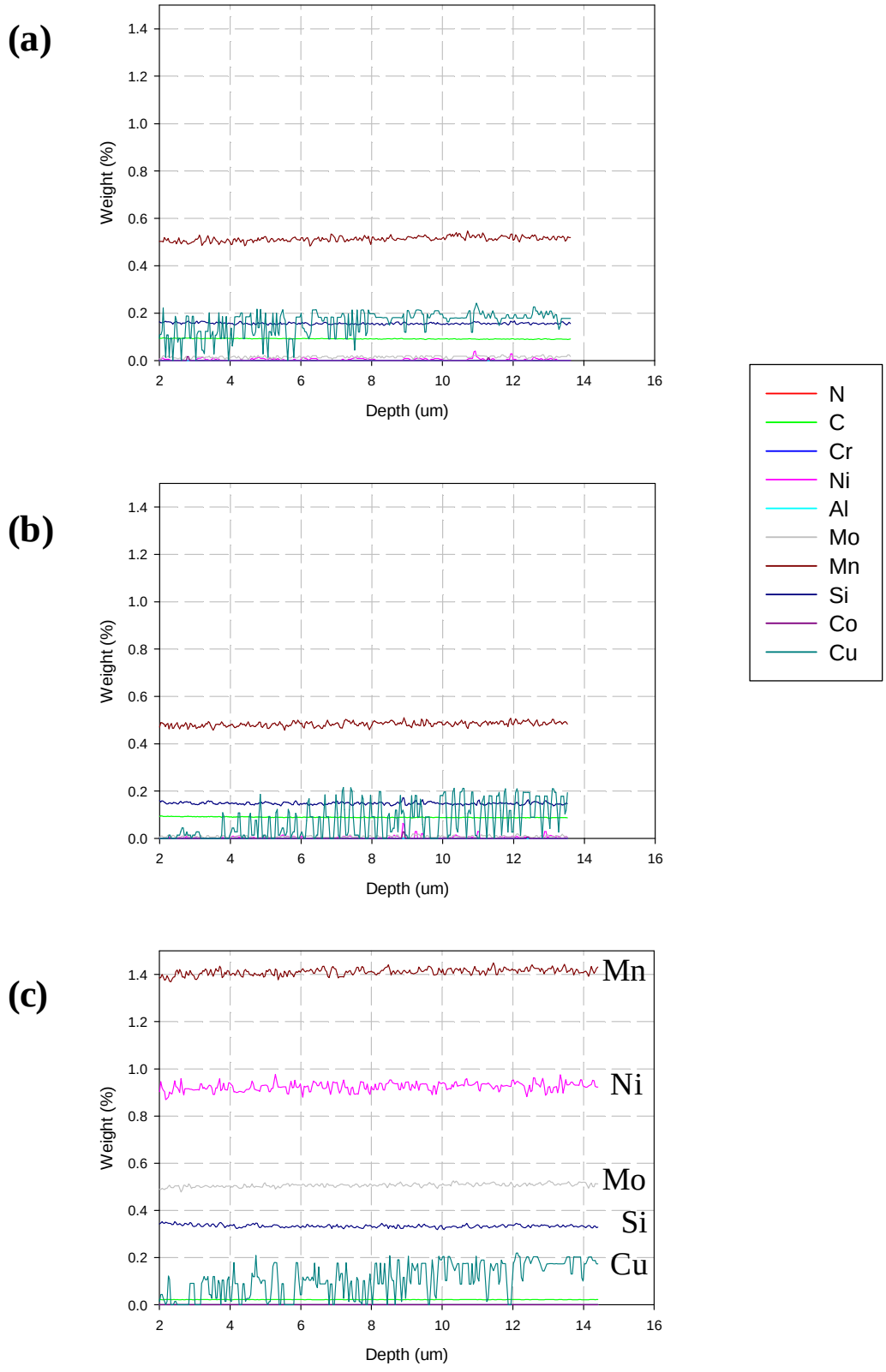

Figure 5.17 - Glow Discharge Spectroscopy (GDS) for Weld N°2. (a) Parent Plate Material, (b) HAZ (c) Weld Material.

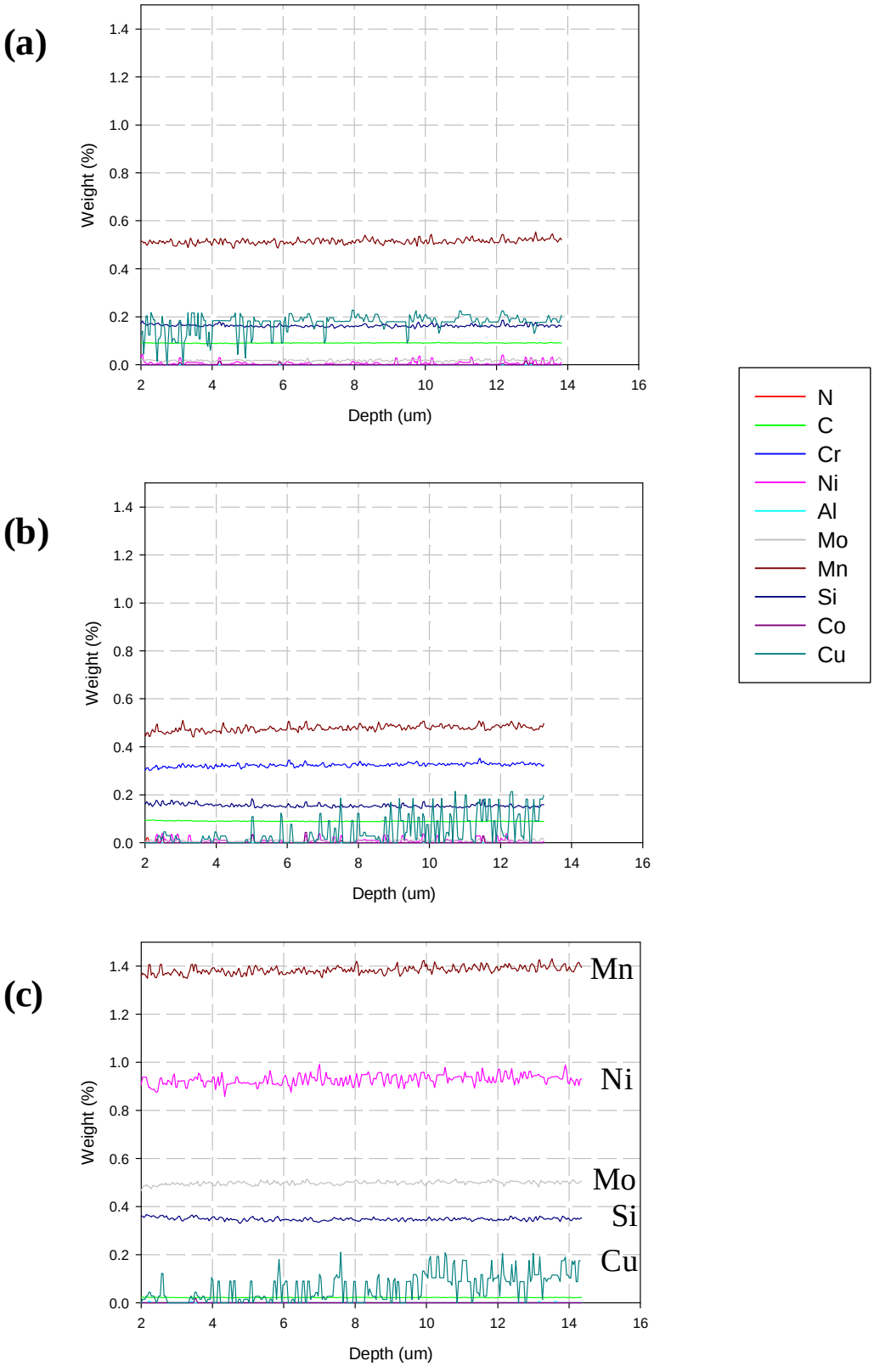

Figure 5.18 - Hardness profiles for both Weld N°1 and Weld N°2 in both weld metal conditions, AR and 5%SA for Line 1.

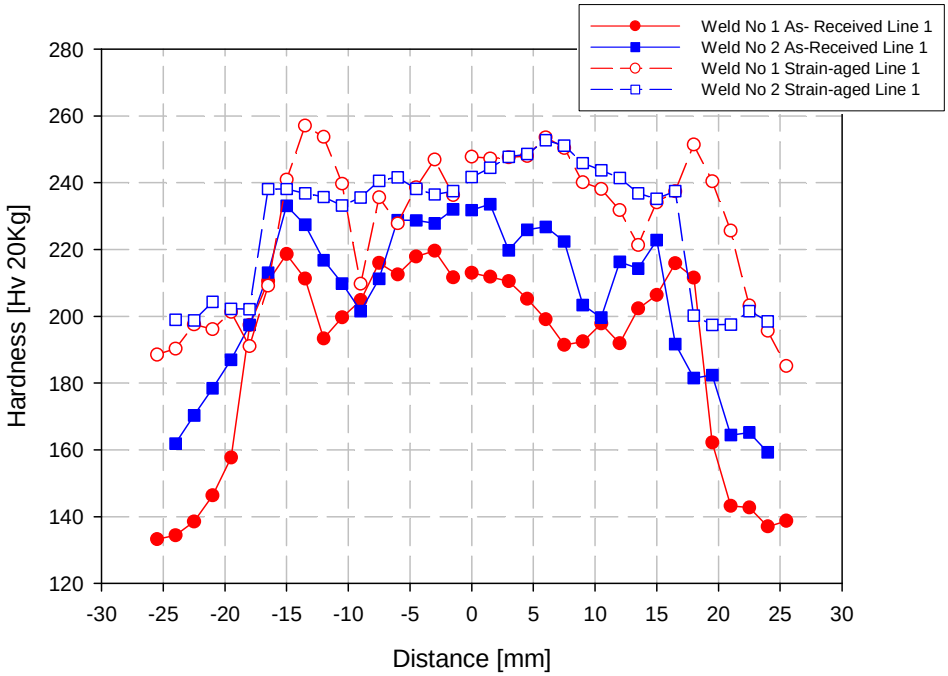

Figure 5.19 - Hardness profiles for both Weld N°1 and Weld N°2 in both weld metal conditions, AR and 5%SA for Line 2.

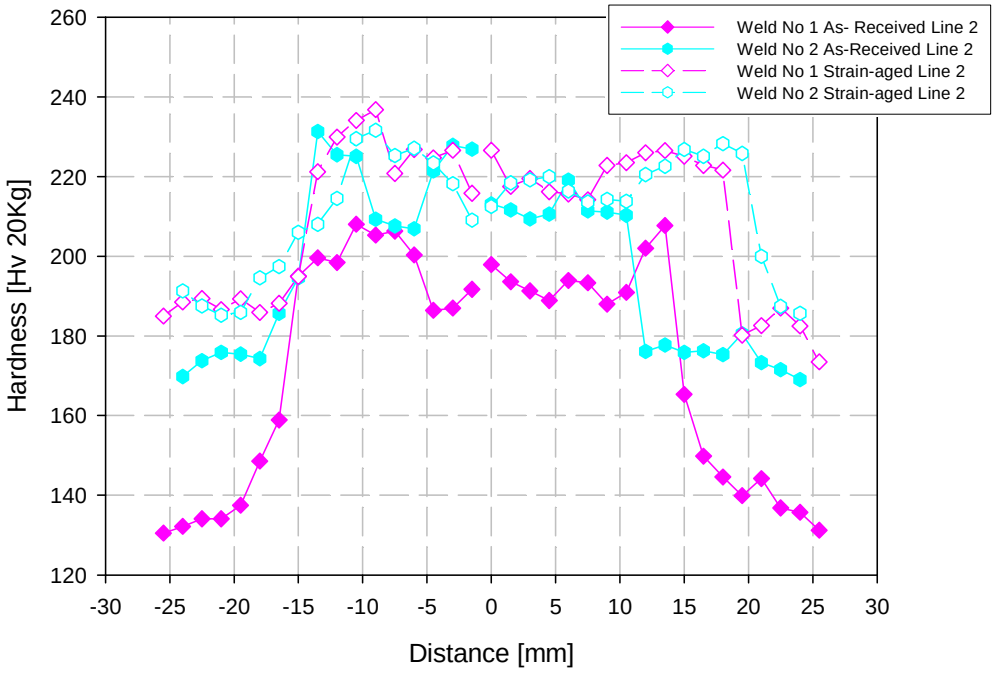

Figure 5.20 - Hardness profiles for both Weld N°1 and Weld N°2 in both weld metal conditions, AR and 5%SA for Line 3.

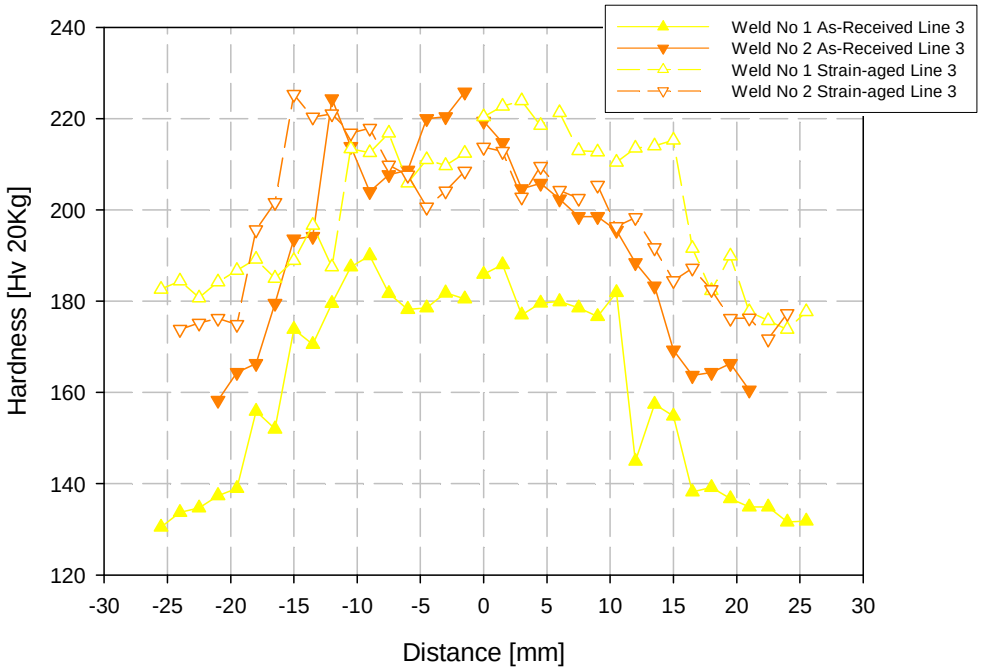

Figure 5.21 - Average hardness values for parent plate, as-deposited and reheated microstructures for both Weld N°1 and Weld N°2 in both weld metal conditions, AR and 5%SA.

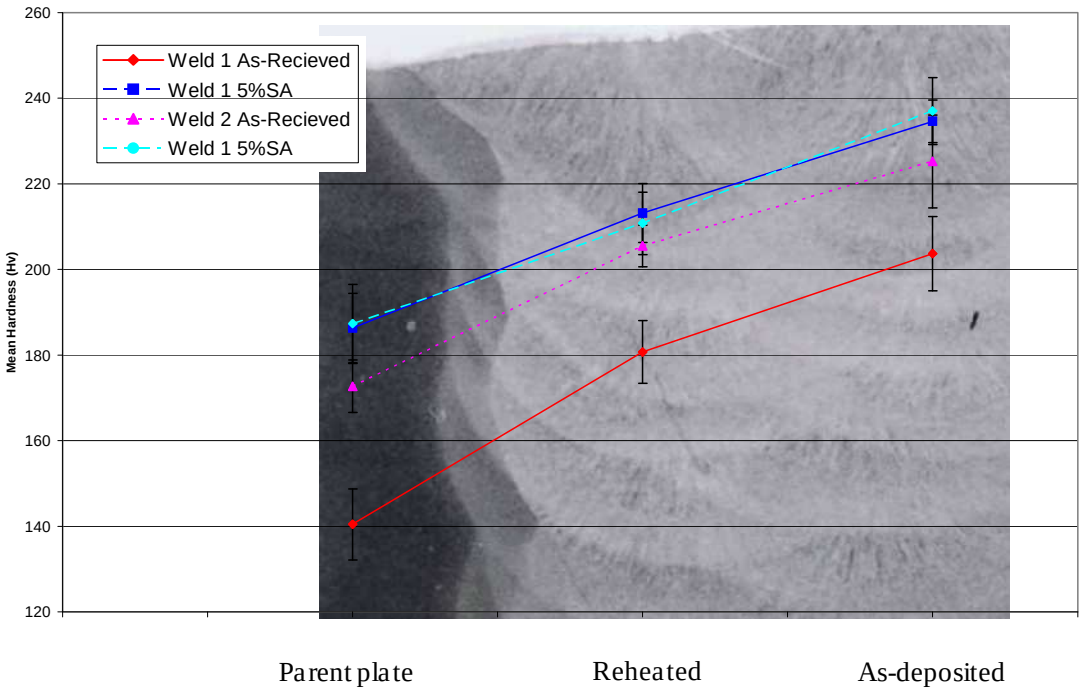

Figure 5.22 - Macrohardness indentations for ADAR, RHAR, AD5%SA and RH5%SA weld conditions.

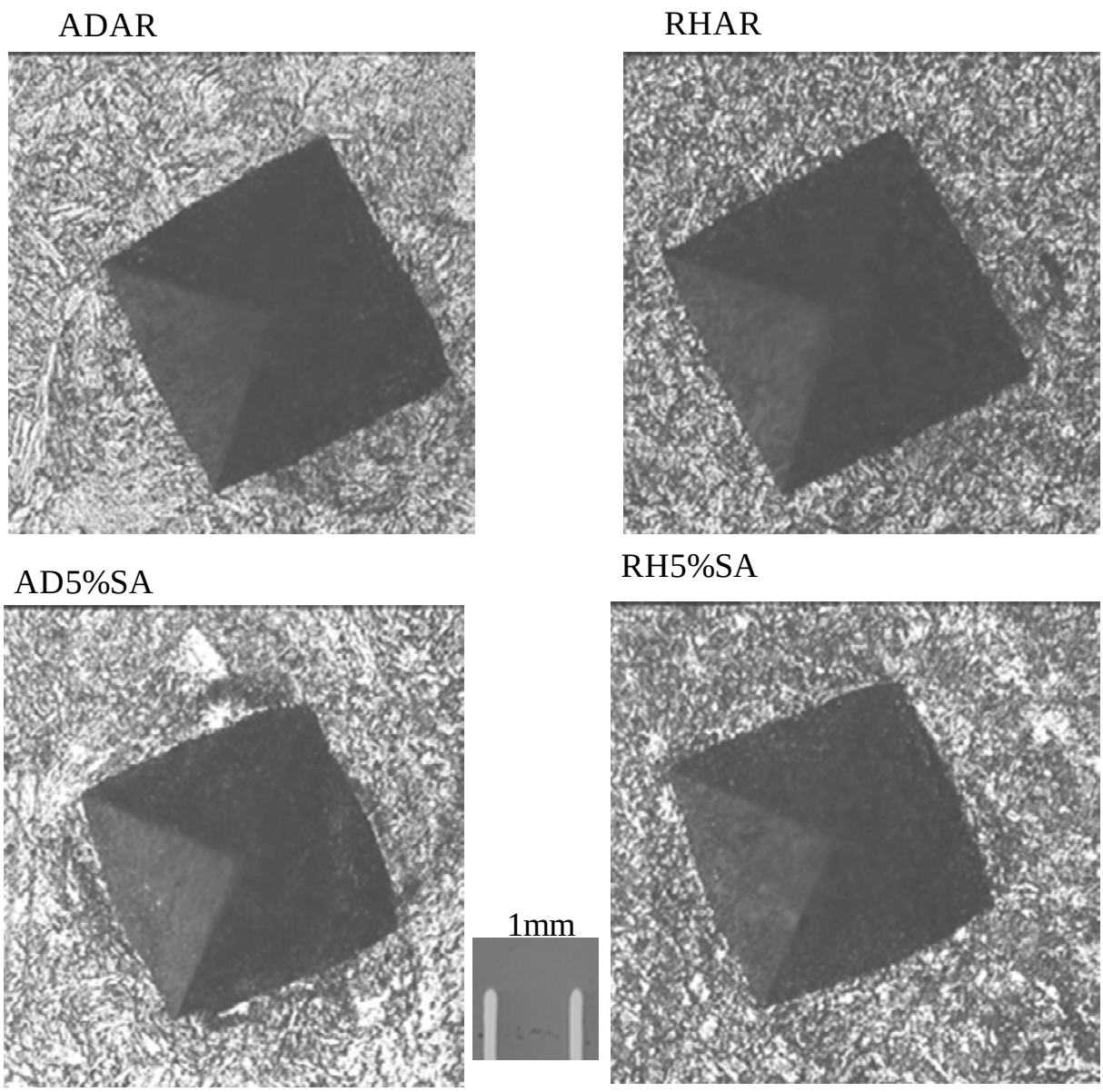

Figure 5.23 - Microhardness profiles for Weld N°1 for both microstructural conditions, AD and RH and in both weld metal conditions, AR and 5%SA.

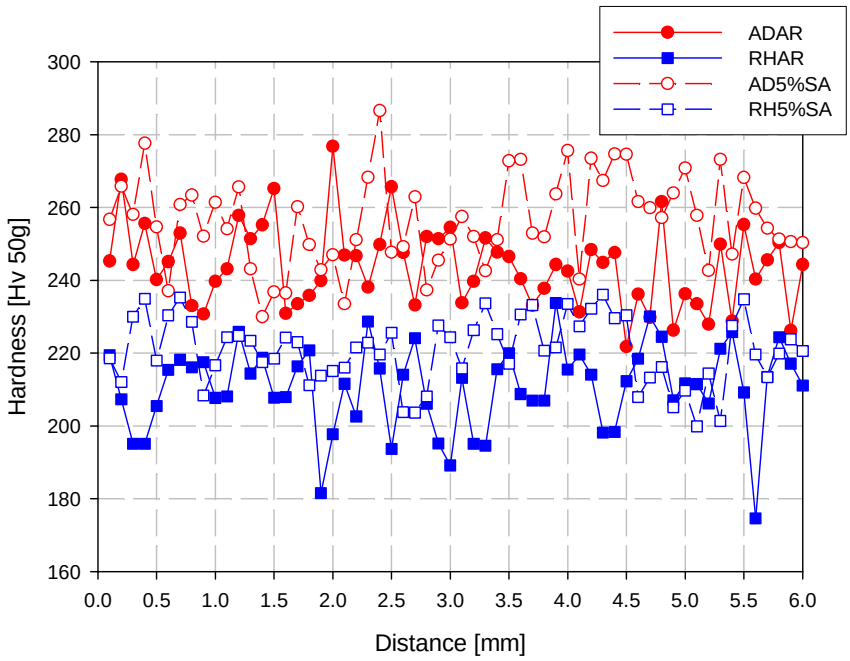

Figure 5.24 - Microhardness profiles for Weld N°2 for both microstructural conditions, AD and RH and in both weld metal conditions, AR and 5%SA.

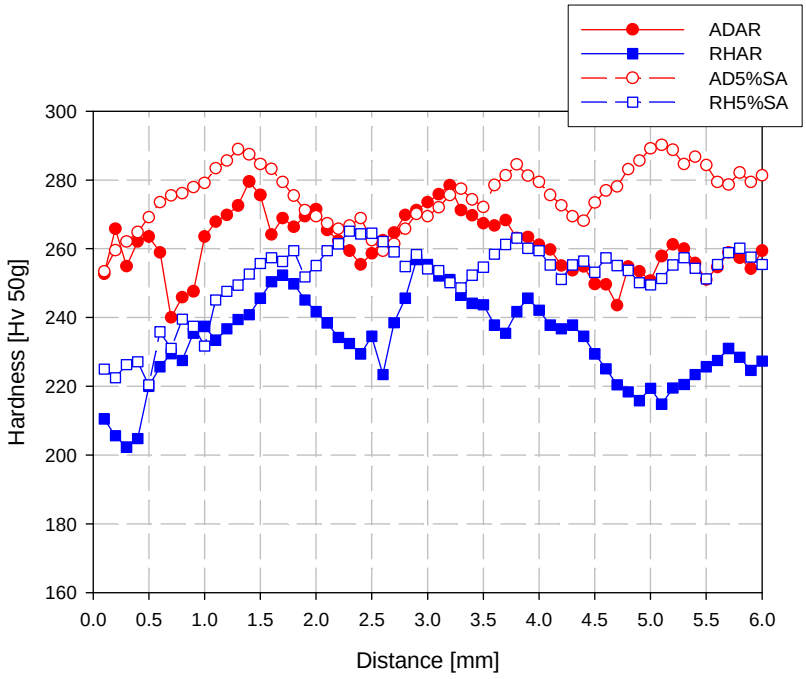

Figure 5.25 - Microhardness indentations for ADAR, RHAR, AD5%SA and RH5%SA weld conditions.

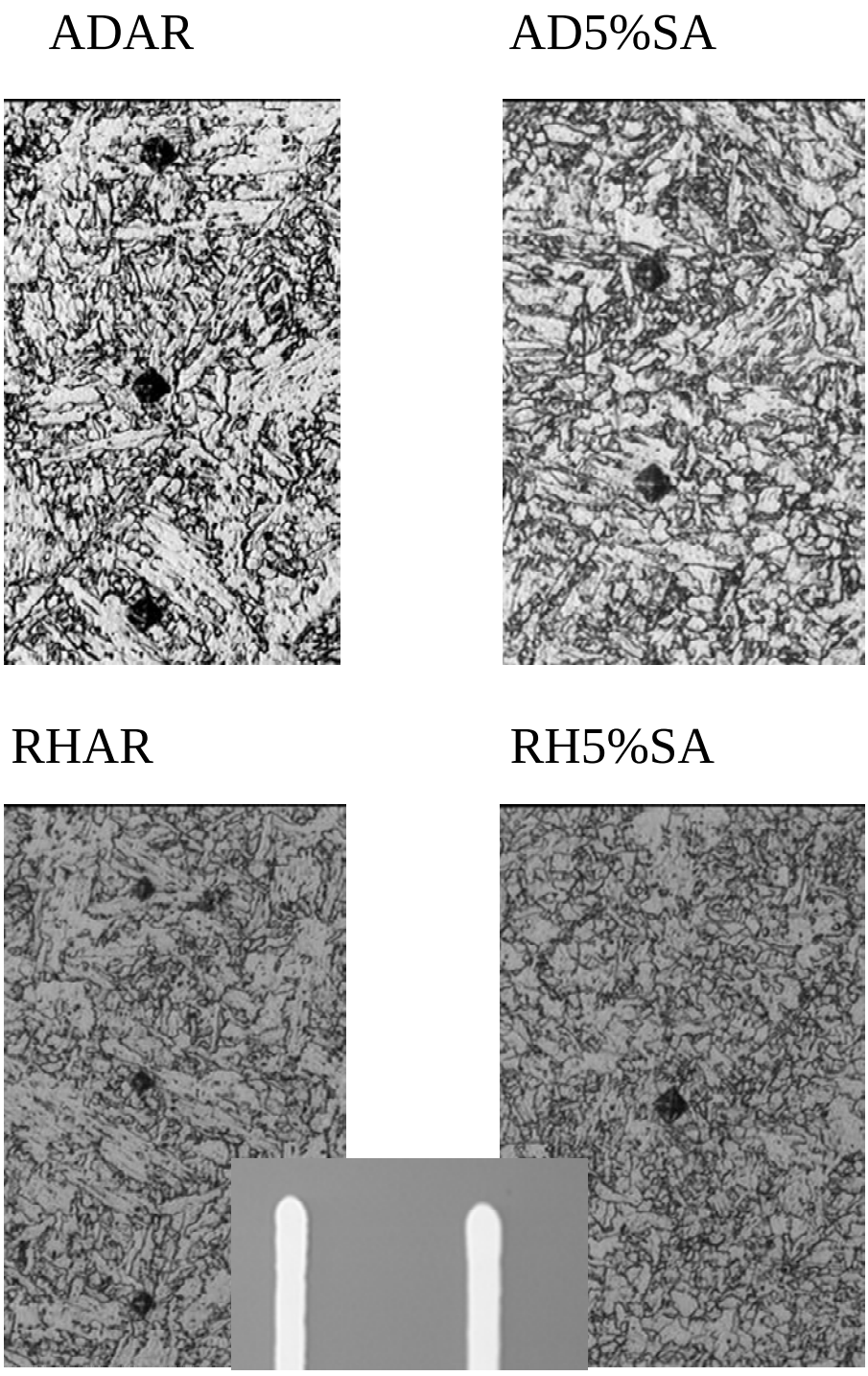

Table 6.1 - Flow Properties, Yield Stress, Ultimate Tensile Stress and Work Hardening Exponent, *n*, for Weld N^{o}1 for the as-deposited as-received microstructural condition.

Specimen	Teperature ^{o}C	Upper Yield MPa	Lower Yield MPa	0.2% Proof Stress MPa	UTS MPa	Elastic Strain %	Total Strain %	*n*	k
7	-196			892	909	10.23	12.41	0.07	1138.68
8	-196			860	860	0.29	7.70	0.01	923.94
9	-196			810	803	0.21	6.99	0.01	534.77
13	-160	6534	646		728	10.05	21.89	0.14	1091.54
14	-120	582	579		672	12.30	25.24	0.14	1000.59
15	-120			506	621	11.47	22.85	0.17	988.96
19	-100	515	511		628	11.82	23.39	0.16	970.20
20	-100	504	500		605	12.44	24.27	0.15	923.87
25	-80	486	479		596	12.92	24.59	0.16	931.41
21	-80			469	566	13.43	24.93	0.19	942.30
26	-60			454	576	11.91	23.57	0.17	927.21
30	-40			479	559	12.06	26.39	0.15	864.00
31	-40			497	588	10.74	23.84	0.14	883.86
36	-20			442	543	11.96	24.35	0.17	878.30
32	-20	475	472		581	12.02	26.07	0.17	924.34
38	20			464	559	9.60	22.63	0.13	771.95
2	20			475	570	11.41	25.93	0.17	925.85
1	20			475	566	12.42	26.46	0.19	948.86
3	20			480	570	12.78	25.46	0.18	941.00

Table 6.2 - Flow Properties, Yield Stress, Ultimate Tensile Stress and Work Hardening Exponent, *n*, for Weld N°1 for the reheated as-received microstructural condition.

Specimen	Teperature °C	Upper Yield MPa	Lower Yield MPa	0.2% Proof Stress MPa	UTS MPa	Elastic Strain %	Total Strain %	*n*	K
11	-196			771	791	17.11	37.59	0.08	1049.22
12	-196	803	754		788	0.20	26.55	0.09	1033.91
10	-160	630	592		690	14.69	26.59	0.14	1023.57
16	-120	508	491		621	15.92	28.43	0.16	965.50
18	-100	533	504		628	14.52	28.25	0.14	933.86
22	-100	449	445		577	14.67	27.55	0.17	913.41
23	-80	513	475		603	18.22	29.57	0.18	959.94
24	-80			468	566	10.11	27.73	0.14	844.10
28	-60			468	533	11.74	26.78	0.12	774.99
29	-60	436	434		555	14.60	26.47	0.20	540.00
33	-40	468	429		557	15.19	29.25	0.18	530.00
34	-40	443	435		555	15.08	31.03	0.19	535.00
35	-20	431	410		521	16.14	35.95	0.17	500.00
4	20	427	411		515	20.03	36.01	0.20	495.00
5	20	417	411		515	19.49	35.72	0.20	500.00
39	20	412	410		510	16.09	32.05	0.17	500.00
6	20			506	525	9.72	24.92	0.08	692.18

Table 6.3 - Flow Properties, Yield Stress, Ultimate Tensile Stress and Work Hardening Exponent, *n*, for Weld N^{o}1 for the mixed microstructural as-received condition.

Specimen	Teperature ^{o}C	Upper Yield MPa	Lower Yield MPa	0.2% Proof Stress MPa	UTS MPa	Elastic Strain %	Total Strain %	*n*	k
2	-196	742	718		814	5.98	12.65	0.14	1232.91
3	-160	670	623		706	9.62	22.20	0.14	991.22
11	-160	559	539		649	9.83	21.77	0.16	1033.24
4	-130	586	571		686	10.82	22.63	0.19	1159.25
12	-120	588	556		680	11.25	25.29	0.18	1116.02
5	-100	458	437		576	14.21	23.25	0.19	928.99
13	-100	457	433		5423	11.06	22.62	0.17	864.12
7	-80	535	512		624	13.60	26.21	0.18	1027.06
6	-60	503	459		580	14.61	31.73	0.19	959.14
14	-60	507	488		606	14.42	27.54	0.19	997.43
8	-40	492	427		584	10.49	25.48	0.19	933.58
15	-40	502	474		591	14.31	30.88	0.21	1032.88
9	-20	4780	441		556	14.11	30.44	0.19	923.03
1	20	426	420		525	13.02	28.98	0.19	883.43
10	20	461	441		535	10.67	23.84	0.11	744.78

Table 6.4 - Flow Properties, Yield Stress, Ultimate Tensile Stress and Work Hardening Exponent, *n*, for Weld N^{o}1 for the transverse microstructural as-received condition.

Specimen	Teperature ^{o}C	Upper Yield MPa	Lower Yield MPa	0.2% Proof Stress MPa	UTS MPa	Elastic Strain %	Total Strain %	*n*	k
1	-196	802	782		830	11.37	20.89	011	1183.15
3	-196	822	795		832	13.62	26.13	0.13	1221.05
4	-160	752	712		792	15.04	24.69	0.14	1191.83
5	-160	683	680		785	14.10	24.93	0.17	1245.23
6	-120	700	697		788	7.93	20.95	0.14	1178.92
7	-120	664	643		748	13.65	24.81	0.16	1166.24
8	-100			664	699	9.70	20.68	0.08	932.57
9	-100	592	590		709	12.77	23.04	0.17	1135.58
10	-80	597	561		699	13.27	22.45	0.16	1069.77
11	-80	566	551		672	14.19	25.07	0.18	1109.87
12	-60	533	530		650	15.71	28.21	0.21	1137.14
13	-60	535	525		644	13.23	24.77	0.18	1070.52
14	-40	510	500		619	11.69	23.28	0.20	1079.35
2	-40			534	645	15.57	26.71	0.20	1107.96
15	-20	514	506		621	13.83	27.68	0.20	1077.19
16	-20	512	505		610	12.40	24.02	0.19	1028.25
17	20	520	515		614	17.57	32.25	0.24	1121.94
18	20	477	468		568	13.63	26.74	0.20	972.45

Table 6.5 - Flow Properties, Yield Stress, Ultimate Tensile Stress and Work Hardening Exponent, *n*, for Weld N^{o}2 for the as-deposited as-received microstructural condition.

Specimen	Teperature ^{o}C	Upper Yield MPa	Lower Yield MPa	0.2% Proof Stress MPa	UTS MPa	Elastic Strain %	Total Strain %	*n*	K
3	-196			863	922	7.53	9.43	0.12	1327.17
6	-196			882	906	3.01	4.88	0.09	1270.23
7	-160			752	869	9.37	16.32	0.17	1435.96
8	-160			819	835	5.85	16.69	0.07	1076.76
12	-160			836	869	4.93	16.93	0.09	1179.99
34	-120			556	674	10.04	21.98	0.15	1059.34
35	-120			570	734	10.56	22.42	0.19	1255.61
14	-100			709	712	3.38	15.00	0.04	849.20
18	-100	592	570		687	10.71	23.31	0.16	1087.51
20	-80			537	658	11.18	29.53	0.20	1127.69
19	-80			595	738	9.69	22.83	0.19	1273.43
24	-60			523	661	11.84	30.41	0.20	1145.55
25	-60			531	667	10.19	22.52	0.20	1164.22
29	-40			468	628	11.85	24.63	0.23	1159.46
26	-40	514	506		623	14.30	28.68	0.21	1090.94
31	-20			497	610	9.45	22.63	0.18	1032.89
40	20			430	541	11.29	24.92	0.14	809.88
30	20			468	610	10.16	24.29	0.21	1086.42
2	20			490	588	11.03	24.79	0.17	969.00
1	20			525	610	7.82	20.02	0.15	970.36

Table 6.6 - Flow Properties, Yield Stress, Ultimate Tensile Stress and Work Hardening Exponent, *n*, for Weld N^{o}2 for the reheated as-received microstructural condition.

Specimen	Teperature ^{o}C	Upper Yield MPa	Lower Yield MPa	0.2% Proof Stress MPa	UTS MPa	Elastic Strain %	Total Strain %	*n*	K
10	-196			887	965	6.60	17.10	0.10	1351.76
9	-196	902	875		922	12.30	14.45	0.13	1367.85
42	-160	674	655		733	6.45	16.53	0.11	1053.85
15	-160			646	801	12.17	24.45	0.19	1345.35
43	-120	620	583		682	12.21	24.51	0.15	1060.34
22	-100	613	608		714	9.12	21.87	0.17	1164.40
21	-100			591	722	9.79	21.74	0.20	1260.69
27	-80			511	672	10.68	23.87	0.23	1243.15
23	-80	572	545		653	11.86	25.99	0.18	1078.61
28	-60	513	499		616	15.82	30.58	0.21	1068.63
32	-60			506	650	18.17	32.92	0.21	1135.16
33	-40	546	529		619	11.73	27.71	0.19	1035.57
37	-40			500	616	8.80	22.07	0.19	1076.57
41	-20			459	618	12.04	26.68	0.20	1064.82
38	-20			461	602	13.23	28.73	0.21	1072.83
4	20			456	554	14.25	28.74	0.19	922.18
5	20			464	545	10.57	25.23	0.17	898.37

Table 6.7 - Flow Properties, Yield Stress, Ultimate Tensile Stress and Work Hardening Exponent, *n*, for Weld N°2 for the mixed microstructural as-received condition.

Specimen	Teperature °C	Upper Yield MPa	Lower Yield MPa	0.2% Proof Stress MPa	UTS MPa	Elastic Strain %	Total Strain %	*n*	K
1	-196	732	711		762	11.17	23.29	0.12	1110.60
3	-196	857	842		873	2.79	4.93	0.11	1269.56
4	-160	716	685		768	8.01	18.90	0.13	1151.41
5	-160	701	680		758	7.69	18.86	0.13	1130.54
9	-120	591	573		701	11.11	24.69	0.18	1140.11
6	-120			590	729	8.92	20.53	0.19	1250.50
10	-100			546	722	11.30	24.55	0.21	1270.51
11	-100	538	525		667	13.44	28.02	0.20	1140.11
12	-80	490	468		576	11.28	26.16	0.15	1137.62
13	-80			546	700	12.40	24.32	0.19	1184.70
12	-80	490	468		576	11.28	26.16	0.15	869.45
15	-60	538	527		638	12.20	25.53	0.18	1041.01
16	-60	541	521		634	11.30	25.60	0.17	1012.40
14	-40	541	525		627	12.24	25.47	0.16	969.24
17	-40			546	683	13.34	26.38	0.18	1142.65
18	-20	512	482		590	11.93	26.33	0.17	958.31
8	20	533	530		601	7.29	20.47	0.07	766.70
2	20			444	627	6.80	18.00	0.10	885.25
7	20			520	633	7.52	21.05	0.14	984.93

Table 6.8 - Flow Properties, Yield Stress, Ultimate Tensile Stress and Work Hardening Exponent, *n*, for Weld N^{o}2 for the transverse microstructural as-received condition.

Specimen	Teperature ^{o}C	Upper Yield MPa	Lower Yield MPa	0.2% Proof Stress MPa	UTS MPa	Elastic Strain %	Total Strain %	*n*	K
3	-196			789	856	8.98	20.93	0.11	1202.45
4	-196			928	947	5.43	7.56	0.08	1251.41
6	-160			568	822	7.27	19.97	0.17	1328.08
7	-160			641	750	9.655	20.84	0.17	1225.54
5	-160			667	772	7.77	14.42	0.12	1125.11
8	-120			551	739	6.82	20.29	0.15	1167.16
10	-100			472	679	13.21	27.07	0.19	1128.91
9	-100	563	559		692	12.20	25.39	0.18	1139.44
12	-80			472	647	14.00	26.79	0.25	1237.64
11	-80			500	680	11.83	25.43	0.23	1255.08
14	-60			443	628	17.57	32.68	0.25	1191.37
13	-60			650	701	6.07	19.84	0.13	1077.44
17	-40			439	617	13.83	30.86	0.24	1151.43
16	-40			450	625	11.32	24.85	0.22	1138.15
18	-20			490	592	13.26	28.19	0.19	934.63
15	-20			511	614	9.91	22.77	0.18	1028.94
2	20			488	561	10.26	24.19	0.18	934.35
1	20			588	594	7.68	20.10	0.11	880.82

Table 6.9 - Flow Properties, Yield Stress, Ultimate Tensile Stress and Work Hardening Exponent, *n*, for Weld N^{o}2 for both the as-deposited and reheated microstructural as-received condition with a 5% pre-strain limit.

Specimen	Teperature ^{o}C	Condition	Displacment	0.2% Proof Stress MPa	UTS MPa	Elastic Strain %	Total Strain %
18	20	AD	0.70	415	526	4.75	5.02
15	20	AD	0.71	450	544	4.86	5.11
10	20	AD	0.70	455	534	4.76	5.00
3	20	AD	0.70	457	539	4.80	5.00
16	20	AD	0.69	460	581	4.66	4.93
12	20	AD	0.68	470	586	4.65	4.88
2	20	AD	0.69	475	547	4.55	4.90
14	20	AD	0.70	475	552	4.81	5.00
1	20	AD	0.68	600	601	0.05	4.86
17	20	RH	0.70	345	475	4.68	4.97
9	20	RH	0.70	400	528	4.71	4.98
4	20	RH	0.70	430	545	4.73	5.02
13	20	RH	0.71	460	540	4.54	5.11
5	20	RH	0.69	480	547	4.63	4.90
8	20	RH	0.70	490	546	4.80	5.02
6	20	RH	0.70	458/446*	528	4.69	4.95
7	20	RH	0.67	459/451*	522	4.54	4.78
11	20	RH	0.69	470/459*	535	4.75	4.95

*Upper and Lower yield was observed in these samples

Table 6.10 - Flow Properties, Yield Stress, Ultimate Tensile Stress and Work Hardening Exponent, *n*, for Weld N°2 for both the as-deposited and reheated microstructure, 5%SA condition.

Specimen	Teperature °C	Condition	Upper Yield MPa	Lower Yield MPa	0.2% Proof Stress MPa	UTS MPa	*n*	Elastic Strain %	Total Strain %
3	-196	AD	885	881		885		14.35	0.33
18	-160	AD			745	774	0.09	18.04	5.91
12	-120	AD	781	745		782		24.37	0.94
16	-100	AD	712	690		719	0.11	13.91	4.90
10	-80	AD	533	501		537	0.08	24.65	9.86
14	-80	AD	666	650		686	0.10	26.88	10.32
1	-60	AD	659	636		659		11.65	0.88
2	-20	AD	628	608		635	0.12	20.44	8.41
15	20	AD	592	585		613	0.11	17.88	6.76
4	-196	RH	987	931		987		21.36	0.99
17	-160	RH	703	672		706	0.12	18.85	6.29
13	-120	RH	767	716		767		26.14	0.85
8	-100	RH			690	722	0.10	21.17	8.92
7	-60	RH	661	621		661	0.13	27.19	12.57
9	-40	RH	619	607		654	0.13	27.52	9.98
6	-40	RH	621	613		655	0.12	25.85	11.24
11	-20	RH	635	613		643	0.09	21.69	8.54
5	20	RH	601	581		602	0.10	20.54	6.10

Table 6.11 - Impact results for Weld N°2 for the ADAR microstructural condition.

Spec. No	Test Temp.(°C)	Absorbed Energy (J)	Mean Energy (J)
Ch 15	-196	3	3
Ch 25	-100	4	4
Ch 21	-80	17	
Ch 19	-80	18	17
Ch 31	-60	19	
Ch 33	-60	21	19
Ch 23	-40	10	
Ch 17	-40	12	
Ch 35	-40	23	
Ch 37	-40	30	10
Ch 29	-29	11	
Ch 27	-29	16	11
Ch 11	-17	31	
Ch 1	-17	35	
Ch 13	-17	35	31
Ch 39	0	48	48
Ch 7	20	77	
Ch 9	20	78	77
Ch 5*	40	109	109
Ch 3	100	127	127
Ch 43*	120	129	
Ch 44*	120	131	129
Ch 46*	140	132	
Ch 47*	140	137	132
Ch 49*	160	142	
Ch 51*	160	139	142
Ch 53*	180	141	141
Ch 55*	200	143	143

* Specimen did not break

Table 6.12 - Impact results for Weld N^{o}2 for the RHAR microstructural condition.

Spec. No	Test Temp.(^{o}C)	Absorbed Energy (J)	Mean Energy (J)
Ch 16	-196	4	4
Ch 24	-100	6	6
Ch 20	-80	26	
Ch 22	-80	29	26
Ch 32	-60	38	
Ch 34	-60	44	38
Ch 26	-40	42	
Ch 18	-40	56	
Ch 36	-40	61	42
Ch 30	-29	47	
Ch 28	-29	52	47
Ch 12*	-17	59	
Ch 14	-17	62	
Ch 38	-17	75	59
Ch 40	0	100	100
Ch 10	20	121	
Ch 8	20	130	121
Ch 6*	40	145	145
Ch 2*	100	144	
Ch 4*	100	148	144
Ch 42*	120	151	
Ch 45*	120	155	151
Ch 48*	140	156	
Ch 50*	140	159	156
Ch 52*	160	157	
Ch 54*	160	161	157
Ch 56*	180	167	167
Ch 57*	200	162	162

* Specimen did not break

Table 6.13 - Impact results for Weld N°2 for the AD5%SA microstructural condition.

Spec. No	Test Temp.(°C)	Absorbed Energy (J)	Mean Energy (J)
Ch 33	-196	2	2
Ch 39	-100	3	3
Ch 11	-80	4	
Ch 31	-80	4	4
Ch 15	-60	6	
Ch 21	-60	6	6
Ch 25	-40	11	
Ch 29	-40	12	11
Ch 1	-20	20	
Ch 3	-20	18	20
Ch 27	0	32	32
Ch 9	20	41	
Ch 13	20	33	41
Ch 19	40	80	
Ch 23	40	78	80
Ch 35*	60	90	
Ch 37	60	82	90
Ch 5*	100	96	96
Ch 17*	140	102	102
Ch 7*	180	105	105

* Specimen did not break

Table 6.14 - Impact results for Weld N°2 for the RH5%SA microstructural condition.

Spec. No	Test Temp.(°C)	Absorbed Energy (J)	Mean Energy (J)
Ch 34	-196	2	2
Ch 18	-100	5	5
Ch 16	-80	12	
Ch 40	-80	10	12
Ch 12	-60	16	
Ch 32	-60	22	16
Ch 26	-40	32	
Ch 30	-40	24	32
Ch 2	-20	52	
Ch 4	-20	46	52
Ch 28	0	69	69
Ch 8	20	86	
Ch 14	20	83	86
Ch 20	40	102	
Ch 24*	40	118	102
Ch 36*	60	121	
Ch 38*	60	132	121
Ch 6	100	130	130
Ch 22*	140	139	139
Ch 10*	180	140	140

* Specimen did not break

Table 6.15 - Summary of results for the change in temperature at 40 (J), change in absorbed energy at 40°C and the USE level for the four microstructural conditions.

Microstructual Condition	Temperature change (°C) at 40 J	Temperature change (°C)	Absorbed Energy change (J) at 40°C	Absorbed Energy (J) difference	USE level (J)	USE level difference (J)
ADAR	-10	45	105	32	138	20
RHAR	-55		137		158	
AD5%SA	10	40	70	40	105	35
RH5%SA	-30		110		140	

Table 6.16 - Results from surface analysis of broken halves of Charpy specimens for Weld N^{o}2 in the ADAR microstructural condition. (a) ductile thumbnail, DT; (b) lateral expansion, LE; (c) crystalline area, CA.

Spec. No	Test Temp.(^{o}C)	Absorbed Energy (J)	DT (mm)	LE (mm)	CA (%)
Ch 15	-196	3	0.000	0.000	100
Ch 25	-100	4	0.000	0.000	100
Ch 21	-80	17	0.415	0.349	86
Ch 19	-80	18	0.511	0.423	85
Ch 31	-60	19	0.517	0.475	79
Ch 33	-60	21	0.622	0.521	77
Ch 23	-40	10	0.246	0.137	98
Ch 17	-40	12	0.423	0.283	95
Ch 35	-40	23	0.763	0.584	75
Ch 37	-40	30	0.993	0.525	68
Ch 29	-29	11	0.134	0.260	96
Ch 27	-29	16	0.340	0.291	85
Ch 11	-17	31	1.172	0.711	66
Ch 1	-17	35	1.381	0.623	57
Ch 13	-17	35	1.578	0.782	54
Ch 39	0	48	1.747	0.946	46
Ch 7	20	77	1.847	1.353	40
Ch 9	20	78	2.137	1.488	28
Ch 5*	40	109	2.365	1.743	7
Ch 3	100	127	NA	2.115	0
Ch 43*	120	129	NA	NA	NA
Ch 44*	120	131	NA	NA	NA
Ch 46*	140	132	NA	NA	NA
Ch 47*	140	137	NA	NA	NA
Ch 49*	160	142	NA	NA	NA
Ch 51*	160	139	NA	NA	NA
Ch 53*	180	141	NA	NA	NA
Ch 55*	200	143	NA	NA	NA

* Specimen did not break

Table 6.17 - Results from surface analysis of broken halves of Charpy specimens for Weld N^{o}2 in the RHAR microstructural condition. (a) ductile thumbnail, DT; (b) lateral expansion, LE; (c) crystalline area, CA.

Spec. No	Test Temp.(^{o}C)	Absorbed Energy (J)	DT (mm)	LE (mm)	CA (%)
Ch 16	-196	4	0.000	NA	100
Ch 24	-100	6	0.236	NA	100
Ch 20	-80	26	0.494	NA	96
Ch 22	-80	29	0.577	NA	92
Ch 32	-60	38	0.715	0.245	84
Ch 34	-60	44	1.167	0.487	75
Ch 26	-40	42	0.934	0.569	79
Ch 18	-40	56	1.796	0.612	62
Ch 36	-40	61	1.836	0.846	46
Ch 30	-29	47	1.413	0.747	68
Ch 28	-29	52	1.848	1.357	76
Ch 12*	-17	59	2.146	1.749	59
Ch 14	-17	62	2.685	NA	44
Ch 38	-17	75	2.947	1.156	38
Ch 40	0	100	3.136	1.294	24
Ch 10	20	121	3.347	1.550	13
Ch 8	20	130	3.568	1.975	18
Ch 6*	40	145	NA	1.877	0
Ch 2*	100	144	NA	2.050	0
Ch 4*	100	148	NA	2.255	0
Ch 42*	120	151	NA	1.956	NA
Ch 45*	120	155	NA	2.510	NA
Ch 48*	140	156	NA	2.335	NA
Ch 50*	140	159	NA	NA	NA
Ch 52*	160	157	NA	NA	NA
Ch 54*	160	161	NA	NA	NA
Ch 56*	180	167	NA	NA	NA
Ch 57*	200	162	NA	NA	NA

* Specimen did not break

Table 6.18 - Results from surface analysis of broken halves of Charpy specimens for Weld N^{o}2 in the AD5%SA microstructural condition. (a) ductile thumbnail, DT; (b) lateral expansion, LE; (c) crystalline area, CA.

Spec. No	Test Temp.(^{o}C)	Absorbed Energy (J)	DT (mm)	LE (mm)	CA (%)
Ch 33	-196	2	0.000	0.000	100
Ch 39	-100	3	0.000	0.000	100
Ch 11	-80	4	0.110	0.000	100
Ch 31	-80	4	0.145	0.000	97
Ch 15	-60	6	0.315	0.000	92
Ch 21	-60	6	0.342	0.129	91
Ch 25	-40	11	0.578	0.000	89
Ch 29	-40	12	0.526	0.000	85
Ch 1	-20	20	0.636	0.531	75
Ch 3	-20	18	0.582	0.819	80
Ch 27	0	32	0.679	0.321	67
Ch 9	20	41	0.946	0.728	54
Ch 13	20	33	0.724	1.000	63
Ch 19	40	80	1.136	1.621	45
Ch 23	40	78	1.239	1.304	48
Ch 35*	60	90	1.315	2.373	0
Ch 37	60	82	NA	2.195	0
Ch 5*	100	96	NA	NA	0
Ch 17*	140	102	NA	NA	0
Ch 7*	180	105	NA	NA	0

* Specimen did not break

Table 6.19 - Results from surface analysis of broken halves of Charpy specimens for Weld N^{o}2 in the RH5%SA microstructural condition. (a) ductile thumbnail, DT; (b) lateral expansion, LE; (c) crystalline area, CA.

Spec. No	Test Temp.(^{o}C)	Absorbed Energy (J)	DT (mm)	LE (mm)	CA (%)
Ch 34	-196	2	0	0.000	100
Ch 18	-100	5	0.226	0.000	100
Ch 16	-80	12	0.457	0.375	97
Ch 40	-80	10	0.479	0.451	95
Ch 12	-60	16	0.525	0.678	87
Ch 32	-60	22	0.817	0.896	85
Ch 26	-40	32	0.835	0.925	76
Ch 30	-40	24	0.951	1.237	72
Ch 2	-20	52	1.728	0.146	67
Ch 4	-20	46	1.432	1.553	55
Ch 28	0	69	1.798	0.168	43
Ch 8	20	86	1.895	1.117	34
Ch 14	20	83	1.821	1.757	25
Ch 20	40	102	1.946	1.854	16
Ch 24*	40	118	2.199	1.930	NA
Ch 36*	60	121	NA	NA	NA
Ch 38*	60	132	NA	NA	NA
Ch 6	100	130	NA	NA	NA
Ch 22*	140	139	NA	NA	NA
Ch 10*	180	140	NA	NA	NA

* Specimen did not break

Figure 6.1 - Example of engineering and true stress - true strain curves for Weld N°1 - As - Deposited Microstructure As - Received Condition (ADAR).

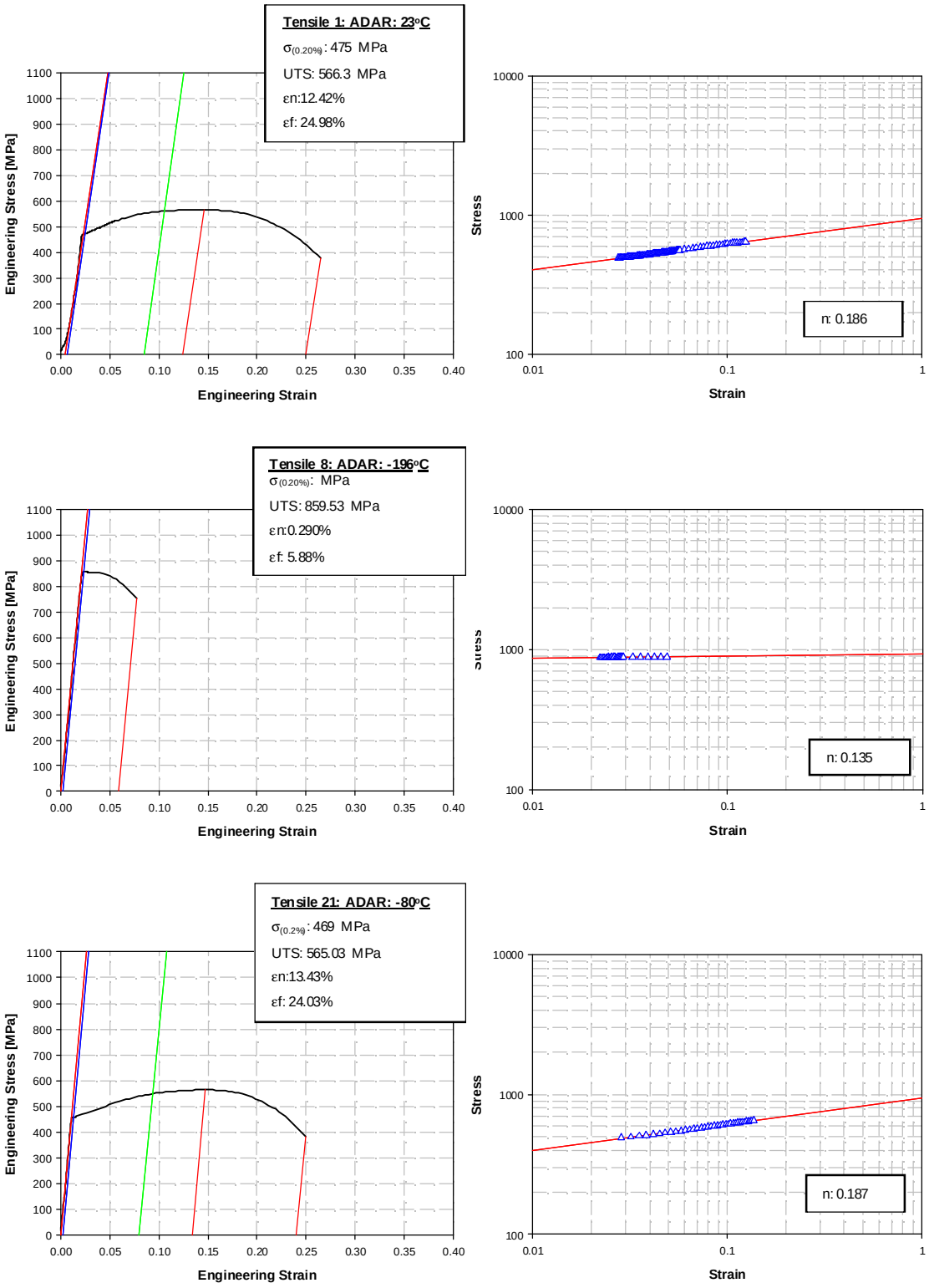

Figure 6.2 - Example of engineering and true stress - true strain curves for Weld N°1 - Reheated Microstructure As - Received Condition (RHAR).

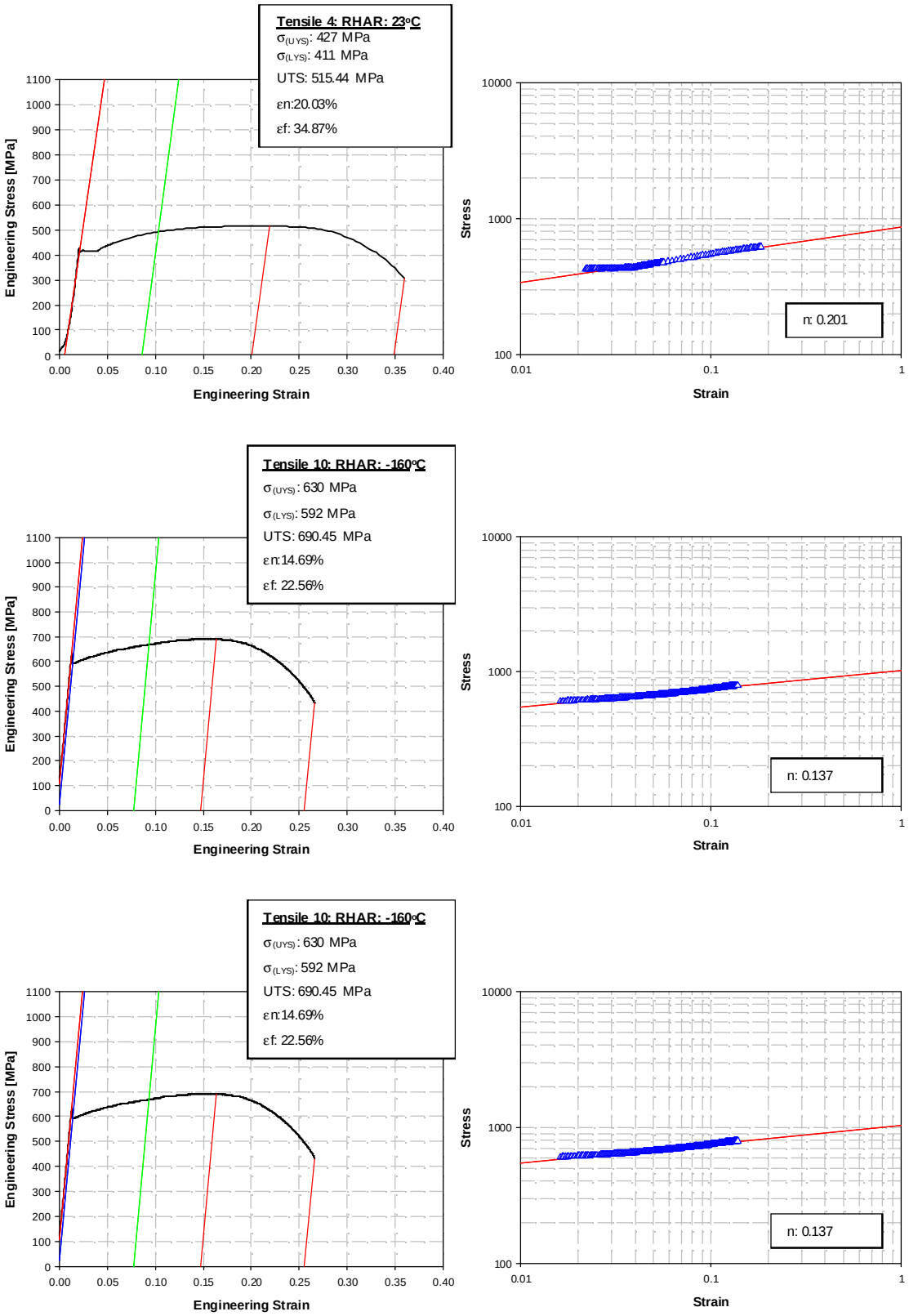

Figure 6.3 - Example of engineering and true stress - true strain curves for Weld N°1 - Mixed Condition.

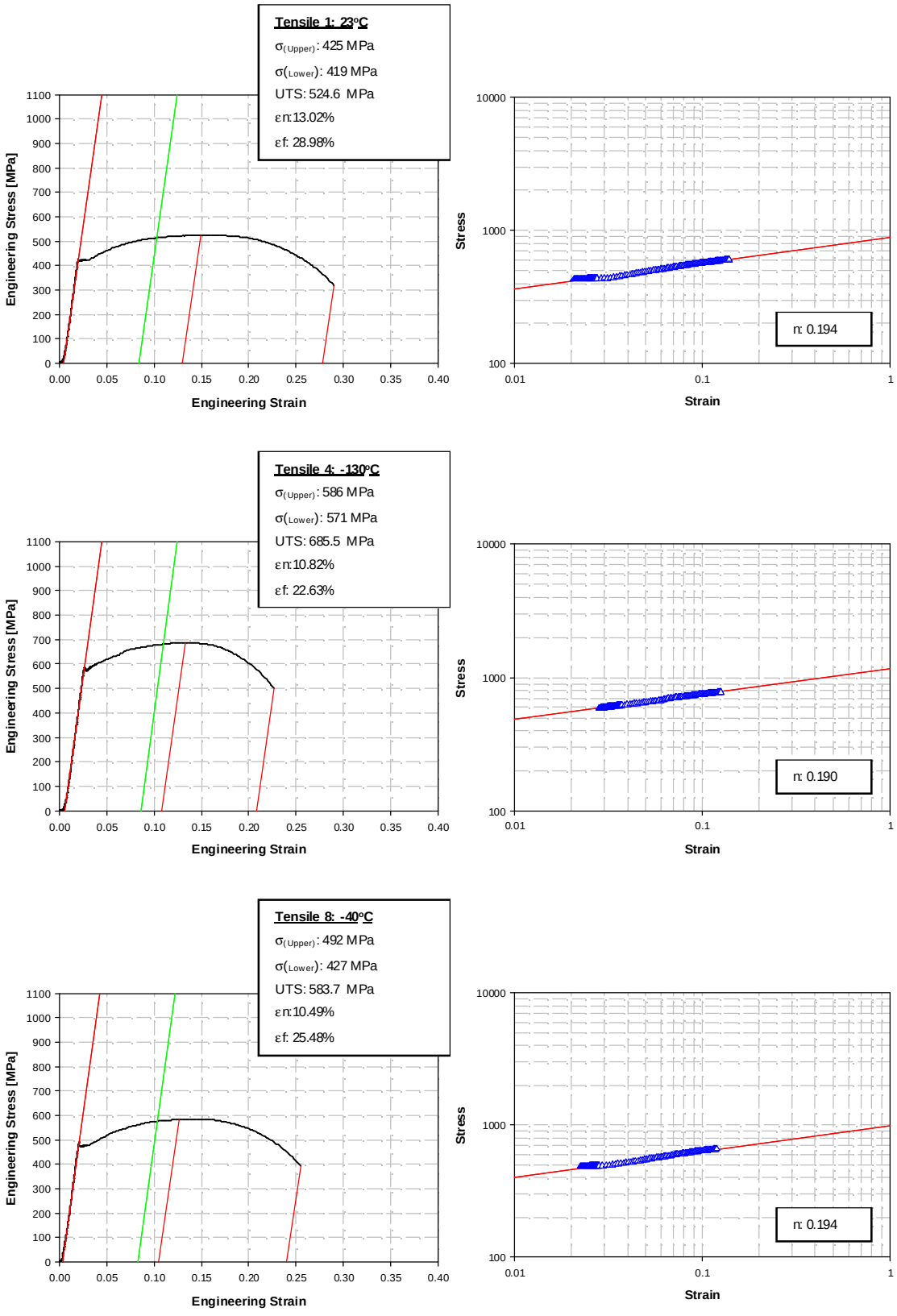

Figure 6.4 - Example of engineering and true stress - true strain curves for Weld N°1 - Transverse Condition.

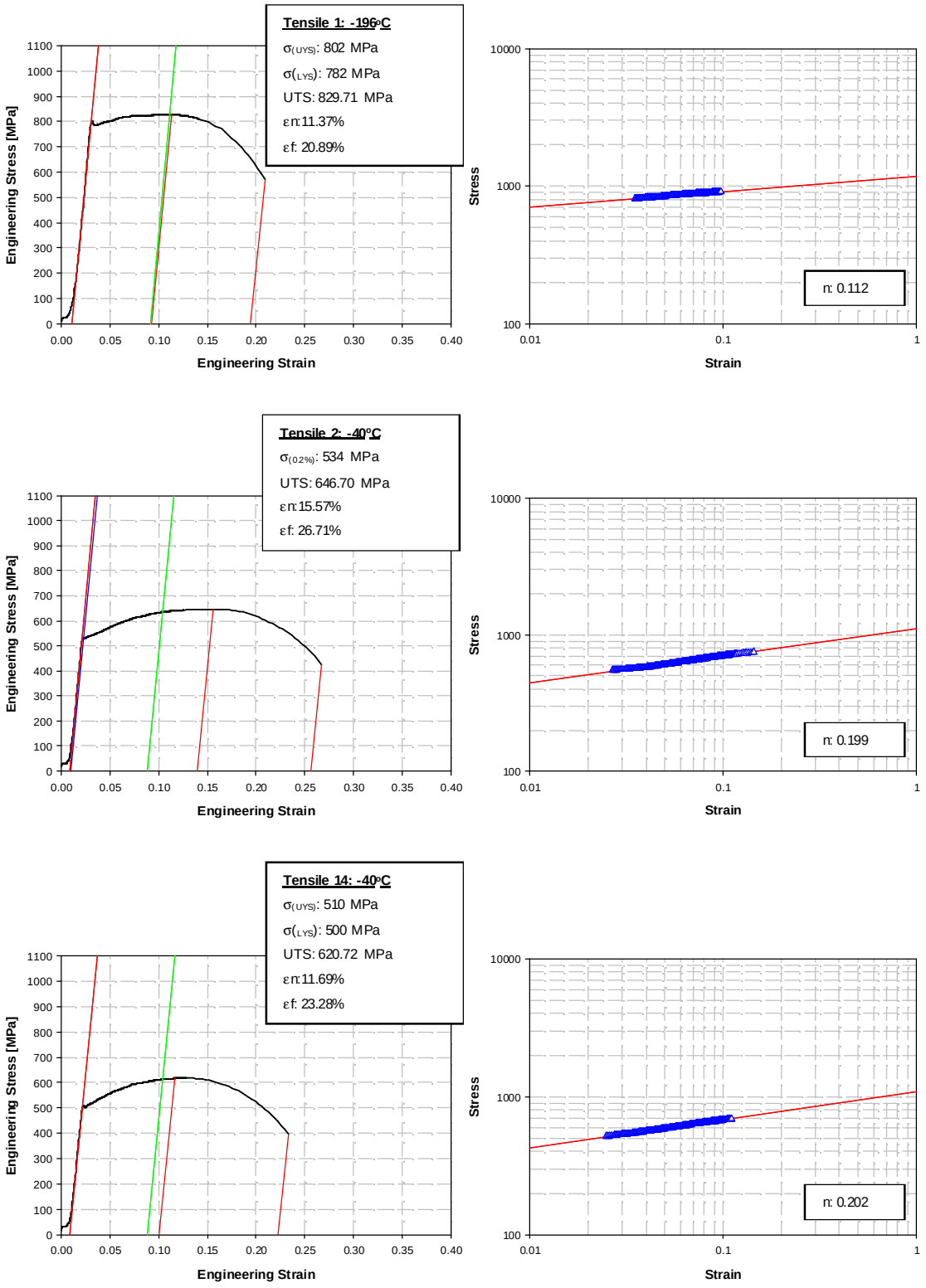

Figure 6.5 - Temperature dependence of flow properties for Weld N°1 in the as-received and mixed microstructural conditions; (a) Yield Stress and (b) Ultimate tensile strength.

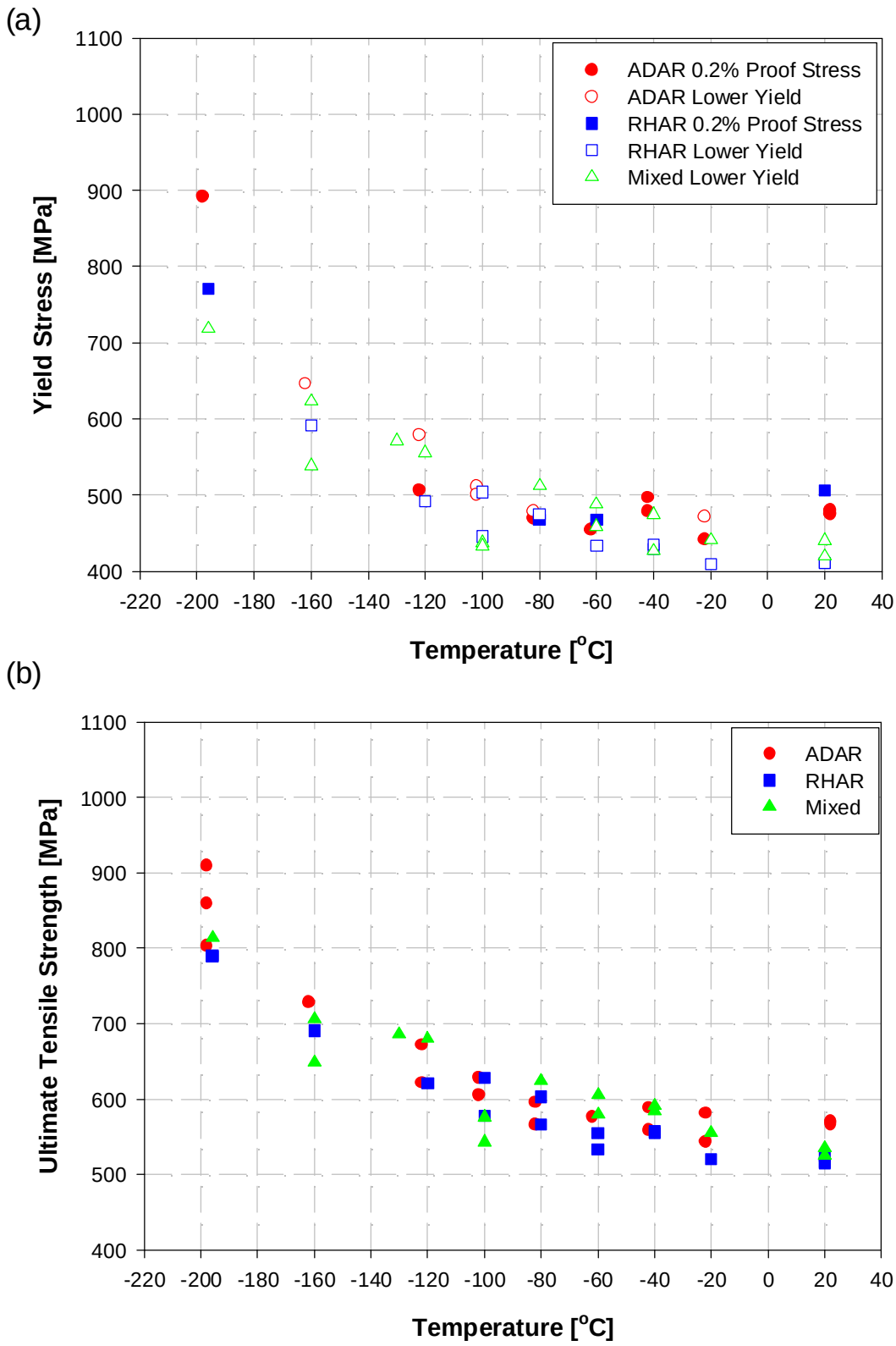

Figure 6.5 - Temperature dependence of flow properties for Weld N°1 in the as-received and mixed microstructural conditions; (c) Total Strain and (d) Work Hardening Exponent, *n*.

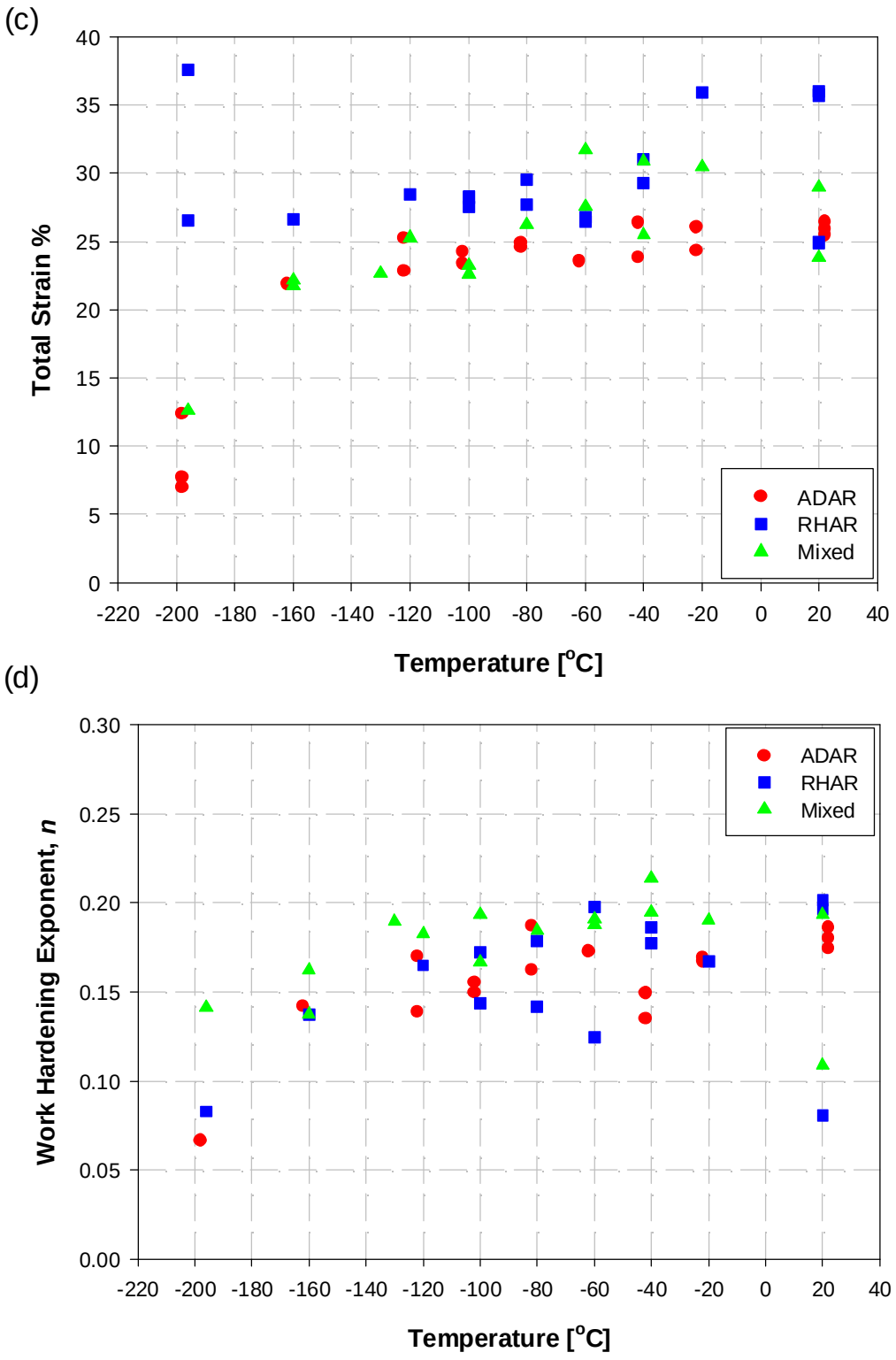

Figure 6.6 - Temperature dependence of flow properties for Weld N°1 in the as-received and transverse microstructural conditions; (a) Yield Stress and (b) Ultimate tensile strength.

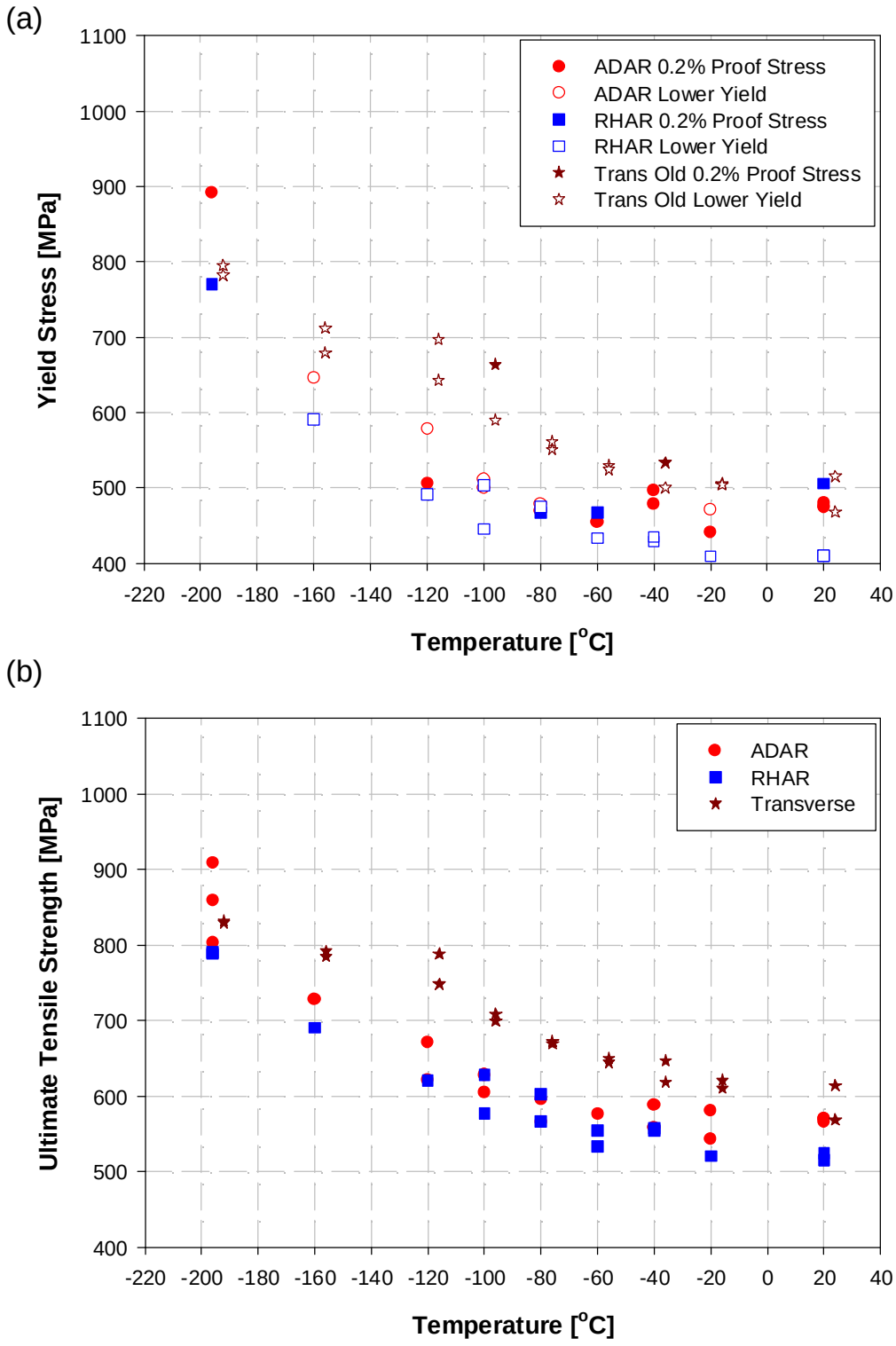

Figure 6.6 - Temperature dependence of flow properties for Weld N°1 in the as-received and transverse microstructural conditions; (c) Total Strain and (d) Work Hardening Exponent, *n*.

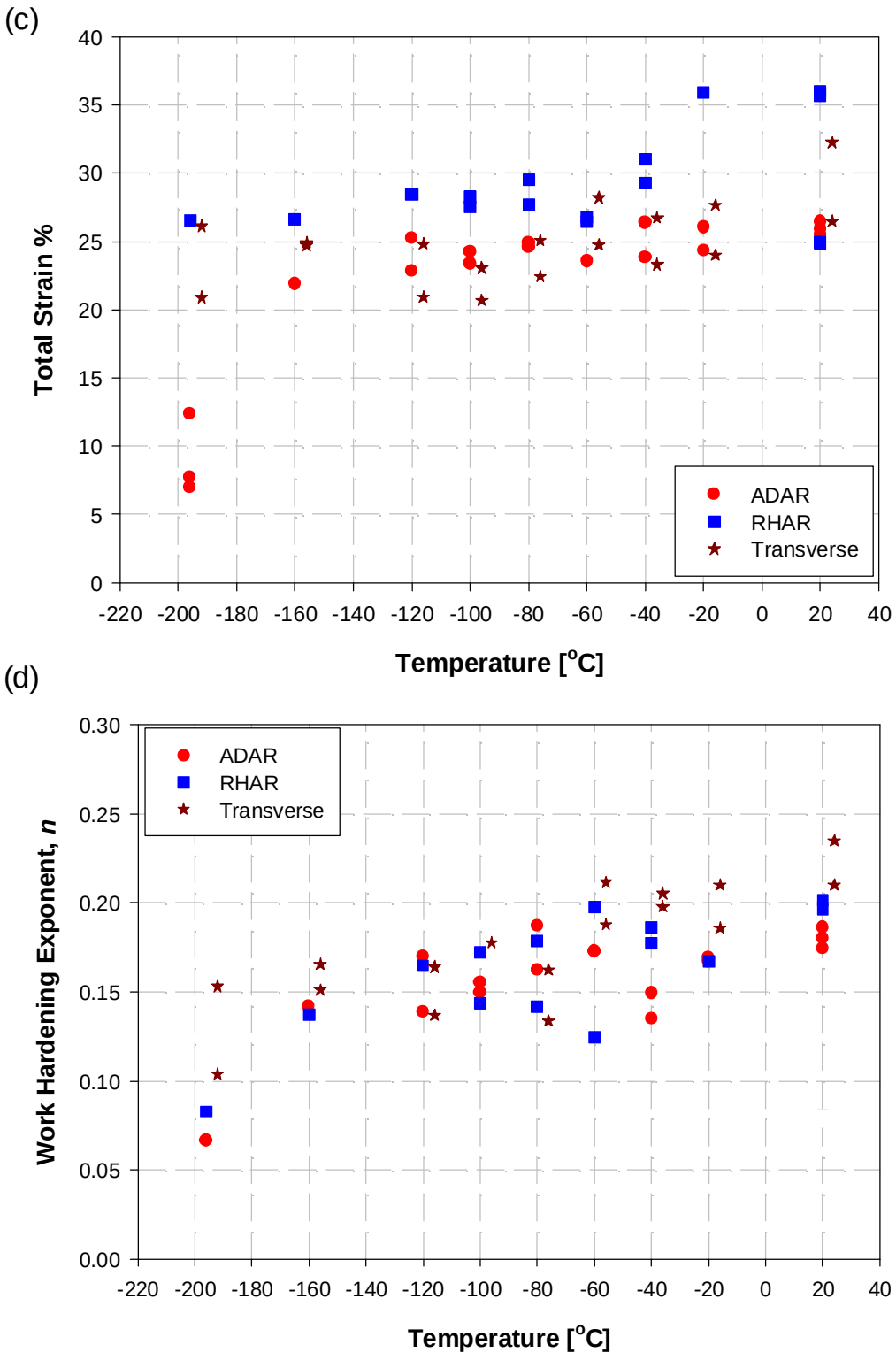

Figure 6.7 - Example of engineering and true stress - true strain curves for Weld N°2 - As - Deposited Microstructure As - Received Condition (ADAR).

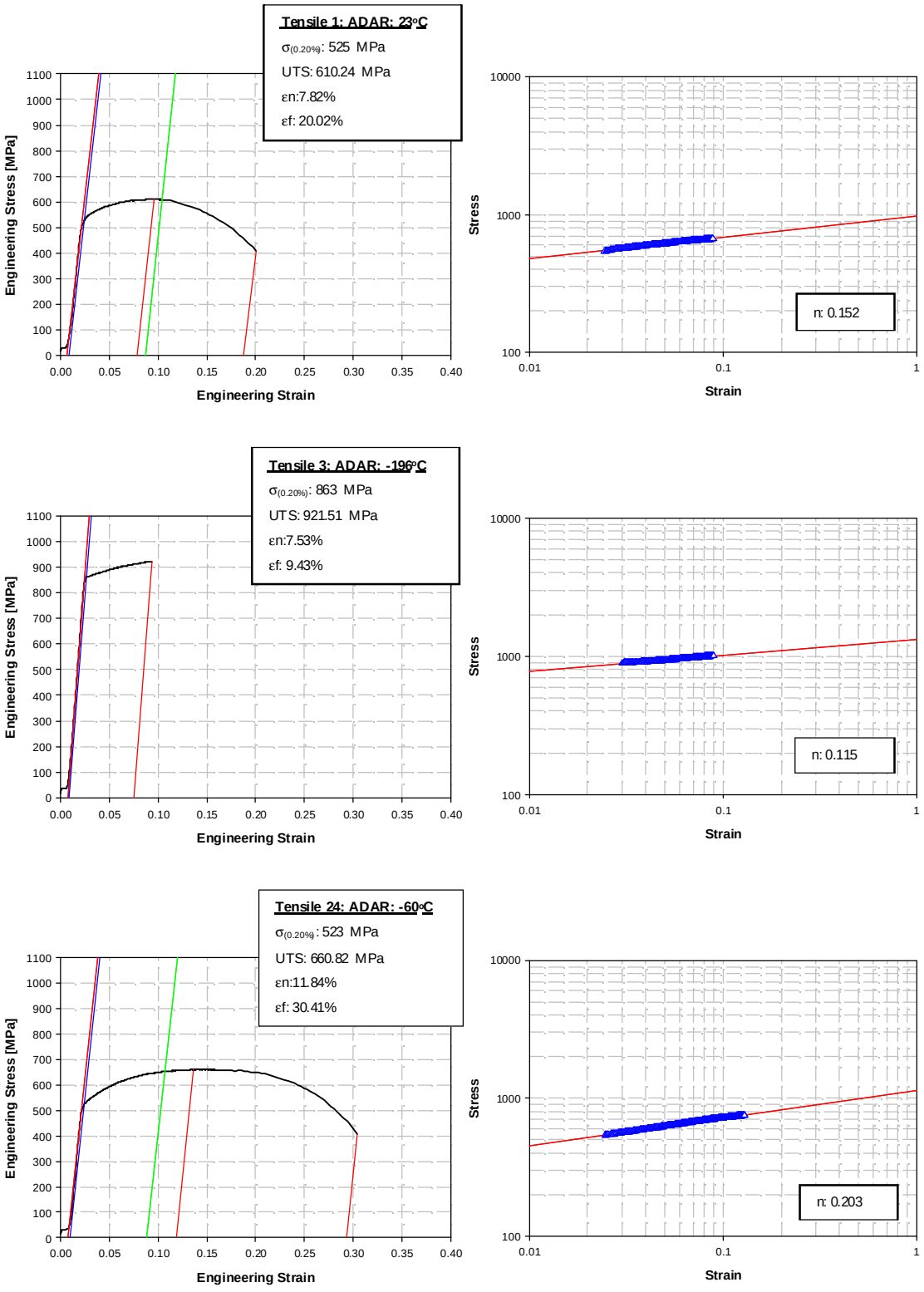

Figure 6.8 - Example of engineering and true stress - true strain curves for Weld N°2 - Reheated Microstructure As - Received Condition (RHAR).

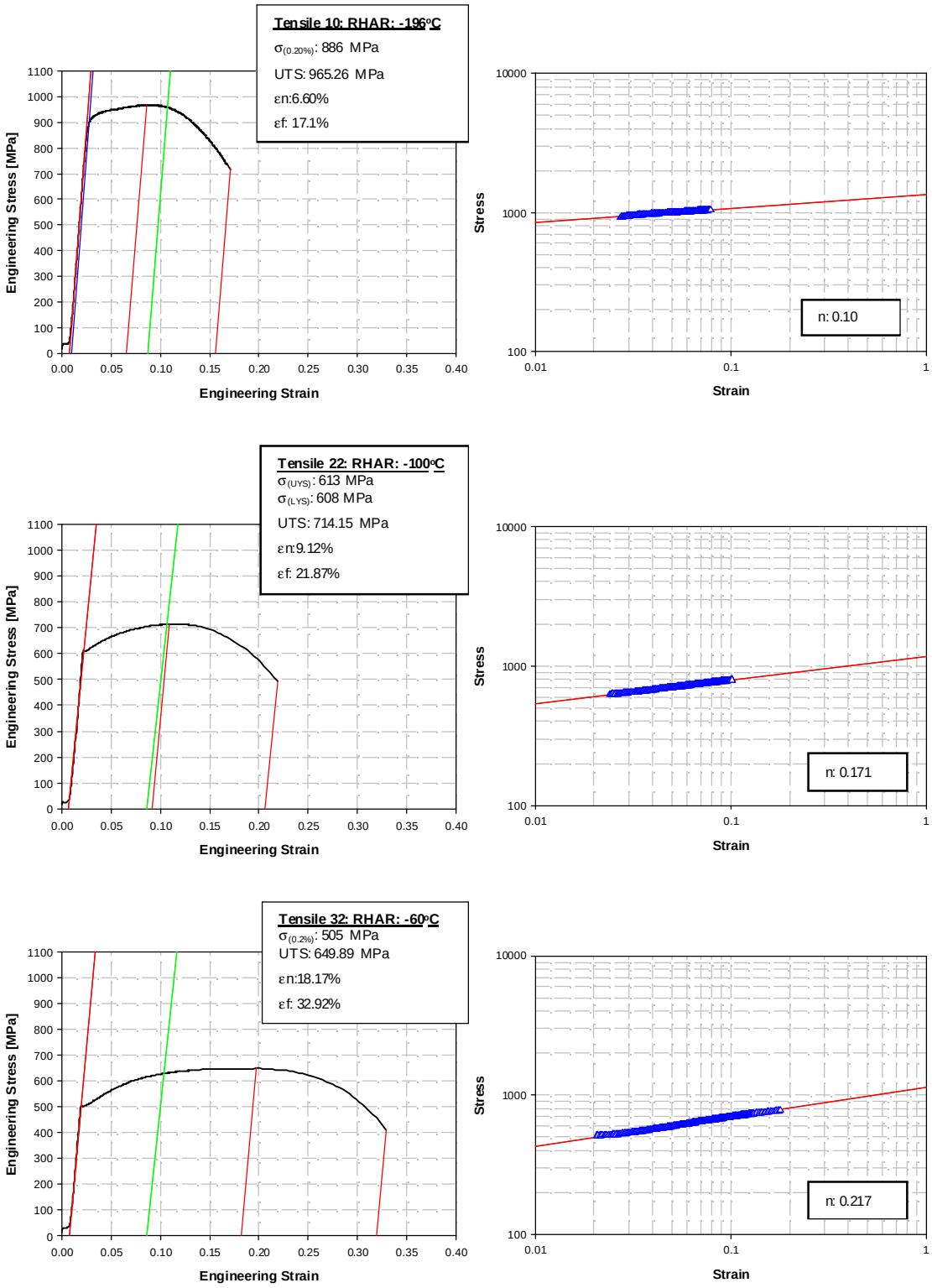

Figure 6.9 - Example of engineering and true stress - true strain curves for Weld N°2 - Mixed Condition.

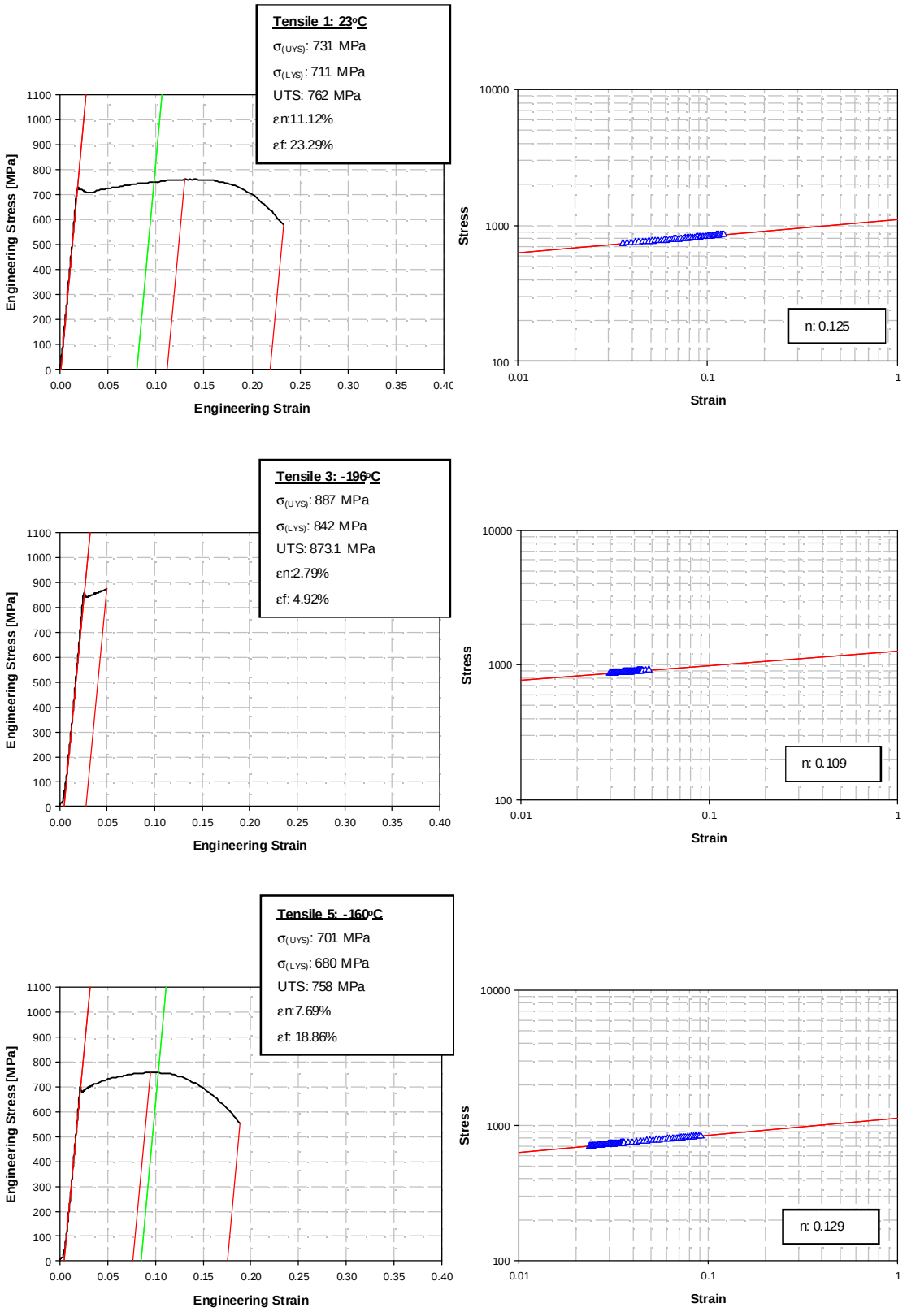

Figure 6.10 - Example of engineering and true stress - true strain curves for Weld N°2 - Transverse Condition.

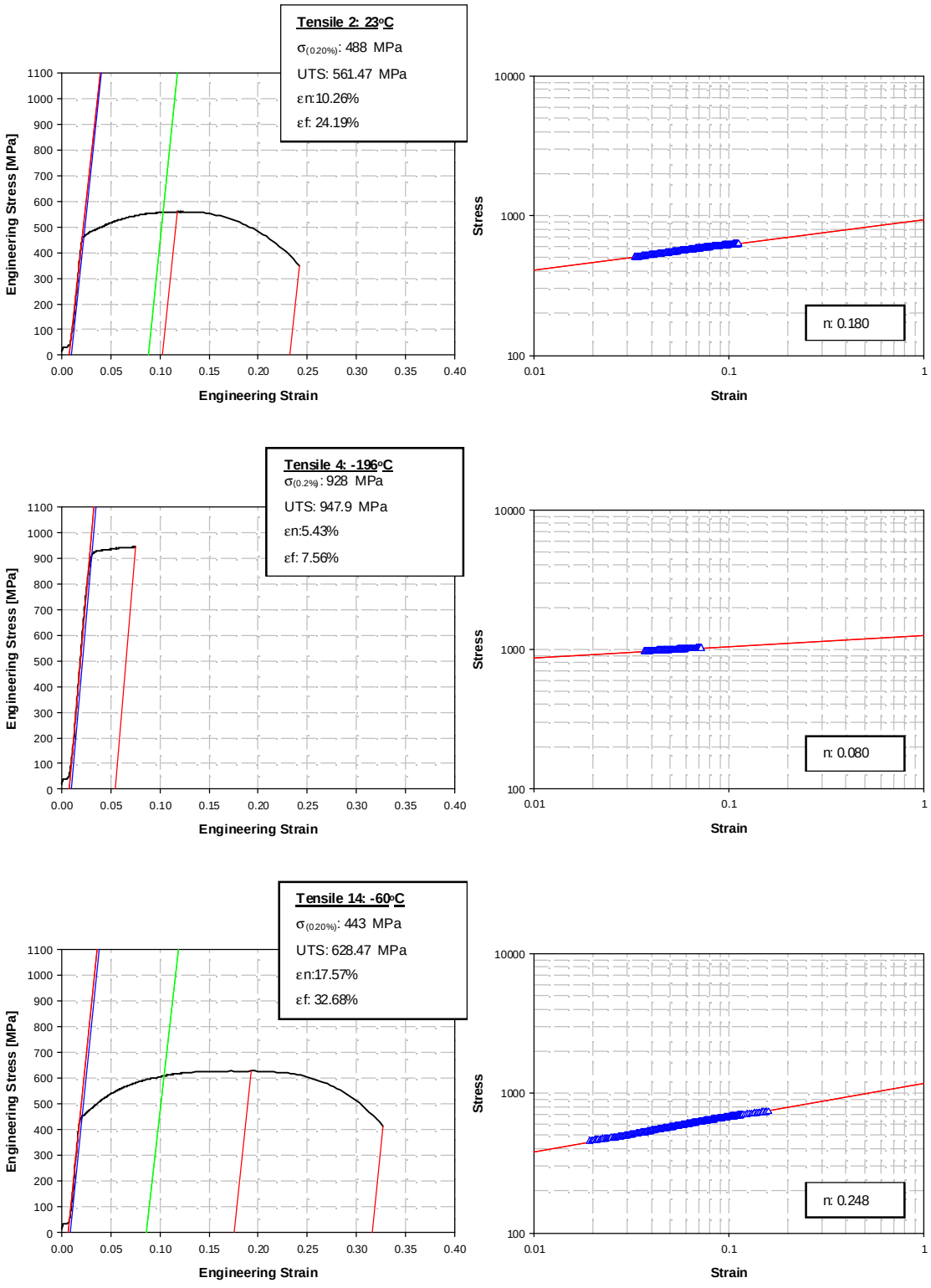

Figure 6.11 - Temperature dependence of flow properties for Weld N°2 in the as-received and mixed microstructural conditions; (a) Yield Stress and (b) Ultimate tensile strength.

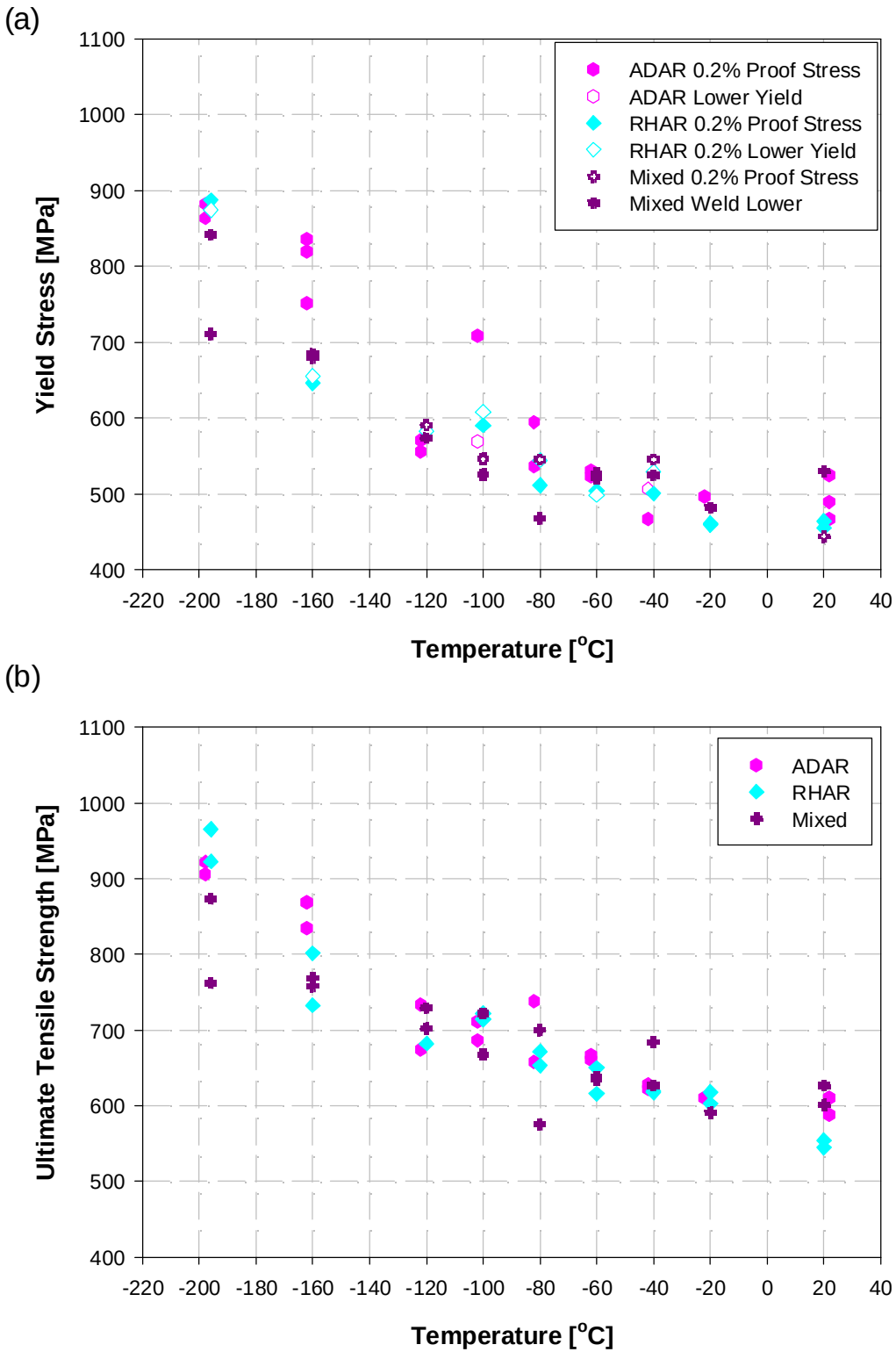

Figure 6.11 - Temperature dependence of flow properties for Weld N°2 in the as-received and mixed microstructural conditions; (c) Total Strain and (d) Work Hardening Exponent, *n*.

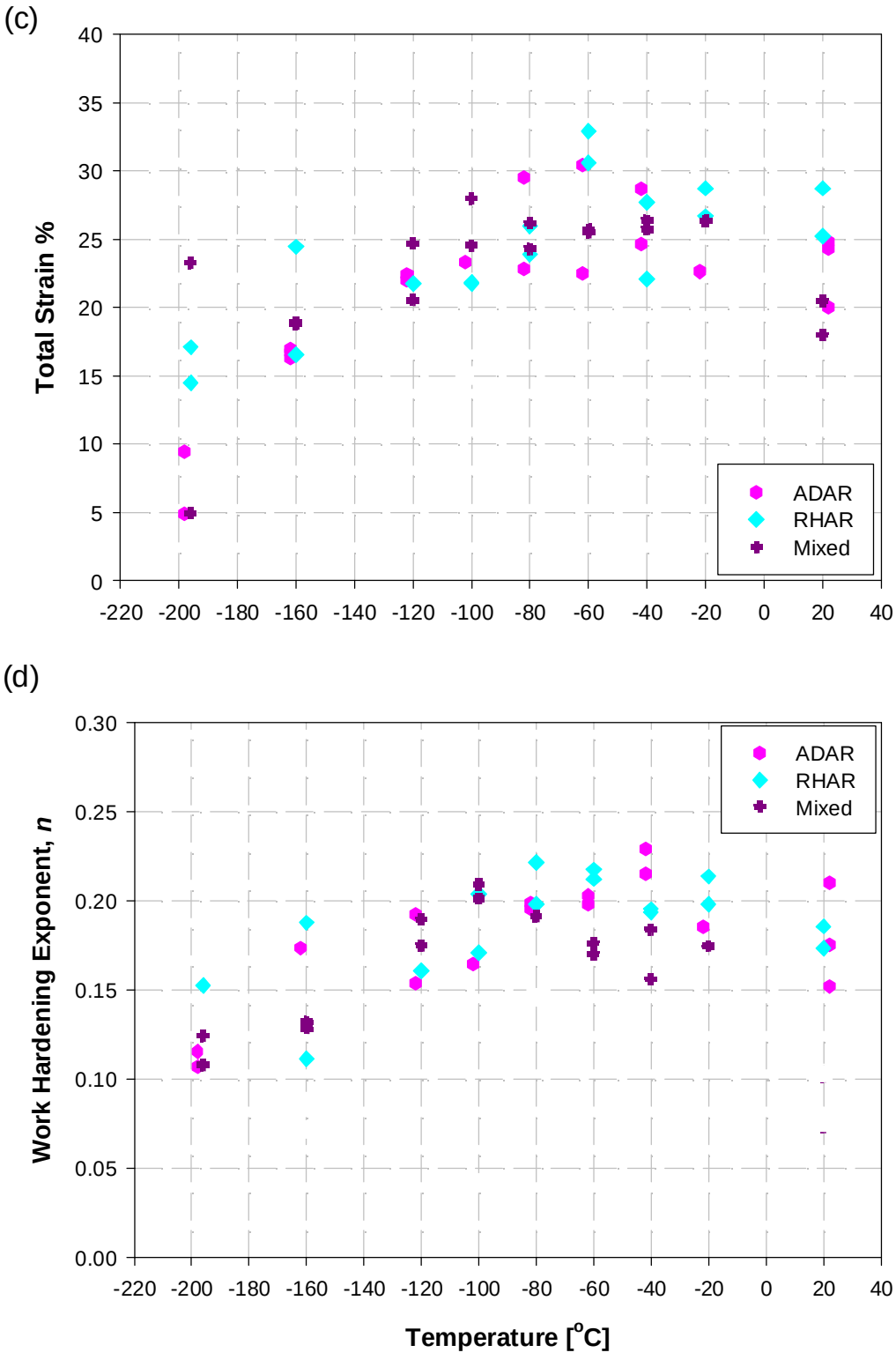

Figure 6.12 - Temperature dependence of flow properties for Weld N°2 in the as-received and transverse microstructural conditions; (a) Yield Stress and (b) Ultimate tensile strength.

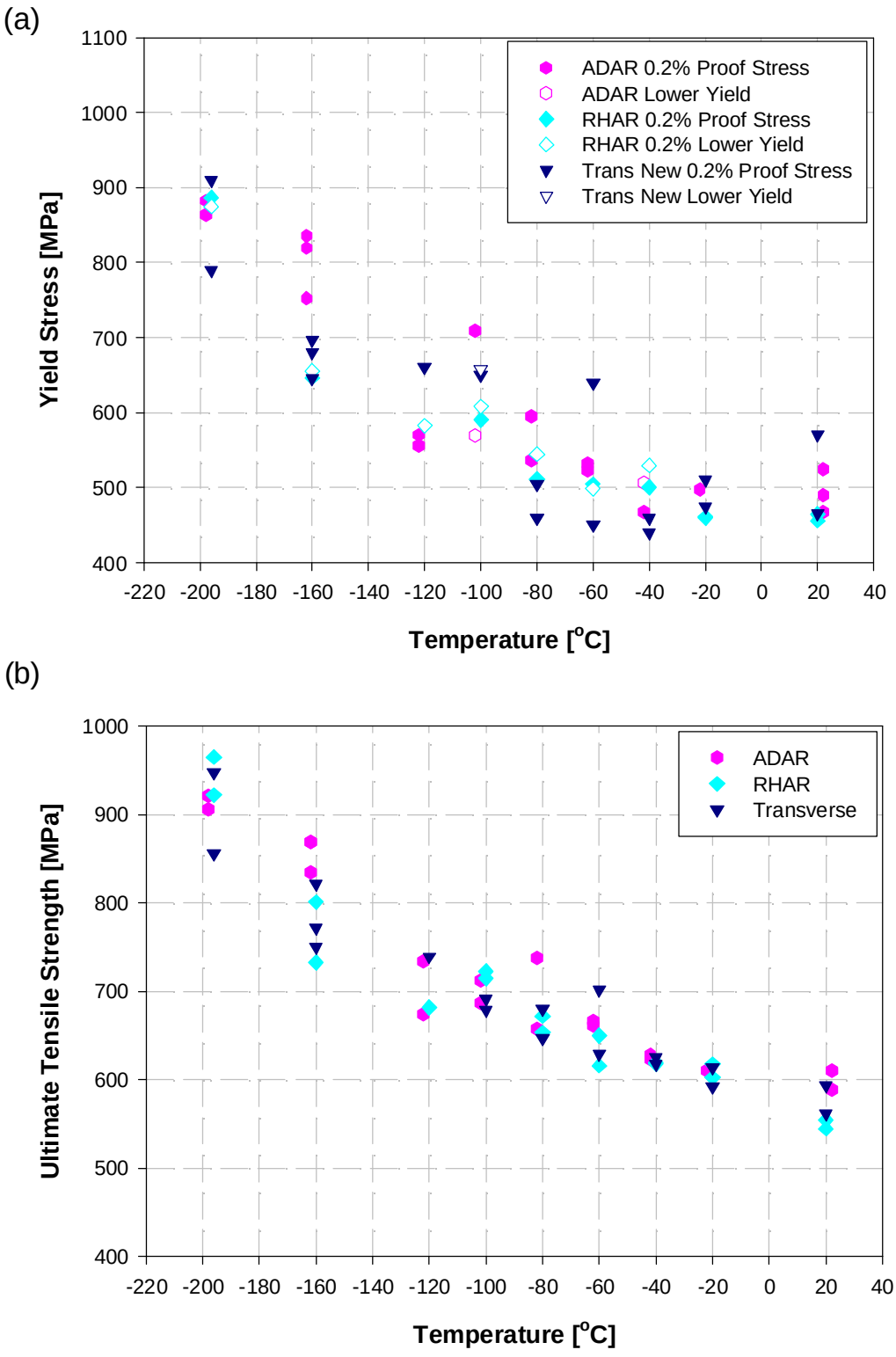

Figure 6.12 - Temperature dependence of flow properties for Weld N°2 in the as-received and transverse microstructural conditions; (c) Total Strain and (d) Work Hardening Exponent, *n*.

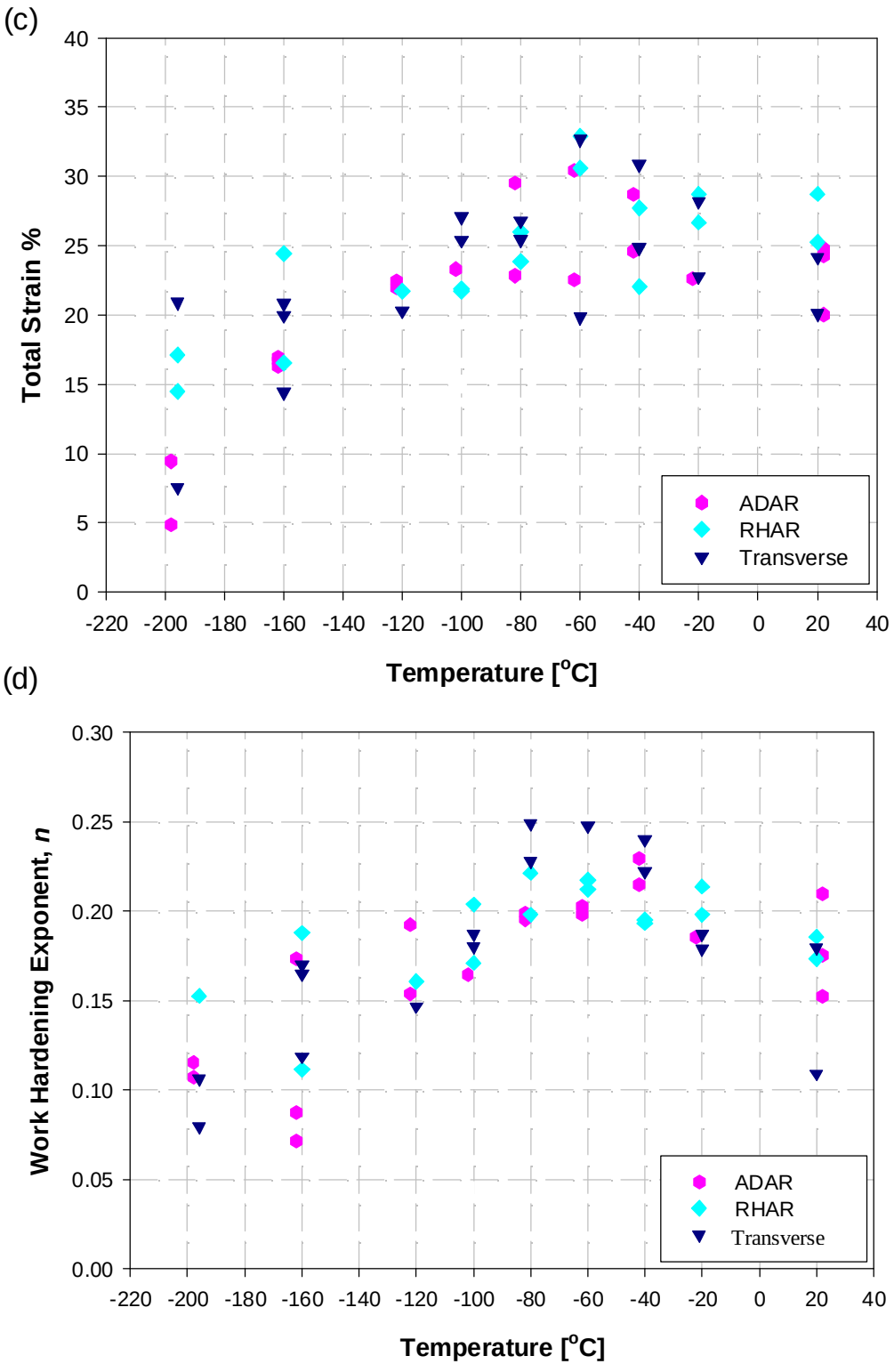

Figure 6.13 - Example of engineering and true stress - true strain curves for Weld N°2 Pre-strain As - deposited condition.

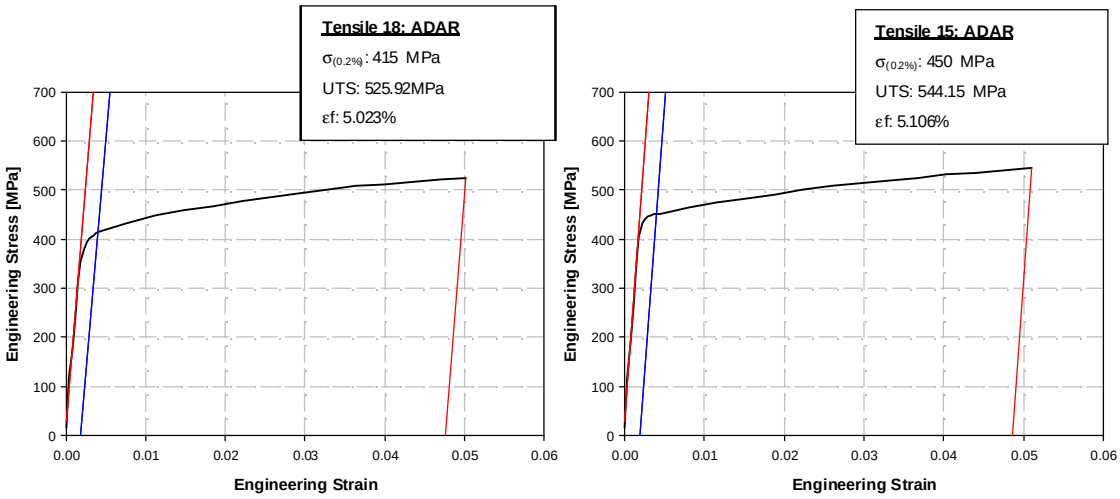

Figure 6.14 - Example of engineering and true stress - true strain curves for Weld N°2 Pre-strain Reheated condition.

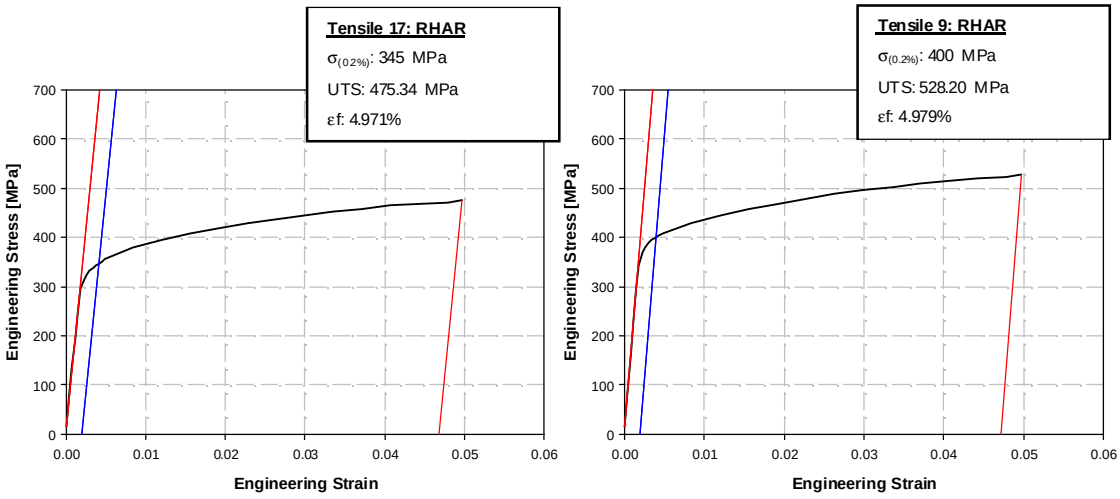

Figure 6.15 - Example of engineering and true stress - true strain curves for Weld N°2 As - deposited Strain Aged (5%SA) microstructural condition.

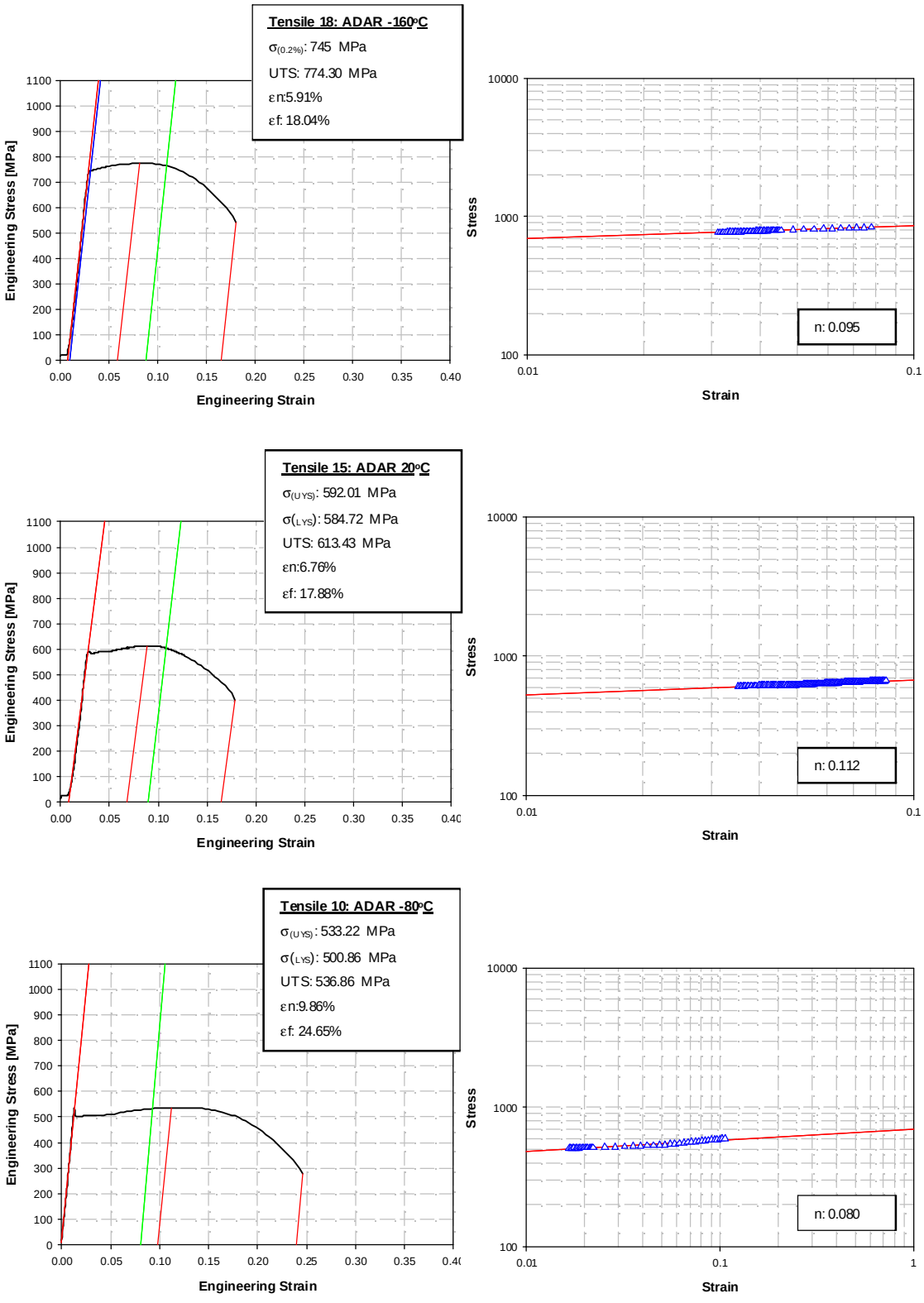

Figure 6.16 - Example of engineering and true stress - true strain curves for Weld N°2 Reheated Strain Aged (5%SA) microstructural condition.

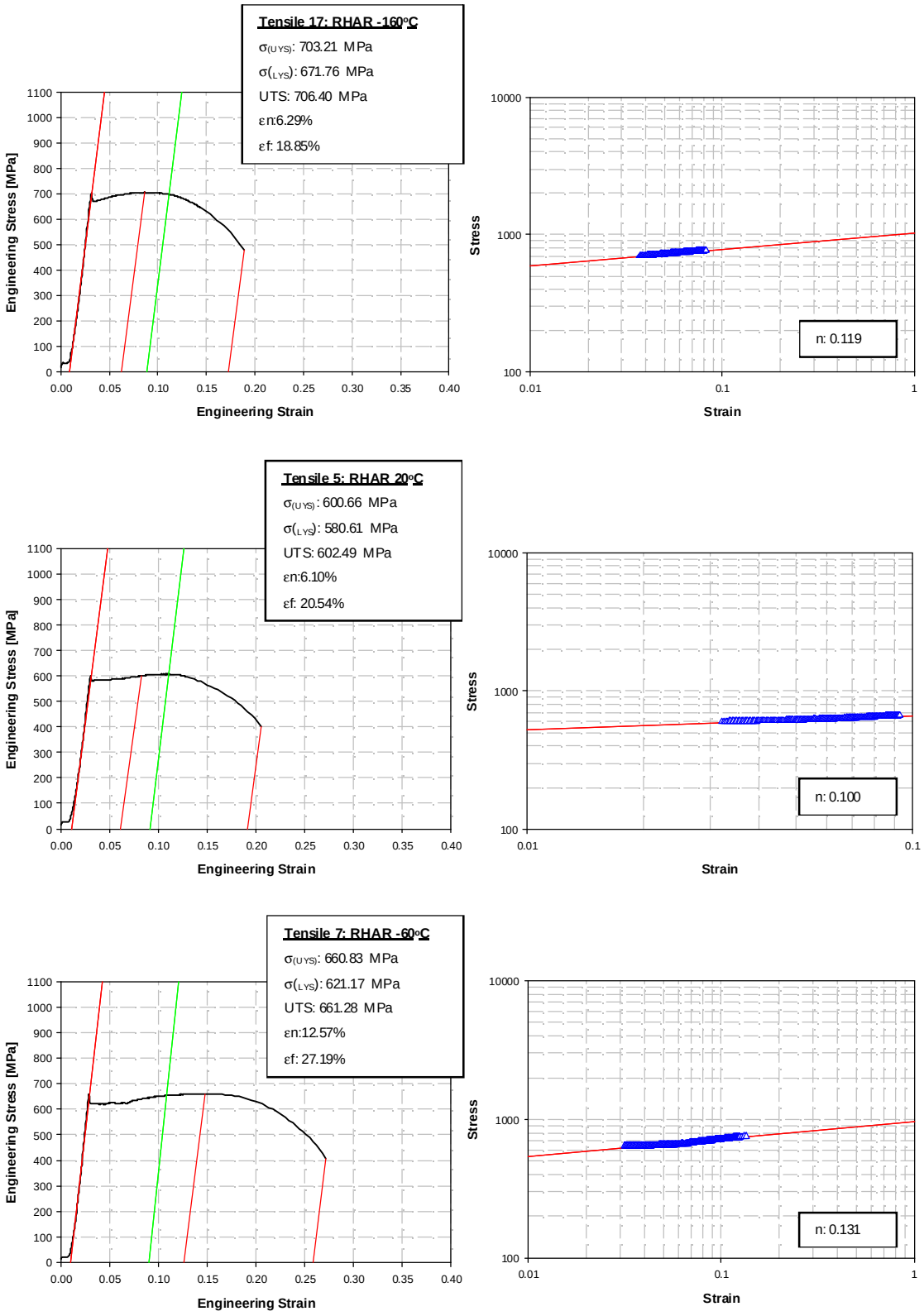

Figure 6.17 - Temperature dependence of flow properties for Weld N°2 in the AD5%SA and RH5%SA microstructural conditions; (a) Yield Stress and (b) Ultimate tensile strength.

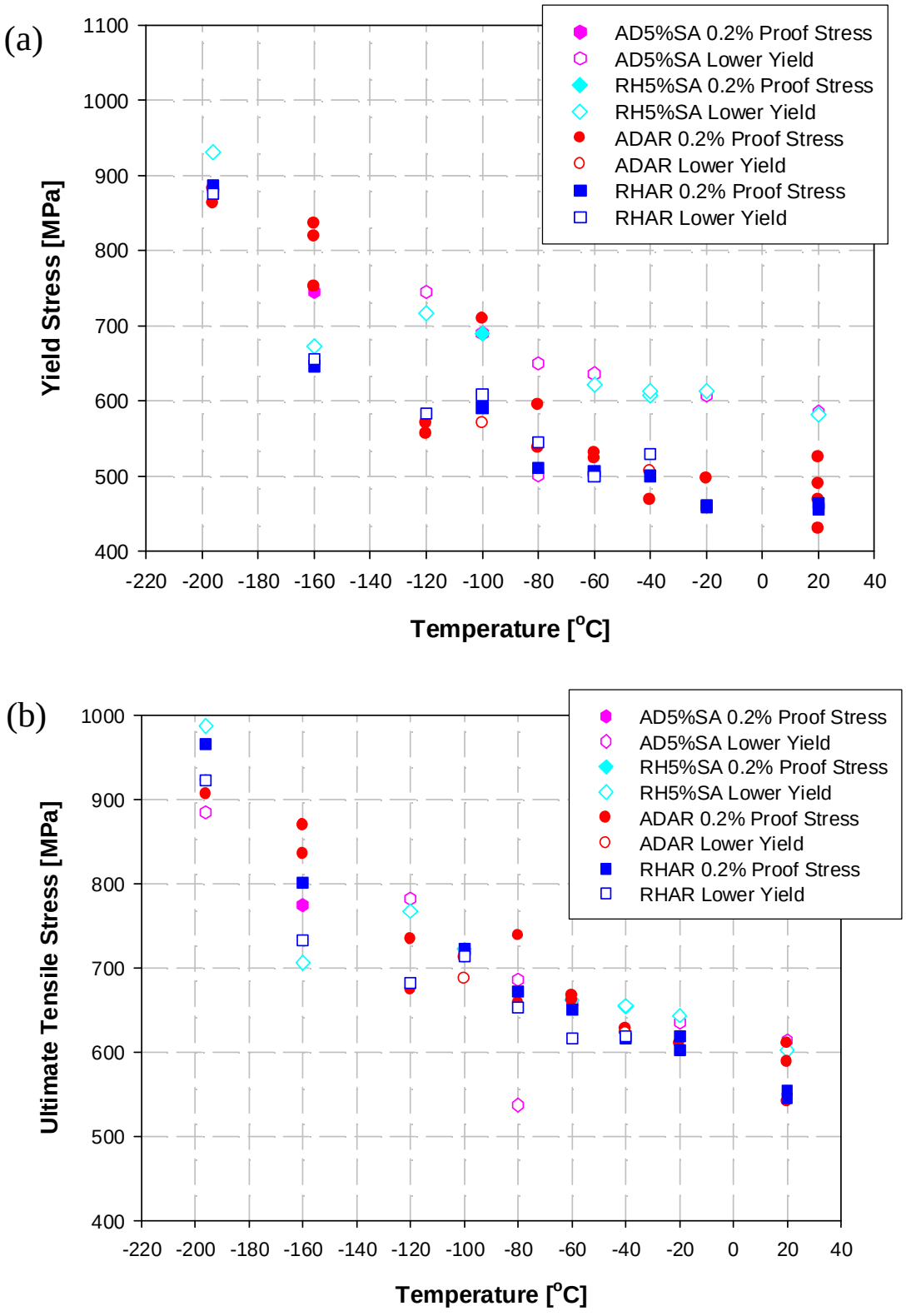

Figure 6.17 - Temperature dependence of flow properties for Weld N°2 in the AD5%SA and RH5%SA microstructural conditions; (c) Total Strain and (d) Work Hardening Exponent, *n*.

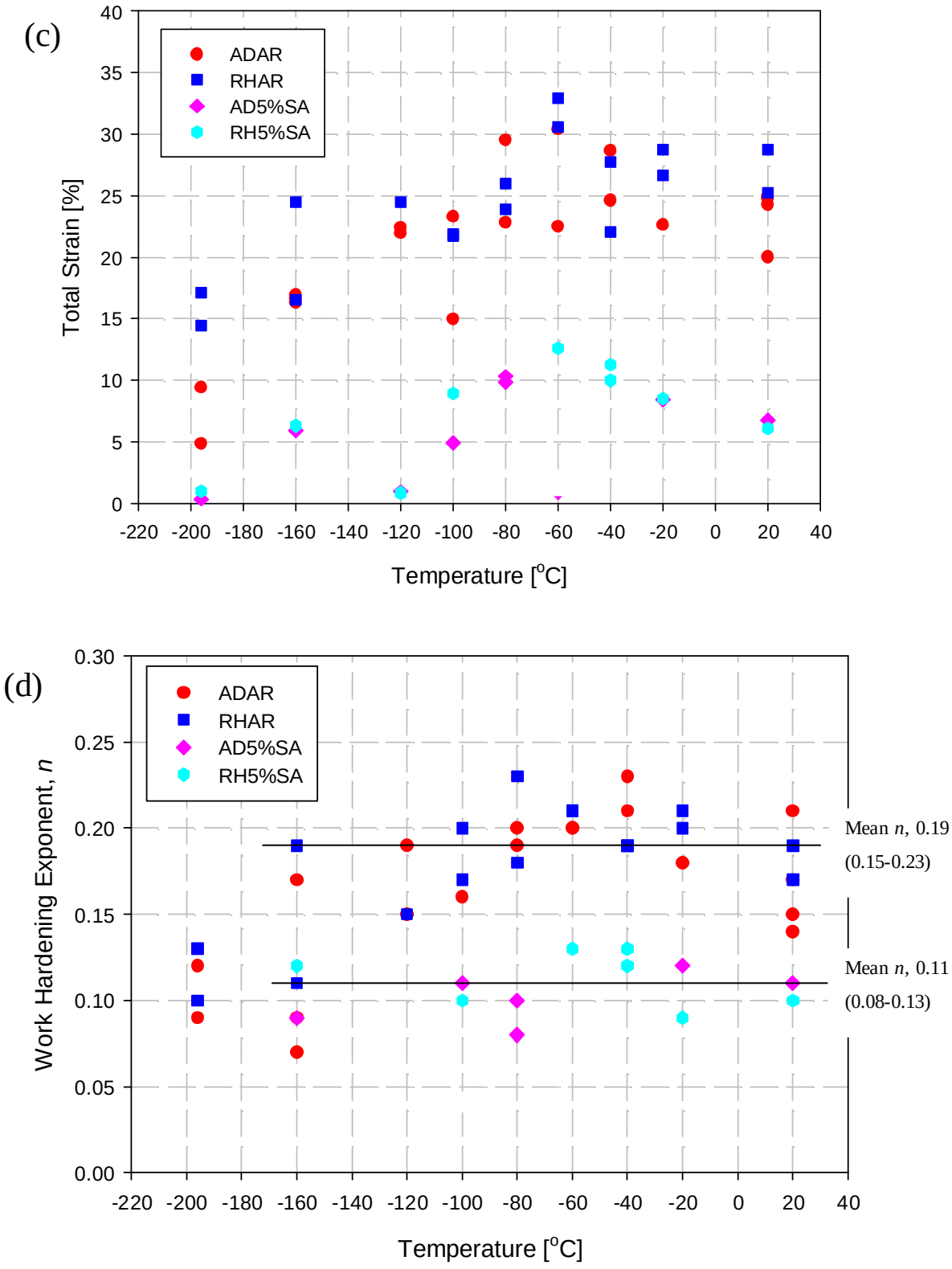

Figure 6.18 - Charpy Impact energy transition curves for Weld N°2 for both microstructure and in both weld metal conditions.

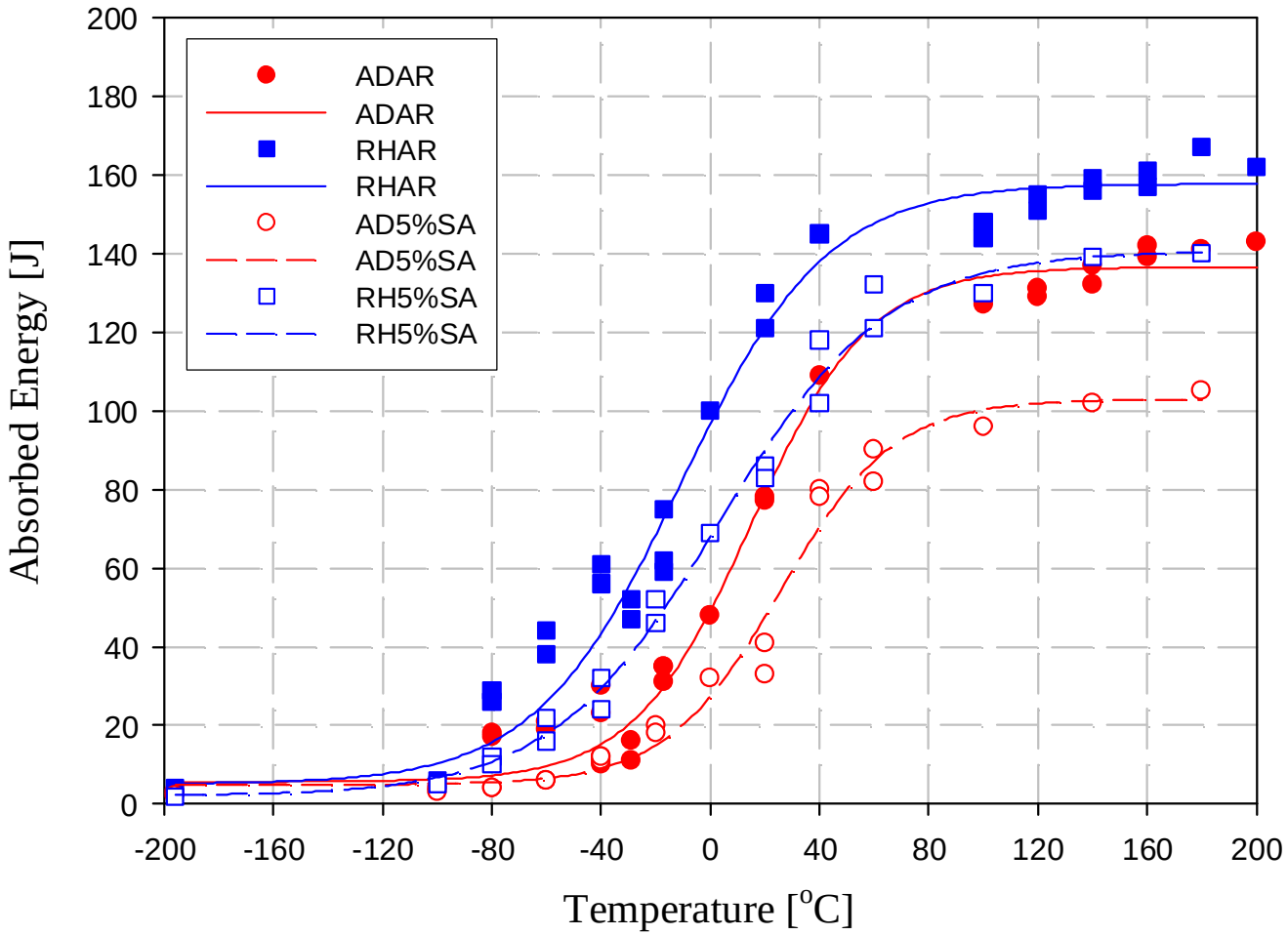

Figure 6.19 - Charpy Impact energy transition curves for Weld N^{o}2 for both the as-deposited and reheated microstructures and in the as - received weld metal condition.

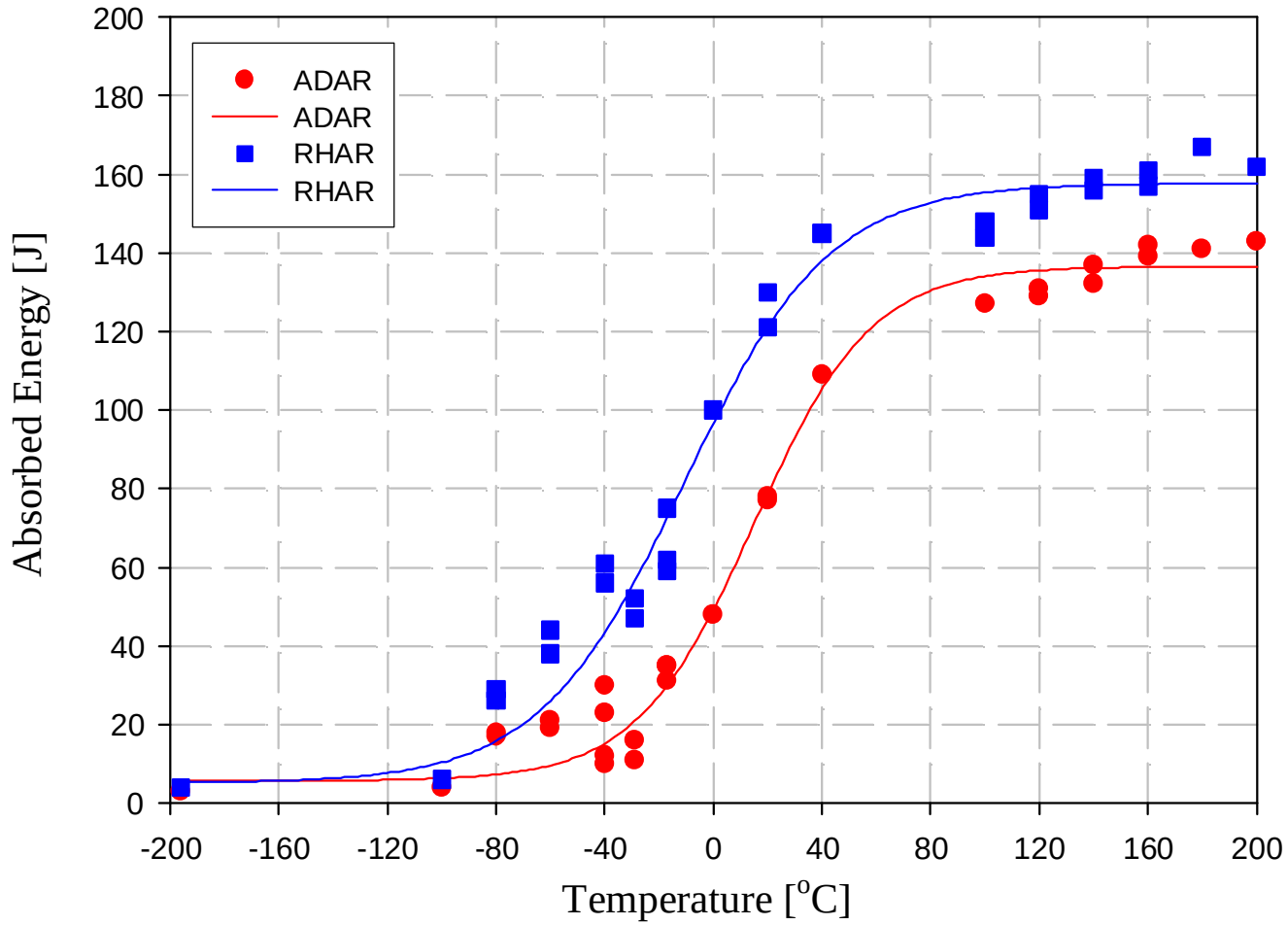

Figure 6.20 - Charpy Impact energy transition curves for Weld N^{o}2 for both the as-deposited and reheated microstructures and in the strain aged weld metal condition.

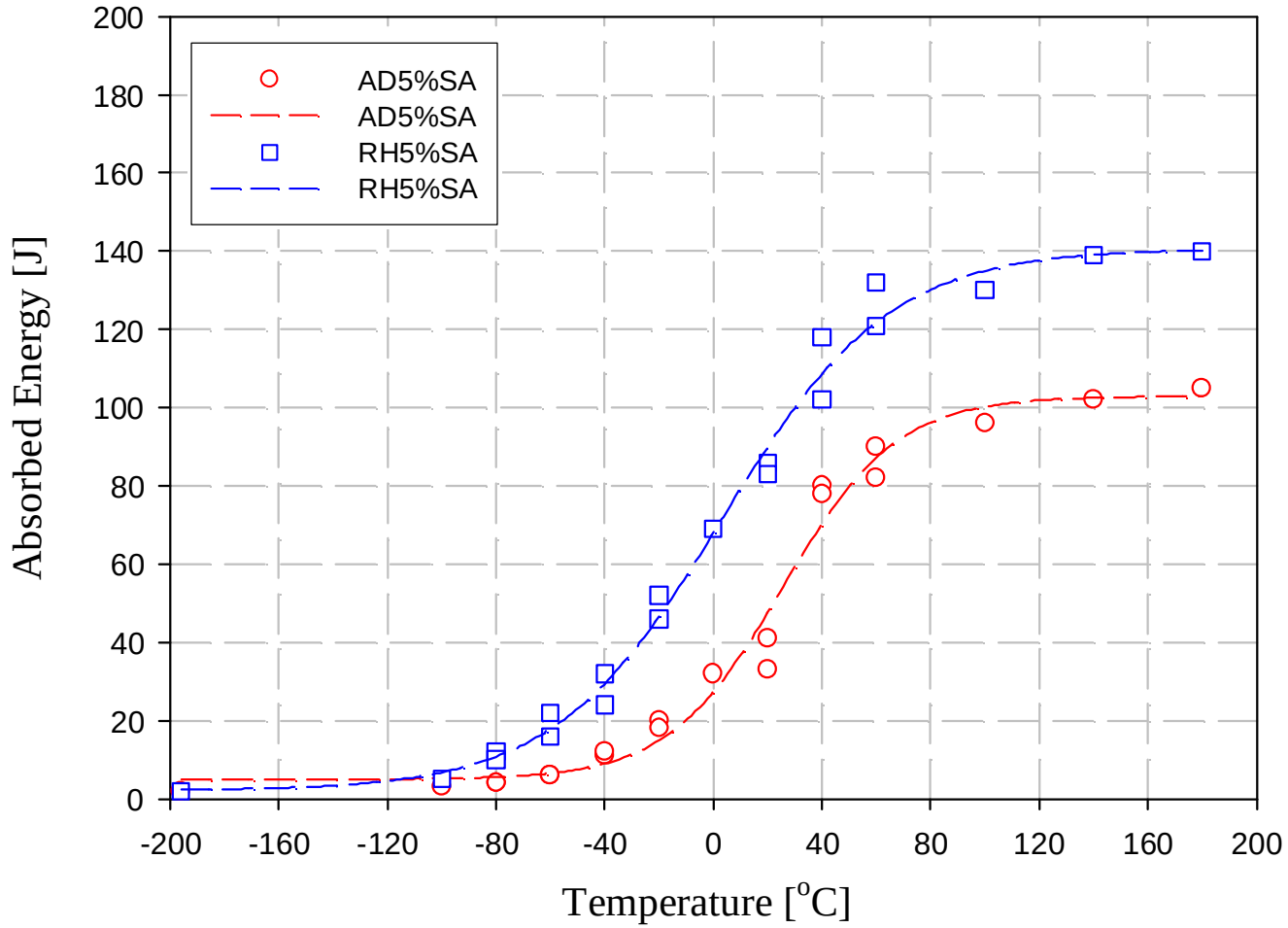

Figure 6.21 - Charpy Impact energy transition curves for Weld N°2 for the as-deposited microstructure and in both weld metal conditions.

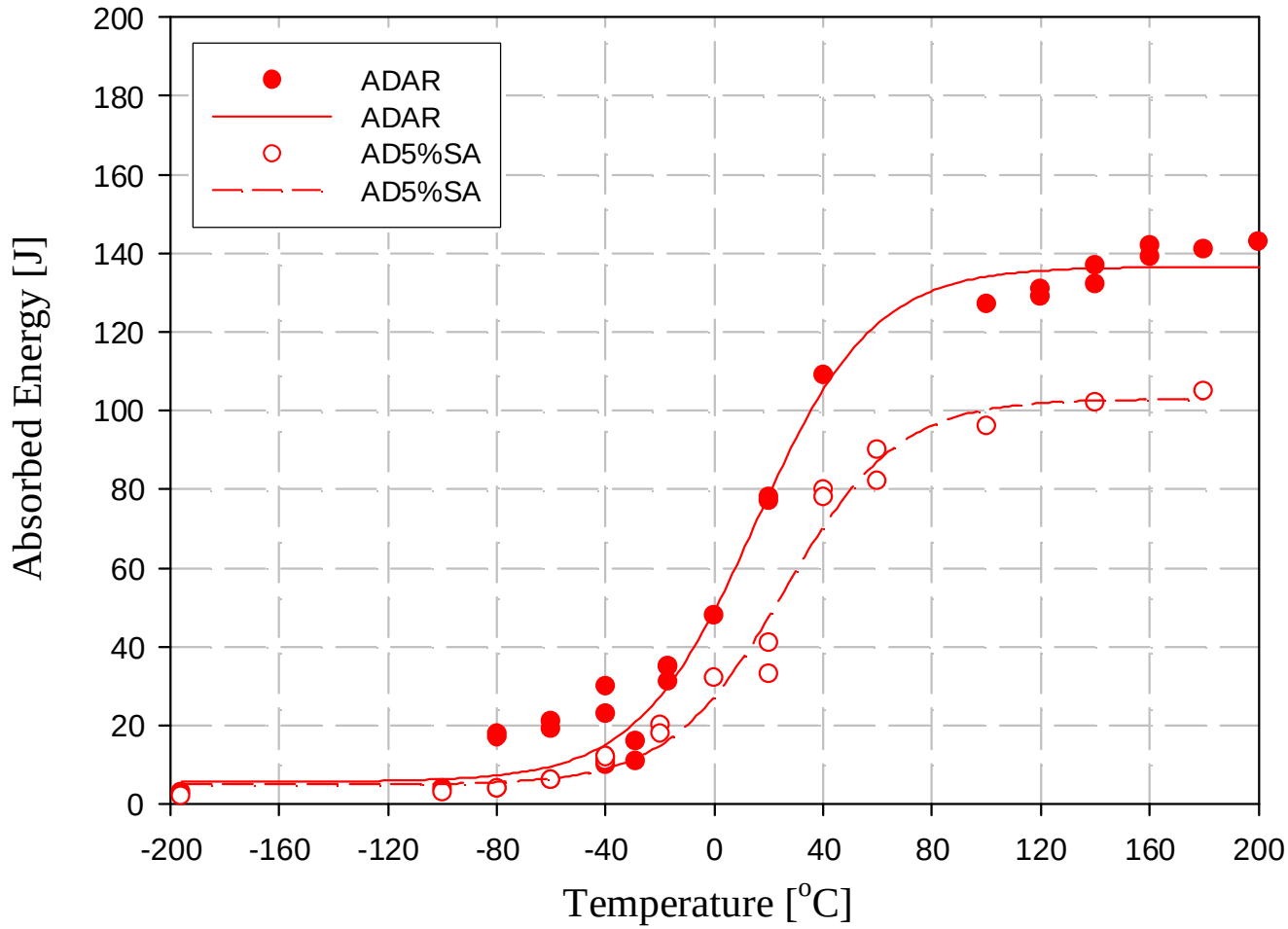

Figure 6.22 - Charpy Impact energy transition curves for Weld Nº2 for the reheated microstructure and in both weld metal conditions.

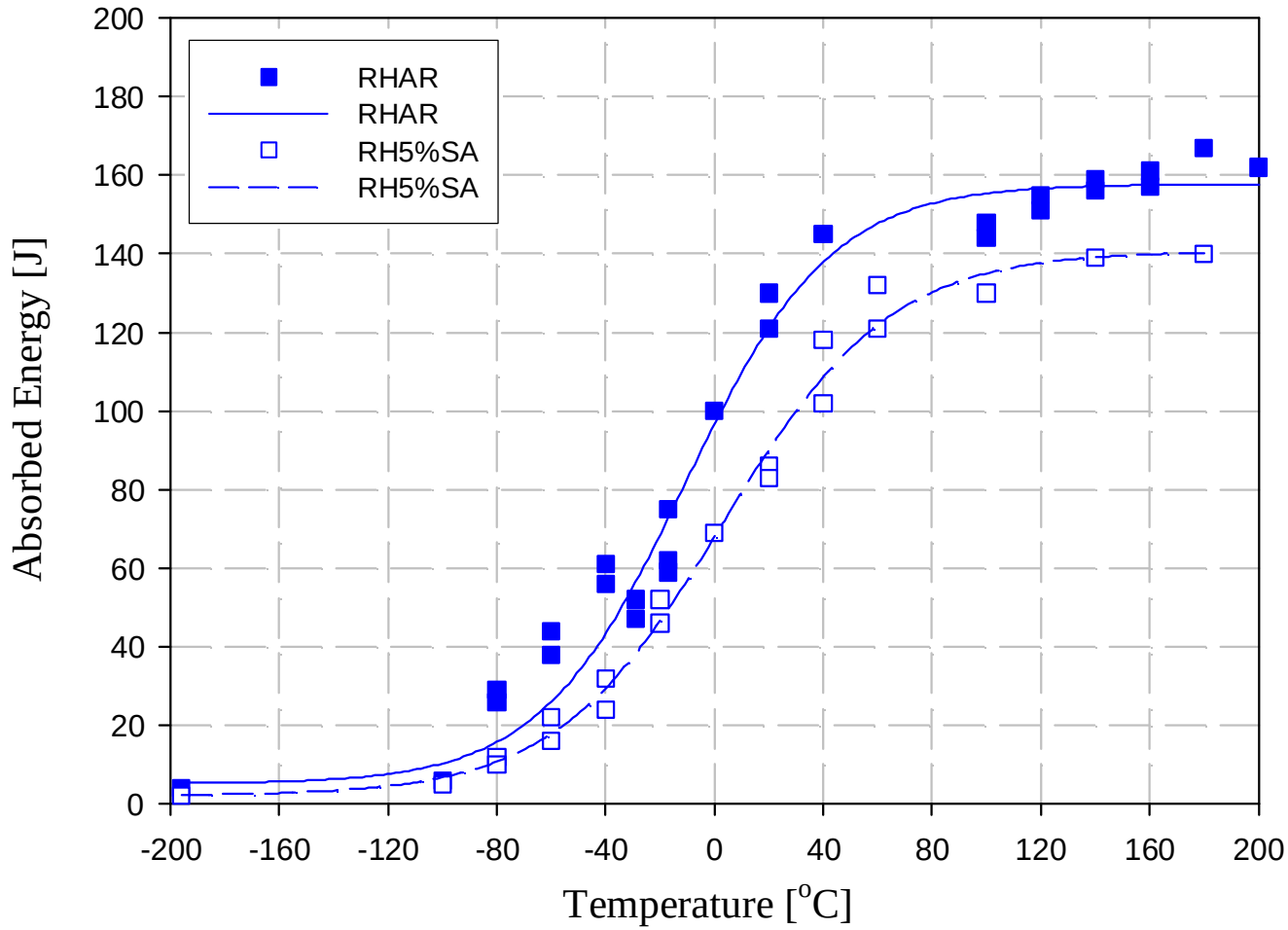

Figure 6.23 - Transition curves for Weld N°2 for both microstructure and in both weld metal conditions.

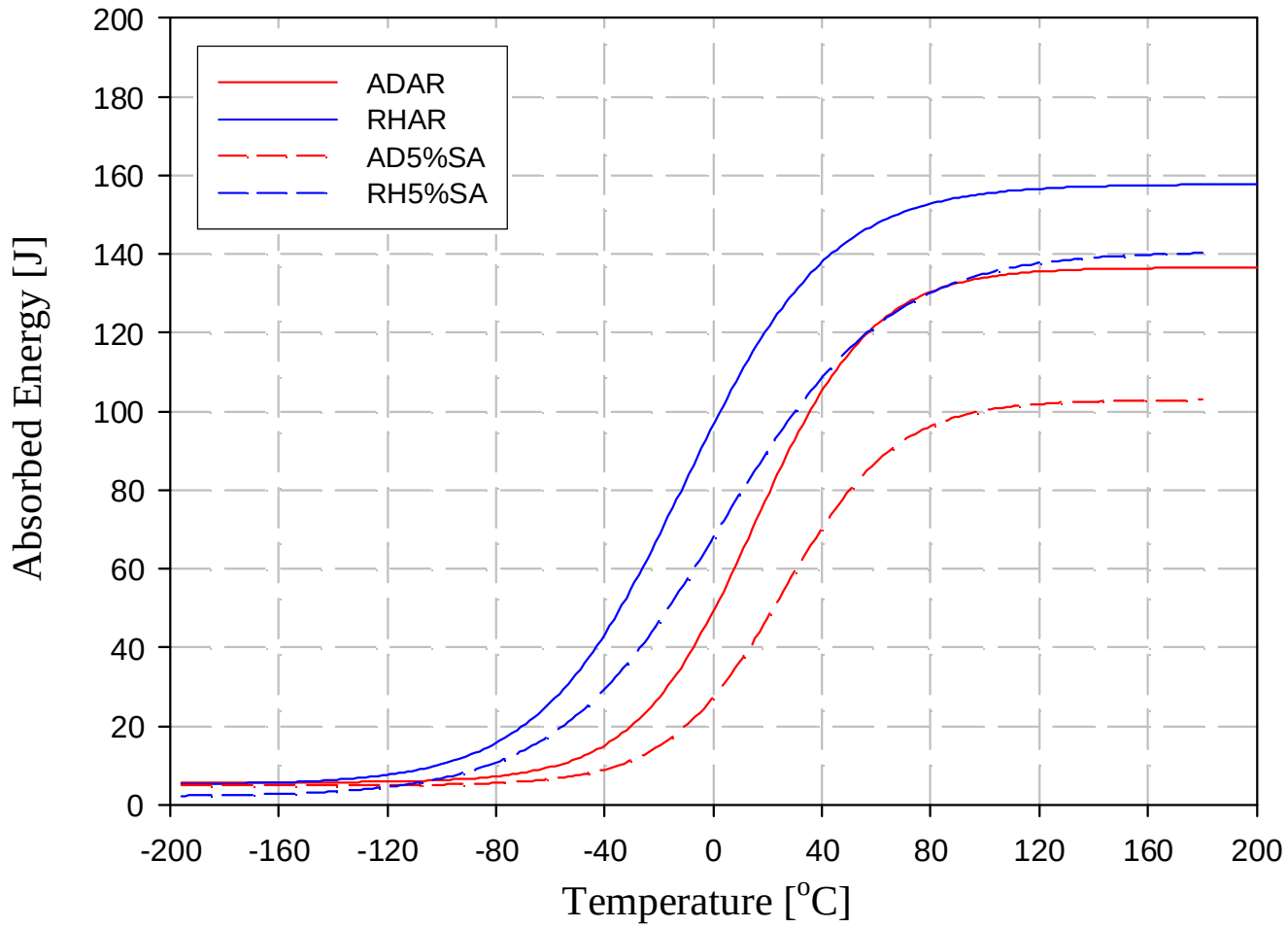

Figure 6.24 - Charpy Impact energy transition curves for Weld N°2 for both microstructure and in both weld metal conditions showing both 40J level and 40°C values.

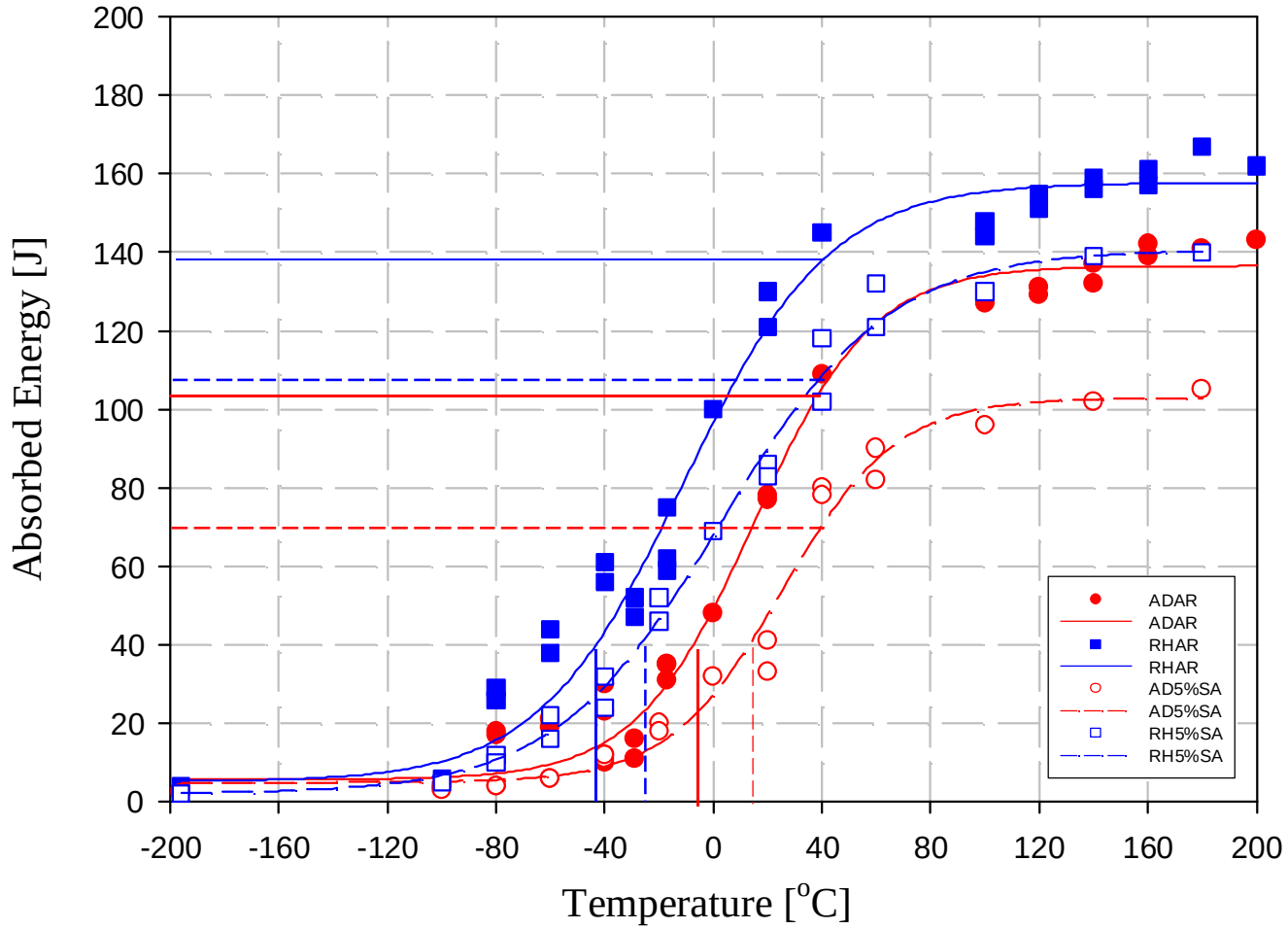

Figure 6.25 - Results from surface analysis of broken halves of Charpy specimens Weld N^{o}2 for both microstructural in both the as-received and strain aged conditions. (a) ductile thumbnail, DT; (b) lateral expansion, LE; (c) crystalline area, CA.

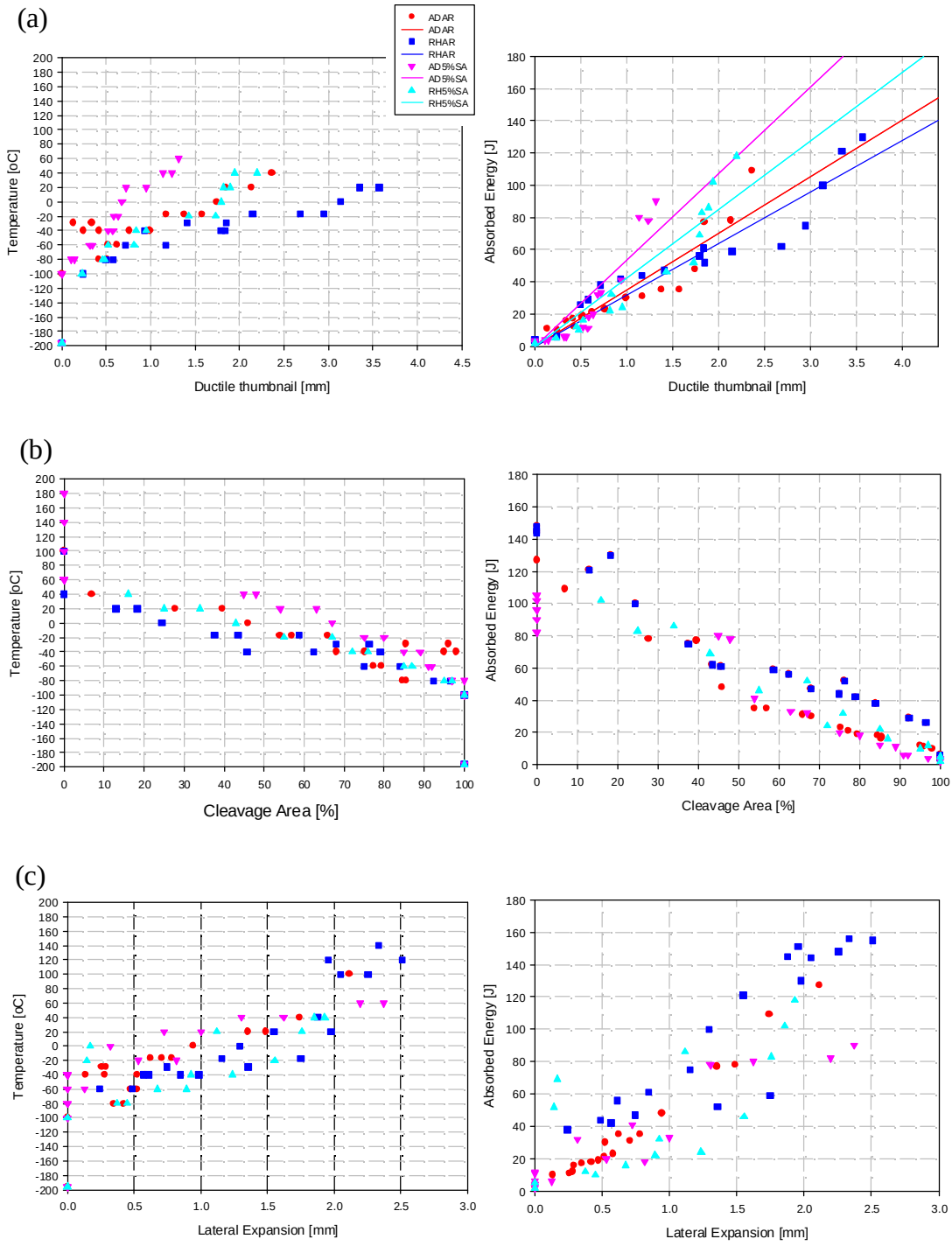

Figure 6.26 - Results from surface analysis of broken halves of Charpy specimens for Weld N°2 for both ADAR and RHAR conditions. (a) ductile thumbnail, DT; (b) lateral expansion, LE; (c) crystalline area, CA.

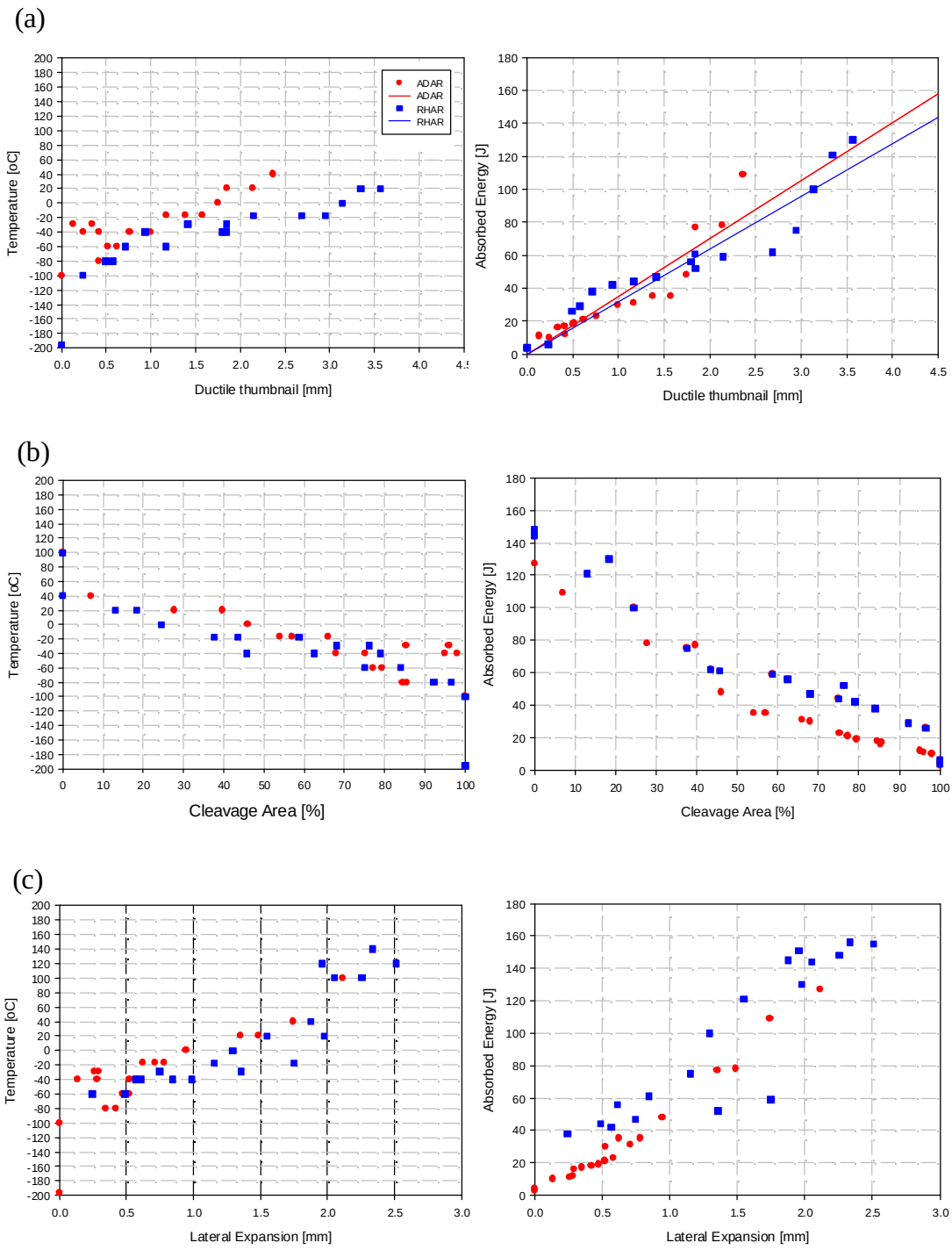

Figure 6.27 - Results from surface analysis of broken halves of Charpy specimens for Weld N°2 for both AD5%SA and RH5%SA conditions. (a) ductile thumbnail, DT; (b) lateral expansion, LE; (c) crystalline area, CA.

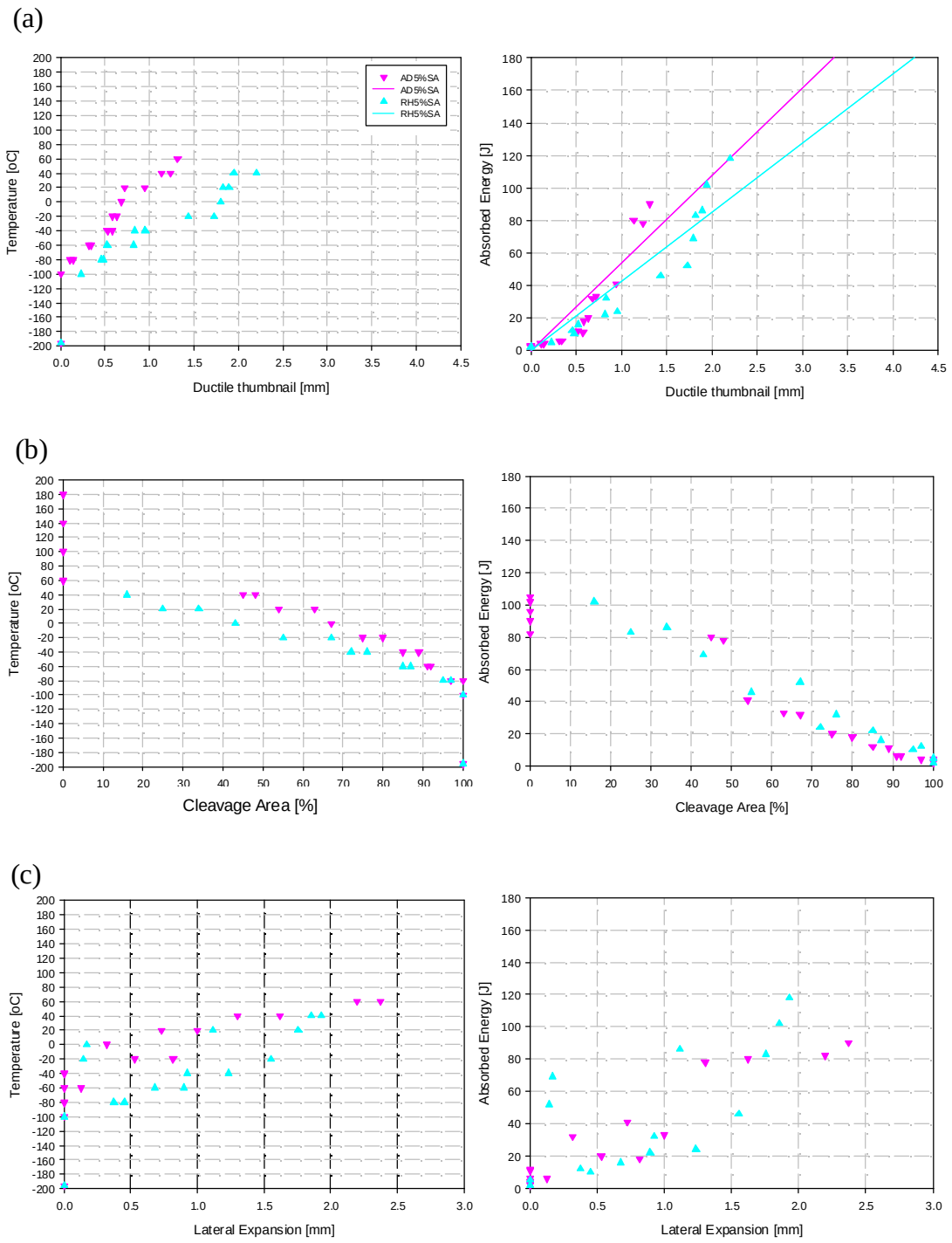

Figure 6.28 - Results from surface analysis of broken halves of Charpy specimens for Weld N°2 for the AD microstructure in the AR and 5%SA conditions. (a) ductile thumbnail, DT; (b) lateral expansion, LE; (c) crystalline area, CA.

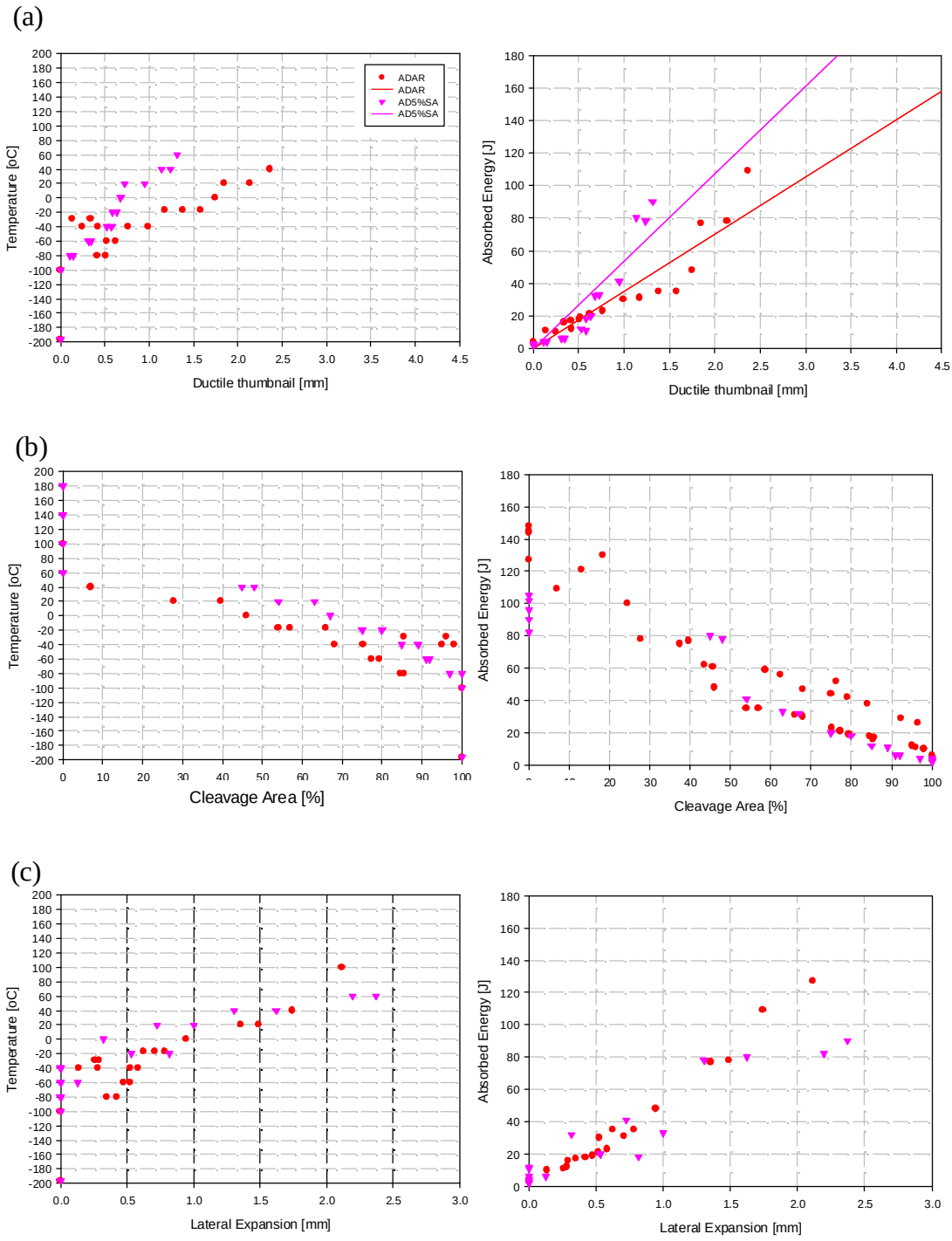

Figure 6.29 - Results from surface analysis of broken halves of Charpy specimens for Weld N°2 for the RH microstructure in the AR and 5%SA conditions. (a) ductile thumbnail, DT; (b) lateral expansion, LE; (c) crystalline area, CA.

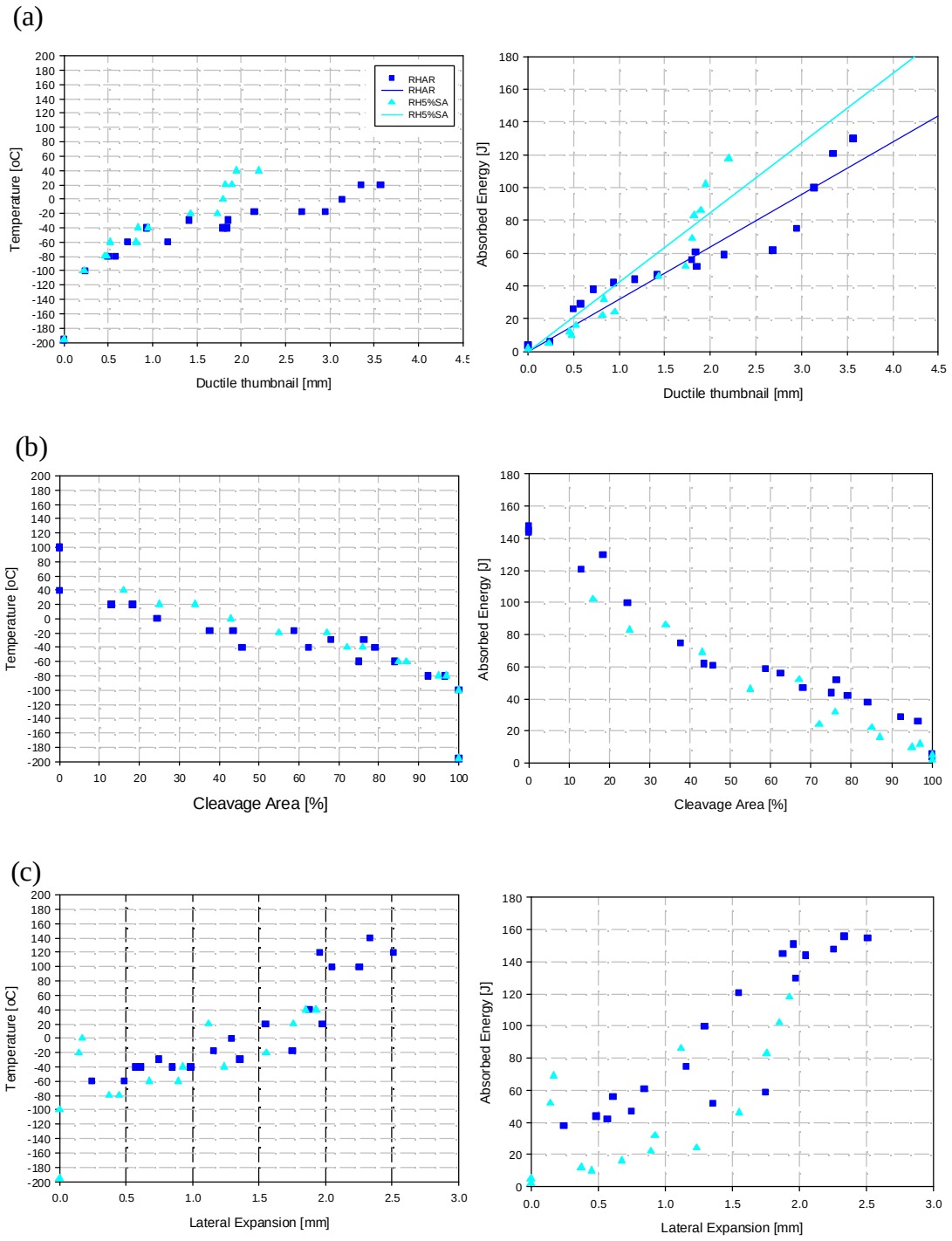

Figure 6.30 - Typical fracture surface of tensile specimens for the AD weld metal region tested at -196°C; (a) fracture surface exhibiting no localized deformation - necking, cleavage steps indicatewd with arrow, (b) cleavage fracture micromechanism.

(a)

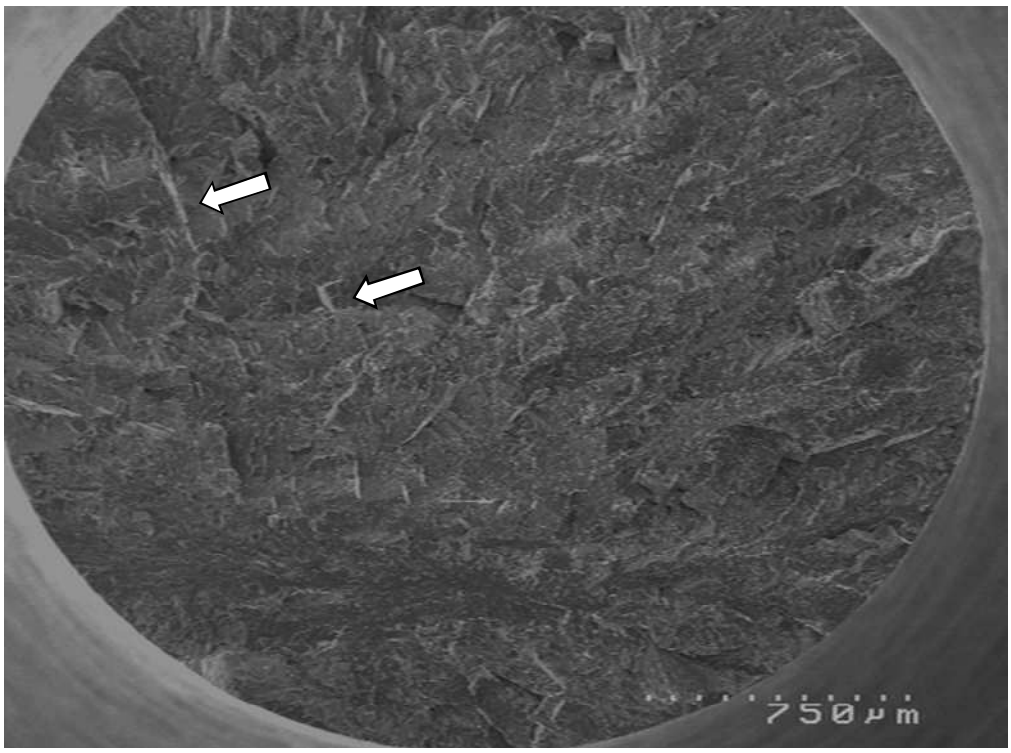

(b)

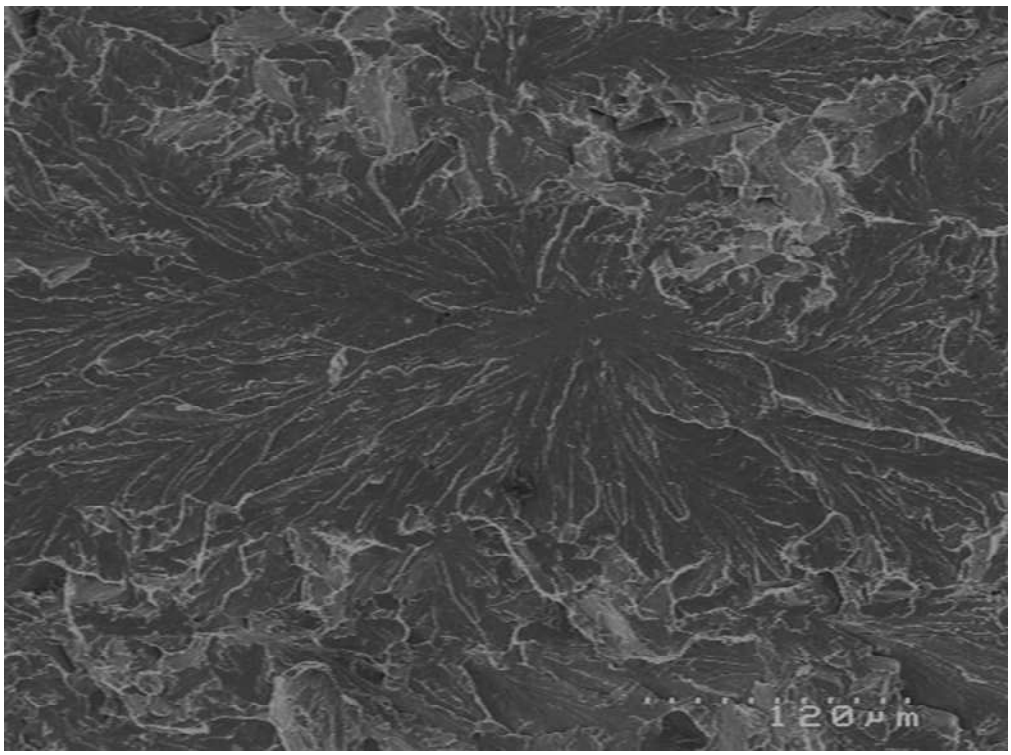

Figure 6.31 - Cleavage fracture initiation site at -196°C; (a) initiation site (framed); (b) magnification of site; (c) detail of initiation site.

(a)

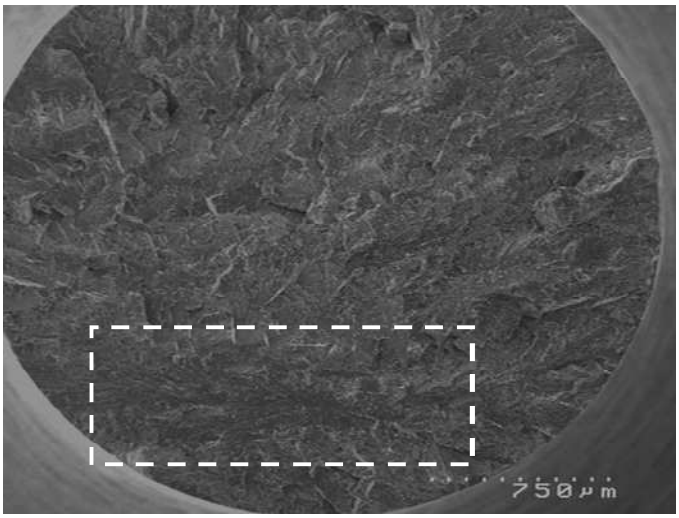

(b)

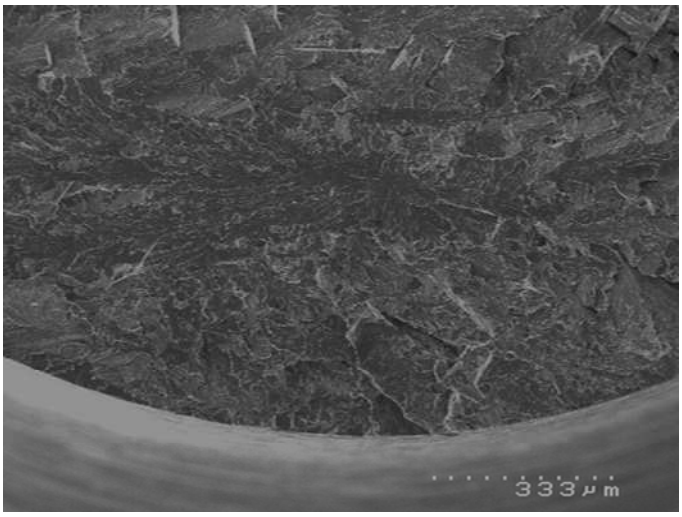

(c)

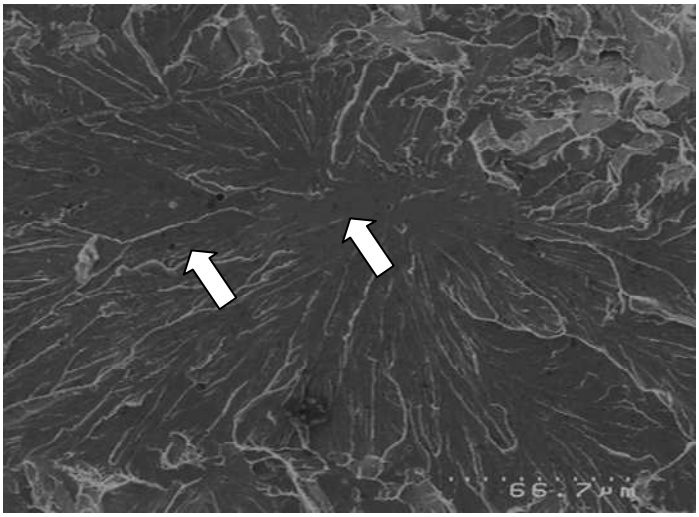

Figure 6.32 - Typical fracture surface of tensile specimens for the RH weld metal region tested at -196^{o}C; (a) fracture surface exhibiting reasonable deformation - necking, (b) Quasi - cleavage fracture micromechanism (cleavage facets surrounded by microvoids).

(a)

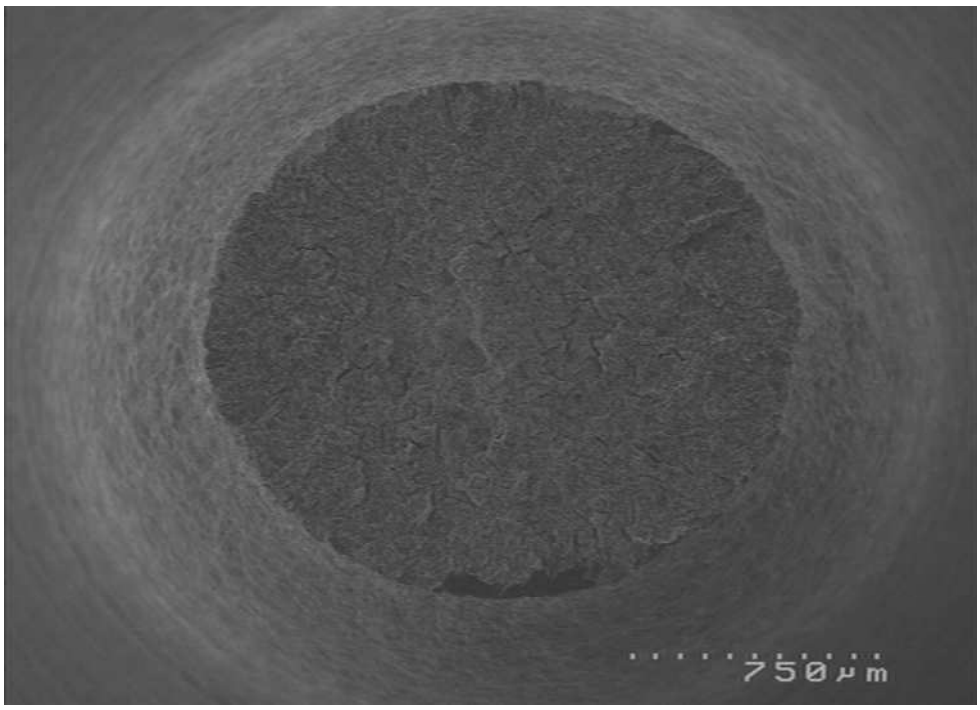

(b)

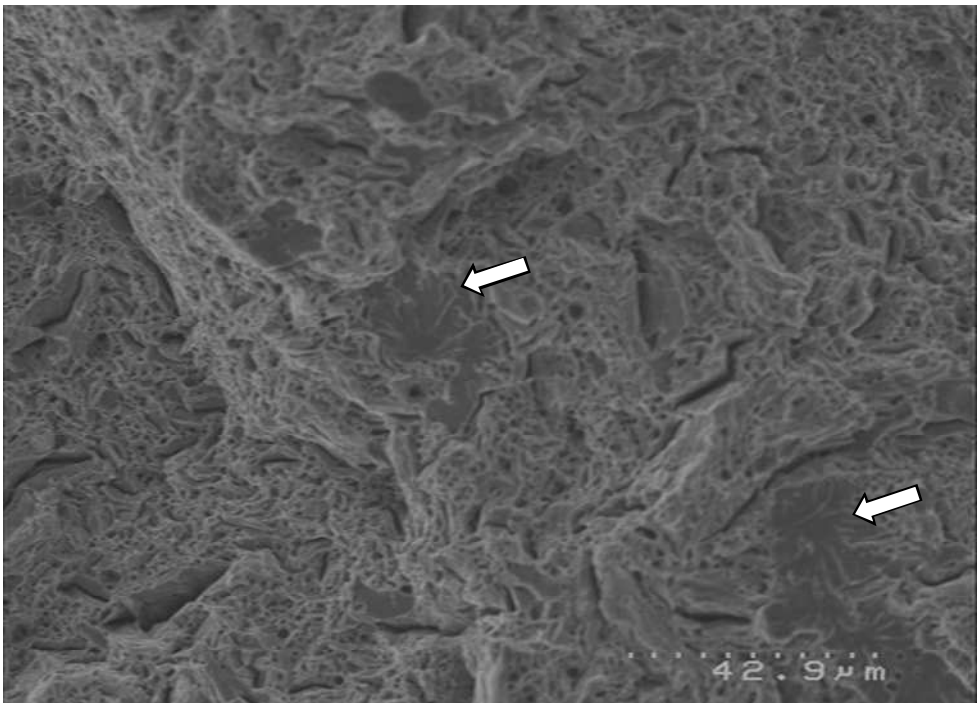

Figure 6.33 - Typical fracture surface of tensile specimen for the AD weld metal tested at 20^{o}C

(a)

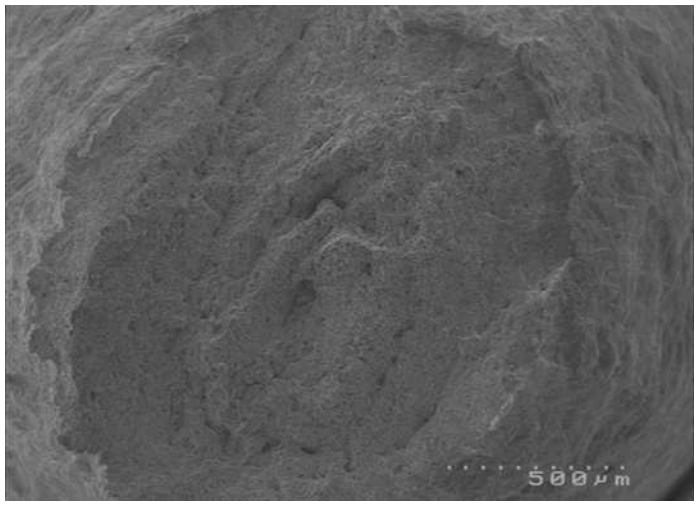

(b)

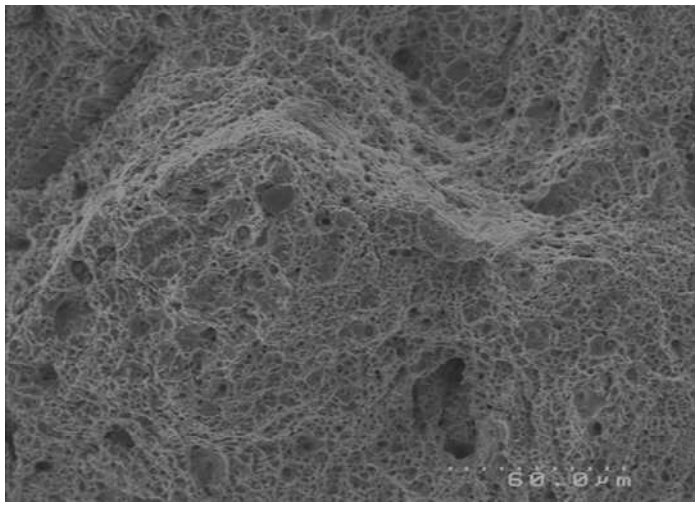

(c)

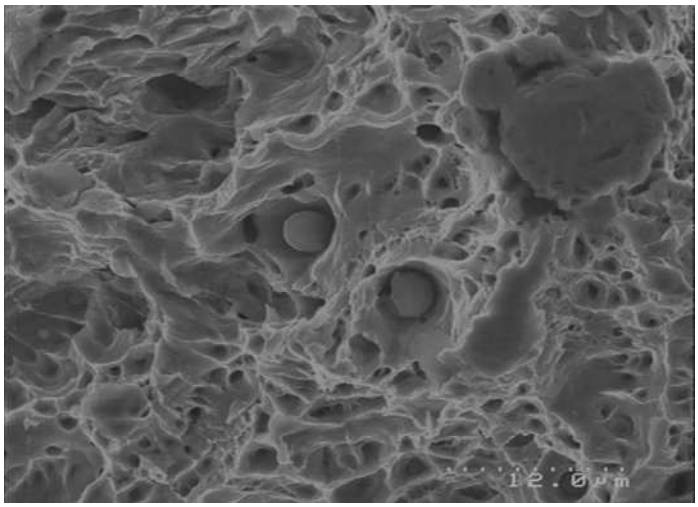

Figure 6.34 - Typical fracture surface of tensile specimen for the RH weld metal tested at 20°C

(a)

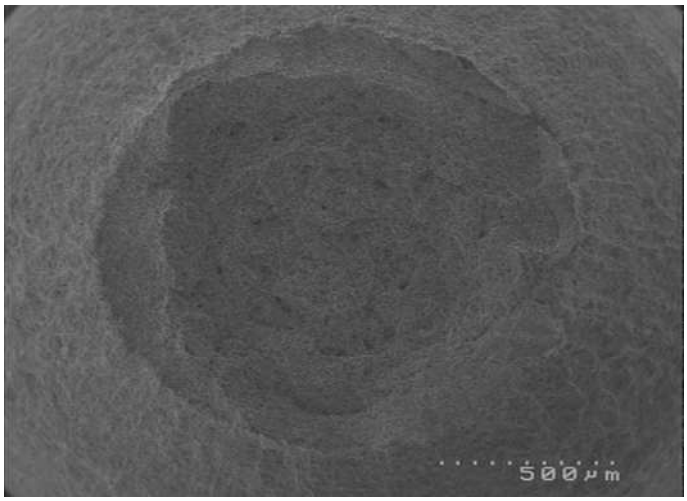

(b)

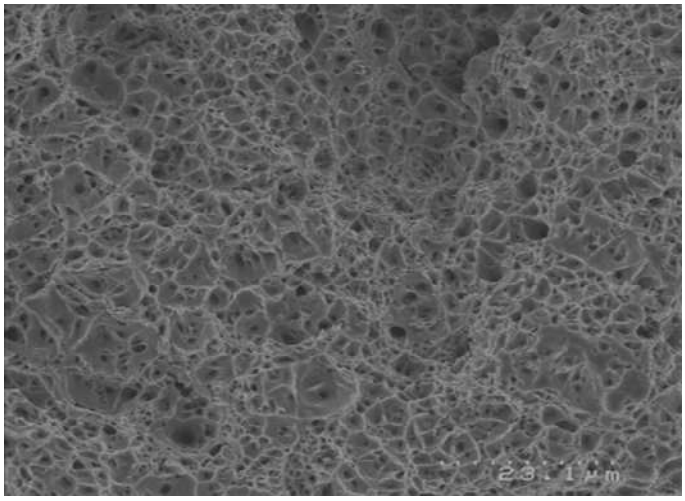

(c)

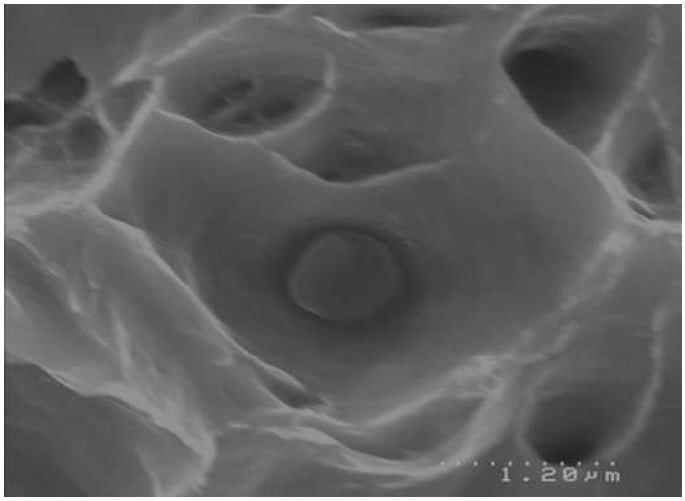

Figure 6.35 - Typical fracture surface of tensile specimen for the AD weld metal tested at -120°C; (a) fracture surface showing mixed fracture mechanisms; (b) magnification of cleavage steps and microvoid coalescence; (c) magnification of cleavage; (d) magnification of microvoid coalescence; (e) magnification of inclusions.

(a)

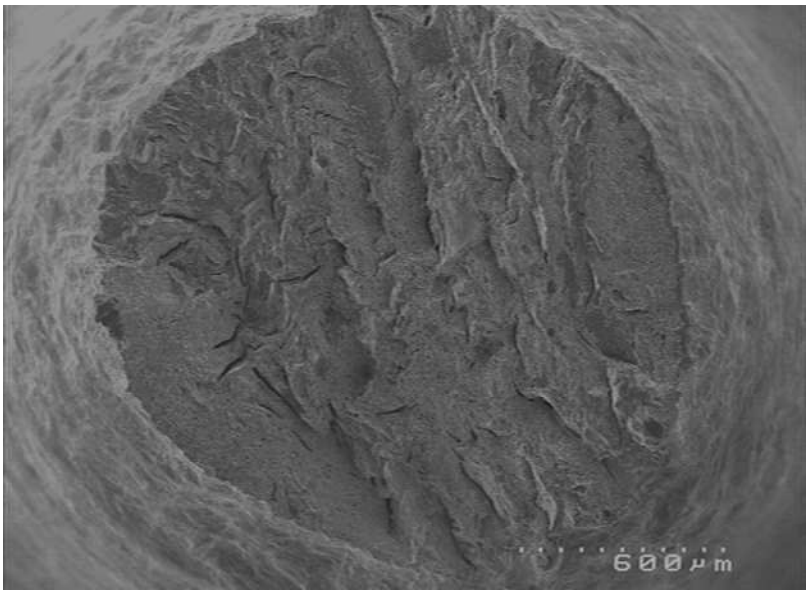

(b)

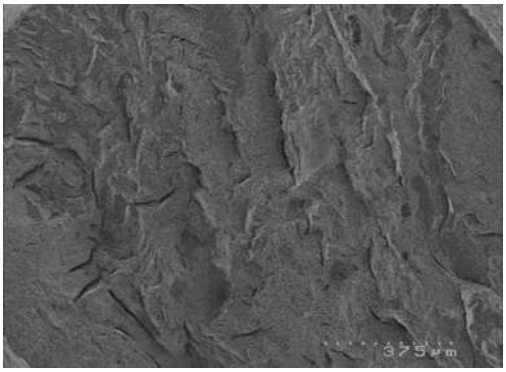

(d)

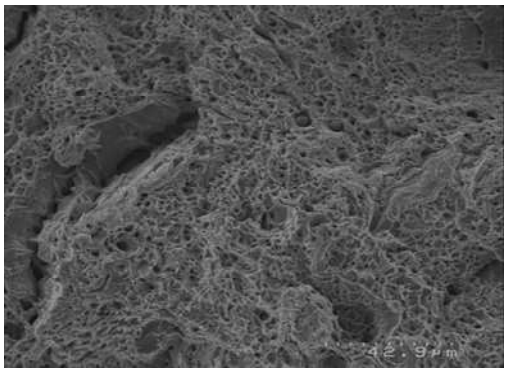

(c)

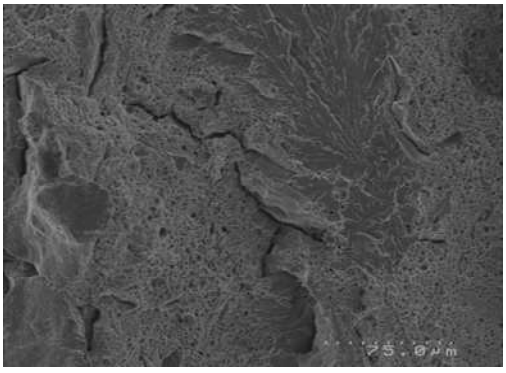

(e)

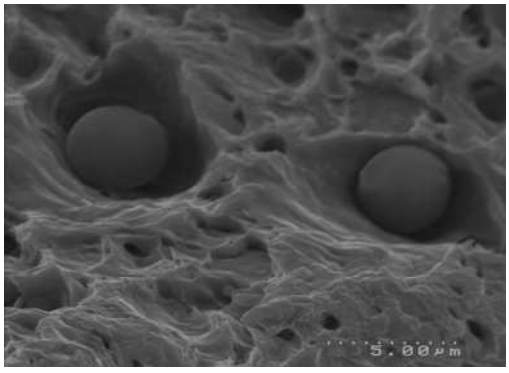

Figure 6.36 - Typical fracture surface of tensile specimen for the RH weld metal tested at -160^{o}C; (a) fracture surface showing quasi - cleavage fracture; (b) magnification of microvoid coalescence; (c) magnification of inclusions.

(a)

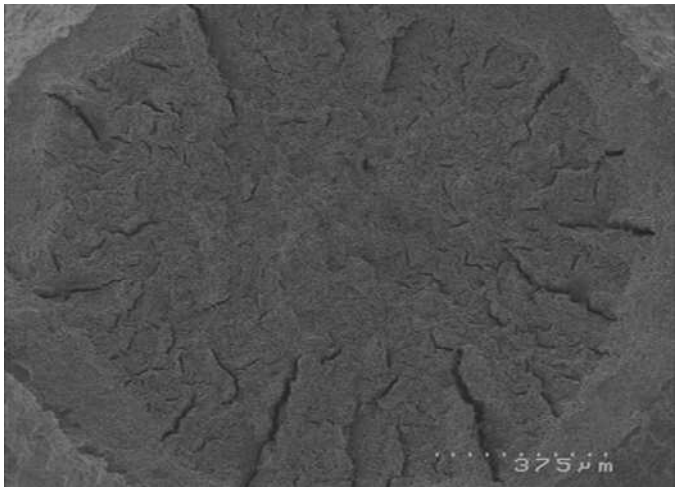

(b)

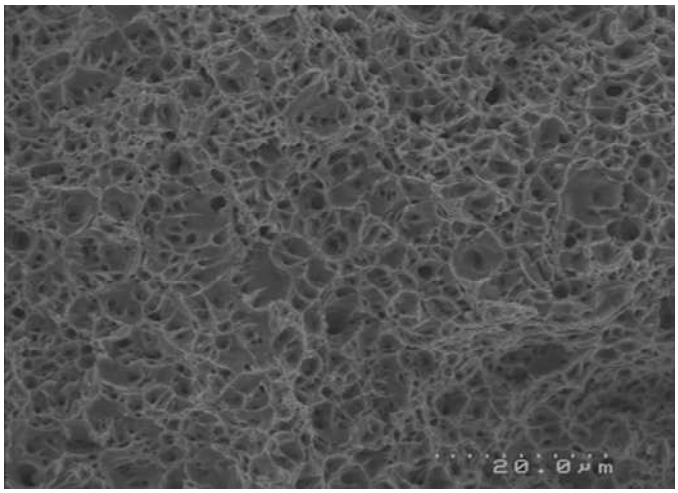

(c)

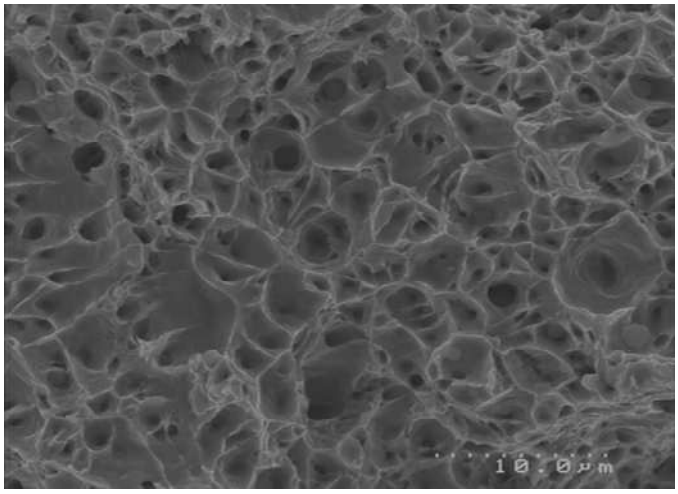

Figure 6.37 - Typical fracture surfaces for Mixed and Transverse microstructures; (a) tensile specimen 2, 8mm diameter, tested at -196 ^{o}C, (b) Tensile specimen 4, 8mm diameter, tested at -130 ^{o}C; (c) Tensile specimen 5, 8mm diameter, tested at -100 ^{o}C; (d) Tensile specimen 1, 8mm diameter, tested at 20 ^{o}C.

(a) (b)

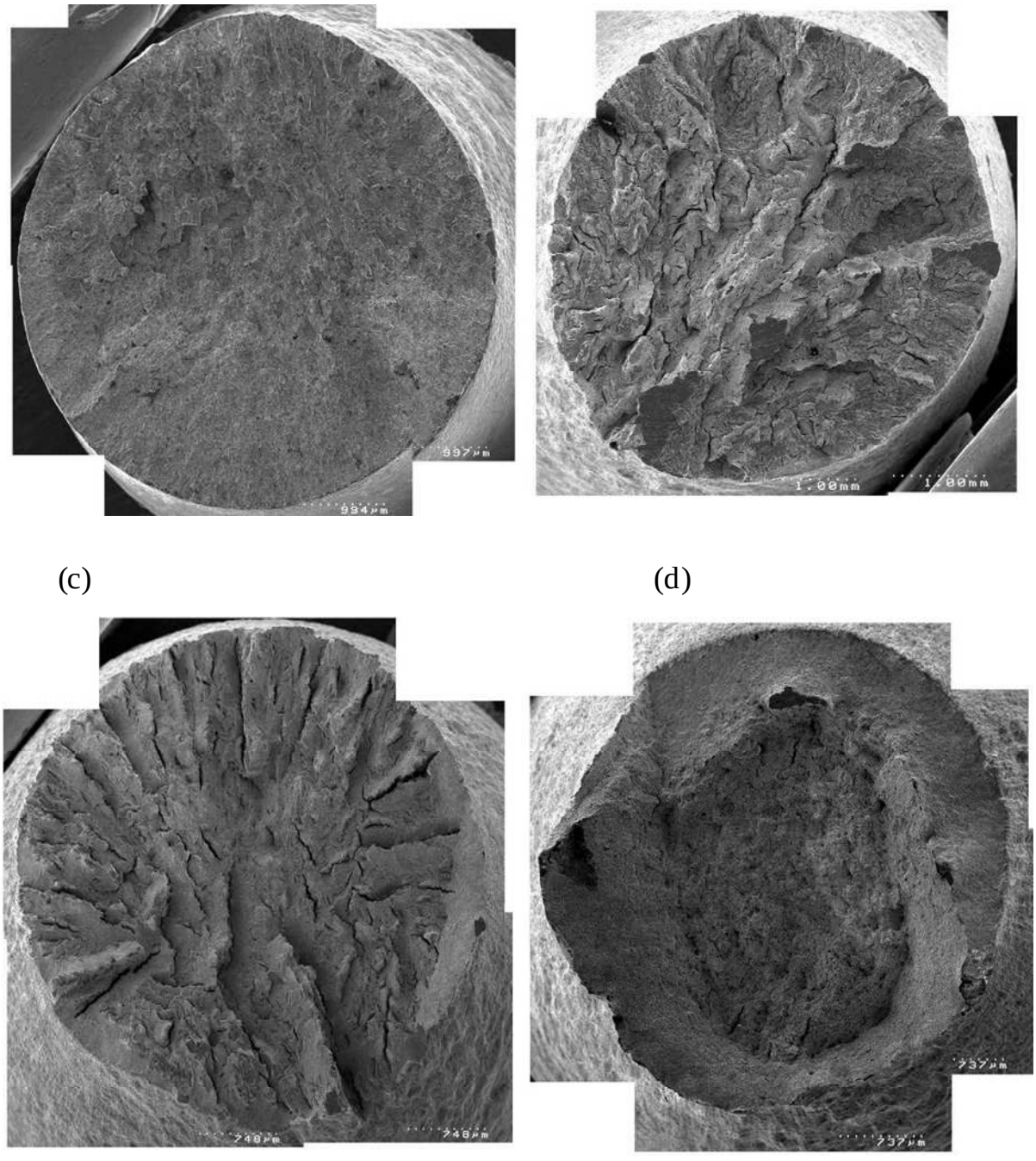

(c) (d)

Figure 6.38 - Typical fracture surfaces for Transverse microstructures; (a) typical fracture surface, tested at -196 ^{o}C; (b) magnification of quasi - cleavage fracture; (c) typical fracture surface, tested at -40^{o}C; (d) magnification of microvoid coalescence; (e) typical fracture surface, tested at 20^{o}C, (f) magnification of microvoid coalescence.

(a)

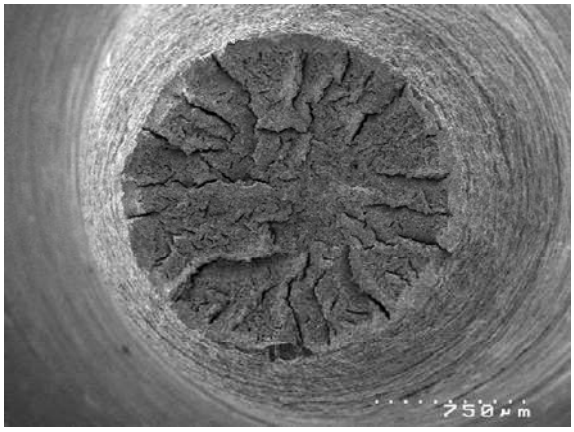

(b)

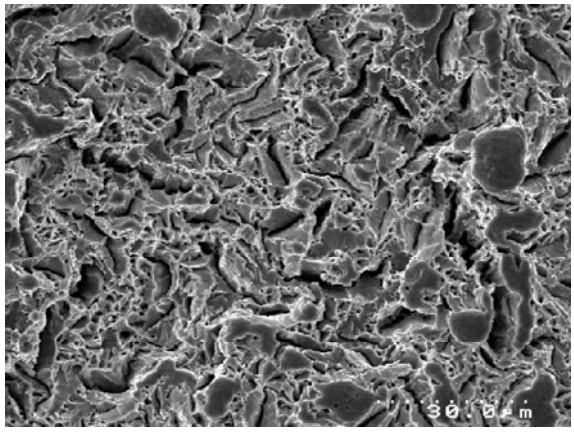

(c)

(d)

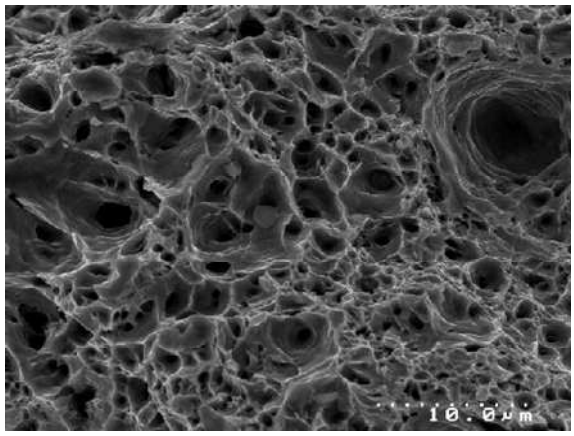

(e)

(f)

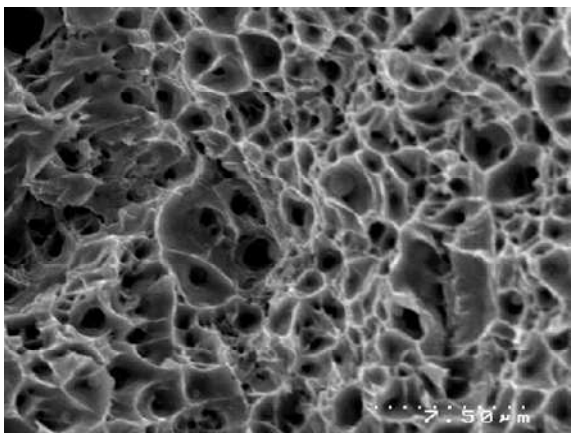

Figure 6.39 - Charpy impact fracture surfaces for the ADAR microstructural condition.

Spec	°C	J
1AD	-17	35

Spec	°C	J
3AD	100	127

Spec	°C	J
5AD	40	109

Spec	°C	J
7AD	20	77

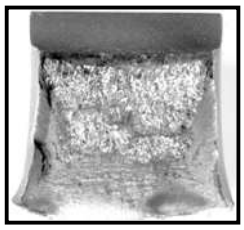

Spec	°C	J
9AD	20	78

Spec	°C	J
11AD	-17	31

Spec	°C	J
13AD	-17	35

Spec	°C	J
15AD	-196	3

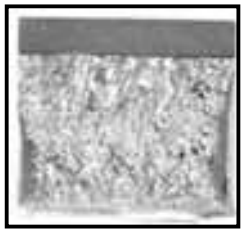

Spec	°C	J
17AD	-40	12

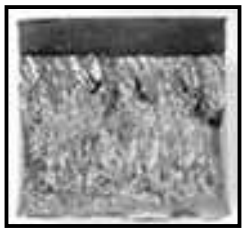

Spec	°C	J
19AD	-80	18

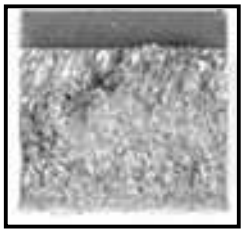

Spec	°C	J
21AD	-80	17

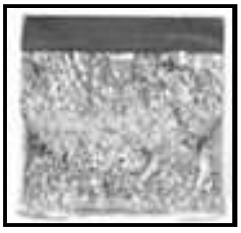

Spec	°C	J
23AD	-40	10

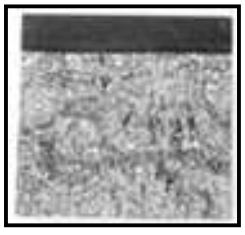

Spec	°C	J
25AD	-100	4

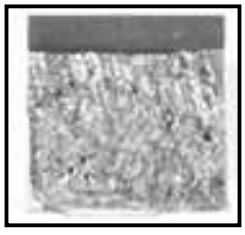

Spec	°C	J
27AD	-29	16

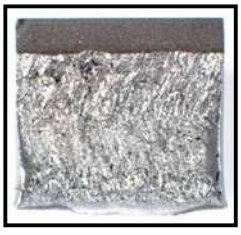

Spec	°C	J
29AD	-29	11

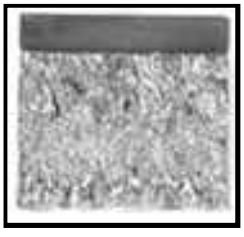

Spec	°C	J
31AD	-60	19

Figure 6.39 - Charpy impact fracture surfaces for the ADAR microstructural condition.

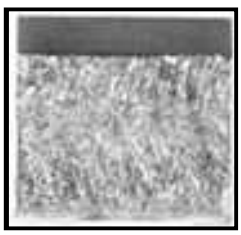

Spec	°C	J
33AD	-60	21

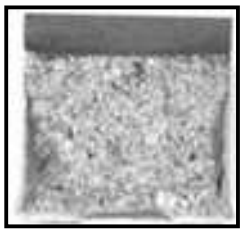

Spec	°C	J
35AD	-40	23

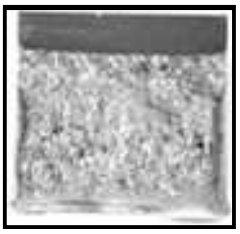

Spec	°C	J
37AD	-40	30

Spec	°C	J
39AD	0	48

Figure 6.40 - Charpy impact fracture surfaces for the RHAR microstructural condition.

Spec	°C	J
2RH	100	144

Spec	°C	J
4RH	100	148

Spec	°C	J
6RH	40	145

Spec	°C	J
8RH	20	130

Spec	°C	J
10RH	20	121

Spec	°C	J
12RH	-17	59

Spec	°C	J
14RH	-17	62

Spec	°C	J
16RH	-196	4

Spec	°C	J
18RH	-40	56

Spec	°C	J
20RH	-80	26

Spec	°C	J
22RH	-80	29

Spec	°C	J
24RH	-100	6

Spec	°C	J
26RH	-40	42

Spec	°C	J
30RH	-29	47

Spec	°C	J
28RH	-29	52

Spec	°C	J
32RH	-60	38

Figure 6.40 - Charpy impact fracture surfaces for the RHAR microstructural condition.

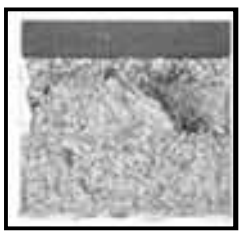

Spec	°C	J
34RH	-60	44

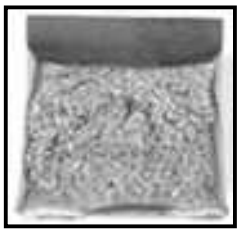

Spec	°C	J
36RH	-40	61

Spec	°C	J
38RH	-17	75

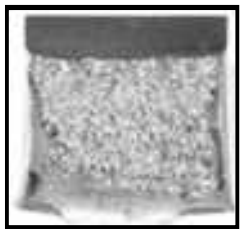

Spec	°C	J
40RH	0	100

Figure 6.41 - Charpy impact fracture surfaces for the AD5%SA microstructural condition.

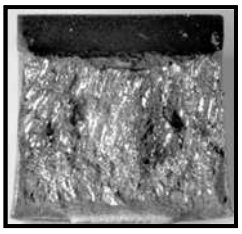

Spec	°C	J
1AD	-20	20

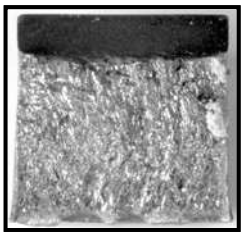

Spec	°C	J
3AD	-20	18

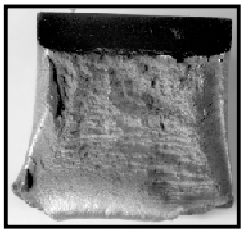

Spec	°C	J
5AD	100	96

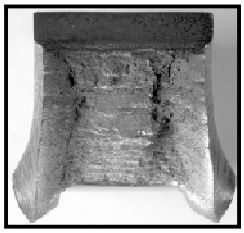

Spec	°C	J
7AD	180	105

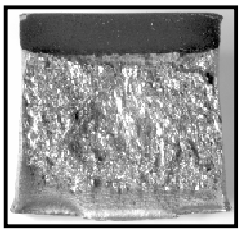

Spec	°C	J
9AD	20	41

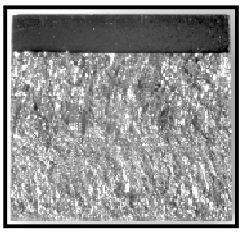

Spec	°C	J
11AD	-80	4

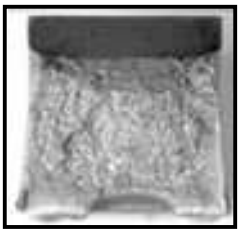

Spec	°C	J
13AD	20	33

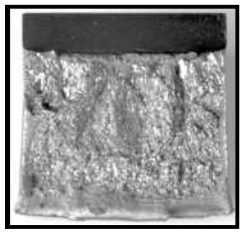

Spec	°C	J
15AD	-60	6

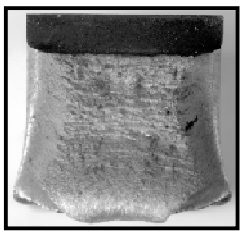

Spec	°C	J
17AD	140	102

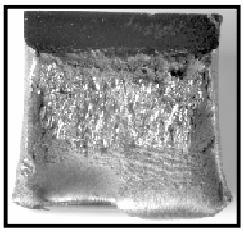

Spec	°C	J
19AD	40	80

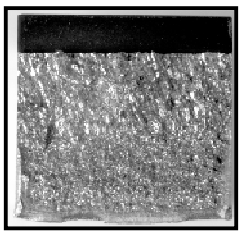

Spec	°C	J
21AD	-60	6

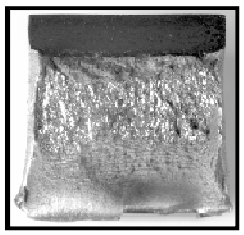

Spec	°C	J
23AD	40	78

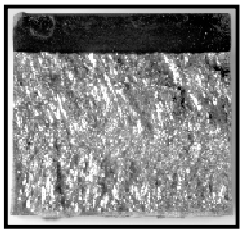

Spec	°C	J
25AD	-40	11

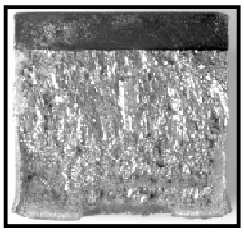

Spec	°C	J
27AD	0	32

Spec	°C	J
29AD	-40	12

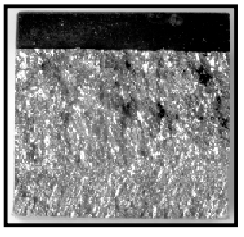

Spec	°C	J
31AD	-80	4

Figure 6.41 - Charpy impact fracture surfaces for the AD5%SA microstructural condition.

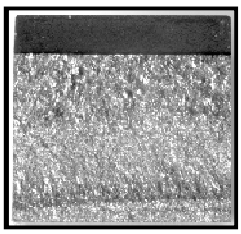

Spec	°C	J
33AD	-196	2

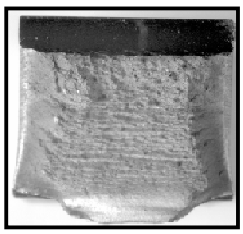

Spec	°C	J
35AD	60	90

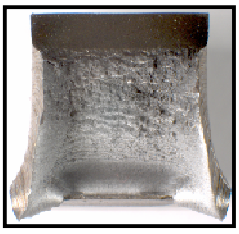

Spec	°C	J
37AD	60	82

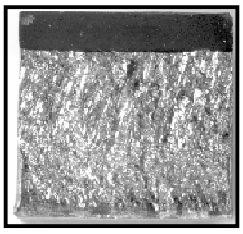

Spec	°C	J
39AD	-100	3

Figure 6.42 - Charpy impact fracture surfaces for the RH5%SA microstructural condition.

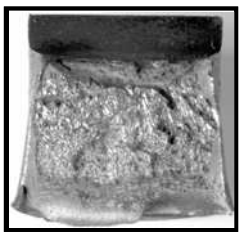

Spec	°C	J
2RH	-20	52

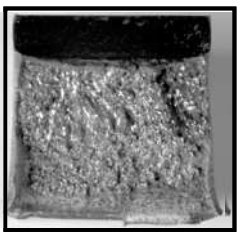

Spec	°C	J
4RH	-20	46

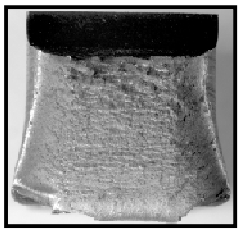

Spec	°C	J
6RH	100	130

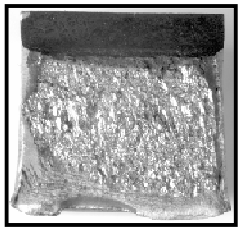

Spec	°C	J
8RH	20	86

Spec	°C	J
10RH	180	140

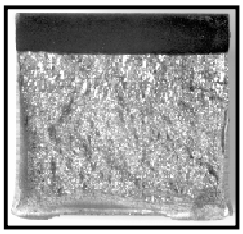

Spec	°C	J
12RH	-60	16

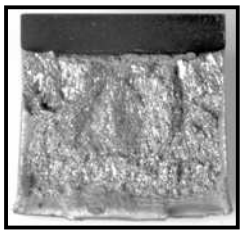

Spec	°C	J
14RH	20	83

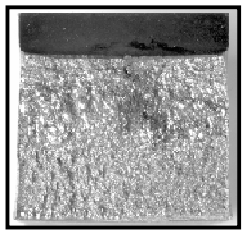

Spec	°C	J
16RH	-80	12

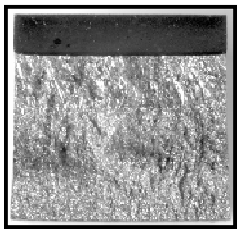

Spec	°C	J
18RH	-100	5

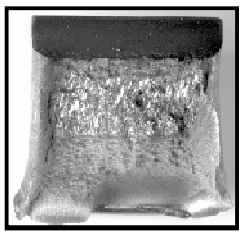

Spec	°C	J
20RH	40	102

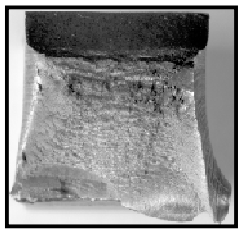

Spec	°C	J
22RH	140	139

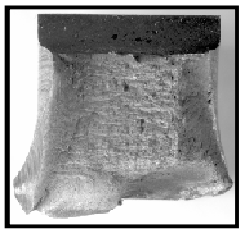

Spec	°C	J
24RH	40	118

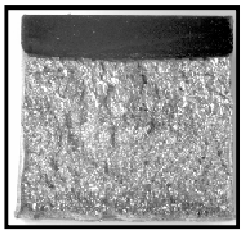

Spec	°C	J
26RH	-40	32

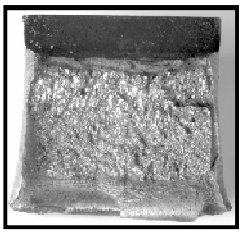

Spec	°C	J
28RH	0	69

Spec	°C	J
30RH	-40	24

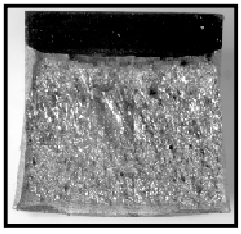

Spec	°C	J
32RH	-60	22

Figure 6.42 - Charpy impact fracture surfaces for the RH5%SA microstructural condition.

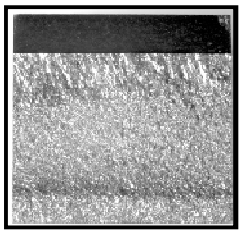

Spec	°C	J
34RH	-196	2

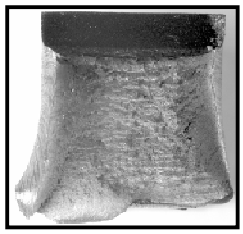

Spec	°C	J
36RH	60	121

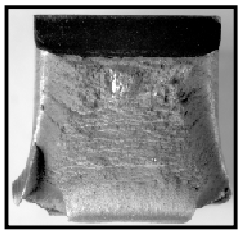

Spec	°C	J
38RH	60	132

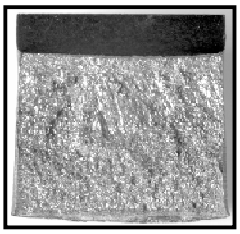

Spec	°C	J
40RH	-80	10

Figure 6.43 - Charpy impact fracture surfaces showing cleavage fracture through the transition region to fully ductile fracture.

Spec	°C	J
15AD	-196	3

Spec	°C	J
11AD	-17	31

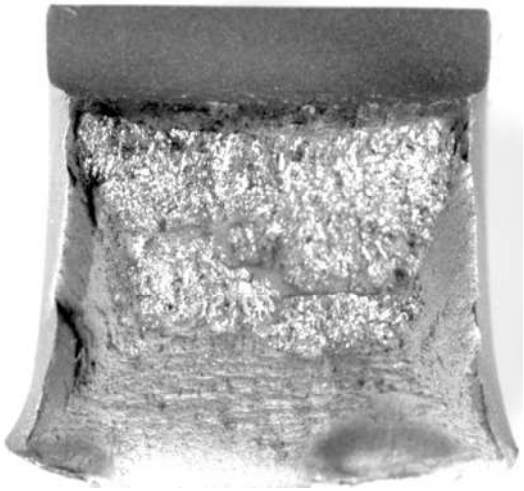

Spec	°C	J
9AD	20	78

Spec	°C	J
3AD	100	127

Figure 6.44 - Comparison between cleavage facets on the fracture surface for the AD and RH microstructure structure tested at -196^{o}C for both the as - received (AR) and the strain - aged (5%SA) conditions.

ADAR

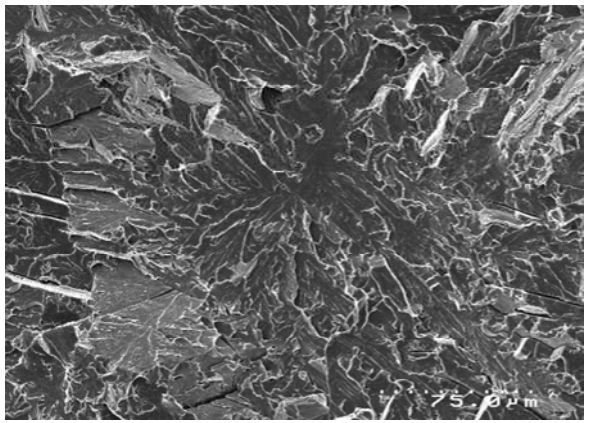

RHAR

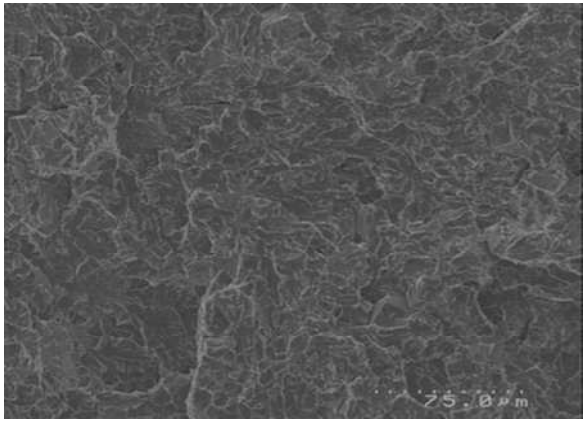

AD5%SA

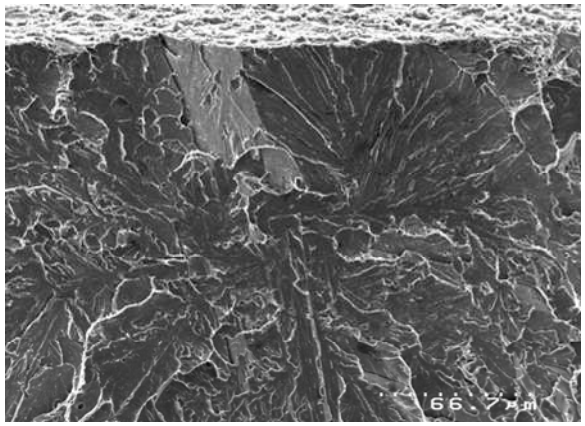

RH5%SA

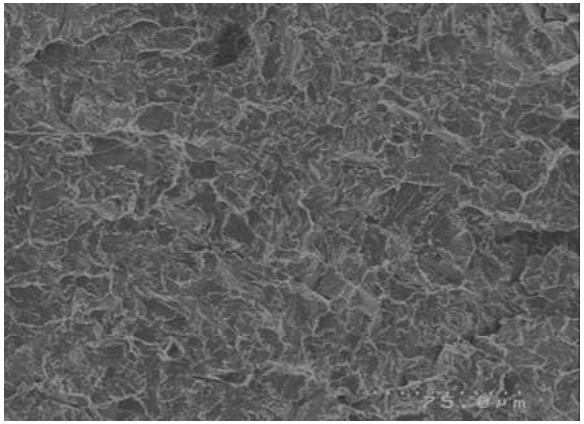

Figure 6.45 - Cleavage initiation site located on an ADAR specimen tested at -80°C; (a) overall cleavage initiation site, arrowed; (b) magnification of cleavage region with cleavage steps arrowed with secondary cracks; (c) magnification of the initiation site.

(a)

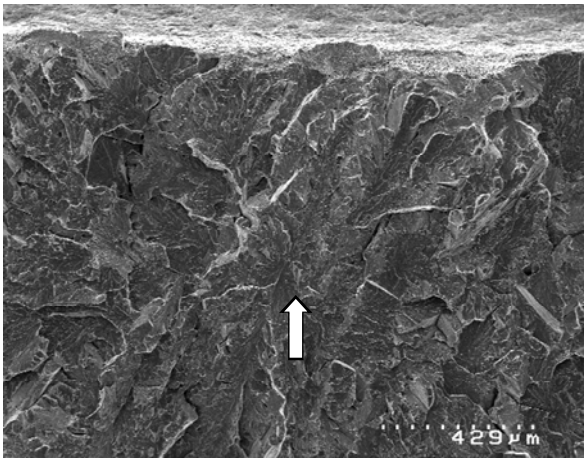

(b)

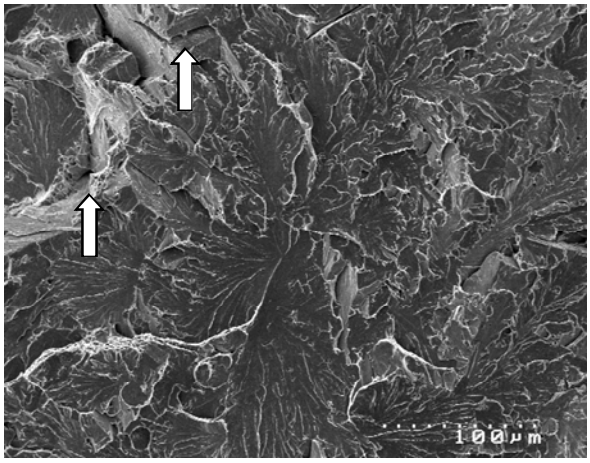

(c)

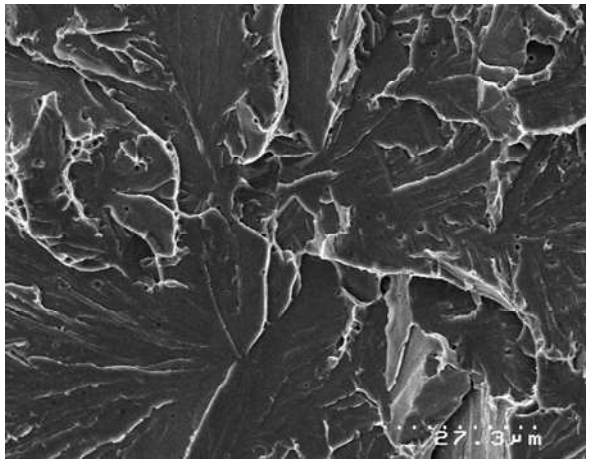

Figure 6.46 - Cleavage initiation site located on an ADAR specimen tested at -80°C; (a) overall cleavage initiation site, arrowed; (b) magnification of cleavage region with secondary crack through site; (c) magnification of the initiation site.

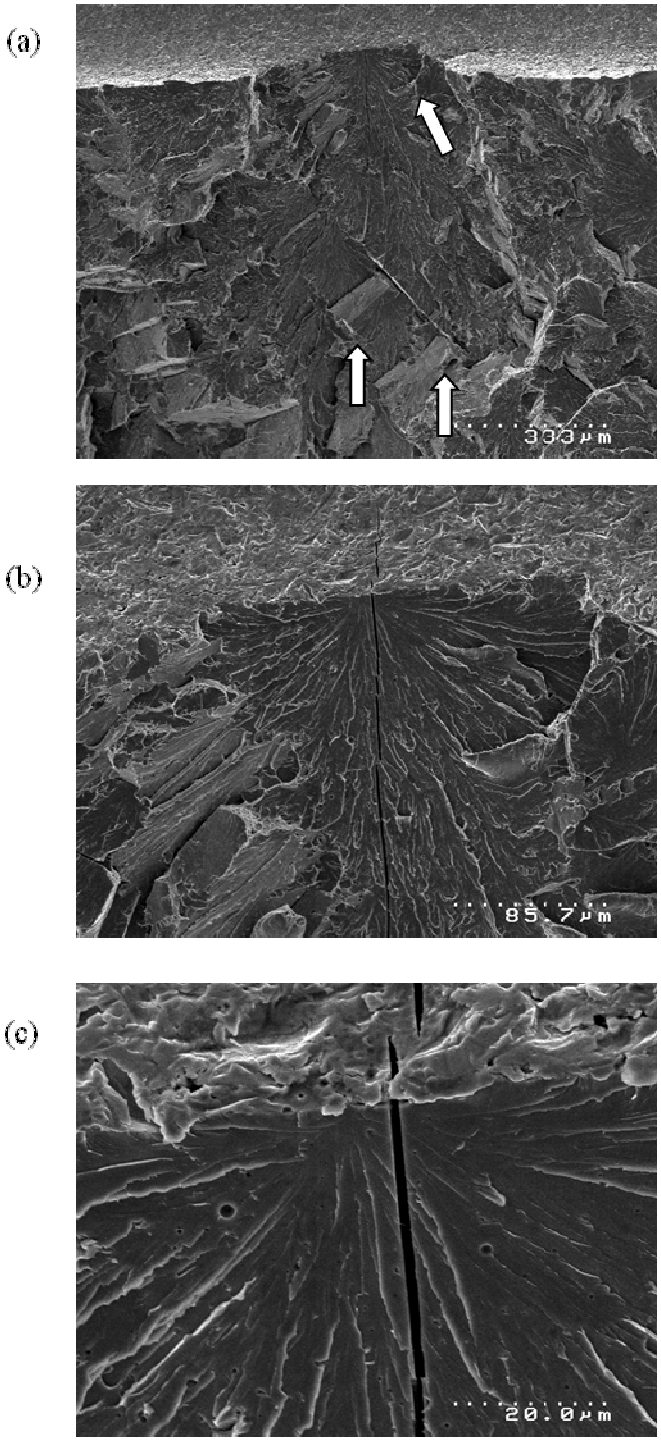

Figure 6.47 - Cleavage initiation site located on an AD5%SA specimen tested at -196°C; (a) overall cleavage initiation site, arrowed; (b) magnification of cleavage region; (c) magnification of the initiation site showing several inclusions.

(a)

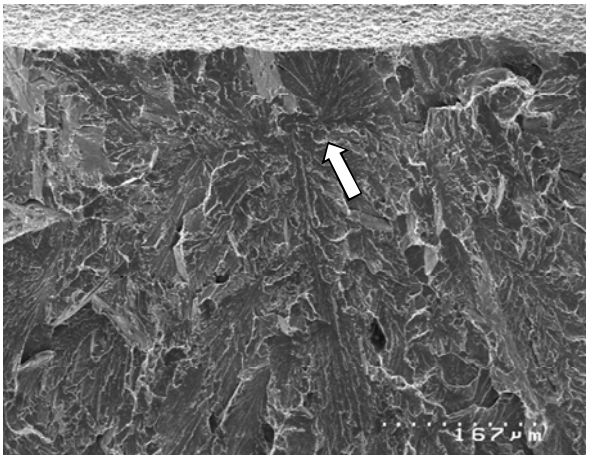

(b)

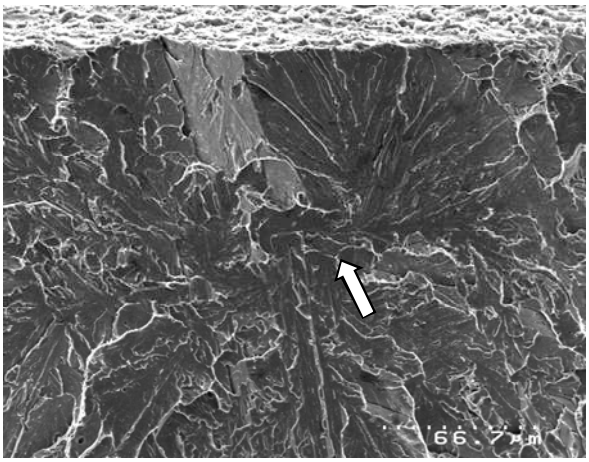

(c)

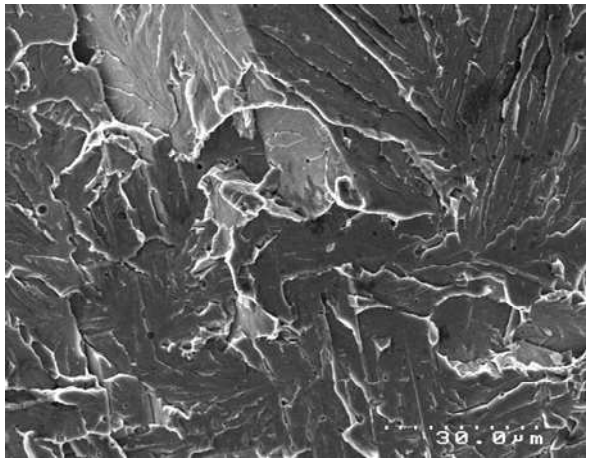

Figure 6.48 - Cleavage initiation site located on an AD5%SA specimen tested at -100°C; (a) overall cleavage initiation site, arrowed also arrowed are cleavage steps; (b) magnification of cleavage region with secondary cracks; (c) magnification of the initiation site showing inclusions at the centre.

(a)

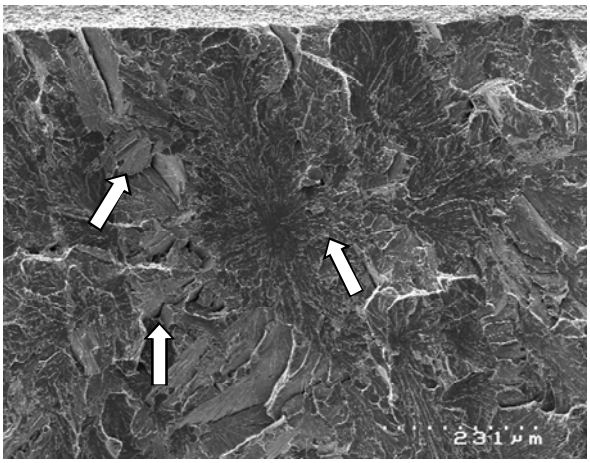

(b)

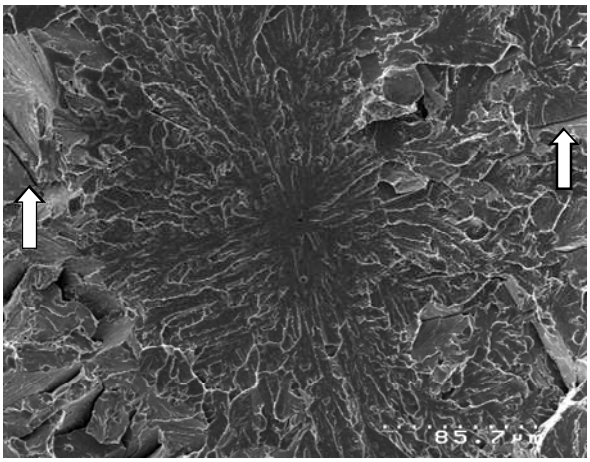

(c)

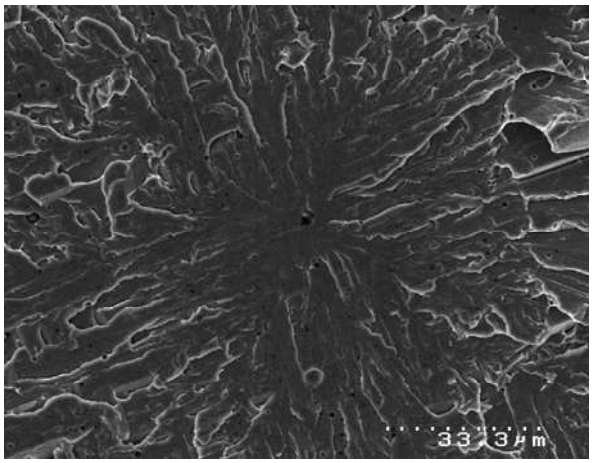

Figure 6.49 - Cleavage initiation site located on an RHAR specimen tested at -100°C; (a) overall cleavage initiation site, arrowed also arrowed are cleavage steps; (b) magnification of cleavage region with secondary cracks; (c) magnification of the initiation site showing inclusions at the centre.

(a)

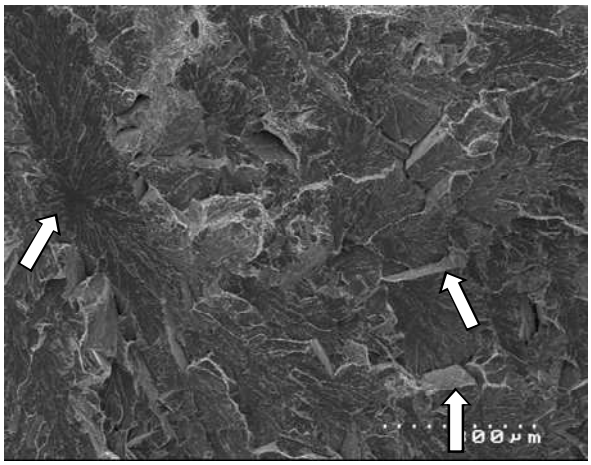

(b)

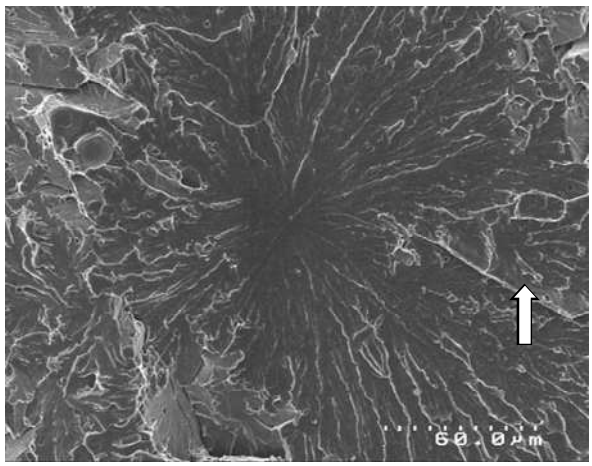

(c)

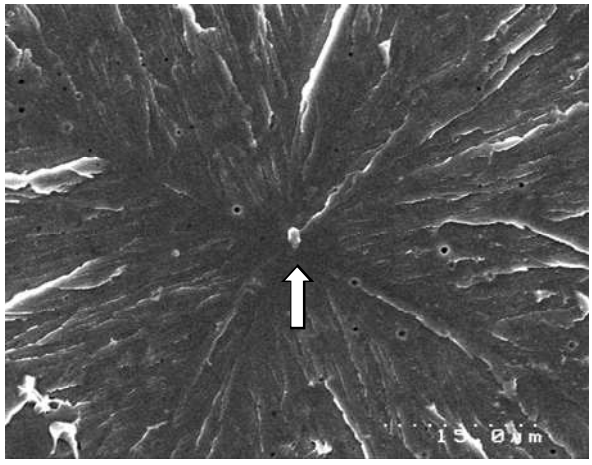

Figure 6.50 - Cleavage initiation site located on an RH5%SA specimen tested at -196°C; (a) overall cleavage initiation site, arrowed also arrowed are cleavage steps; (b) magnification of cleavage region with secondary cracks; (c) magnification of the initiation site showing several inclusions.

(a)

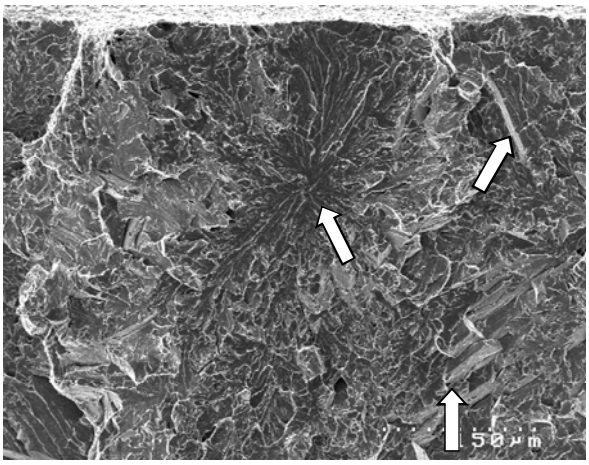

(b)

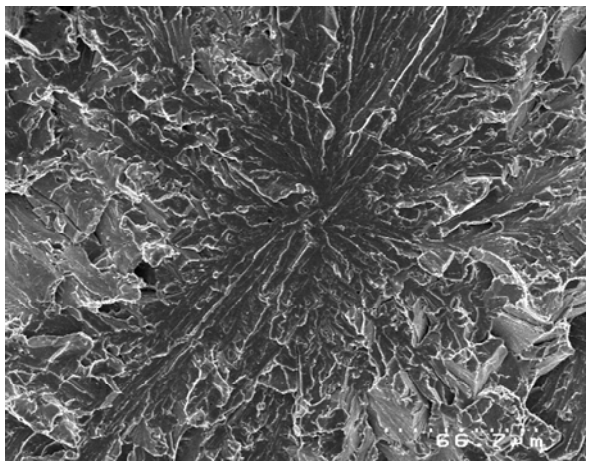

(c)

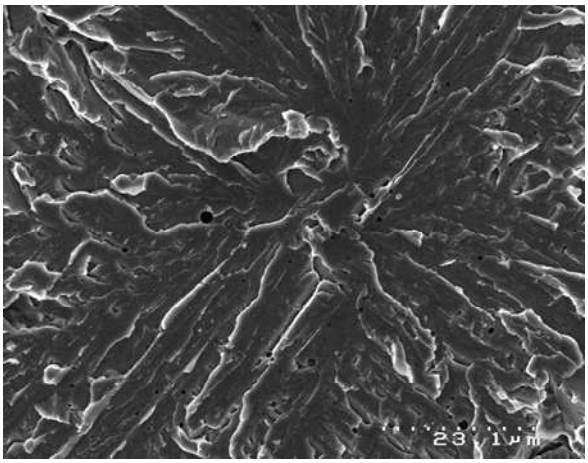

Figure 6.51 - General appearance of microvoids on the fracture surface for the AD Charpy specimens in the as - received condition, tested on the upper shelf.

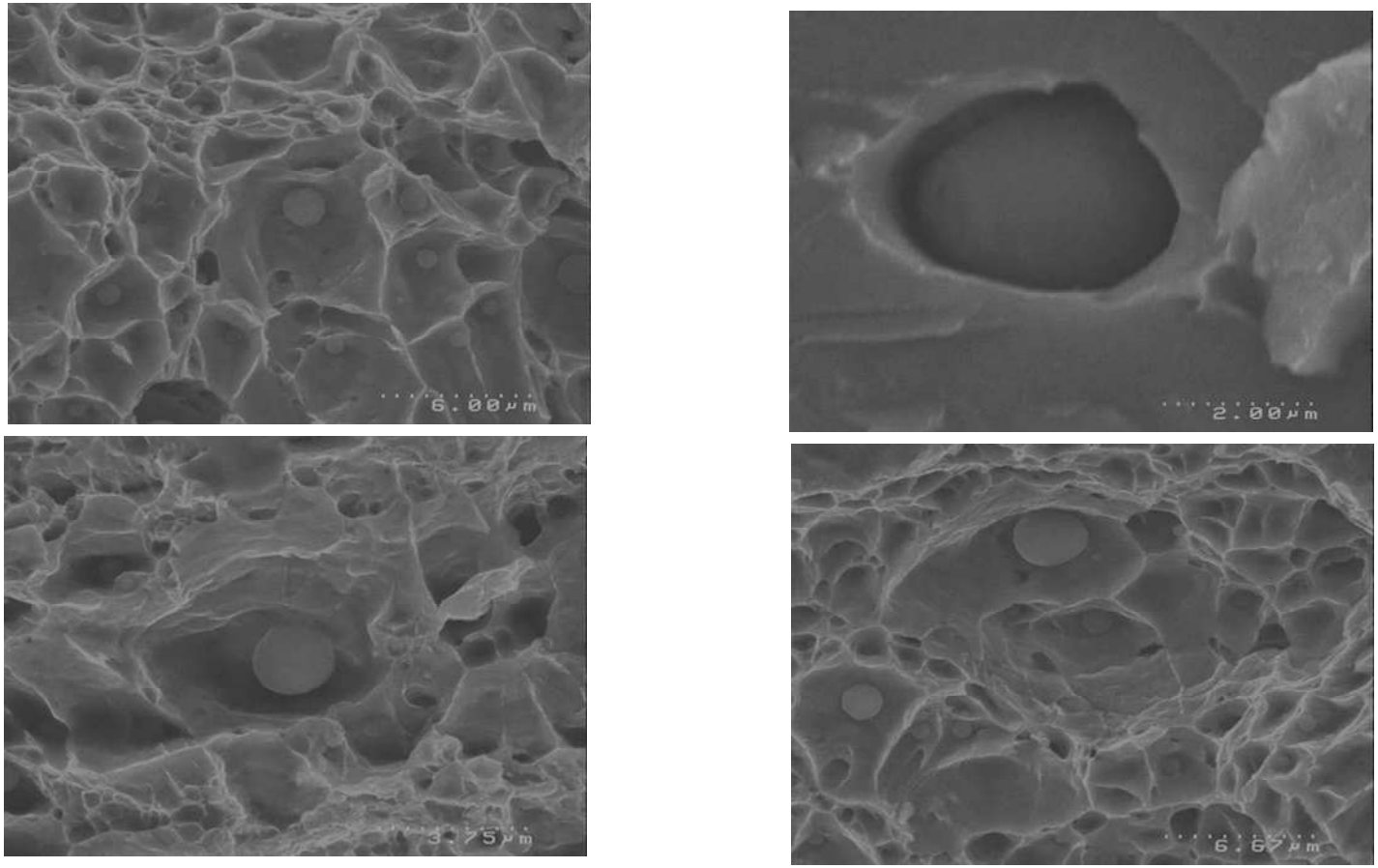

Figure 6.52 - General appearance of microvoids on the fracture surface for the RH Charpy specimens in the as - received condition, tested on the upper shelf.

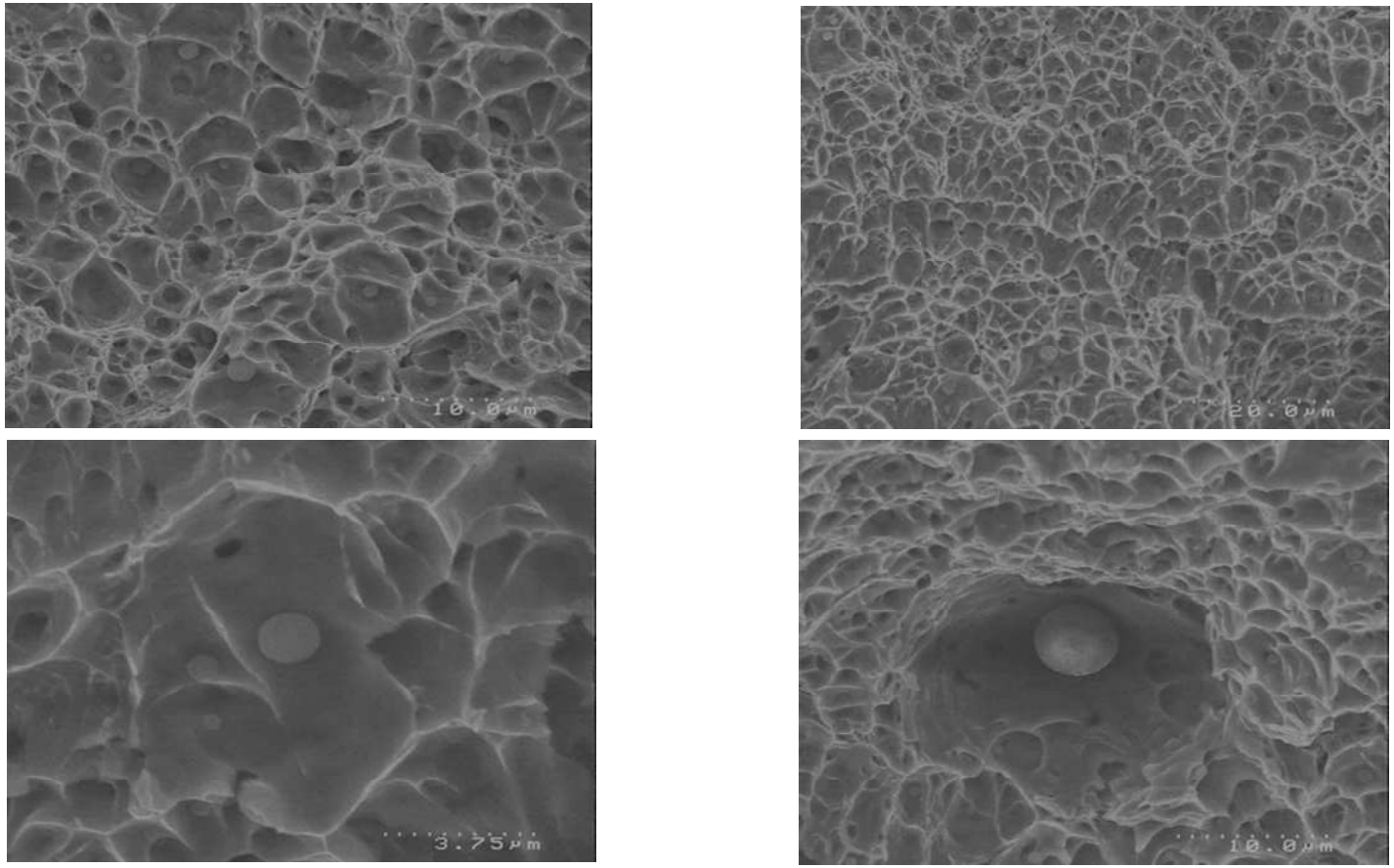

Figure 6.53 - General appearance of microvoids on the fracture surface for the AD Charpy sp strain and aged condition, tested on the upper shelf.

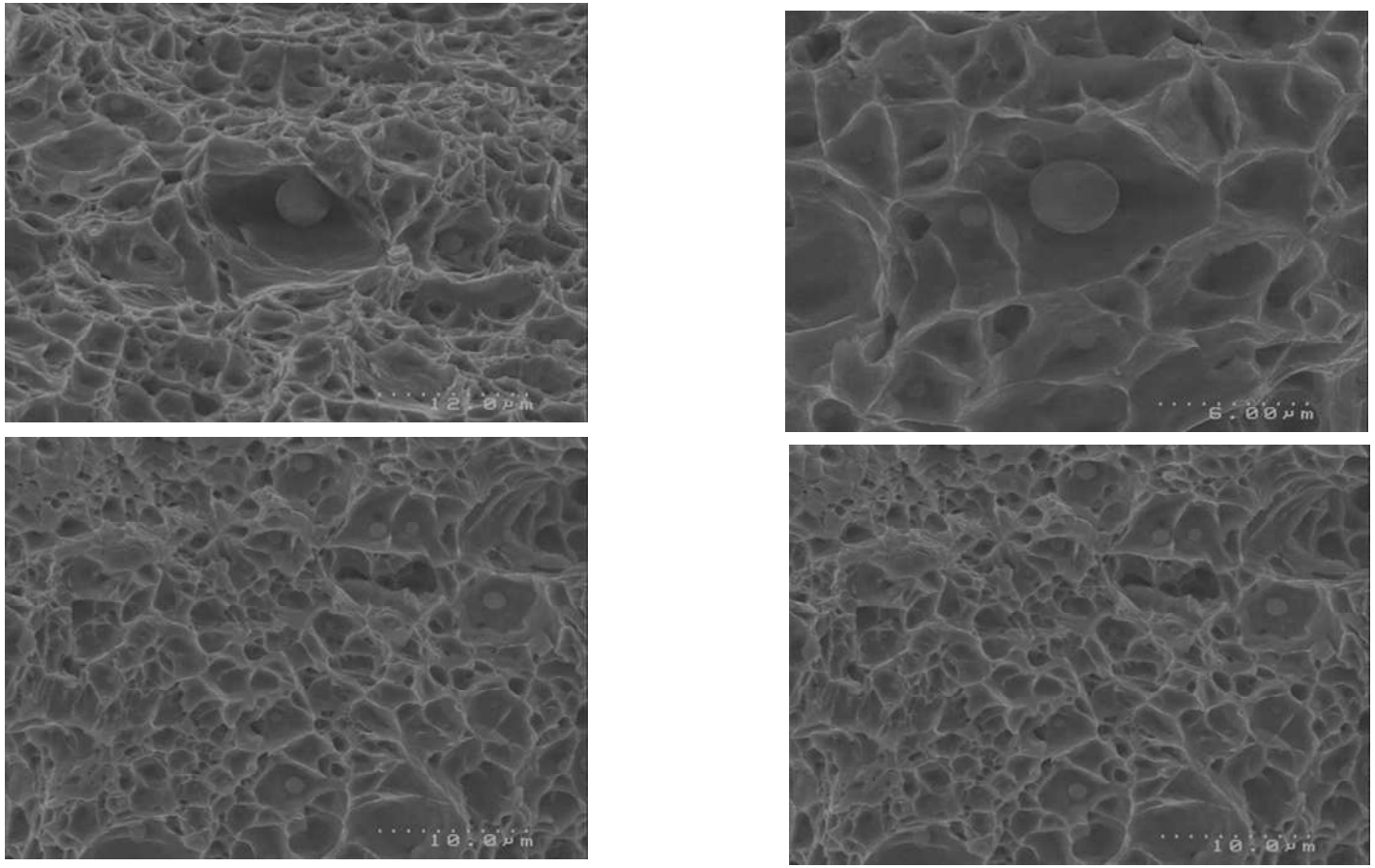

Figure 6.54 - General appearance of microvoids on the fracture surface for the RH Charpy specimens in the strain and aged condition, tested on the upper shelf.

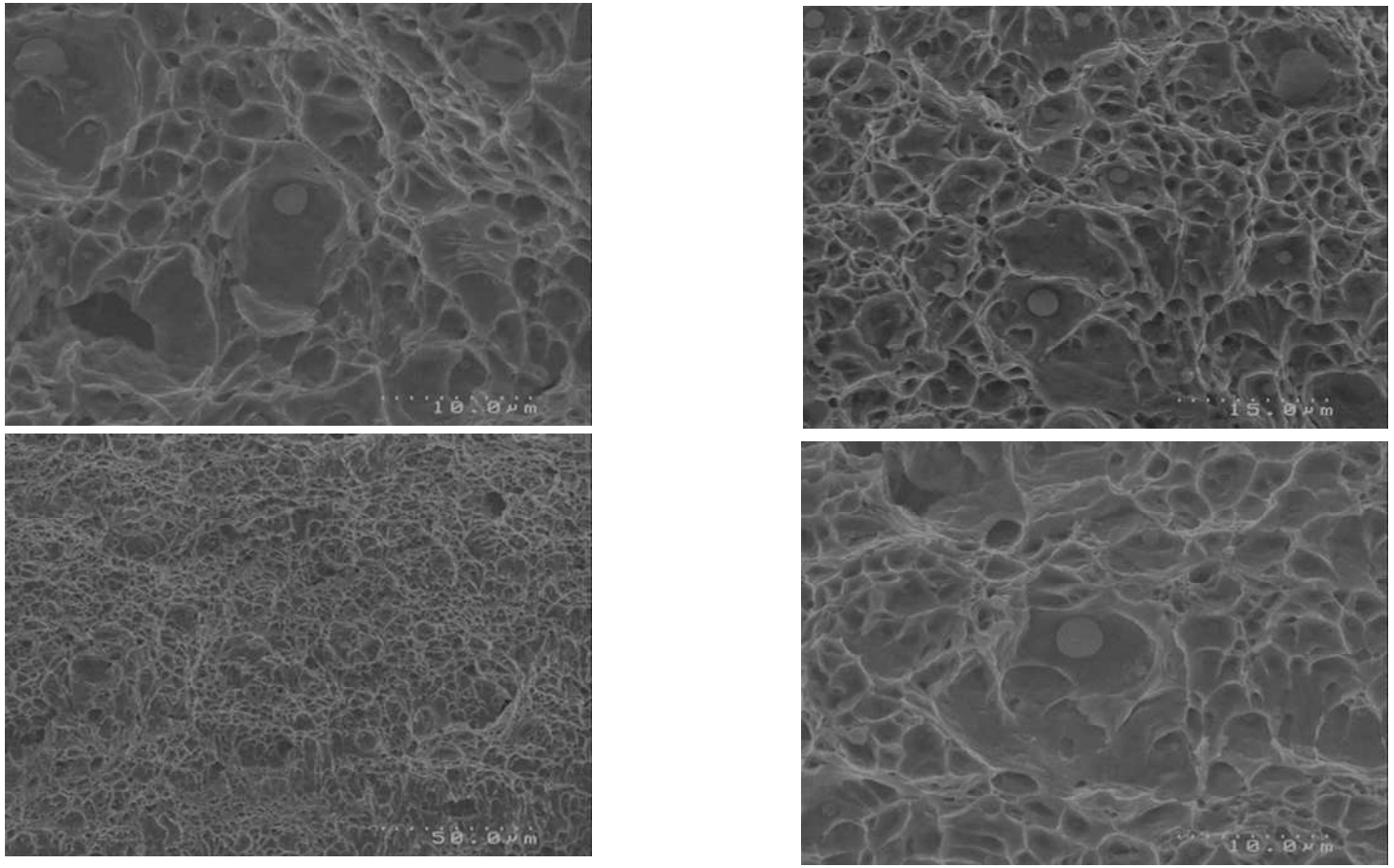

Table 7.1 - Values of local cleavage fracture stress, σ_{X0}, obtained from Griffiths and Owen FEM analysis and stress intensification at the cleavage initiation site for both microstructures in both conditions for Weld N°2, tested at various temperatures.

Weld Condition	Specimen	Temp [°C]	Distance from the notch X_0 [µm]	σ_{X0} [MPa]	Mean σ_{X0} [MPa]
ADAR	AD1*	-196	187	1514	1910
	AD2	-196	222	1897	
	AD3	-196	207	1827	
	AD4	-196	239	1975	
	AD1	-196	245	1940	
	AD2	-196	NA	NA	
RHAR	RH5	-196	236	2003	2078
	RH6	-196	267	2020	
	RH7	-196	305	2046	
	RH8	-196	289	2221	
	RH9	-196	NA	NA	
	RH3	-196	NA	NA	
	RH4	-196	320	2099	
	RH5	-196	NA	NA	
AD5%SA	ADSA1	-196	182	1629	1710
	ADSA2	-196	196	1688	
	ADSA3	-196	NA	NA	
	ADSA4	-196	205	1768	
	ADSA5	-196	212	1737	
RH5%SA	RHSA6	-196	201	1739	1808
	RHSA7	-196	212	1814	
	RHSA8	-196	235	1786	
	RHSA9	-196	214	1832	
	RHSA10	-196	244	1869	
	RHSA11	-196	NA	NA	

*Excluded from mean calculation

Table 7.2 - Maximum principal stress of the weld metal for both the ADAR and RHAR conditions, tested at -196°C.

Specimen	Dimensions [mm]	Notch Depth [mm]	Span [mm]	T [°C]	Max Load [kN]	Nom Stress σ_{nom} [Mpa]	Ligament Size W-a [mm]	Yield Stress σ_y [MPa]	Nom Stress/Yield Stress	L/LGY	R Griffiths Max	R (σ_{yymax}/σ_y)	Max Fracture Stress σ_{yymax} [MPa]	Mean Fracture Stress σ_{yymax} [MPa]
AD – 1*	10x10	3.33	40/20	-196	11.70	791	6.66	870	0.910	0.423		1.84	1600	
AD - 2	10x10	3.33	40/20	-196	21.24	1437	6.66	870	1.651	0.768	2.62	2.32	2018	
AD - 3	10x10	3.33	40/20	-196	21.28	1439	6.66	870	1.654	0.769		2.32	2020	
AD - 4	10x10	3.33	40/20	-196	22.12	1496	6.66	870	1.720	0.800		2.36	2051	
AD - 1	*12.7x12.7*	*4.33*	*63.5/38.1*	*-196*	*35.61*	*1489*	*8.47*	*870*	*1.712*	*0.796*	*2.62*	*2.35*	*2047*	
AD - 2	*12.7x12.7*	*4.33*	*63.5/38.1*	*-196*	*42.63*	*1783*	*8.47*	*870*	*2.049*	*0.953*		*2.52*	*2196*	**1989**
RH - 5	10 x10	3.33	40/20	-196	23.82	1611	6.66	874.57	1.842	0.857		2.42	2118	
RH - 6	10x10	3.33	40/20	-196	25.63	1733	6.66	874.57	1.982	0.922		2.49	2179	
RH - 7	10x10	3.33	40/20	-196	25.76	1742	6.66	874.57	1.992	0.926	2.62	2.50	2184	
RH - 8	10x10	3.33	40/20	-196	28.63	1936	6.66	874.57	2.214	1.030		2.60	2276	
RH - 9	10x10	3.33	40/20	-196	32.00	2164	6.66	874.57	2.475	1.151		2.72	NA	**2212**
RH - 3	*12.7x12.7*	*4.33*	*63.5/38.1*	*-196*	*47.66*	*1993*	*8.47*	*874.57*	*2.279*	*1.060*		*2.63*	*2291*	
RH - 4	*12.7x12.7*	*4.33*	*63.5/38.1*	*-196*	*43.76*	*1830*	*8.47*	*874.57*	*2.092*	*0.973*	*2.62*	*2.55*	*2226*	
RH - 5	*12.7x12.7*	*5.33*	*63.5/38.1*	*-196*	*55.94*	*2339*	*8.47*	*874.57*	*2.675*	*1.244*			*0*	

*Excluded from mean calculation

Table 7.3 - Maximum principal stress of the weld metal for both microstructures in the strain-aged condition, tested at -196°C.

Specimen	Dimensions [mm]	Notch Depth [mm]	Span [mm]	T [°C]	Max Load [kN]	Nom Stress σ_{nom} [Mpa]	Ligament Size W-a [mm]	Yield Stress σ_y [MPa]	Nom Stress/Yield Stress	L/LGY	R Griffiths Max	R (σ_{yymax}/σ_y)	Max Fracture Stress σ_{yymax} [MPa]	Mean Fracture Stress σ_{yymax} [MPa]
ADSA - 1	10x10	3.33	40/20	-196	11.97	810	6.66	987.00	0.820	0.381		1.77	1744	
ADSA - 2	10 x10	3.33	40/20	-196	12.04	814	6.66	987.00	0.825	0.384		1.77	1748	
ADSA - 3	10x10	3.33	40/20	-196	12.66	856	6.66	987.00	0.868	0.403	2.62	1.81	1782	
ADSA - 4	10x10	3.33	40/20	-196	13.81	934	6.66	987.00	0.946	0.440		1.87	1843	
ADSA - 5	10x10	3.33	40/20	-196	14.09	953	6.66	987.00	0.966	0.449		1.88	1858	**1795**
RHSA - 6	10x10	3.33	40/20	-196	15.65	1058	6.66	930.00	1.138	0.529		2.01	1866	
RHSA - 7	10x10	3.33	40/20	-196	16.25	1099	6.66	930.00	1.182	0.550		2.04	1894	
RHSA - 8	10x10	3.33	40/20	-196	17.28	1169	6.66	930.00	1.257	0.584	2.62	2.09	1939	
RHSA - 9	10x10	3.33	40/20	-196	18.55	1255	6.66	930.00	1.349	0.627		2.14	1994	
RHSA - 10	10x10	3.33	40/20	-196	19.1	1292	6.66	930.00	1.389	0.646		2.17	2017	
RHSA - 11	10x10	3.33	40/20	-196	25.35	1715	6.66	930.00	1.844	0.857		2.42	2253	**1994**

Table 7.4 - Summary table for all the blunt notch specimens, tested for both microstructures in both the as-received and strain aged microstructural conditions.

Weld Condition	Specimen	Max Load [kN]	R (σ_{yymax}/σ_y)	Max Fracture Stress σ_{yymax} [MPa]	Fracture Stress σ_{yymax} [MPa]	Distance from the notch X_0 [µm]	σ_{X0} [MPa]	Mean σ_{X0} [MPa]
ADAR	AD – 1*	11.70	1.84	1600	1989	187	1514	1910
	AD - 2	21.24	2.32	2018		222	1897	
	AD - 3	21.28	2.32	2020		207	1827	
	AD - 4	22.12	2.36	2051		239	1975	
	AD - 1	*35.61*	*2.35*	*2047*		245	1940	
	AD - 2	*42.63*	*2.52*	*2196*		NA	NA	
RHAR	RH - 5	23.82	2.42	2118	2212	236	2003	2078
	RH - 6	25.63	2.49	2179		267	2020	
	RH - 7	25.76	2.50	2184		305	2046	
	RH - 8	28.63	2.60	2276		289	2221	
	RH - 9	32.00	2.72	NA		NA	NA	
	RH - 3	*47.66*	*2.63*	*2291*		NA	NA	
	RH - 4	*43.76*	*2.55*	*2226*		320	2099	
	RH - 5	*55.94*		*0*		NA	NA	
AD5%SA	ADSA - 1	11.97	1.77	1744	1795	182	1629	1710
	ADSA - 2	12.04	1.77	1748		196	1688	
	ADSA - 3	12.66	1.81	1782		NA	NA	
	ADSA - 4	13.81	1.87	1843		205	1768	
	ADSA - 5	14.09	1.88	1858		212	1737	
RH5%SA	RHSA - 6	15.65	2.01	1866	1994	201	1739	1808
	RHSA - 7	16.25	2.04	1894		212	1814	
	RHSA - 8	17.28	2.09	1939		235	1786	
	RHSA - 9	18.55	2.14	1994		214	1832	
	RHSA - 10	19.1	2.17	2017		244	1869	
	RHSA - 11	25.35	2.42	2253		NA	NA	

N/A - Site could not be established

*Excluded from mean calculation

Figure 7.1 - Photograph of a slow blunt notch test specimen.

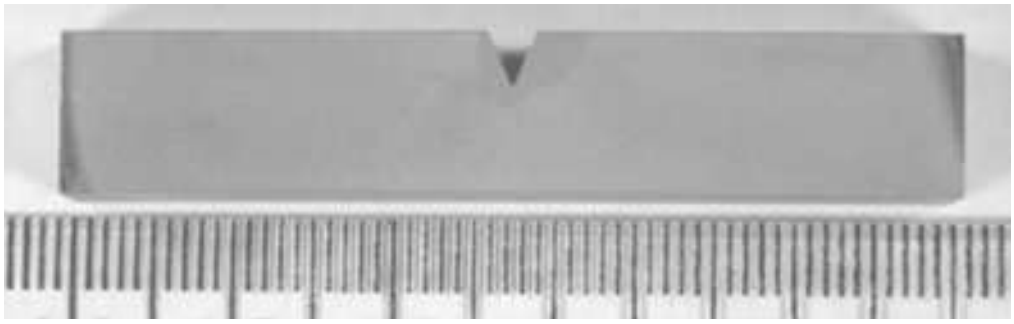

Figure 7.2 - Magnification of the blunt notch root. (a) ADAR Specimen 1; (b) RHAR Specimen 1 and (c) AD5%SA Specimen 1 and (d) RH5%SA Specimen 1.

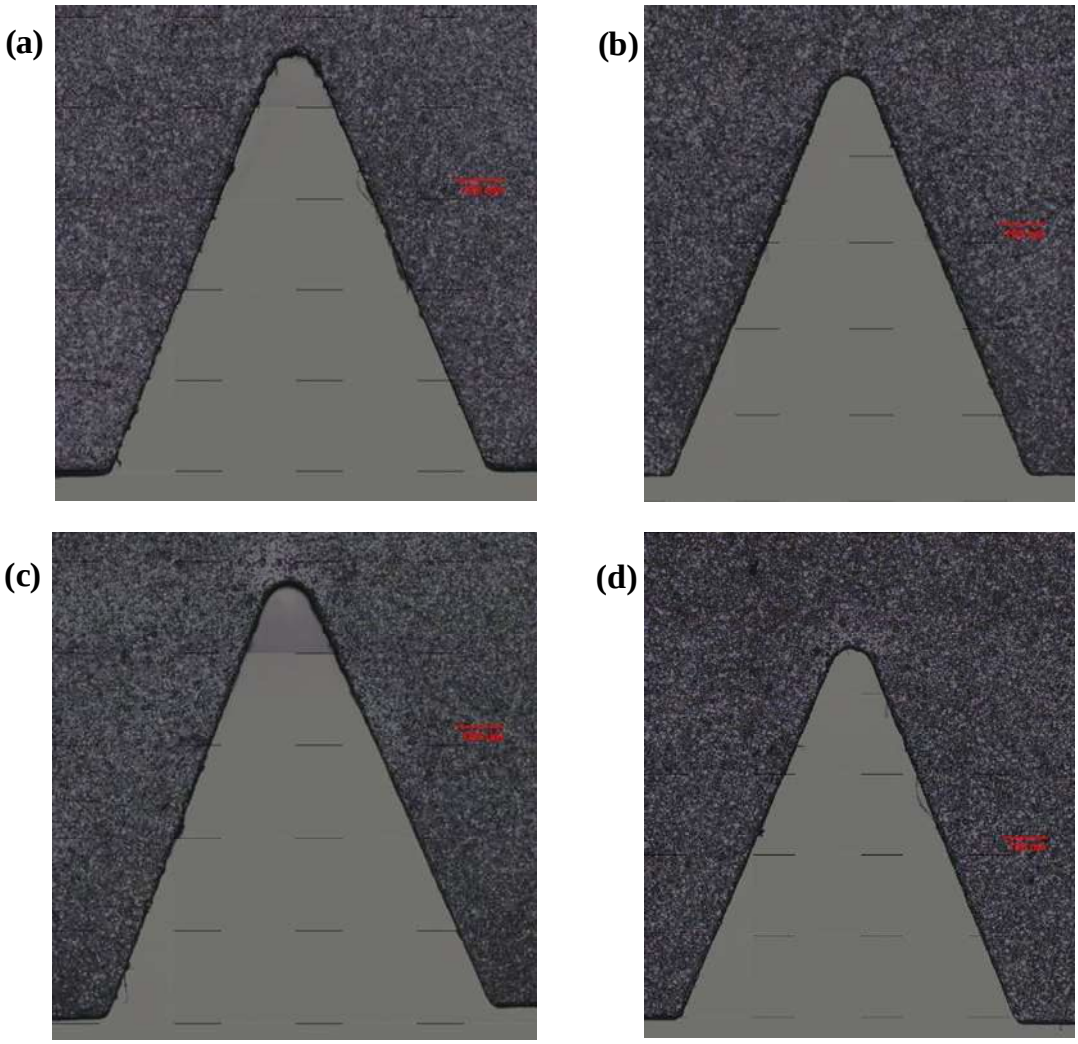

Figure 7.3 - Local cleavage fracture stress, σ_{X0}, for the as-deposited and reheated microstructural conditions in both the as-received (AR) and strain and aged condition (5%SA).

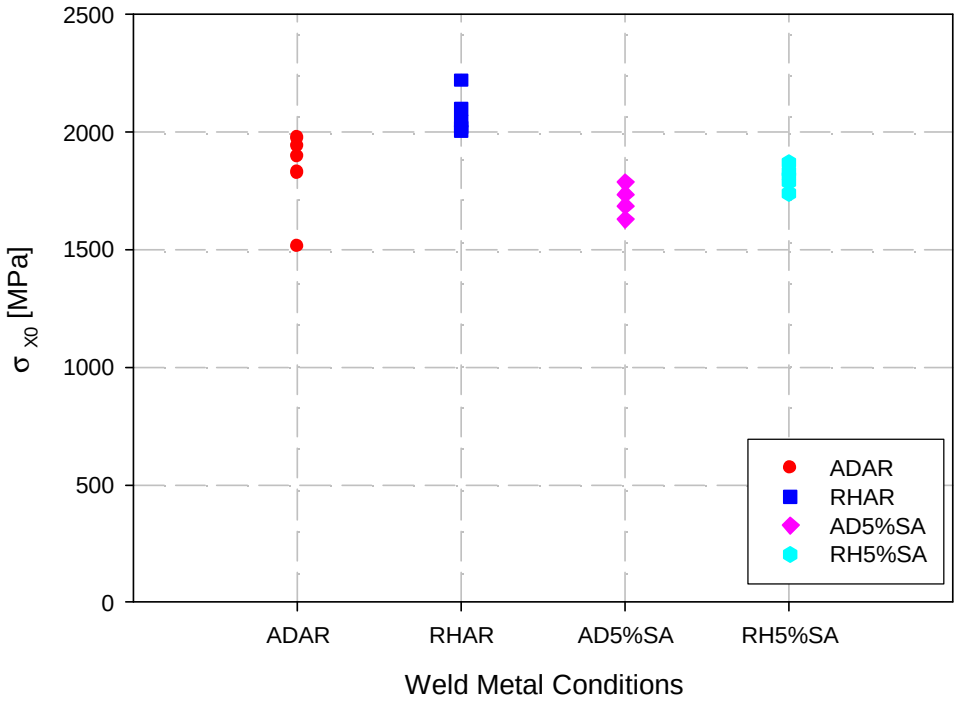

Figure 7.4 - Maximum principal tensile stress at fracture, σ_{yymax}, for the as-deposited and reheated microstructural conditions in both the as-received (AR) and strain and aged condition (5%SA).

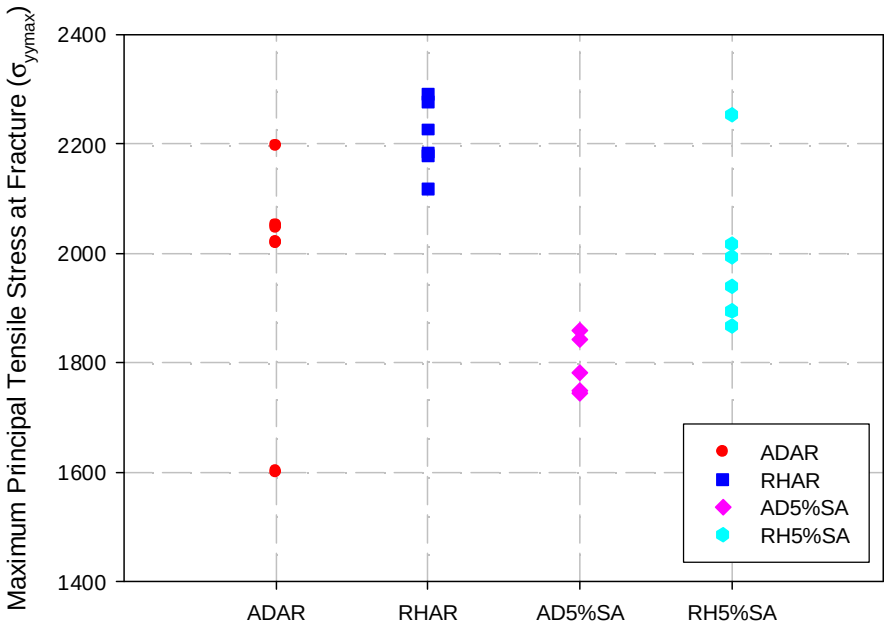

Figure 7.5 - Relationship between local cleavage fracture stress, σ_{X0}, and maximum principal tensile stress, σ_{yymax}. Graph depicts the four various microstructural conditions.

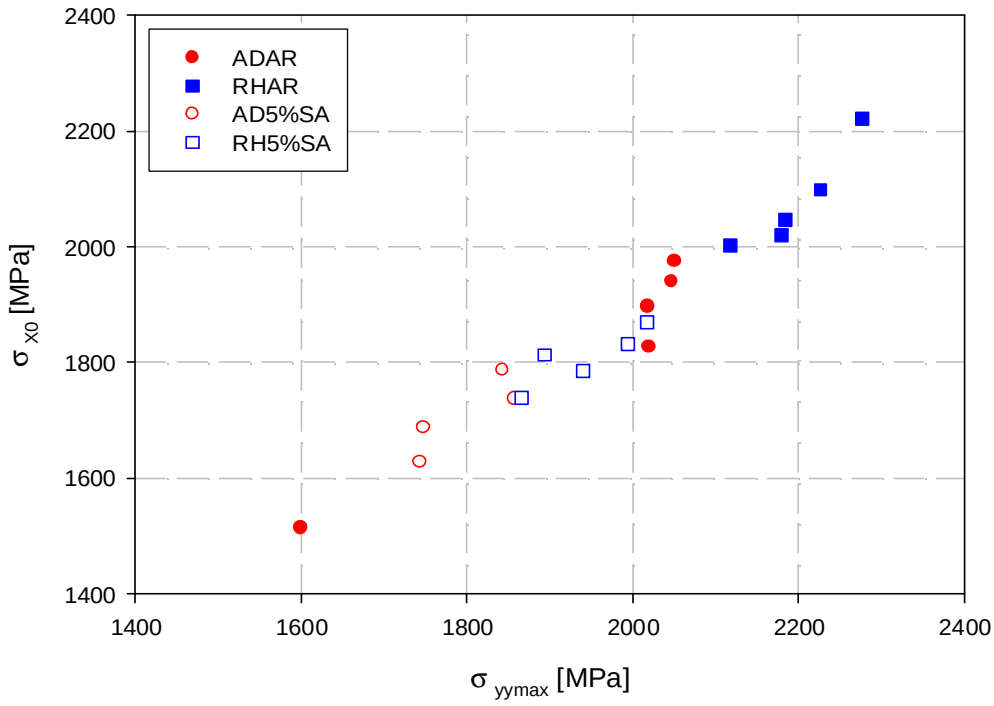

Figure 7.6 - Cleavage initiation site locations plot of stress intensification factor R versus distance below the notch root X_0.

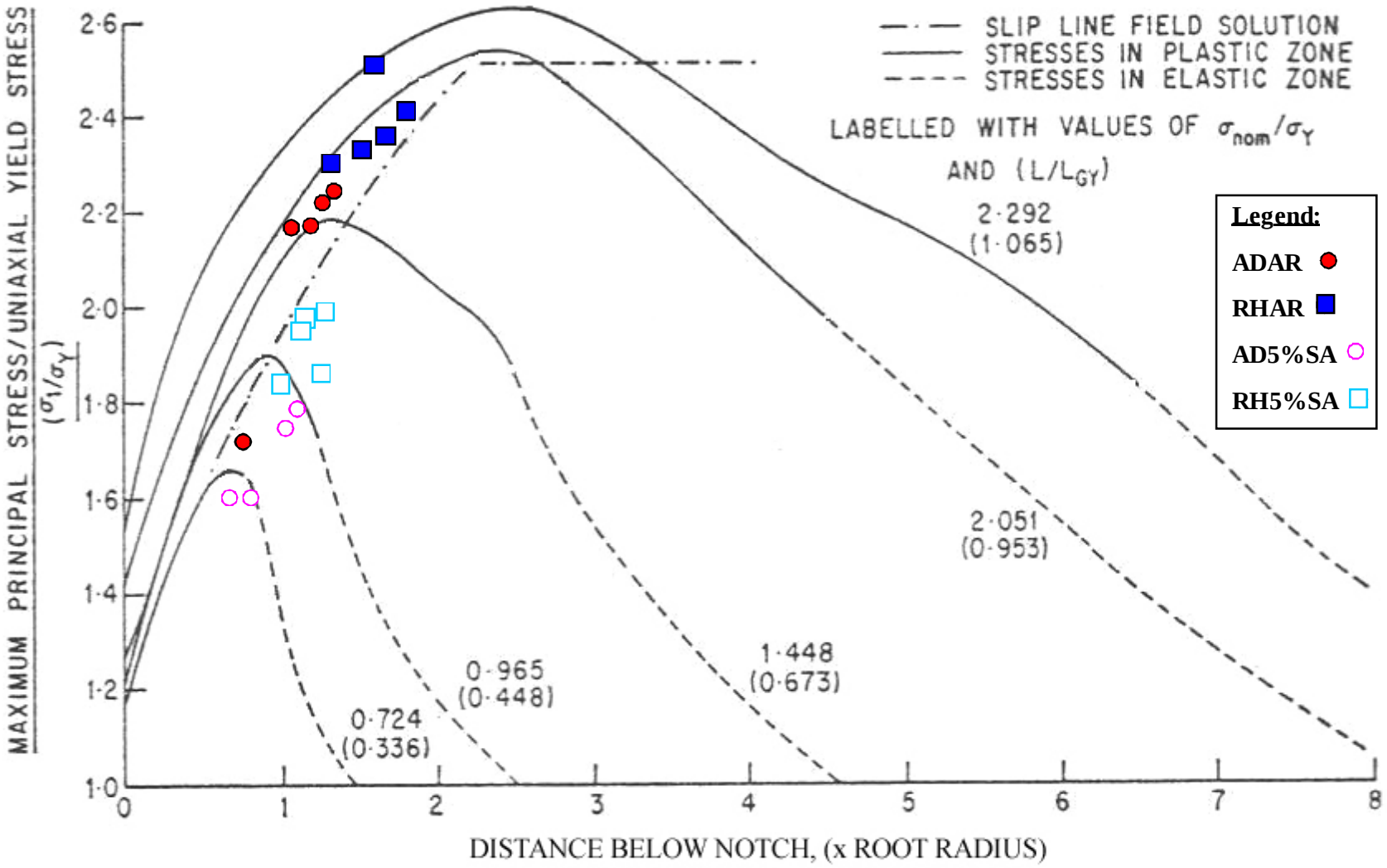

Figure 7.7 - Stress intensification ratio R, at the cleavage initiation site for the as-deposited and reheated microstructure for both the as-received and strain aged microstructural condition.

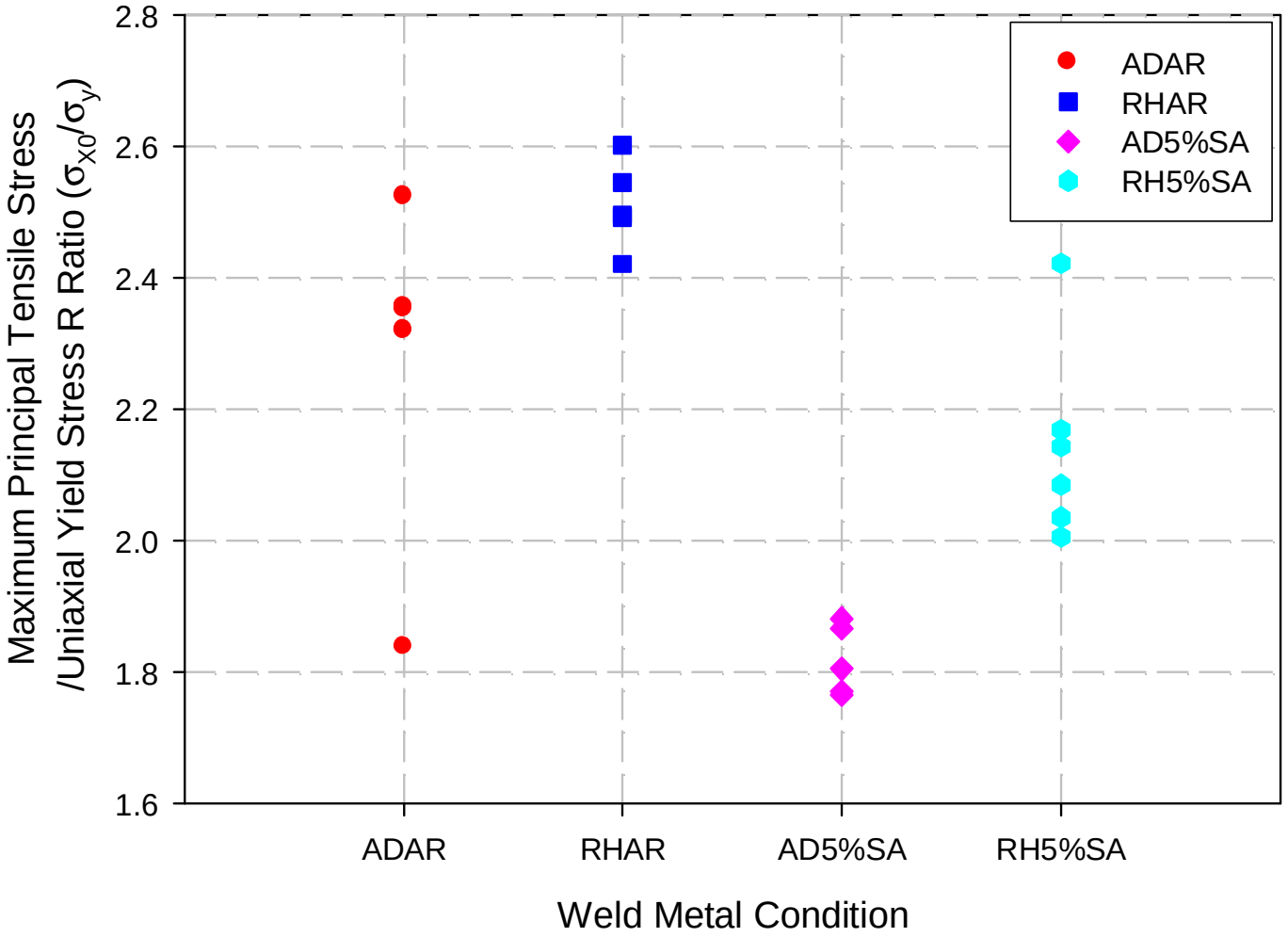

Figure 7.8 - Plot of X_0 distance for all four weld metal conditions.

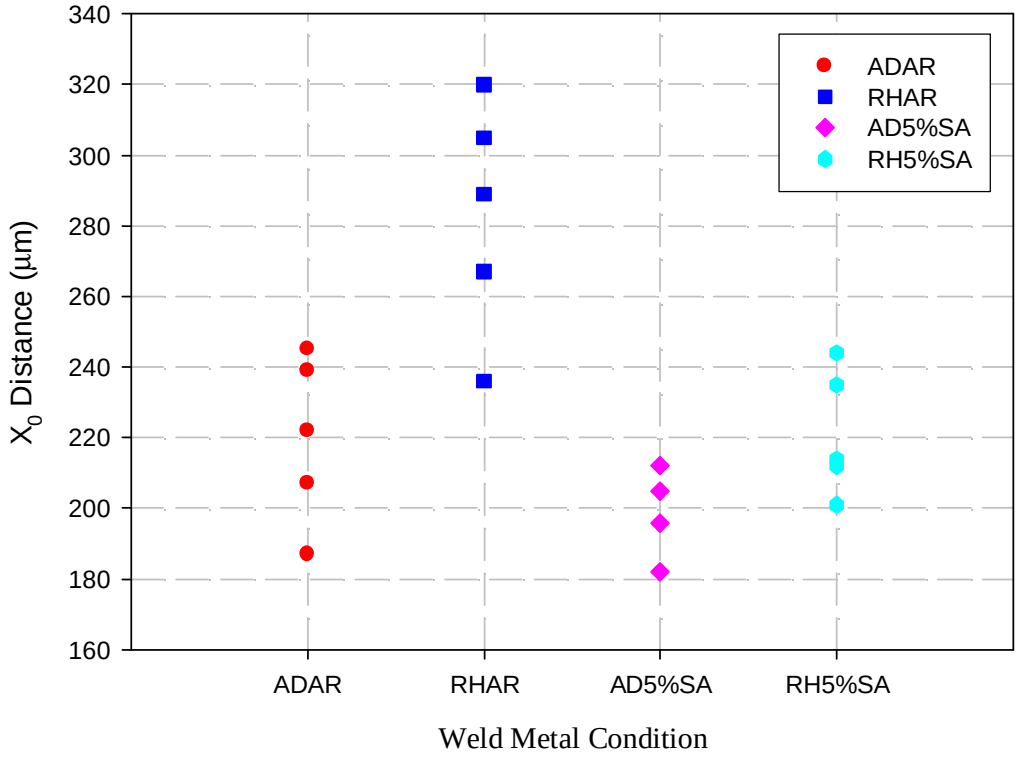

Figure 7.9 - The spread of plasticity from the notch root (after Griffiths and Owen).

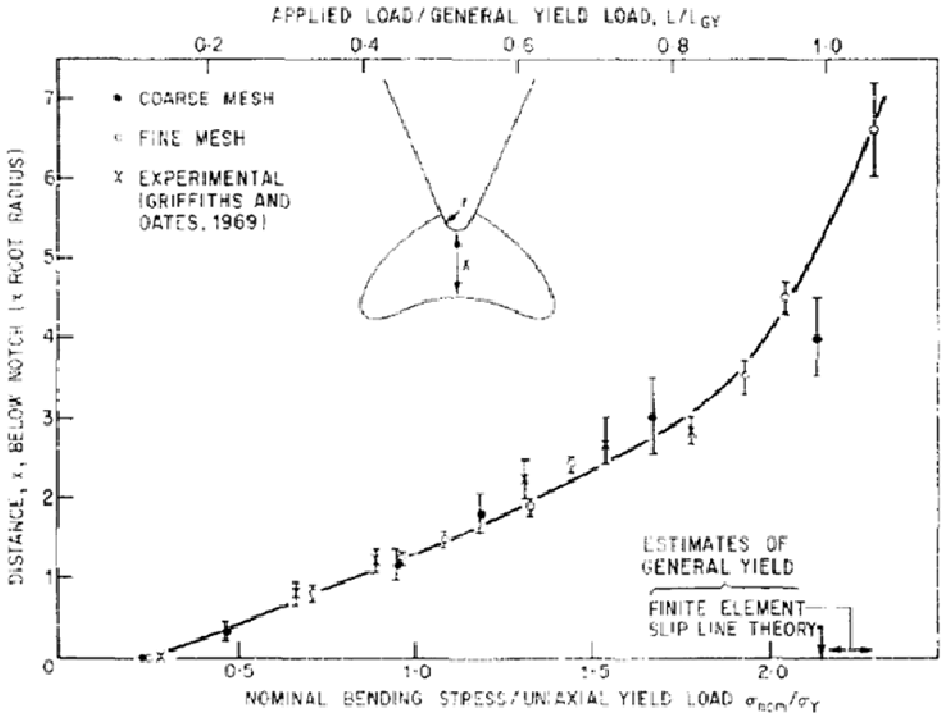

Figure 7.10 - Local cleavage fracture stress, σ_{X0}, for the as-deposited and reheated microstructural conditions in both the as-received (AR) and strain and aged condition (5%SA).

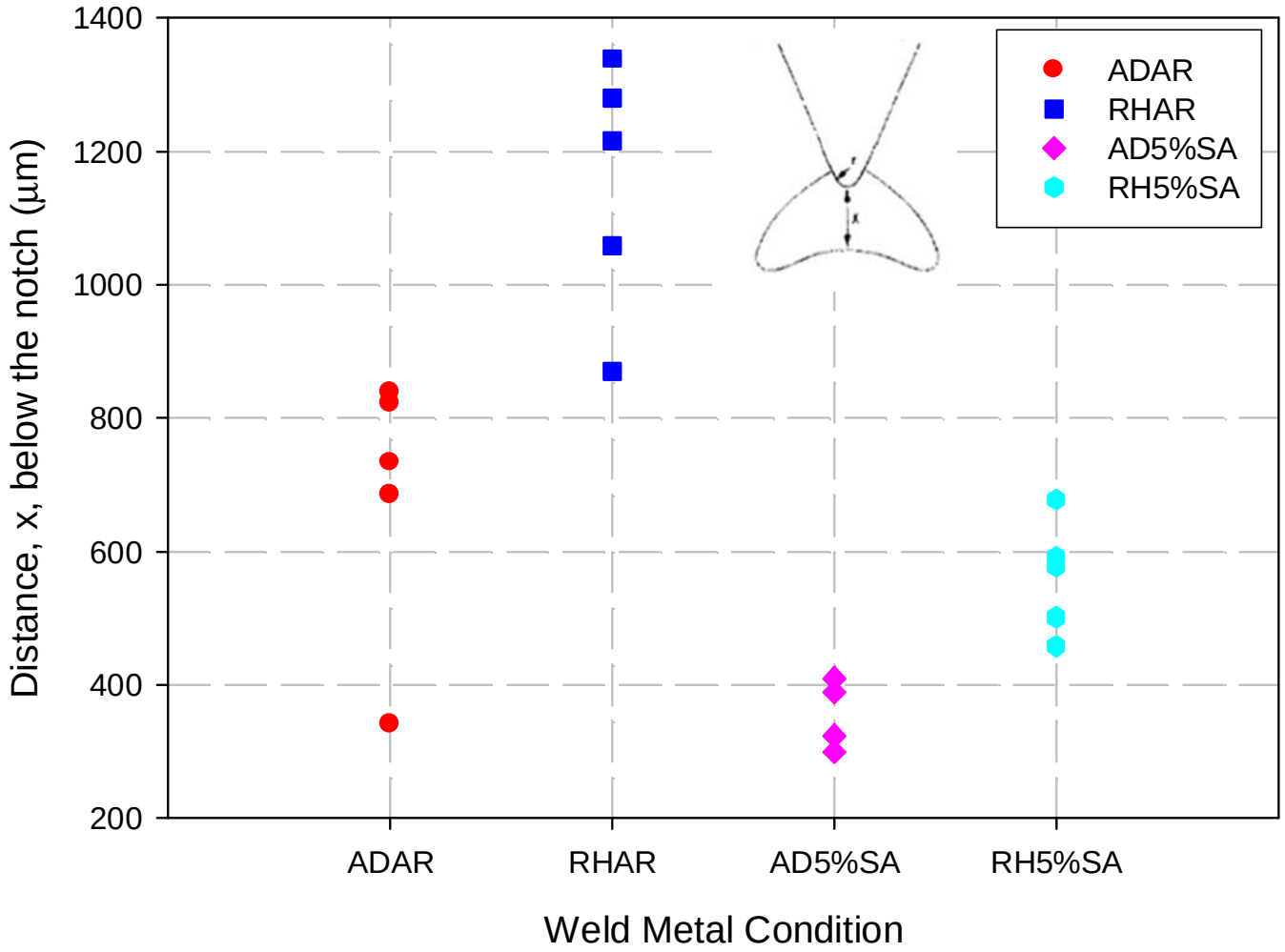

Figure 7.11 - The general appearance of the fracture surfaces of the slow blunt notch specimens; (a) as-deposited and (b) reheated microstructure.

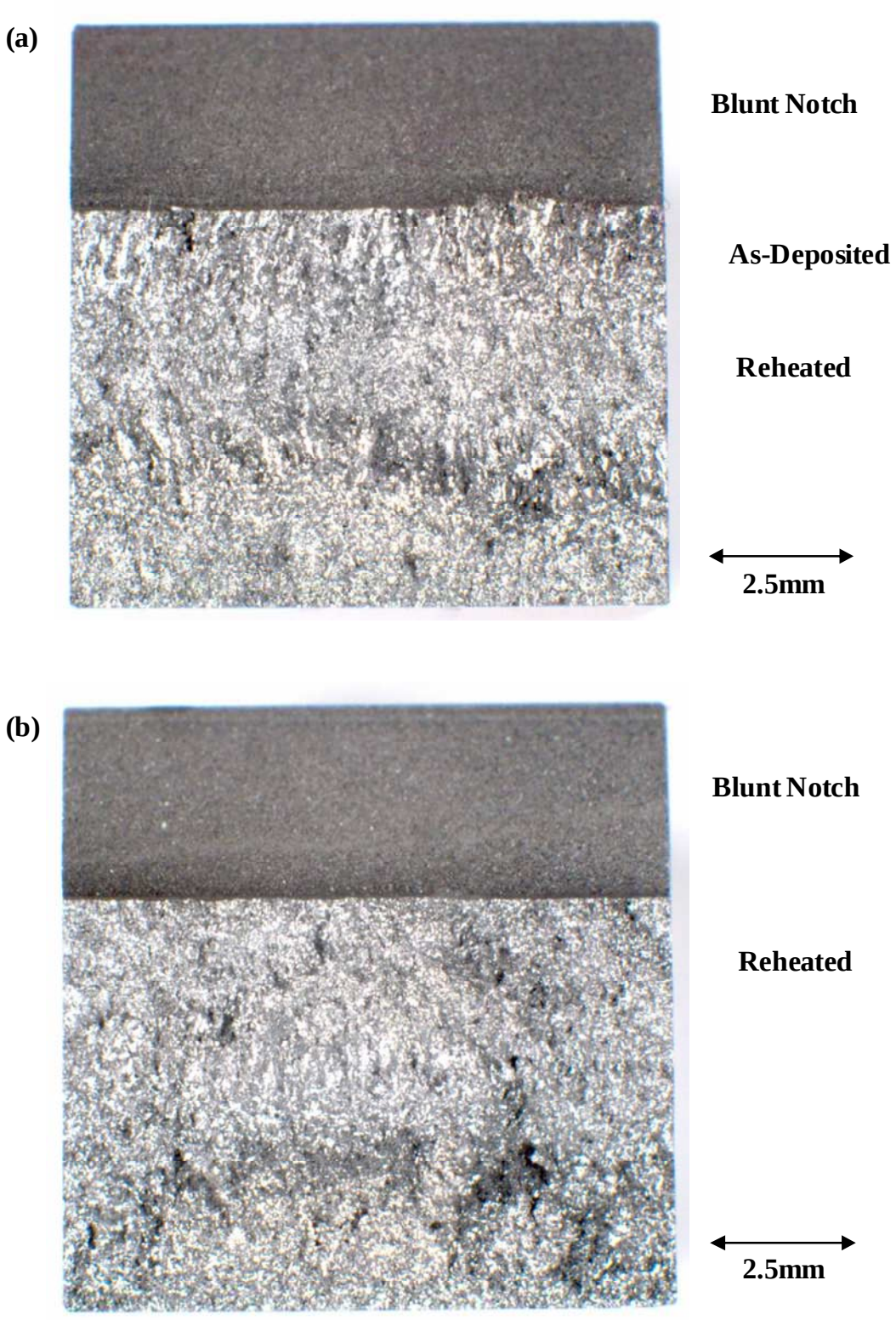

Figure 7.12 - Fracture initiation of blunt notch specimen RHAR4 tested at -196°C; (a) overall fracture initiation (site framed), (b) magnification framed area, (c) secondary cracking noted near to initiation site (arrowed), (d) non metallic inclusion initiation site (arrowed).

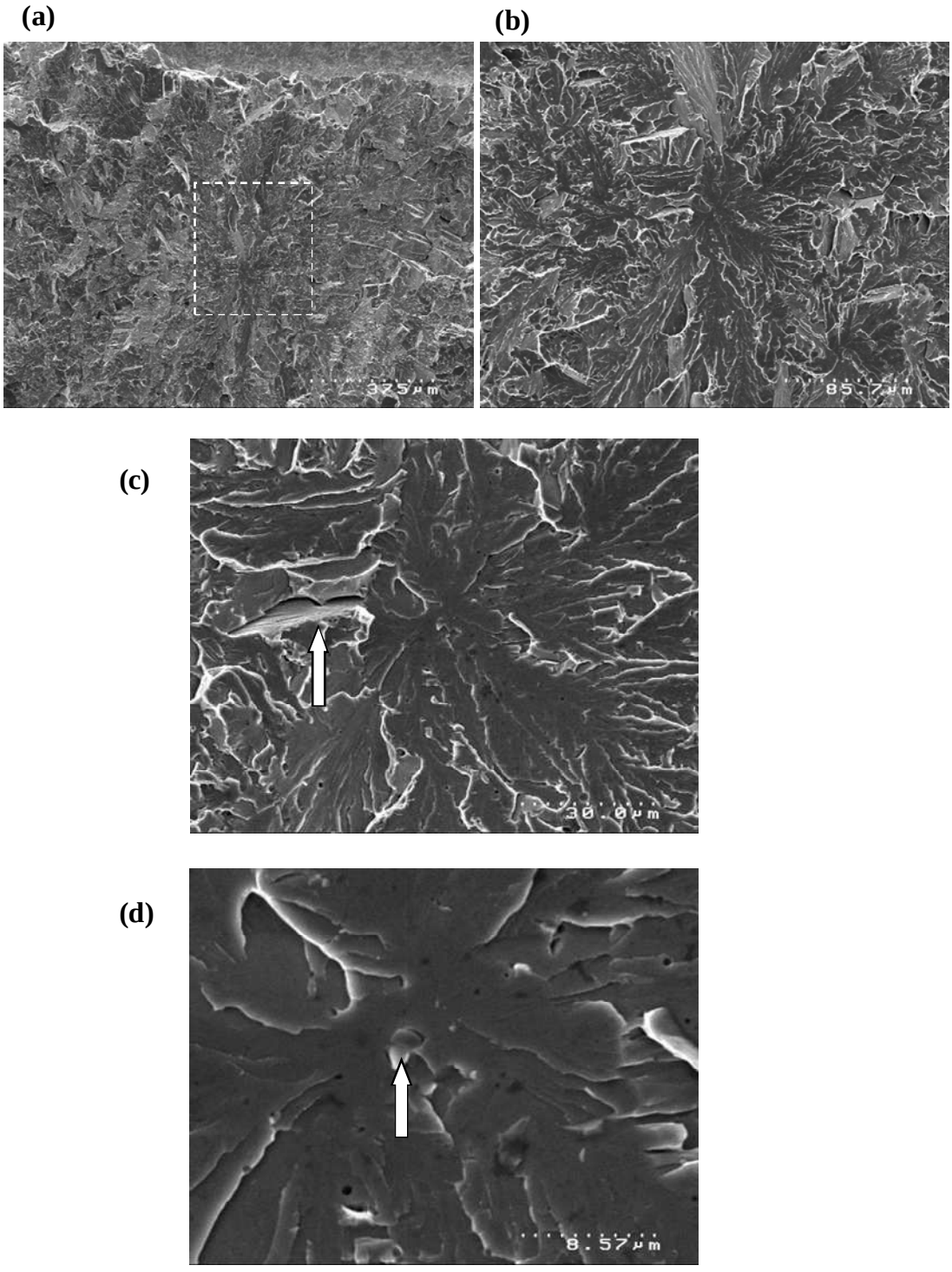

Figure 7.13 - Fracture initiation of blunt notch specimen ADAR4 tested at -196°C; (a) overall fracture initiation (site framed), (b) magnification framed area, (c) cleavage steps noted near to initiation site (arrowed), (d) cleavage initiation site, and decohered inclusion (arrowed).

(a)

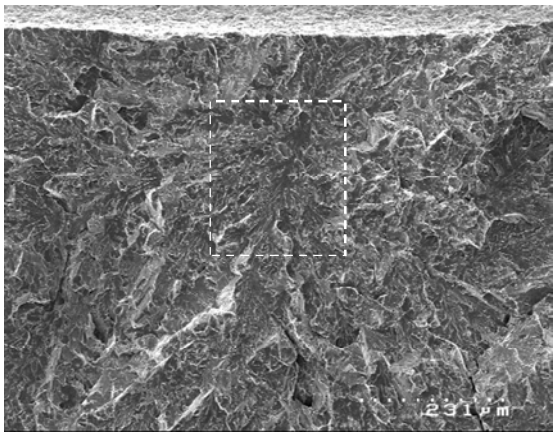

(b)

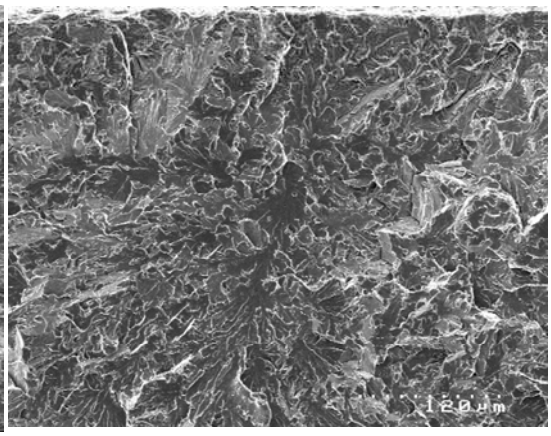

(c)

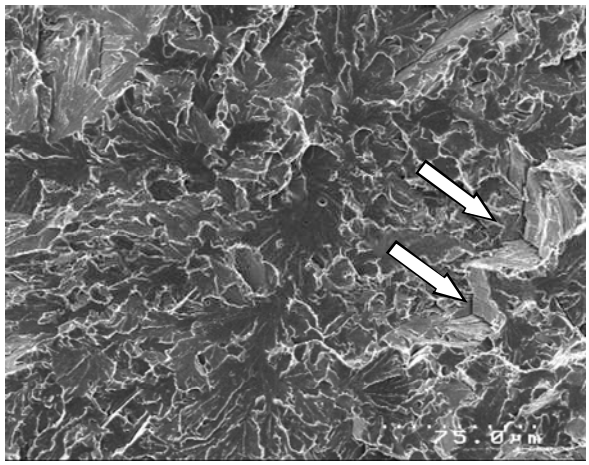

(d)

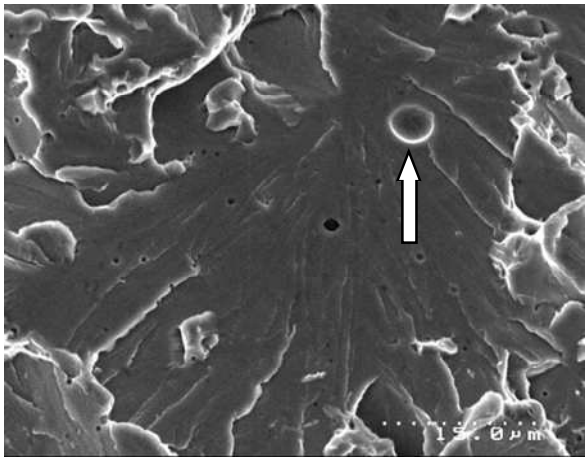

Figure 7.14 - Fracture initiation of blunt notch specimen AD5%SA tested at -196°C; (a) overall fracture initiation (site framed), (b) magnification framed area, (c) non metallic inclusion initiation site (arrowed).

(a)

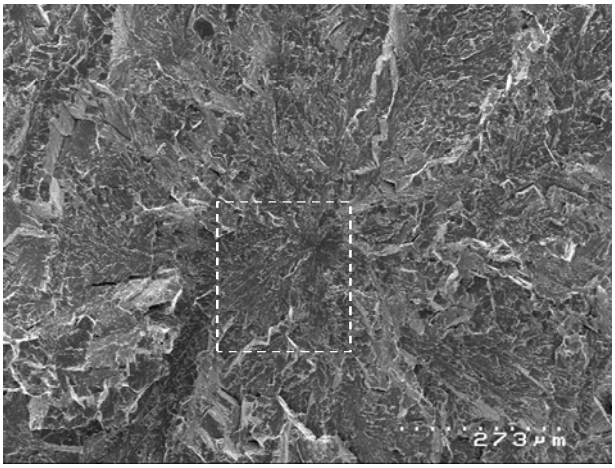

(b)

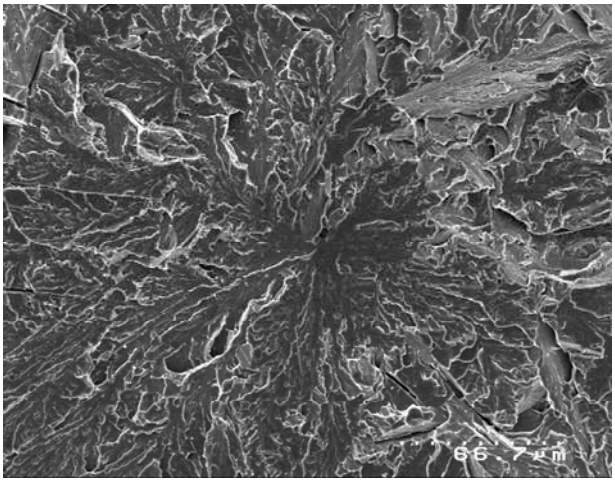

(c)

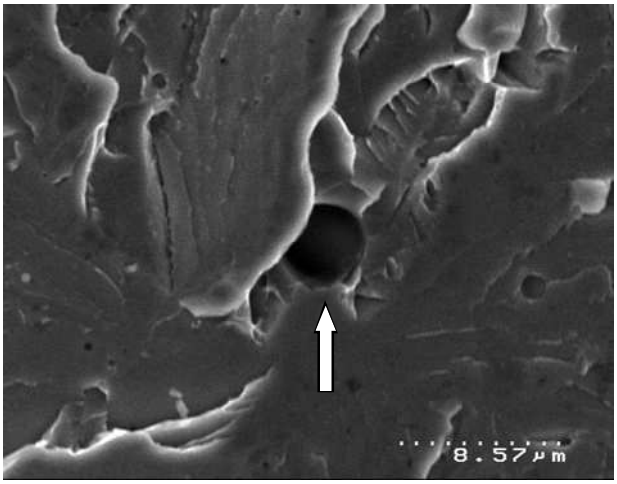

Figure 7.15 - Fracture initiation of blunt notch specimen RH5%SA10 tested at -196°C; (a) overall fracture initiation (site framed), (b) magnification framed area secondary cracking and cleavage steps noted (arrowed), (c) cleavage initiation site, (d) magnification of frames area from (c).

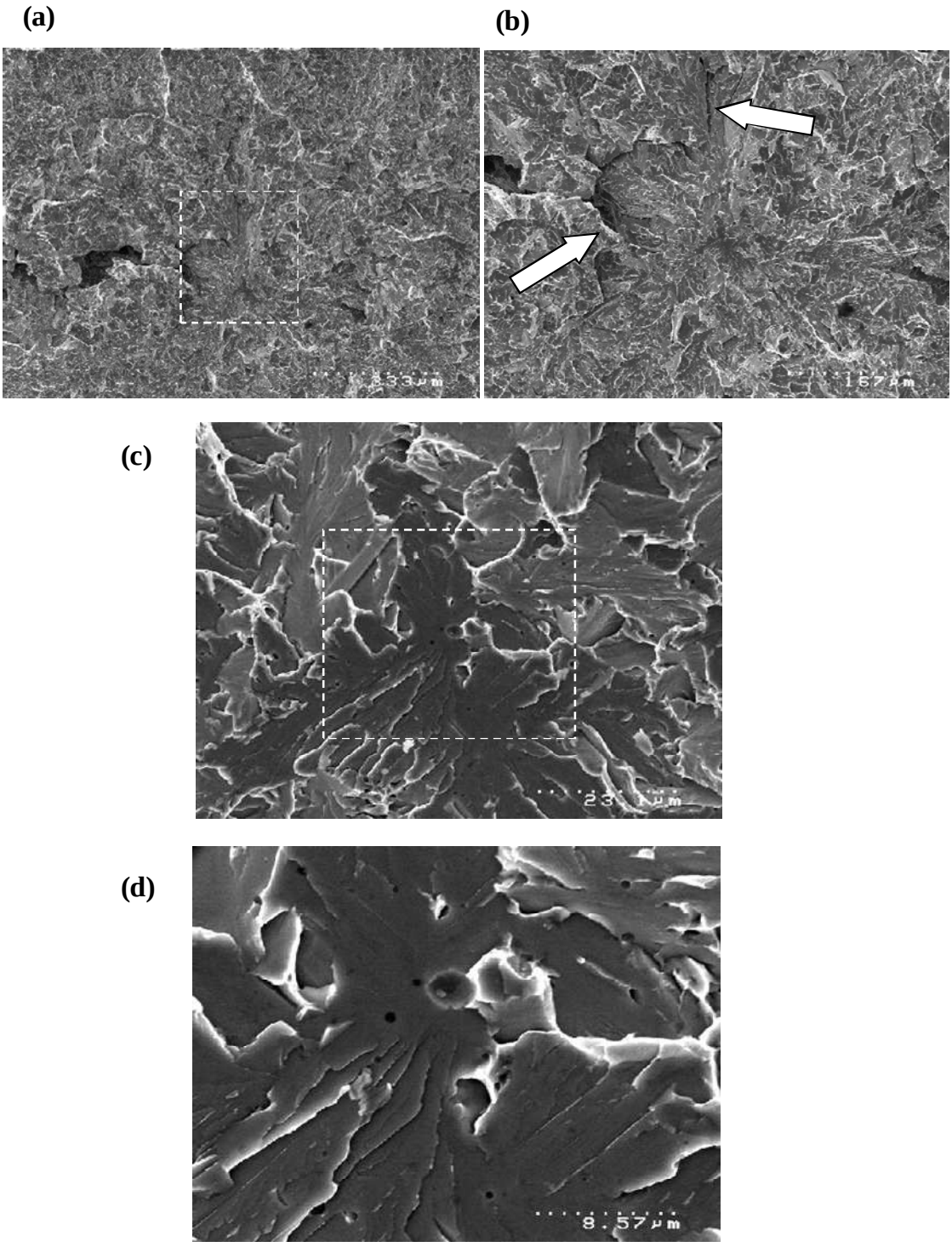

Figure 7.16 - Fracture initiation of blunt notch specimen AD5%SA5 tested at -196°C; (a) overall fracture initiation (site framed), (b) magnification framed area, cleavage fracture steps (arrowed), (c) secondary cracking near initiation site (arrowed), (d) initiation site.

(a)

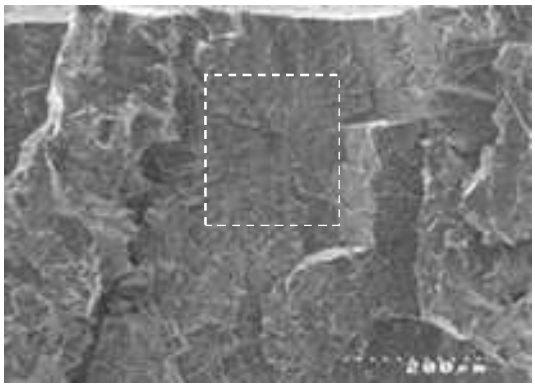

(b)

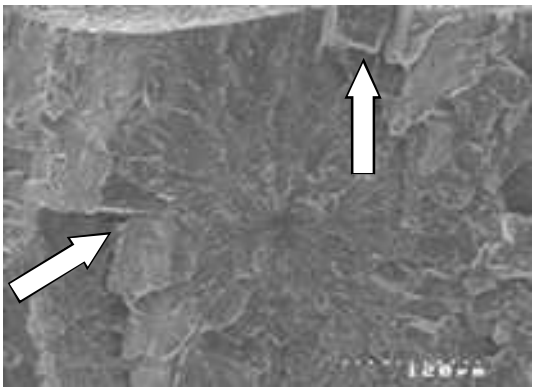

(c)

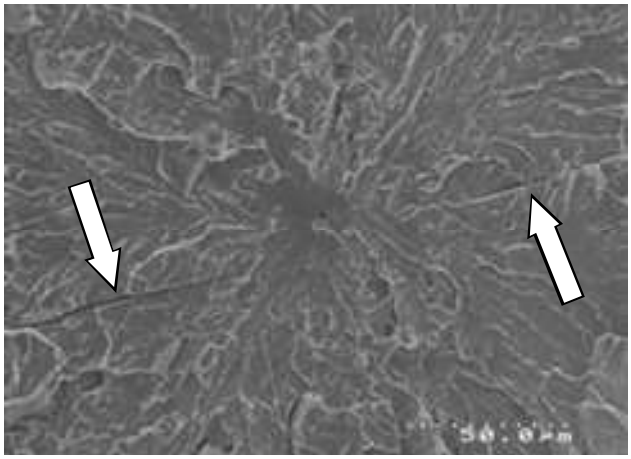

(d)

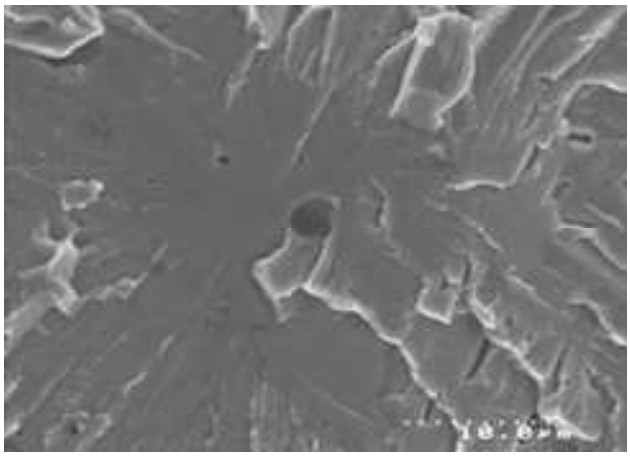

Figure 7.17 - Fracture initiation of blunt notch specimen RH5%SA8 tested at -196°C; (a) overall fracture initiation (site framed), (b) magnification framed area, (c) secondary cracking noted near to initiation site (arrowed).

(a)

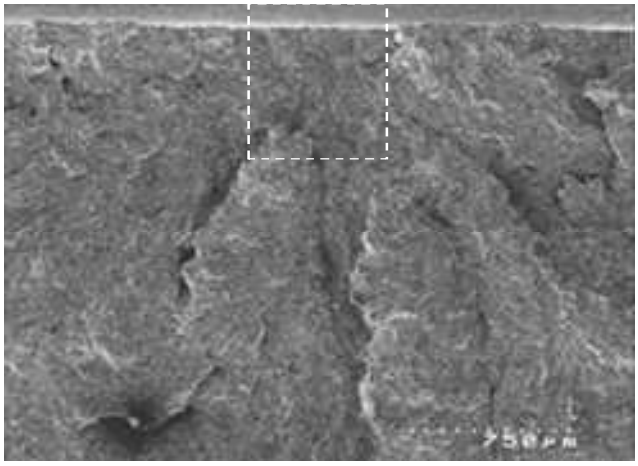

(b)

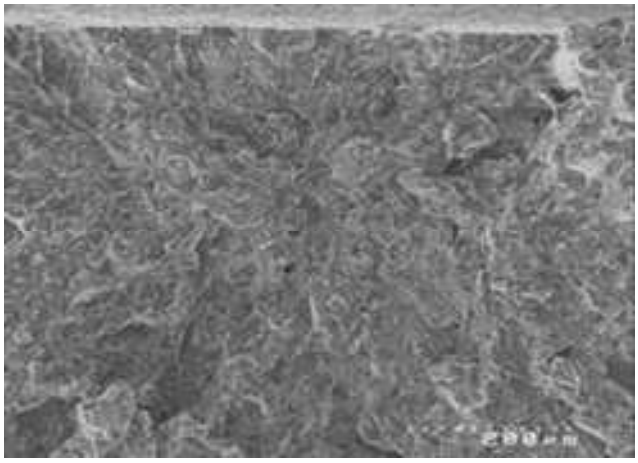

(c)

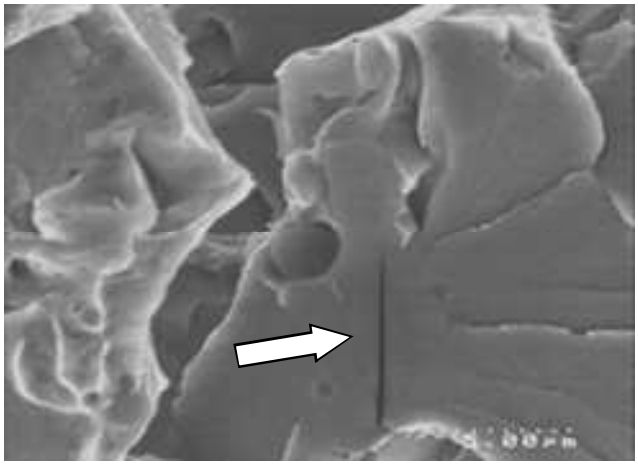

Figure 7.18 - Fracture initiation of blunt notch specimen ADAR1 tested at -196°C; (a) overall fracture initiation (site framed), (b) magnification framed area, (c) secondary cracking and cleavage steps noted near to initiation site, (d) cleavage initiation site, decohered inclusion (arrowed).

(a)

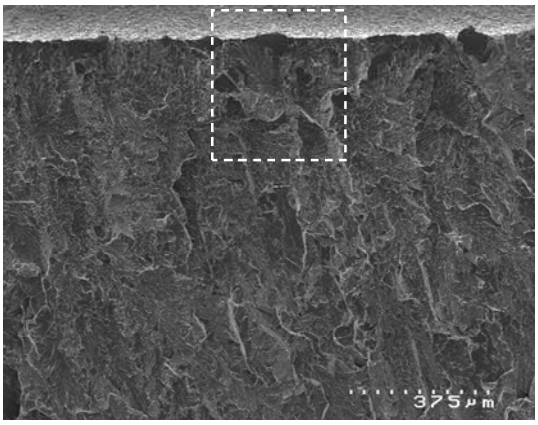

(b)

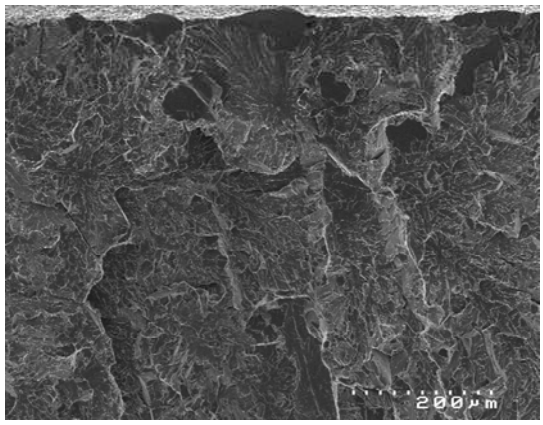

(c)

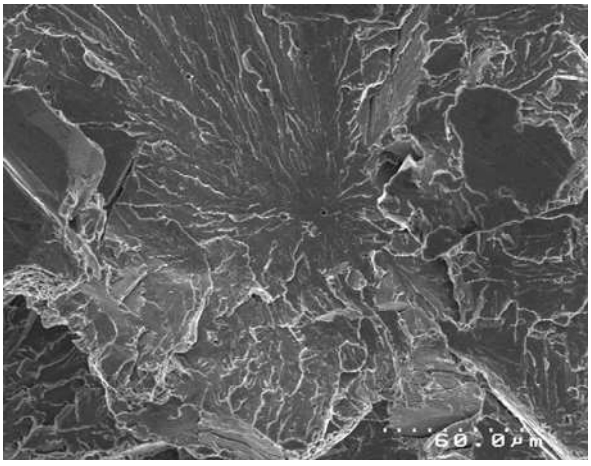

(d)

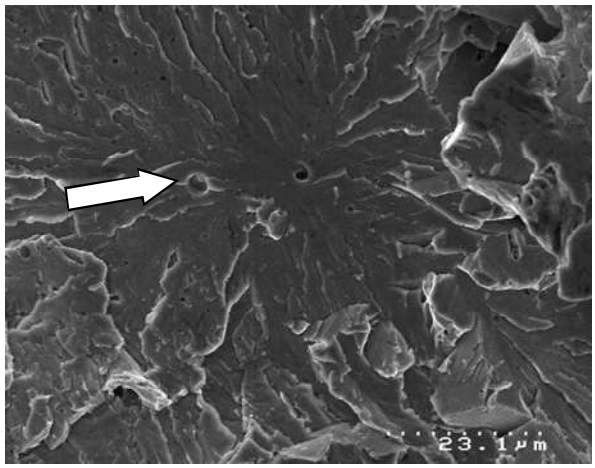

Figure 7.19 - Fracture initiation of blunt notch specimen RH5%SA tested at -196°C; (a) overall fracture initiation (site framed), (b) magnification framed area, (c) non metallic inclusion initiation site (arrowed).

(a)

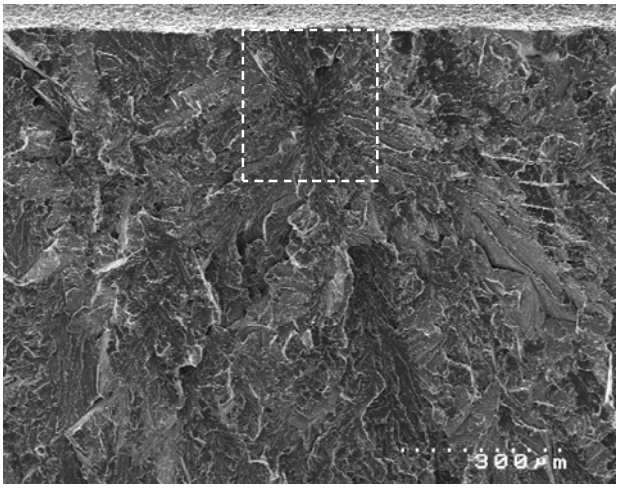

(b)

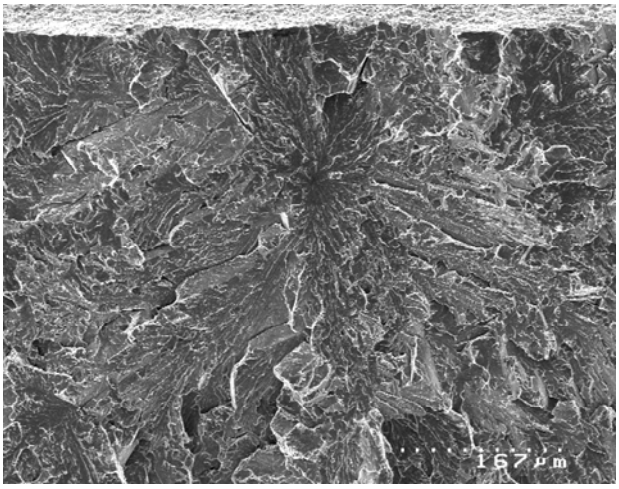

(c)

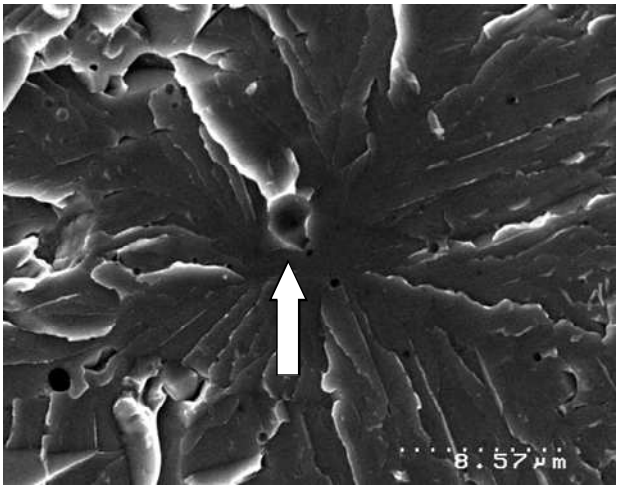

Figure 7.20 - Fracture initiation of blunt notch specimen AD5%SA tested at -196°C; (a) overall fracture initiation (site framed), (b) magnification framed area, cleavage steps noted (arrowed), (c) cleavage initiation site, no inclusion observed.

(a)

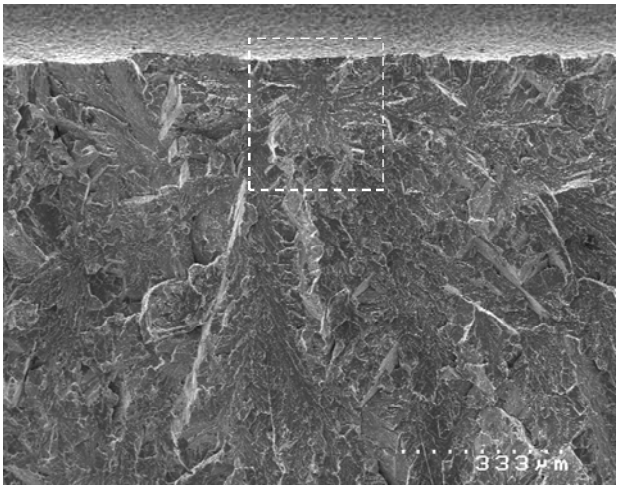

(b)

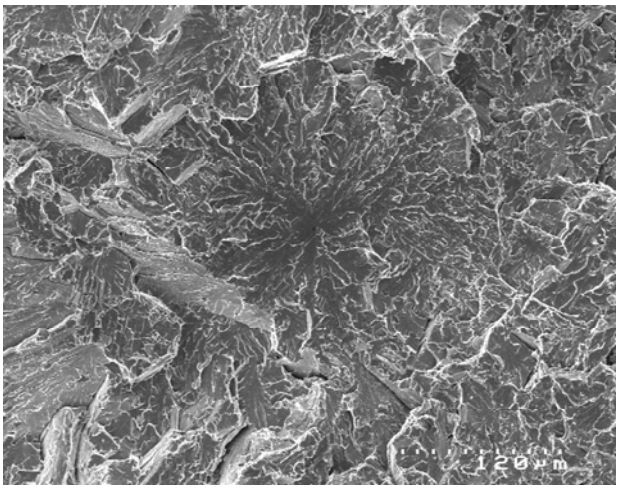

(c)

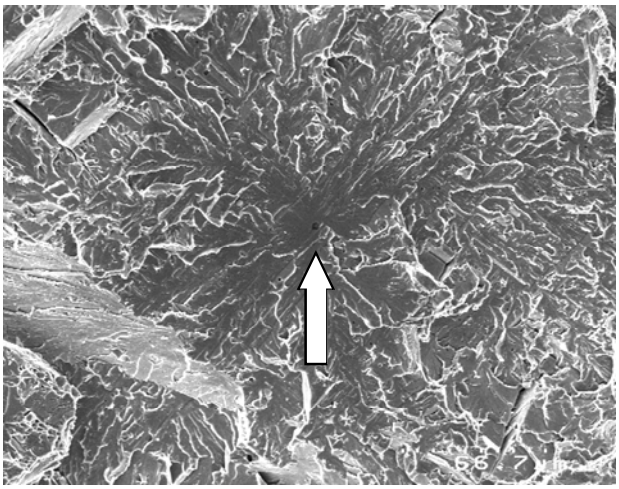

Figure 7.21 - Fracture initiation of blunt notch specimen AD5%SA4 tested at -196°C; (a) overall fracture initiation (site framed), (b) magnification framed area cleavage steps noted (arrowed), (c) secondary cracking noted near to initiation site (arrowed).

(a)

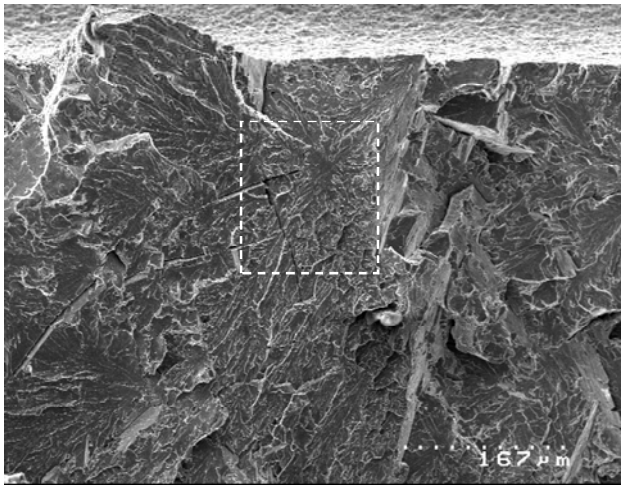

(b)

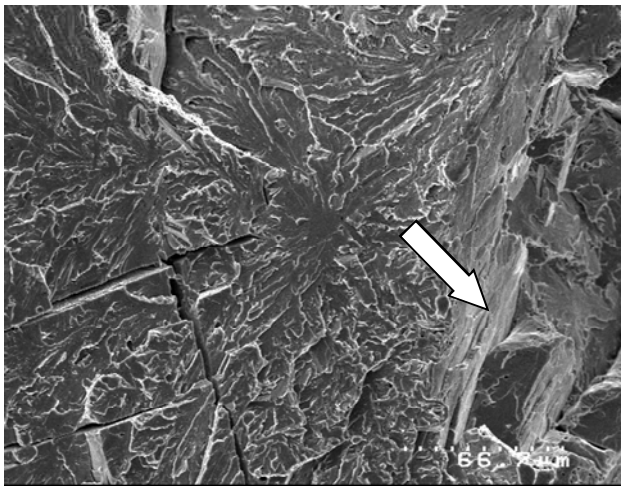

(c)

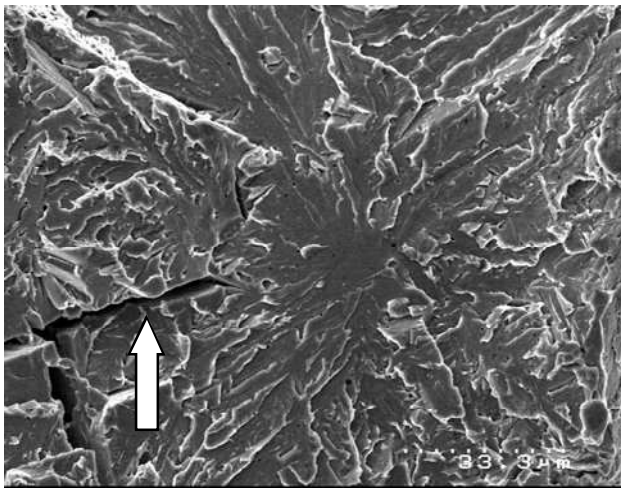

Table 8.1 - CTOD values for the ADAR weld metal condition for Weld N^{o}1.

Spec	Temp	Fm	a0	Δa	B	W	a_0/W	$f(a_0/W)$	V_p	Span	σyield	Z	E	CTOD	CTOD
	^{o}C	kN	mm	mm	mm	mm			mm	mm		mm		mm	Designations
19	-196	6130	3.55	0.000	10	10	0.35	1.75	0.00	40	890	2	206	0.005	C
37	-196	3310	6.12	0.000	10	10	0.61	3.95	0.00	40	890	2	206	0.007	C
29	-120	8403	4.17	0.098	10	10	0.42	2.08	0.00	40	625	2	206	0.017	C
7	-100	6669	3.53	0.112	10	10	0.35	1.75	0.08	40	600	2	206	0.033	C
31	-100	6134	4.32	0.145	10	10	0.43	2.17	0.20	40	600	2	206	0.063	C
9	-80	10833	3.67	0.203	10	10	0.37	1.81	0.29	40	580	2	206	0.113	U
27	-80	7403	3.71	0.216	10	10	0.37	1.83	0.25	40	580	2	206	0.088	U
45	-80	9243	5.94	0.289	10	10	0.59	3.69	0.21	40	580	2	206	0.106	U
53	-80	5947	4.34	0.297	10	10	0.43	2.18	0.36	40	580	2	206	0.106	U
55	-80	6531	3.73	0.305	10	10	0.37	1.84	0.20	40	580	2	206	0.070	U
47	-60	4125	6.19	N/A	10	10	0.62	4.06	0.85	40	580	2	206	0.150	M
11	-60	7000	2.78	0.364	10	10	0.28	1.44	0.50	40	580	2	206	0.195	U
33	-60	10359	6.04	0.458	10	10	0.60	3.83	0.29	40	580	2	206	0.143	U
35	-60	11076	3.75	0.489	10	10	0.38	1.85	0.42	40	580	2	206	0.154	U
25	-40	6643	4.13	N/A	10	10	0.41	2.05	1.02	40	542	2	206	0.294	M
15	-40	7700	2.78	0.545	10	10	0.28	1.44	0.72	40	542	2	206	0.280	U
1	20	6801	3.95	0.189	10	10	0.39	1.95	0.40	40	488	2	206	0.128	C
3	20	7156	4.29	N/A	10	10	0.43	2.15	1.30	40	488	2	206	0.364	M
5	20	6753	4.54	N/A	10	10	0.45	2.31	1.36	40	488	2	206	0.357	M
49	20	7912	5.20	N/A	10	10	0.52	2.84	1.48	40	488	2	206	0.348	M

Table 8.2 - CTOD values for the RHAR weld metal condition for Weld N^{o}1.

Spec	Temp	Fm	a0	Δa	B	W	a_0/W	$f(a_0/W)$	V_p	Span	σyield	Z	E	CTOD	CTOD
	^{o}C	kN	mm	mm	mm	mm			mm	mm		mm		mm	Designations
10	-196	6000	2.90	0.000	10	10	0.29	1.48	0.00	40	837	2	206	0.003	**C**
42	-196	6850	3.17	0.000	10	10	0.32	1.59	0.00	40	837	2	206	0.005	C
40	-122	9569	2.76	0.000	10	10	0.28	1.43	0.14	40	583	2	206	0.064	C
30	-102	7867	3.60	0.232	10	10	0.36	1.78	0.25	40	553	2	206	0.091	U
38	-100	12348	2.43	0.249	10	10	0.24	1.32	0.25	40	553	2	206	0.118	U
23	-80	5786	2.80	N/A	10	10	0.28	1.45	0.79	40	533	2	206	0.299	M
48	-80	6614	3.00	N/A	10	10	0.30	1.52	0.79	40	533	2	206	0.289	M
22	-80	6850	5.82	N/A	10	10	0.58	3.52	1.44	40	533	2	206	0.292	M
36	-80	7663	3.94	0.358	10	10	0.39	1.95	0.83	40	533	2	206	0.254	U
16	-80	10696	2.85	N/A	10	10	0.28	1.46	0.69	40	533	2	206	0.273	M
50	-62	7325	4.31	N/A	10	10	0.43	2.16	1.16	40	510	2	206	0.325	M
18	-62	10004	6.18	N/A	10	10	0.62	4.05	1.39	40	510	2	206	0.332	M
32	-62	13027	3.33	N/A	10	10	0.33	1.66	0.93	40	510	2	206	0.344	M
4	-42	7147	4.04	N/A	10	10	0.40	2.00	1.41	40	493	2	206	0.415	M
14	-42	7158	3.48	N/A	10	10	0.35	1.72	1.19	40	493	2	206	0.395	M
24	-42	10440	2.55	N/A	10	10	0.25	1.35	1.05	40	493	2	206	0.429	M
56	-42	10727	3.11	N/A	10	10	0.31	1.57	1.16	40	493	2	206	0.427	M
8	-42	15594	3.14	0.426	10	10	0.31	1.58	1.05	40	493	2	206	0.408	U
46	-40	8040	4.00	N/A	10	10	0.40	1.98	1.35	40	493	2	206	0.404	M
34	22	10283	3.03	N/A	10	10	0.30	1.53	1.57	40	430	2	206	0.579	M
6	25	12144	2.74	N/A	10	10	0.27	1.43	1.50	40	430	2	206	0.594	M
28	25	13809	3.78	N/A	10	10	0.38	1.87	1.76	40	430	2	206	0.582	M

Table 8.3 - CTOD values for the AD5%SA weld metal condition for Weld N^{o}1.

Spec	Temp	Fm	a0	Δa	B	W	a_0/W	$f(a_0/W)$	V_p	Span	σyield	Z	E	CTOD	CTOD
	^{o}C	kN	mm	mm	mm	mm			mm	mm		mm		mm	Designations
37	-122	12068	3.67	0.000	10	10	0.37	1.81	0.00	40	765	2	206	0.022	C
39	-118	6418	2.66	0.000	10	10	0.27	1.40	0.00	40	765	2	206	0.004	C
7	-80	6155	3.25	0.000	10	10	0.32	1.62	0.00	40	735	2	206	0.005	C
49	-80	6666	3.95	0.000	10	10	0.39	1.95	0.00	40	735	2	206	0.008	C
3	-62	6186	3.44	0.000	10	10	0.34	1.71	0.04	40	719	2	206	0.017	C
43	-62	6710	4.70	0.000	10	10	0.47	2.43	0.06	40	719	2	206	0.027	C
19	-58	8625	2.98	0.134	10	10	0.30	1.51	0.01	40	719	2	206	0.012	C
55	-58	6517	3.73	0.159	10	10	0.37	1.84	0.04	40	719	2	206	0.020	C
23	-40	9456	2.80	0.178	10	10	0.28	1.45	0.11	40	703	2	206	0.050	U
53	-40	5690	4.34	0.224	10	10	0.43	2.18	0.22	40	703	2	206	0.065	U
33	-20	9315	2.72	0.351	10	10	0.27	1.42	0.15	40	687	2	206	0.067	U
17	18	4580	5.00	0.397	10	10	0.50	2.66	0.50	40	656	2	206	0.119	M
35	20	10007	3.03	0.410	10	10	0.30	1.53	0.20	40	656	2	206	0.084	U
5	20	12590	2.90	N/A	10	10	0.29	1.48	0.22	40	656	2	206	0.100	M
25	22	10625	2.78	N/A	10	10	0.28	1.44	0.12	40	656	2	206	0.058	U

Table 8.4 - CTOD values for the RH5%SA weld metal condition for Weld N^{o}1.

Spec	Temp	Fm	a0	Δa	B	W	a_0/W	$f(a_0/W)$	V_p	Span	σyield	Z	E	CTOD	CTOD
	^{o}C	kN	mm	mm	mm	mm			mm	mm		mm		mm	Designations
22	-120	7890	2.89	0.000	10	10	0.29	1.48	0.00	40	735	2	206	0.007	C
42	-82	3933	4.86	0.000	10	10	0.49	2.55	0.00	40	692	2	206	0.005	C
16	-82	7728	4.04	0.054	10	10	0.40	2.01	0.00	40	692	2	206	0.012	C
46	-60	6122	5.09	0.107	10	10	0.51	2.74	0.32	40	669	2	206	0.085	C
32	-60	13132	2.61	0.221	10	10	0.26	1.38	0.21	40	669	2	206	0.099	U
8	-60	10473	3.33	0.268	10	10	0.33	1.66	0.28	40	669	2	206	0.109	U
14	-40	6026	2.84	N/A	10	10	0.28	1.46	0.50	40	638	2	206	0.190	U
2	-40	7791	4.82	N/A	10	10	0.48	2.52	0.74	40	638	2	206	0.193	U
28	-40	11013	2.74	N/A	10	10	0.27	1.42	0.50	40	638	2	206	0.204	M
50	-2	7148	4.37	N/A	10	10	0.44	2.20	0.83	40	592	2	206	0.233	M
52	18	8466	3.66	N/A	10	10	0.37	1.80	0.74	40	573	2	206	0.245	M
26	18	10707	2.93	N/A	10	10	0.29	1.49	0.65	40	573	2	206	0.254	M
24	20	12237	2.74	N/A	10	10	0.27	1.42	0.68	40	573	2	206	0.276	M
34	22	10710	3.11	N/A	10	10	0.31	1.57	0.68	40	573	2	206	0.255	M
45	22	6886	4.42	N/A	10	10	0.44	2.23	0.89	40	573	2	206	0.244	M
47	22	10225	4.21	N/A	10	10	0.42	2.10	0.86	40	573	2	206	0.263	M
57	22	8986	4.35	N/A	10	10	0.43	2.19	0.91	40	573	2	206	0.263	M

Table 8.5 - CTOD values for the ADAR weld metal condition for Weld N^{o}2.

Specimen	Condition	Temp	Fm	a0	Δa	B	W	a_0/W	$f(a_0/W)$	V_p	Span	σyield	Z	E	CTOD	CTOD
		^{o}C	kN	mm	mm	mm	mm			mm	mm		mm		mm	Designations
32	ADAR	-120	2795	1.98	0	10	10	0.20	1.17	0.04	40	562	2	206	0.027	C
31	ADAR	-120	5780	2.17	0	10	10	0.22	1.23	0.08	40	562	2	206	0.048	C
24	ADAR	-120	6708.3	2.08	0	10	10	0.21	1.20	0.08	40	562	2	206	0.050	C
33	ADAR	-100	3945	1.89	0.112	10	10	0.19	1.14	0.05	40	561	2	206	0.029	C
21	ADAR	-100	7018.3	1.45	0.154	10	10	0.14	1.00	0.08	40	561	2	206	0.056	C
35	ADAR	-80	6590	2.84	0.214	10	10	0.28	1.46	0.13	40	565	2	206	0.066	U
28	ADAR	-80	6735	2.26	0.188	10	10	0.23	1.26	0.12	40	565	2	206	0.072	C
27	ADAR	-80	6228.3	1.98	0.222	10	10	0.20	1.17	0.32	40	565	2	206	0.200	U
39	ADAR	-80	6649.2	2.35	0.254	10	10	0.23	1.29	0.15	40	565	2	206	0.084	U
42	ADAR	-80	7011.7	2.99	0.258	10	10	0.30	1.52	0.30	40	565	2	206	0.147	U
30	ADAR	-60	7508.3	1.90	0.275	10	10	0.19	1.14	0.18	40	526	2	206	0.112	U
37	ADAR	-60	9710.8	1.54	0.285	10	10	0.15	1.03	0.36	40	526	2	206	0.246	U
43	ADAR	-60	6003.3	2.09	0.296	10	10	0.21	1.20	0.32	40	526	2	206	0.193	U
29	ADAR	-60	3219.2	2.99	N/A	10	10	0.30	1.52	0.63	40	526	2	206	0.303	M
11	ADAR	-40	7262.5	1.09	0.317	10	10	0.11	0.88	0.33	40	467	2	206	0.252	U
40	ADAR	-40	6965.8	2.26	N/A	10	10	0.23	1.26	0.56	40	467	2	206	0.322	M
41	ADAR	-20	4144.2	2.35	N/A	10	10	0.23	1.29	0.66	40	497	2	206	0.374	M
9	ADAR	-20	8972.5	1.08	N/A	10	10	0.11	0.88	0.51	40	497	2	206	0.392	M
3	ADAR	20	8658.3	1.35	N/A	10	10	0.14	0.97	0.74	40	477	2	206	0.528	M
5	ADAR	20	7575	1.54	N/A	10	10	0.15	1.03	0.78	40	477	2	206	0.538	M

Table 8.6 - CTOD values for the RHAR weld metal condition for Weld N^{o}2.

Specimen	Condition	Temp	Fm	a0	Δa	B	W	a_0/W	$f(a_0/W)$	V_p	Span	σyield	Z	E	CTOD	CTOD
		^{o}C	kN	mm	mm	mm	mm			mm	mm		mm		mm	Designations
2	RHAR	-120	7641.7	2.06	0	10	10	0.21	1.19	0.14	40	582	2	206	0.086	C
23	RHAR	-120	7961.7	1.66	0	10	10	0.17	1.07	0.14	0.04	582	2	206	0.095	C
1	RHAR	-120	10268	1.06	0.147	10	10	0.11	0.87	0.15	0.04	582	2	206	0.116	C
34	RHAR	-100	7787.5	1.76	0.169	10	10	0.18	1.10	0.17	0.04	590	2	206	0.109	C
19	RHAR	-100	7587.5	1.47	0.173	10	10	0.15	1.01	0.18	0.04	590	2	206	0.127	C
22	RHAR	-100	7781.7	1.69	0.185	10	10	0.17	1.08	0.27	0.04	590	2	206	0.181	C
20	RHAR	-100	3929.2	2.98	0.197	10	10	0.30	1.51	0.60	0.04	590	2	206	0.292	C
18	RHAR	-80	6412.5	2.17	0.225	10	10	0.22	1.23	0.42	0.04	527	2	206	0.248	U
36	RHAR	-80	4284.2	1.45	0.246	10	10	0.14	1.00	0.52	0.04	527	2	206	0.367	U
17	RHAR	-80	11747	0.50	0.269	10	10	0.05	0.62	0.47	0.04	527	2	206	0.413	U
15	RHAR	-60	8398.3	1.18	0.279	10	10	0.12	0.91	0.54	0.04	500	2	206	0.405	U
13	RHAR	-60	9676.7	0.81	0.292	10	10	0.08	0.77	0.54	0.04	500	2	206	0.444	U
16	RHAR	-60	8514.2	1.54	0.299	10	10	0.15	1.03	0.74	0.04	500	2	206	0.509	U
38	RHAR	-60	6937.5	2.08	N/A	10	10	0.21	1.20	0.84	0.04	500	2	206	0.510	M
8	RHAR	-40	8880	1.35	N/A	10	10	0.14	0.97	0.71	0.04	510	2	206	0.509	M
26	RHAR	-40	7250.8	1.90	N/A	10	10	0.19	1.14	0.87	0.04	510	2	206	0.549	M
10	RHAR	-20	7690	1.86	N/A	10	10	0.19	1.13	1.01	0.04	460	2	206	0.642	M
6	RHAR	0	7965	1.38	N/A	10	10	0.14	0.98	0.96	0.04	460	2	206	0.688	M
14	RHAR	20	10063	1.68	N/A	10	10	0.17	1.07	1.18	0.04	455	2	206	0.786	M
12	RHAR	20	9308.3	1.76	N/A	10	10	0.18	1.10	1.18	0.04	455	2	206	0.772	M
7	RHAR	20	7704.2	1.30	N/A	10	10	0.13	0.95	1.05	0.04	455	2	206	0.765	M
4	RHAR	20	7754.2	1.65	0	10	10	0.16	1.06	1.21	0.04	455	2	206	0.811	M

Table 8.7 - CTOD values for the AD5%SA weld metal condition for Weld N^{o}2.

Specimen	Condition	Temp	Fm	a0	Δa	B	W	a_0/W	$f(a_0/W)$	V_p	Span	σyield	Z	E	CTOD	CTOD
		^{o}C	kN	mm	Mm	mm	mm			mm	mm		mm		mm	Designations
17	AD5%SA	-120	4092.5	1.80	0	10	10	0.18	1.11	0.04	40	765	2	206	0.026	C
3	AD5%SA	-100	3222.5	2.79	0	10	10	0.28	1.44	0.07	40	755	2	206	0.034	C
2	AD5%SA	-100	3755	2.79	0.125	10	10	0.28	1.44	0.07	40	755	2	206	0.036	C
14	AD5%SA	-80	6057.5	1.98	0.148	10	10	0.20	1.17	0.08	40	735	2	206	0.047	C
13	AD5%SA	-80	5327.5	2.16	0.157	10	10	0.22	1.23	0.08	40	735	2	206	0.047	C
20	AD5%SA	-60	7535.8	2.07	0.175	10	10	0.21	1.20	0.18	40	719	2	206	0.108	C
18	AD5%SA	-60	7425.8	1.71	0.186	10	10	0.17	1.08	0.23	40	719	2	206	0.151	C
10	AD5%SA	-40	8533.3	1.80	0.202	10	10	0.18	1.11	0.36	40	703	2	206	0.230	U
6	AD5%SA	-40	7146.7	1.62	0.255	10	10	0.16	1.06	0.37	40	703	2	206	0.246	U
25	AD5%SA	-20	3961.7	2.97	0.325	10	10	0.30	1.51	0.66	40	687	2	206	0.321	U
8	AD5%SA	20	8423.3	1.60	N/A	10	10	0.16	1.05	0.59	40	650	2	206	0.402	M
22	AD5%SA	20	4926.7	2.72	N/A	10	10	0.27	1.42	0.88	40	650	2	206	0.455	M

Table 8.8 - CTOD values for the RH5%SA weld metal condition for Weld N^{o}2.

Specimen	Condition	Temp	Fm	a0	Δa	B	W	a_0/W	$f(a_0/W)$	V_p	Span	σyield	Z	E	CTOD	CTOD
		^{o}C	kN	mm	mm	mm	mm			mm	mm		mm		mm	Designations
4	RH5%SA	-120	4405.8	1.98	0	10	10	0.20	1.17	0.06	40	755	2	206	0.034	C
16	RH5%SA	-100	5800.8	1.98	0	10	10	0.20	1.17	0.07	40	710	2	206	0.040	C
15	RH5%SA	-100	6232.5	1.89	0.133	10	10	0.19	1.14	0.07	40	710	2	206	0.044	C
12	RH5%SA	-80	4530.8	2.13	0.168	10	10	0.21	1.22	0.09	40	692	2	206	0.054	C
9	RH5%SA	-80	7716.7	1.89	0.173	10	10	0.19	1.14	0.12	40	692	2	206	0.074	C
19	RH5%SA	-60	7640	2.07	0.196	10	10	0.21	1.20	0.28	40	669	2	206	0.170	C
23	RH5%SA	-60	5550	2.52	0.204	10	10	0.25	1.35	0.32	40	669	2	206	0.173	U
21	RH5%SA	-40	6911.7	1.53	0.224	10	10	0.15	1.03	0.36	40	638	2	206	0.251	U
1	RH5%SA	-40	6392.5	2.07	0.266	10	10	0.21	1.20	0.43	40	638	2	206	0.258	U
24	RH5%SA	-40	5852.5	2.43	0.325	10	10	0.24	1.32	0.47	40	638	2	206	0.261	U
5	RH5%SA	-20	6448.3	2.43	0.363	10	10	0.24	1.32	0.69	40	600	2	206	0.381	U
11	RH5%SA	20	9759.2	1.26	N/A	10	10	0.13	0.94	0.68	40	573	2	206	0.499	M
7	RH5%SA	20	8838.3	1.86	N/A	10	10	0.19	1.13	0.88	40	573	2	206	0.561	M

Table 8.9 - Summary of CTOD values for the ADAR and RHAR weld metal condition for Weld N^{o}1, with the correct CTOD designations, McMeeking analysis and actual measurements.

Specimen	Condition	Temp	Fm	a0	Δa	δ	δ	1.9δ	Actual
		^{o}C	kN	mm	mm	mm	Designation	mm	Measurement
19	ADAR	-196	6130	3.55	0.000	0.005	C	0.009	0.010
37	ADAR	-196	3310	6.12	0.000	0.007	C	0.013	0.014
29	ADAR	-120	8403	4.17	0.098	0.017	C	0.033	0.030
7	ADAR	-100	6669	3.53	0.112	0.034	C	0.064	0.097
31	ADAR	-100	61347	4.32	0.145	0.063	C	0.120	0.154
1	ADAR	20	6801	3.95	0.189	0.129	C	0.244	0.280
9	ADAR	-80	10833	3.67	0.203	0.113	U	0.215	0.190
27	ADAR	-80	7403	3.71	0.216	0.088	U	0.167	0.186
45	ADAR	-80	9243	5.94	0.289	0.106	U	0.202	0.247
53	ADAR	-80	5947	4.34	0.297	0.106	U	0.201	0.265
55	ADAR	-80	6531	3.73	0.305	0.070	U	0.132	0.116
11	ADAR	-60	7000	2.78	0.364	0.195	U	0.370	0.405
33	ADAR	-60	10359	6.04	0.458	0.143	U	0.272	0.296
35	ADAR	-60	11076	3.75	0.489	0.154	U	0.292	0.327
15	ADAR	-40	7700	2.78	0.545	0.280	U	0.531	N/A
10	RHAR	-196	6000	2.90	0.000	0.003	C	0.006	0.009
42	RHAR	-196	6850	3.17	0.000	0.005	C	0.010	0.014
40	RHAR	-122	9569	2.76	0.000	0.064	C	0.122	0.164
30	RHAR	-102	7867	3.60	0.232	0.091	U	0.173	0.196
38	RHAR	-102	12348	2.43	0.249	0.118	U	0.225	0.269
36	RHAR	-82	7663	3.94	0.358	0.254	U	0.483	N/A
8	RHAR	-42	15594	3.14	0.426	0.408	U	0.774	N/A

Table 8.10 - Summary of CTOD values for the AD5%SA and RH5%SA weld metal condition for Weld N^{o}1, with the correct CTOD designations, McMeeking analysis and actual measurements.

Specimen	Condition	Temp	Fm	a0	Δa	δ	δ	1.9δ	Actual
		^{o}C	kN	mm	mm	mm	Designation	mm	Measurement
37	AD5%SA	-122	12068	3.67	0.000	0.022	C	0.042	0.069
39	AD5%SA	-118	6418	2.66	0.000	0.004	C	0.007	0.010
7	AD5%SA	-80	6155	3.25	0.000	0.048	C	0.091	0.126
49	AD5%SA	-80	6666	3.95	0.000	0.008	C	0.015	0.186
3	AD5%SA	-62	6186	3.44	0.000	0.017	C	0.032	0.039
43	AD5%SA	-62	6710	4.70	0.000	0.027	C	0.051	0.053
19	AD5%SA	-58	8625	2.98	0.134	0.012	C	0.023	0.027
55	AD5%SA	-58	6517	3.73	0.159	0.020	C	0.038	0.040
23	AD5%SA	-40	9456	2.80	0.178	0.050	U	0.095	0.125
53	AD5%SA	-40	5690	4.34	0.224	0.067	U	0.128	0.158
33	AD5%SA	-20	9315	2.72	0.351	0.067	U	0.127	0.169
35	AD5%SA	20	10007	3.03	0.410	0.084	U	0.160	0.196
25	AD5%SA	22	10625	2.78	0.397	0.058	U	0.110	0.126
22	RH5%SA	-120	7890	2.89	0.000	0.007	C	0.012	0.010
42	RH5%SA	-82	3933	4.86	0.000	0.005	C	0.010	0.008
16	RH5%SA	-82	7728	4.04	0.054	0.012	C	0.023	0.035
46	RH5%SA	-60	6122	5.09	0.107	0.085	C	0.161	0.190
32	RH5%SA	-60	13132	2.61	0.221	0.099	U	0.189	0.201
8	RH5%SA	-60	10473	3.33	0.268	0.109	U	0.207	0.225
14	RH5%SA	-40	6026	2.84	0.278	0.190	U	0.361	0.396
2	RH5%SA	-40	7791	4.82	0.254	0.193	U	0.366	0.380

Table 8.11 - Summary of CTOD values for the ADAR weld metal condition for Weld N^{o}2, with the correct CTOD designations, McMeeking analysis and actual measurements.

Specimen	Condition	Temp	Fm	a0	Δa	Δ	δ	1.9δ	Actual
		^{o}C	kN	mm	mm	mm	Designation	mm	Measurement
32	ADAR	-120	2795	1.98	0.000	0.027	C	0.051	0.066
31	ADAR	-120	5780	2.17	0.000	0.048	C	0.091	0.113
24	ADAR	-120	6708.3	2.08	0.000	0.050	C	0.095	0.106
33	ADAR	-100	3945	1.89	0.112	0.029	C	0.054	0.076
21	ADAR	-100	7018.3	1.45	0.154	0.056	C	0.106	0.136
28	ADAR	-80	6735	2.26	0.188	0.072	C	0.136	0.176
35	ADAR	-80	6590	2.84	0.214	0.066	U	0.126	0.157
27	ADAR	-80	6228.3	1.98	0.222	0.200	U	0.380	N/A
39	ADAR	-80	6649.2	2.35	0.254	0.084	U	0.160	0.186
42	ADAR	-80	7011.7	2.99	0.258	0.147	U	0.279	0.317
30	ADAR	-60	7508.3	1.90	0.275	0.112	U	0.212	0.236
37	ADAR	-60	9710.8	1.54	0.285	0.246	U	0.468	0.257
43	ADAR	-60	6003.3	2.09	0.296	0.193	U	0.367	N/A
11	ADAR	-40	7262.5	1.09	0.317	0.252	U	0.479	N/A

Table 8.12 - Summary of CTOD values for the RHAR weld metal condition for Weld N^{o}2, with the correct CTOD designations, McMeeking analysis and actual measurements.

Specimen	Condition	Temp	Fm	a0	Δa	δ	δ	1.9δ	Actual
		^{o}C	kN	mm	mm	mm	Designation	mm	Measurement
2	RHAR	-120	7641.7	2.06	0.000	0.086	C	0.163	0.197
23	RHAR	-120	7961.7	1.66	0.000	0.095	C	0.180	0.215
1	RHAR	-120	10268	1.06	0.147	0.116	C	0.221	0.266
34	RHAR	-100	7787.5	1.76	0.169	0.109	C	0.206	0.217
19	RHAR	-100	7587.5	1.47	0.173	0.127	C	0.241	0.285
22	RHAR	-100	7781.7	1.69	0.185	0.181	C	0.345	N/A
20	RHAR	-100	3929.2	2.98	0.197	0.292	C	0.555	N/A
18	RHAR	-80	6412.5	2.17	0.225	0.248	U	0.472	N/A
36	RHAR	-80	4284.2	1.45	0.246	0.367	U	0.698	N/A
17	RHAR	-80	11747	0.50	0.269	0.413	U	0.785	N/A
15	RHAR	-60	8398.3	1.18	0.279	0.405	U	0.770	N/A
13	RHAR	-60	9676.7	0.81	0.292	0.444	U	0.843	N/A
16	RHAR	-60	8514.2	1.54	0.299	0.509	U	0.966	N/A
8	RHAR	-40	8880	1.35	0.342	0.509	U	0.967	N/A
26	RHAR	-40	7250.8	1.90	0.357	0.549	U	1.043	N/A

Table 8.13 - Summary of CTOD values for the AD5%SA and RH5%SA weld metal condition for Weld N^{o}2, with the correct CTOD designations, McMeeking analysis and actual measurements.

Specimen	Condition	Temp	Fm	a0	Δa	δ	δ	1.9δ	Actual
		^{o}C	kN	mm	mm	mm	Designation	mm	Measurement
17	AD5%SA	-120	4092.5	1.80	0.000	0.026	C	0.050	0.057
3	AD5%SA	-100	3222.5	2.79	0.000	0.034	C	0.065	0.080
2	AD5%SA	-100	3755	2.79	0.125	0.036	C	0.068	0.097
14	AD5%SA	-80	6057.5	1.98	0.148	0.047	C	0.089	0.115
13	AD5%SA	-80	5327.5	2.16	0.157	0.047	C	0.090	0.125
20	AD5%SA	-60	7535.8	2.07	0.175	0.108	C	0.205	0.237
18	AD5%SA	-60	7425.8	1.71	0.186	0.151	C	0.287	0.317
10	AD5%SA	-40	8533.3	1.80	0.202	0.230	U	0.437	N/A
6	AD5%SA	-40	7146.7	1.62	0.255	0.246	U	0.468	N/A
25	AD5%SA	-20	3961.7	2.97	0.325	0.321	U	0.611	N/A
4	RH5%SA	-120	4405.8	1.98	0.000	0.034	C	0.065	0.078
16	RH5%SA	-100	5800.8	1.98	0.000	0.040	C	0.077	0.096
15	RH5%SA	-100	6232.5	1.89	0.133	0.044	C	0.083	0.114
12	RH5%SA	-80	4530.8	2.13	0.168	0.054	C	0.102	0.136
9	RH5%SA	-80	7716.7	1.89	0.173	0.074	C	0.140	0.175
19	RH5%SA	-60	7640	2.07	0.196	0.170	C	0.324	0.363
23	RH5%SA	-60	5550	2.52	0.204	0.173	U	0.329	N/A
21	RH5%SA	-40	6911.7	1.53	0.224	0.251	U	0.477	N/A
1	RH5%SA	-40	6392.5	2.07	0.266	0.258	U	0.490	N/A
24	RH5%SA	-40	5852.5	2.43	0.325	0.261	U	0.495	N/A
5	RH5%SA	-20	6448.3	2.43	0.363	0.381	U	0.725	N/A

Figure 8.1 - Weld N°1 - Example of load versus clip gauge displacement curves for the ADAR microstructural condition.

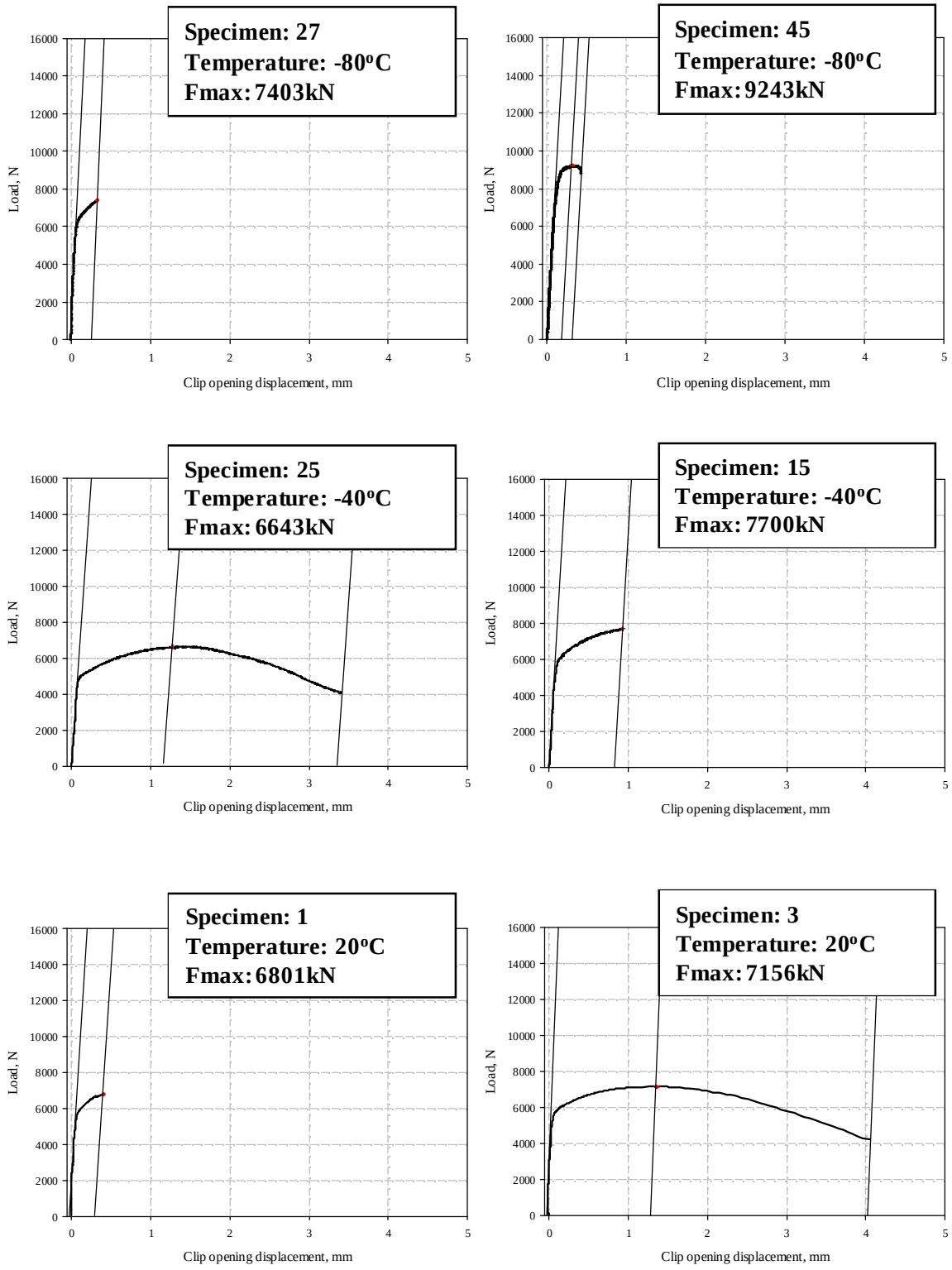

Figure 8.2 - Weld N°1 - Example of load versus clip gauge displacement curves for the RHAR microstructural condition.

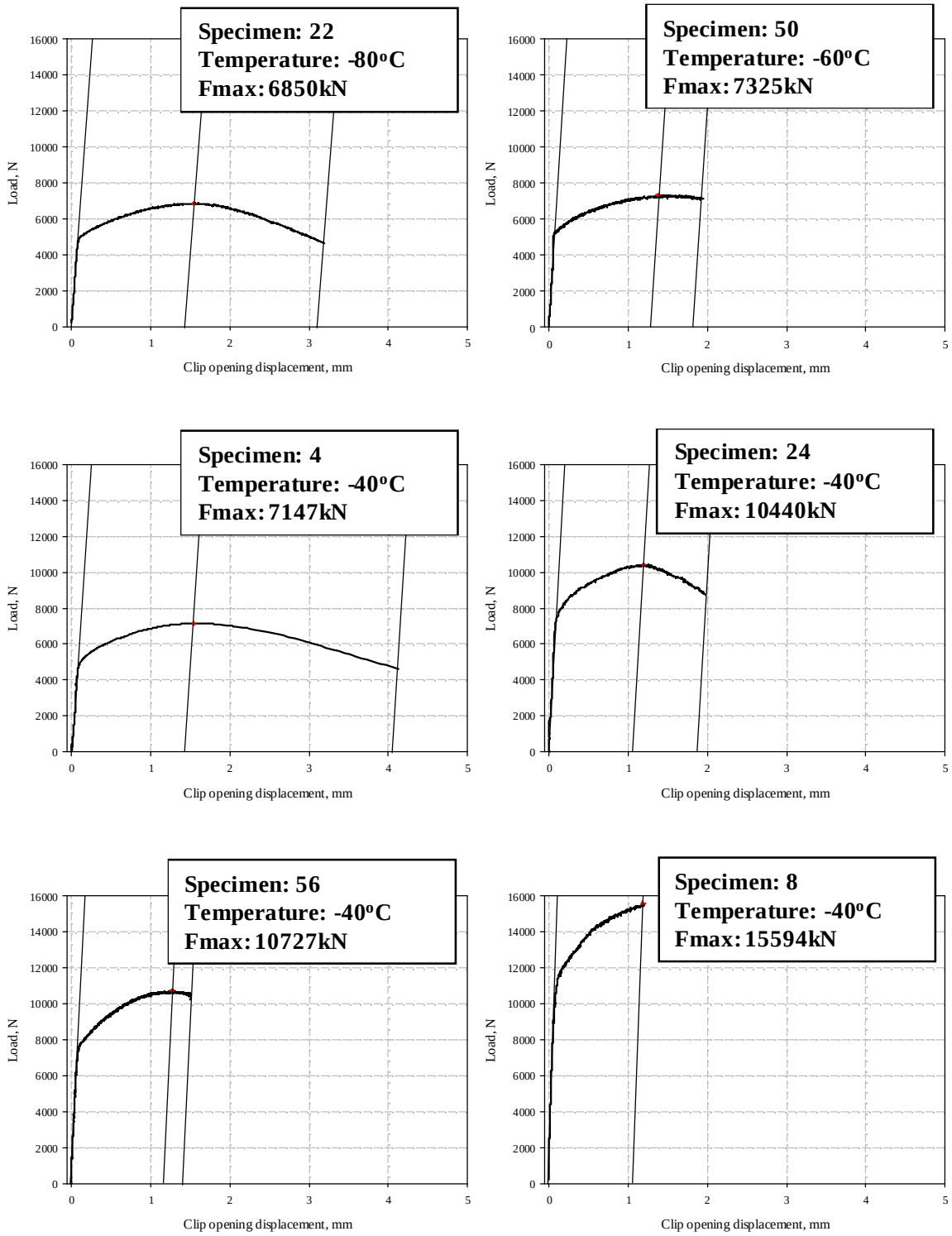

Figure 8.3 - Weld N°1 - Example of load versus clip gauge displacement curves for the AD5%SA microstructural condition.

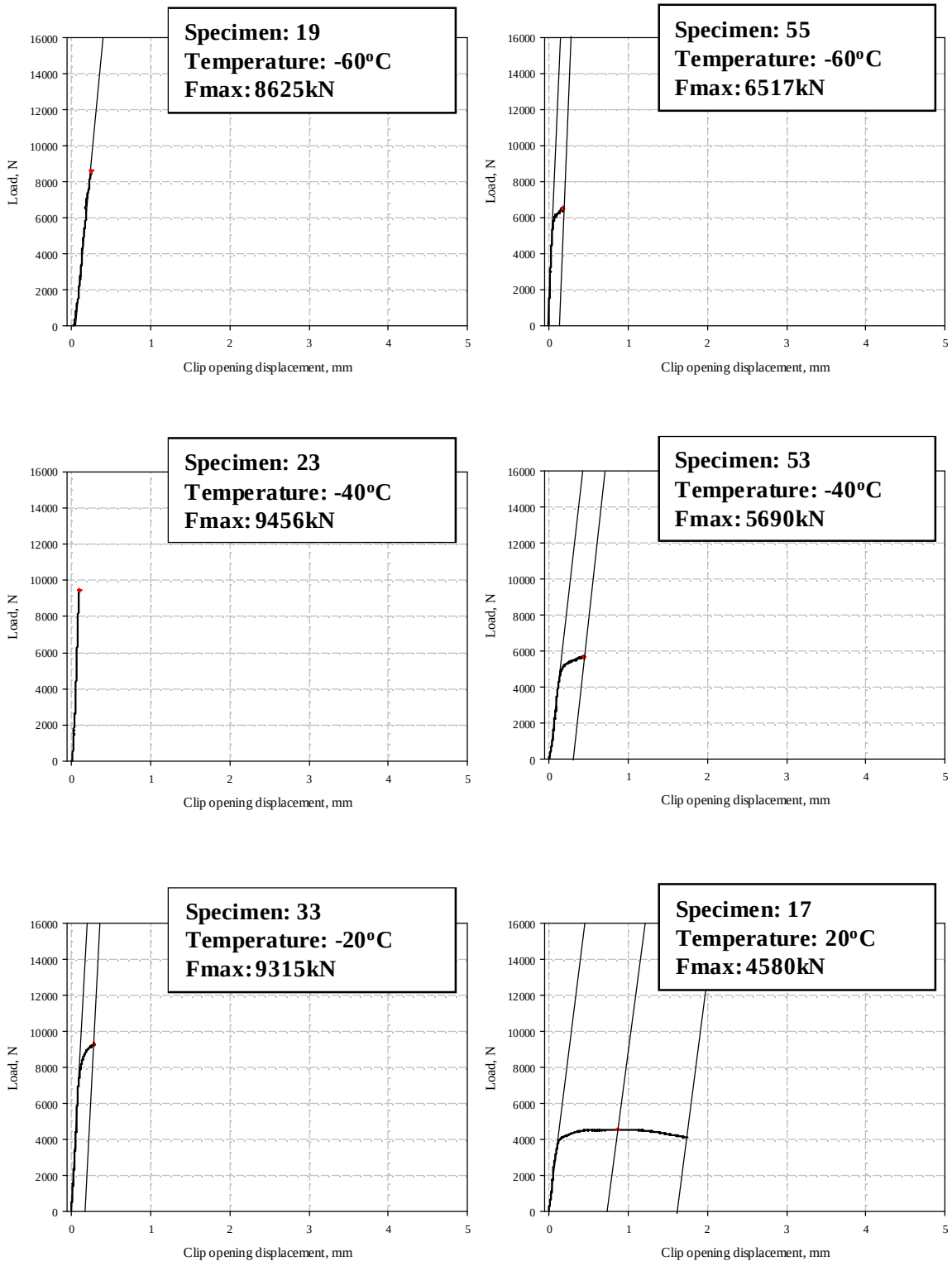

Figure 8.4 - Weld N°1 - Example of load versus clip gauge displacement curves for the RH5%SA microstructural condition.

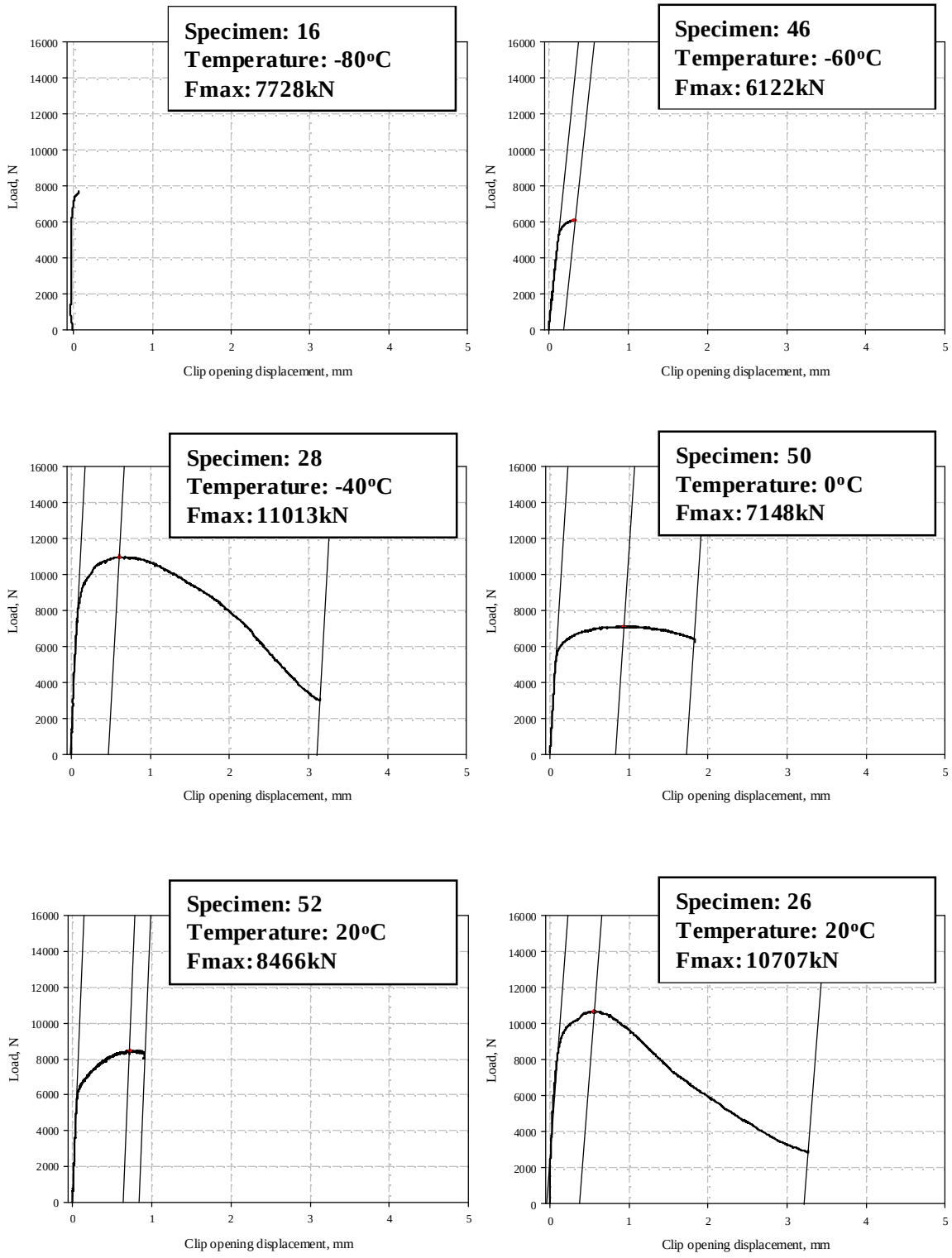

Figure 8.5 - Weld N°1 - CTOD values for both microstructures, as-deposited (AD) and reheated (RH); in both the as-received (AR) and prestrained and aged (5%SA) condition.

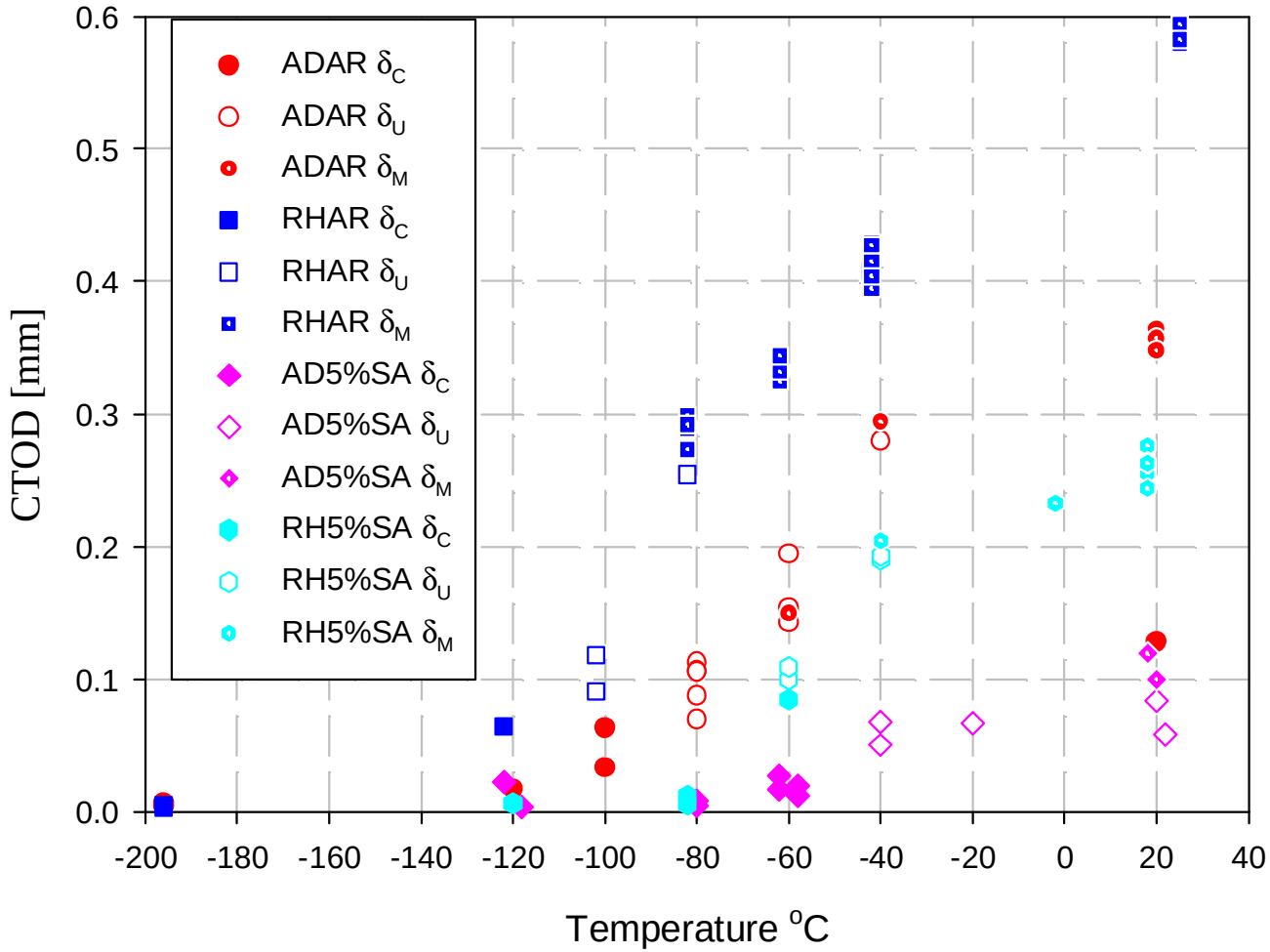

Figure 8.6 - Weld N°1 - CTOD values for both microstructures, as-deposited (AD) and reheated (RH); in the as-received (AR) condition.

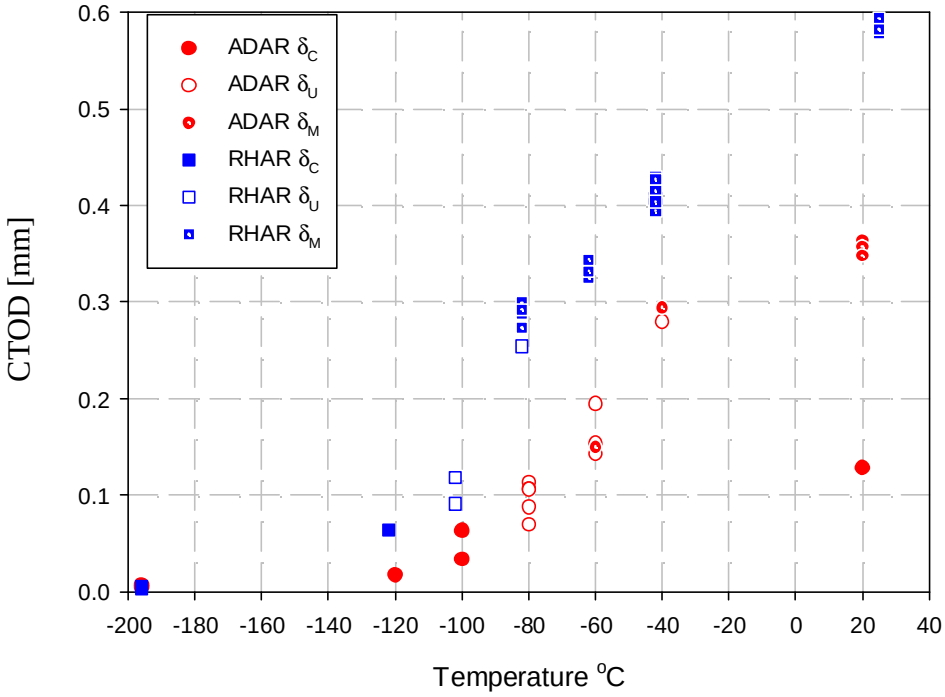

Figure 8.7 - Weld N°1 - CTOD values for both microstructures, as-deposited (AD) and reheated (RH); in the prestrain and aged (5%SA) condition.

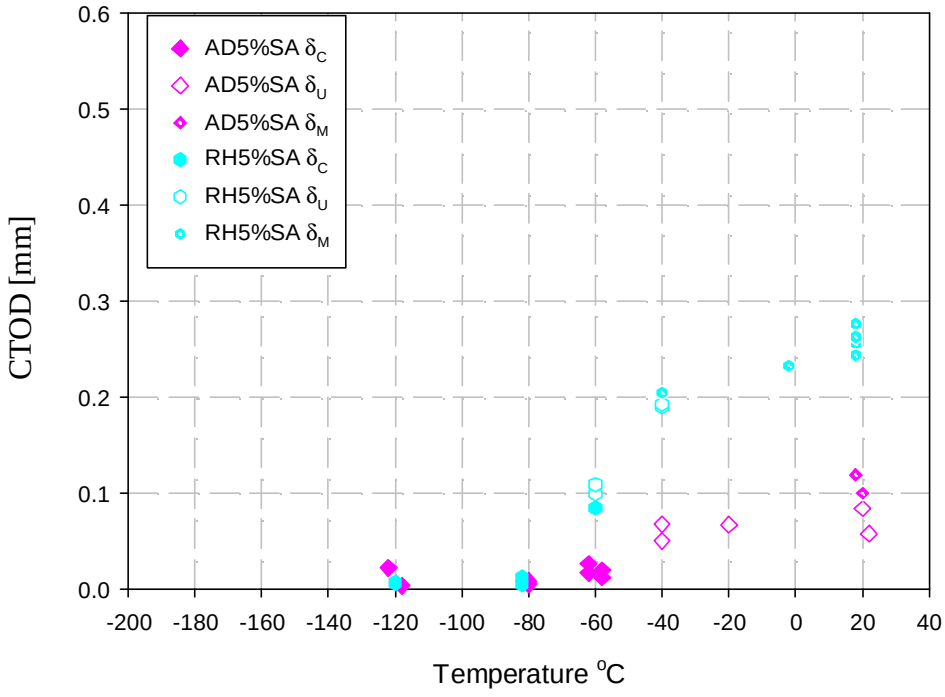

Figure 8.8 - Weld N°1 - CTOD values plotted against the amount of stable crack growth for all microstructures and conditions.

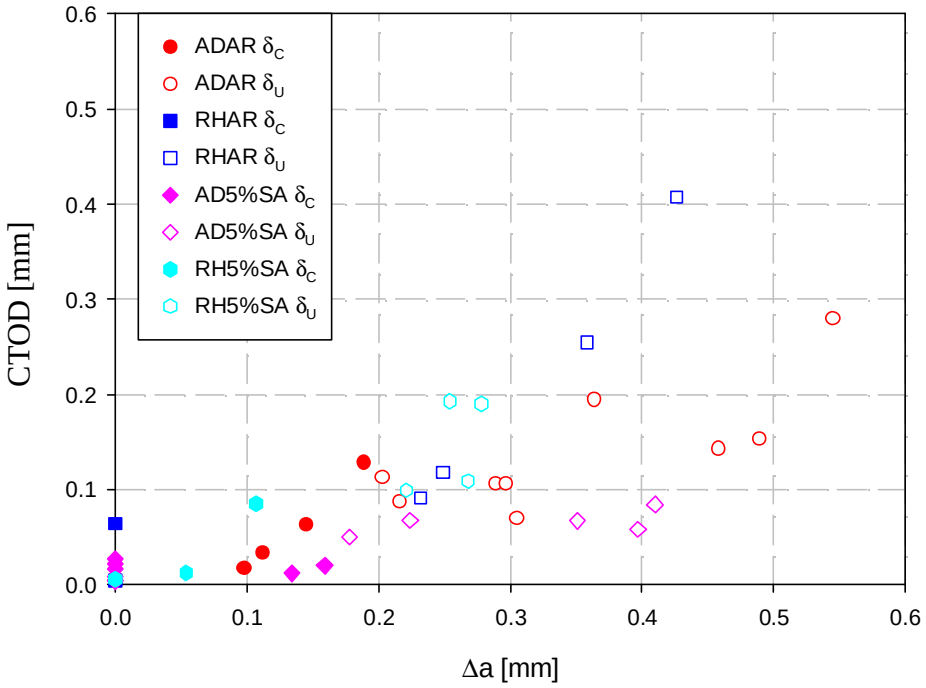

Figure 8.9 - Weld N°1 - Amount of stable crack growth plotted against the test temperature for all microstructures and conditions.

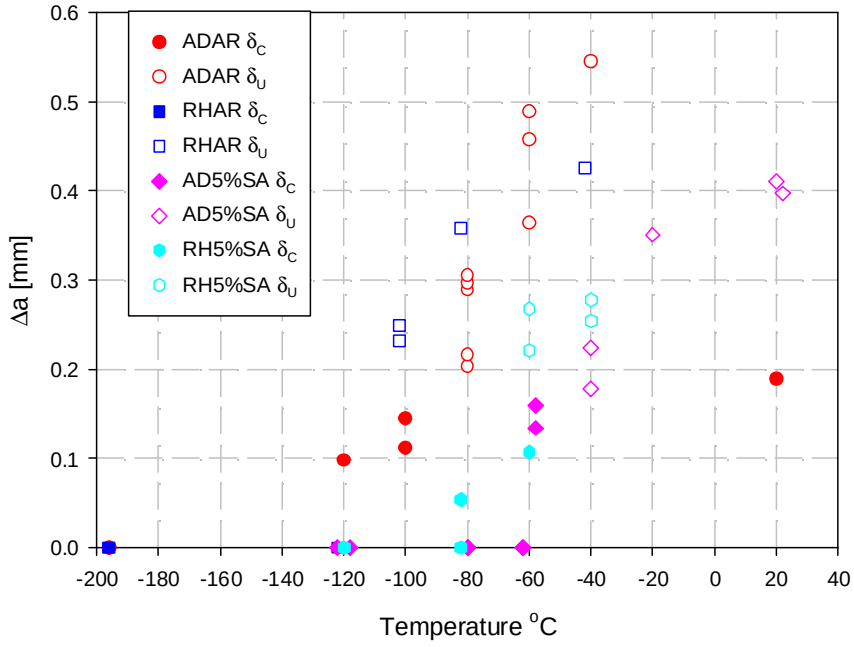

Figure 8.10 - Weld Nº2 - Example of load versus displacement curves for the ADAR microstructural condition.

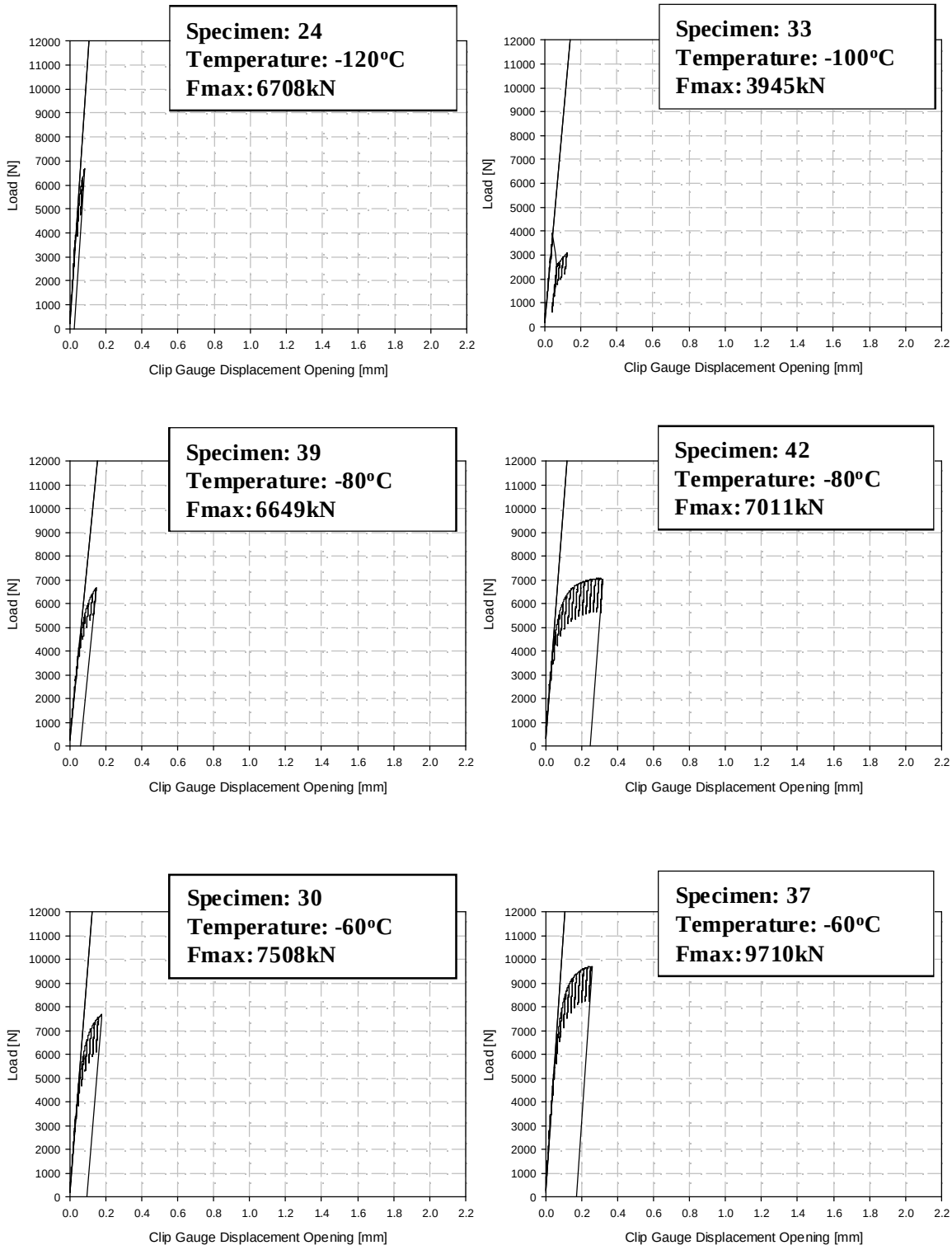

Figure 8.11 - Weld N^{o}2 - Example of load versus displacement curves for the RHAR microstructural condition.

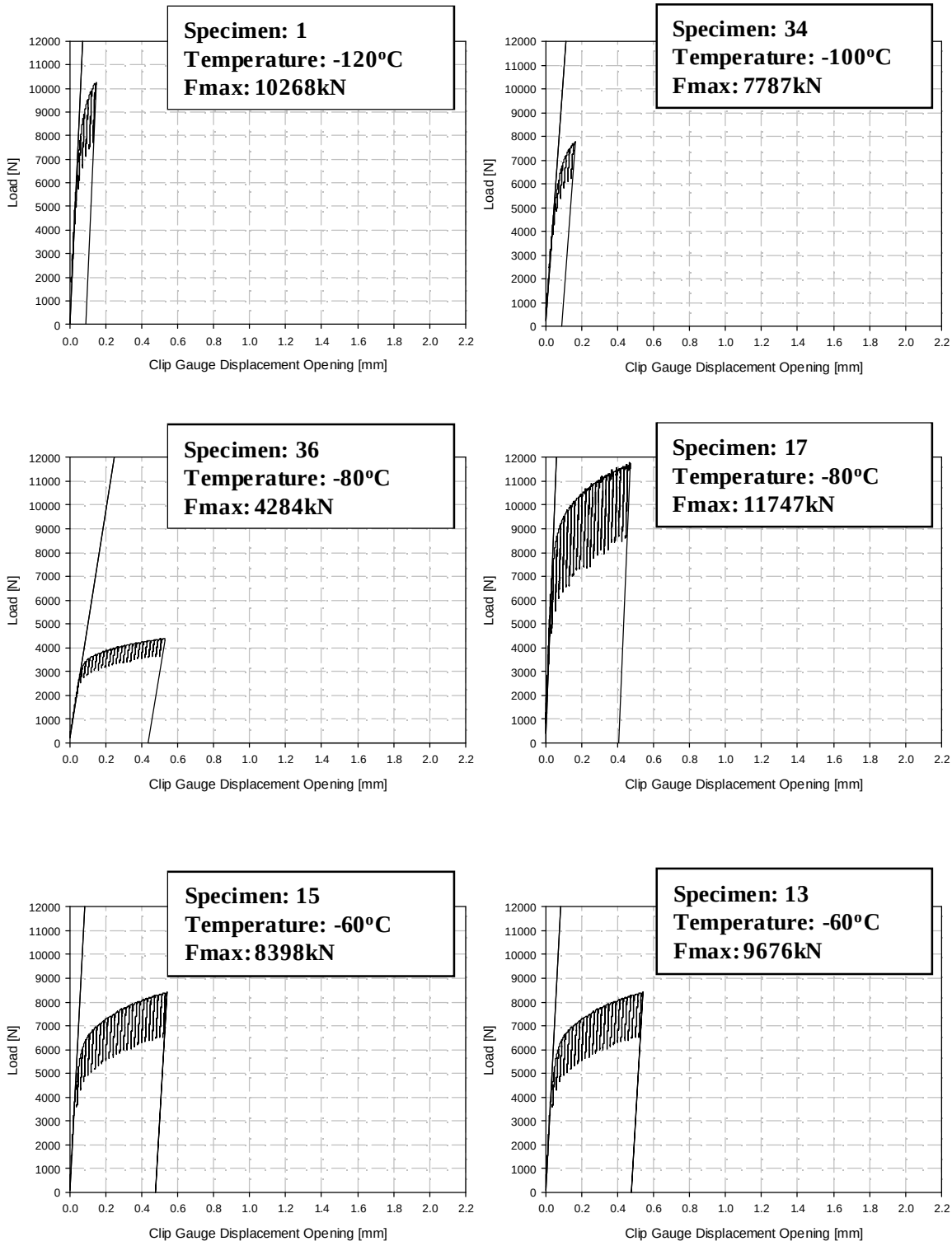

Figure 8.12 - Weld N°2 - Example of load versus displacement curves for the AD5%SA microstructural condition.

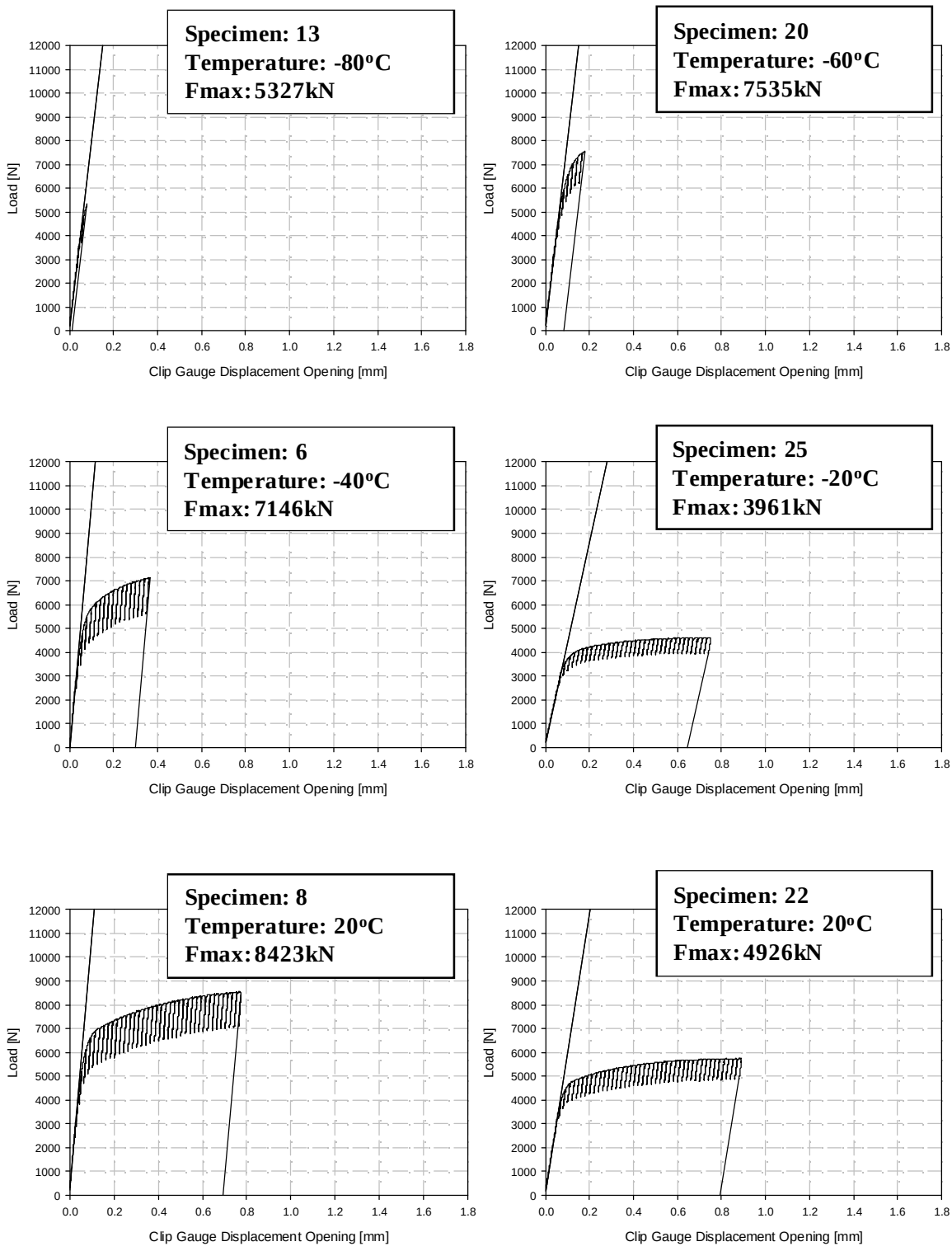

Figure 8.13- Weld N^{o}2 - Example of load versus displacement curves for the RH5%SA microstructural condition.

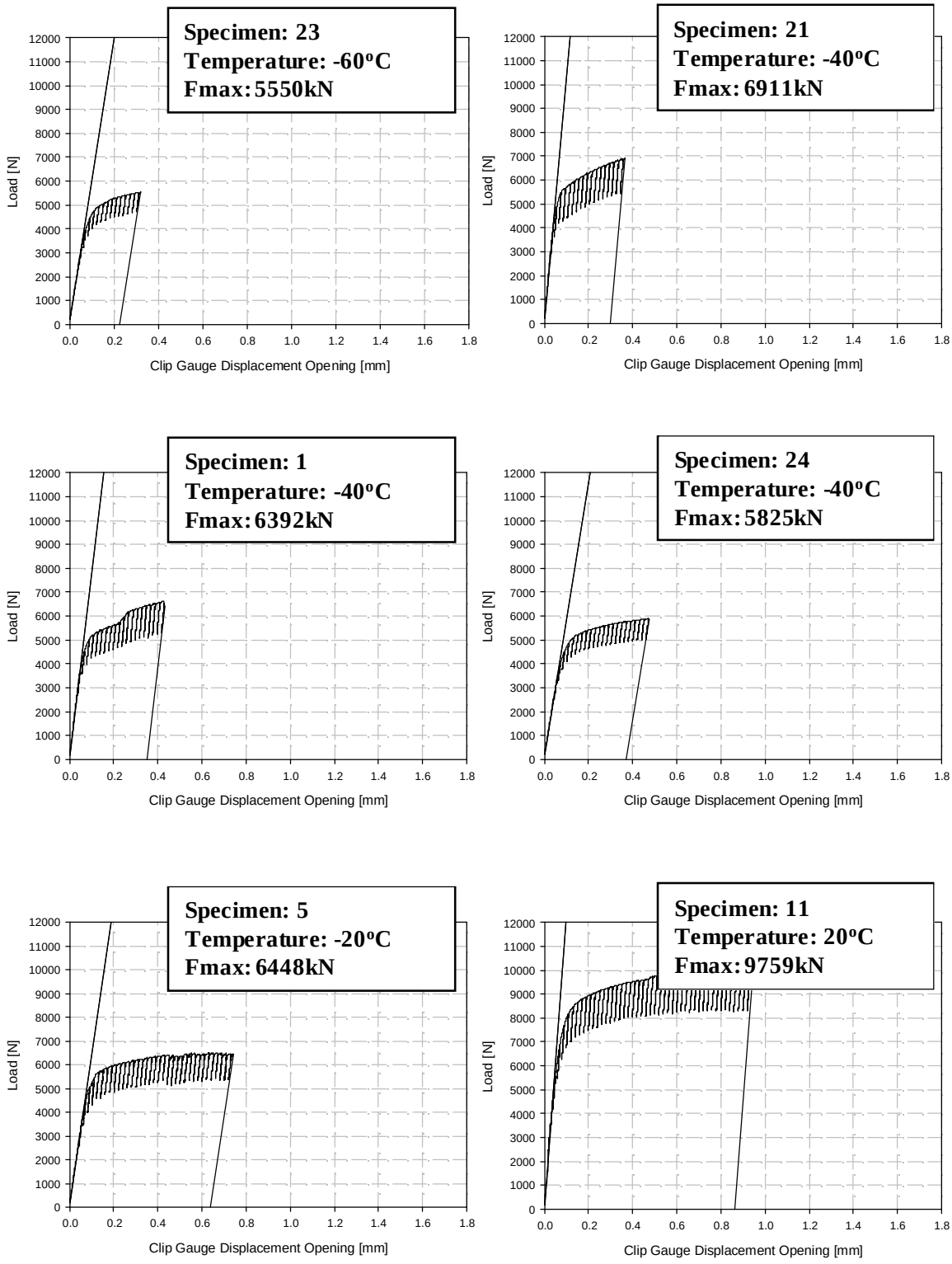

Figure 8.14 - Weld N°2 - CTOD values for both microstructures, as-deposited (AD) and reheated (RH); in both the as-received (AR) and prestrained and aged (5%SA) condition.

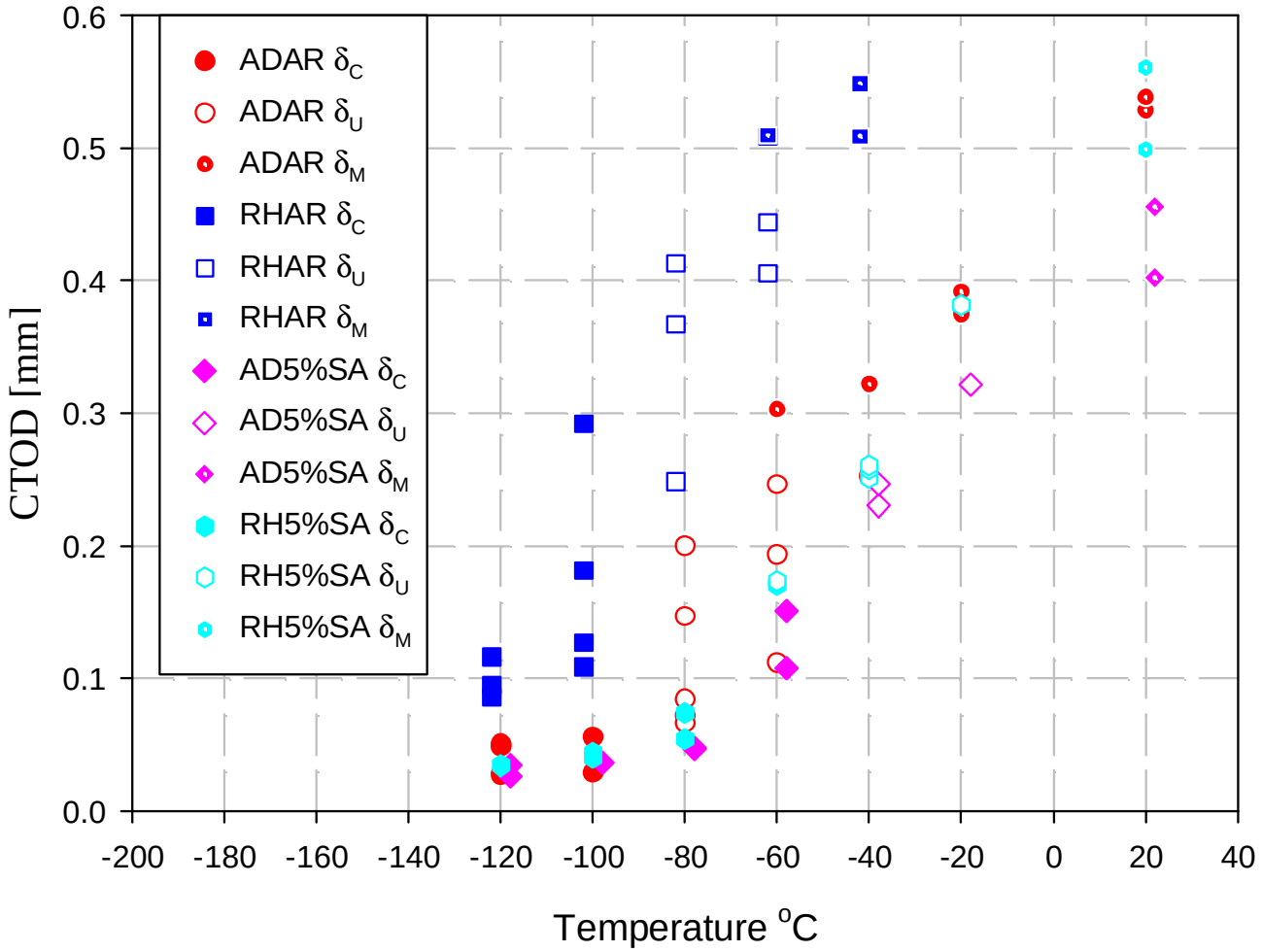

Figure 8.15 - Weld N°2 - CTOD values for both microstructures, as-deposited (AD) and reheated (RH); in the as-received (AR) condition.

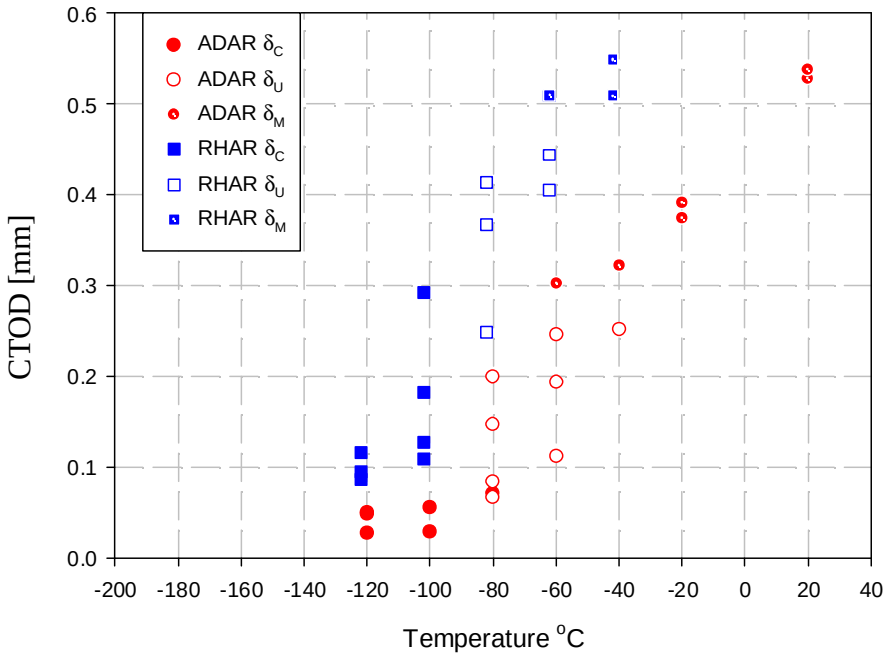

Figure 8.16 - Weld N°2 - CTOD values for both microstructures, as-deposited (AD) and reheated (RH); in the prestrain and aged (5%SA) condition.

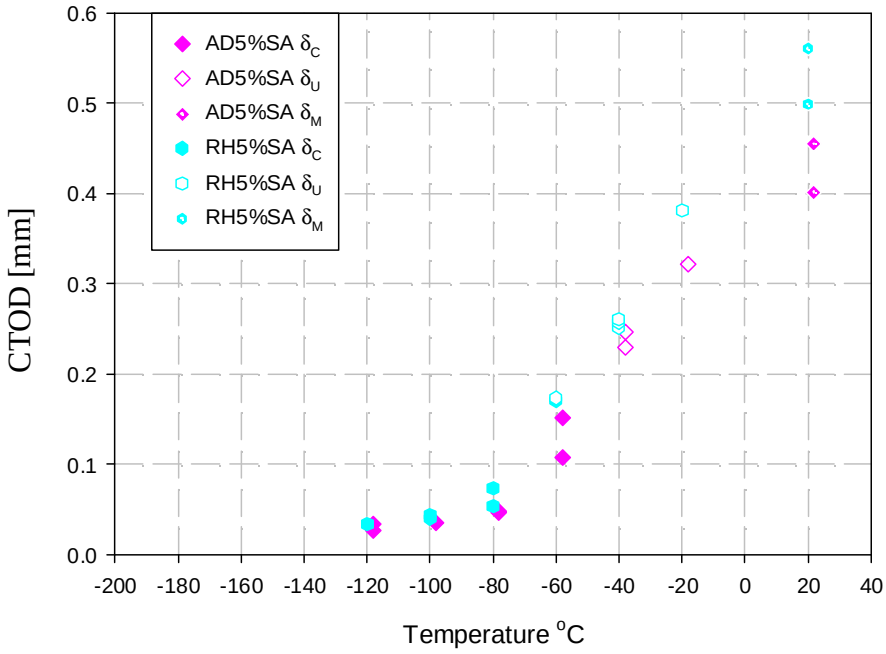

Figure 8.17 - Weld N°2 - CTOD values plotted against the amount of stable crack growth for all microstructures and conditions.

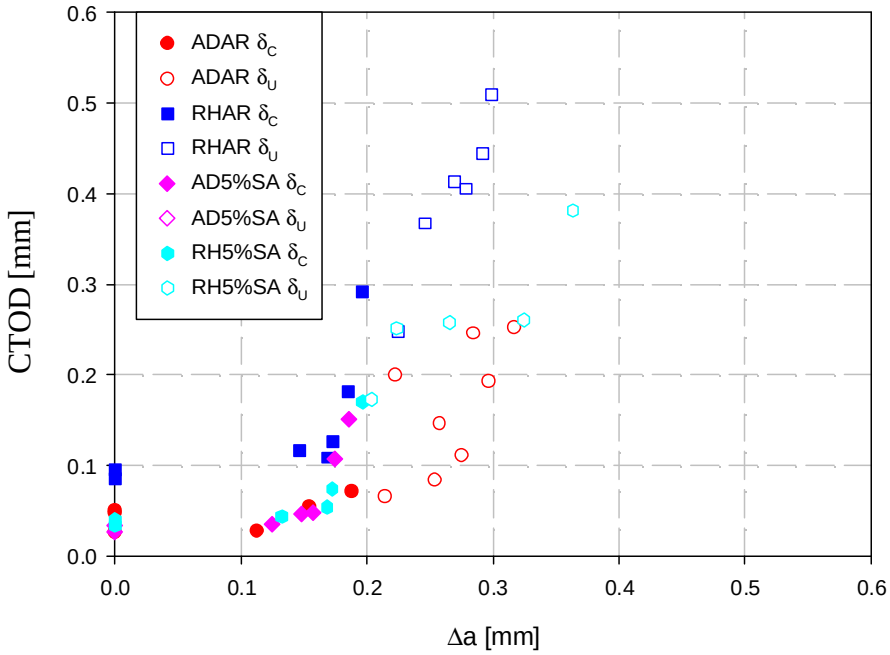

Figure 8.18 - Weld N°2 - Amount of stable crack growth plotted against the test temperature for all microstructures and conditions.

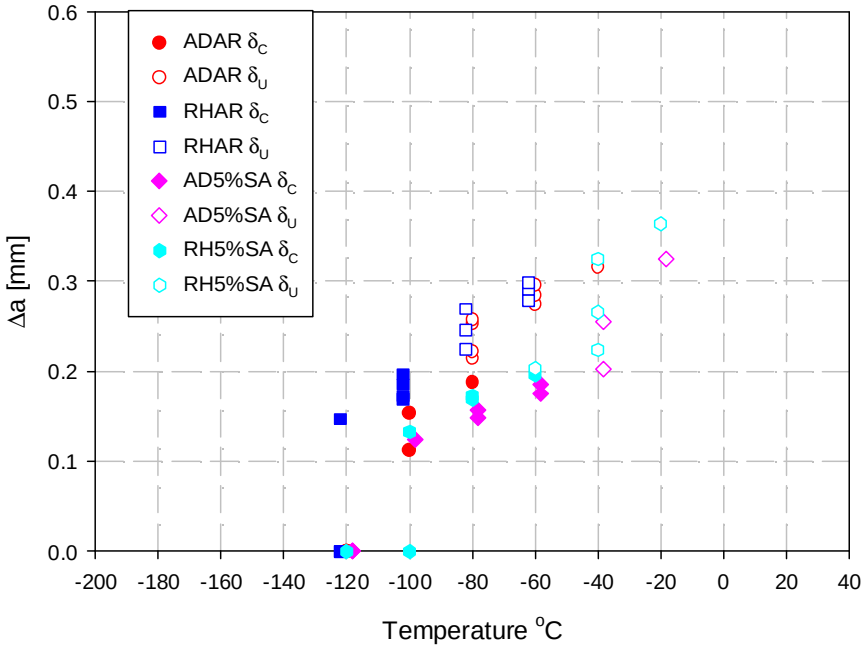

Figure 8.19 - Macroscopic appearance of selected AD specimen (a) tested at -120°C, exhibiting no stable crack extension. (b) tested at -60°C exhibiting a small amount of stable crack extension.

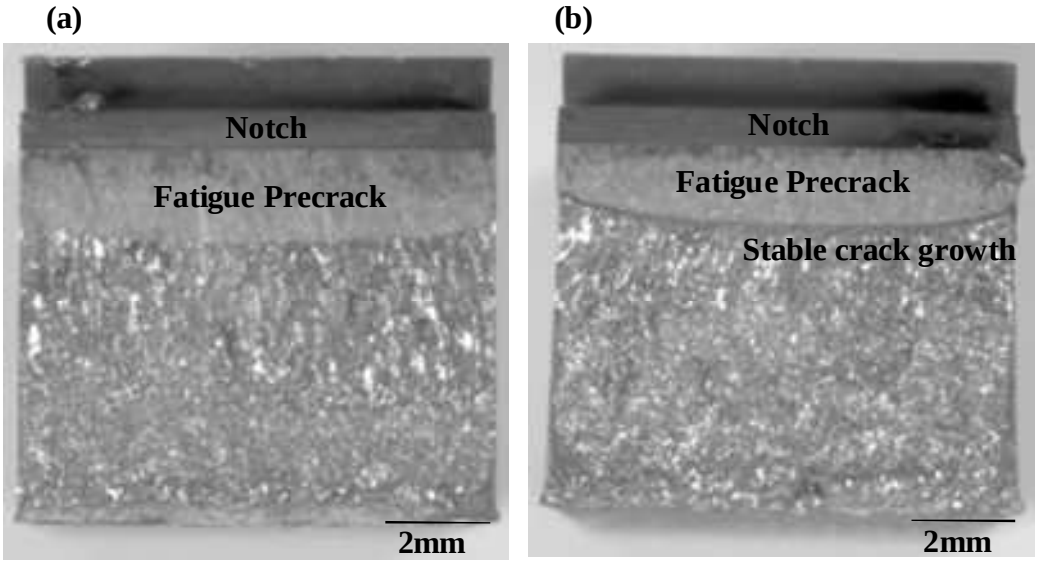

Figure 8.20 - Macroscopic appearance of selected RH specimen (a) tested at -120°C, exhibiting no stable crack extension. (b) tested at -60°C exhibiting a small amount of stable crack extension.

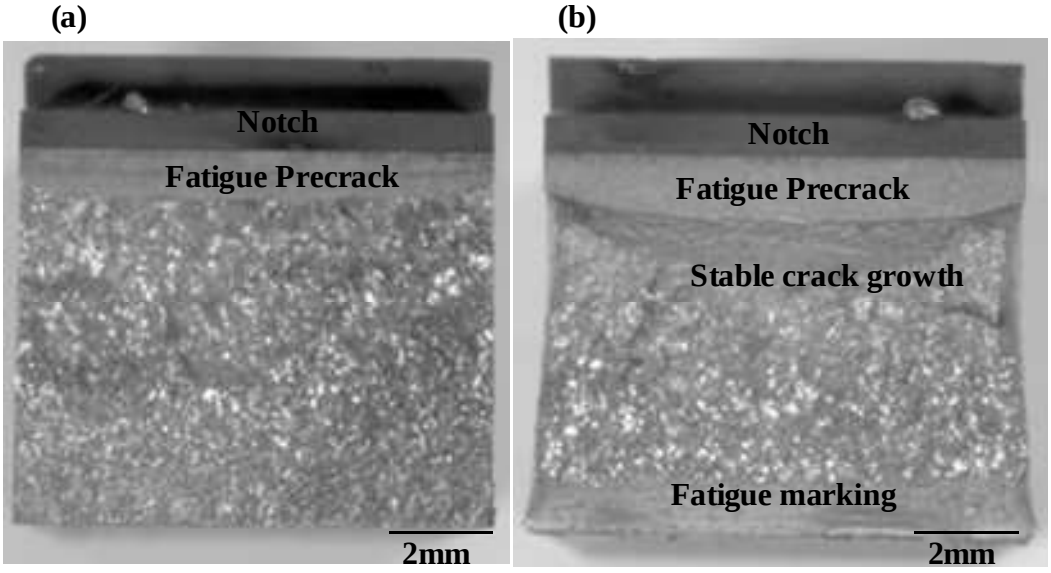

Figure 8.21 - Weld N^{o}1 Sample 9, ADAR; (a) general fracture surface, (b) magnification of framed area, (c) secondary cracking noted near to initiation site (arrowed), (d) non metallic inclusion initiation site (arrowed).

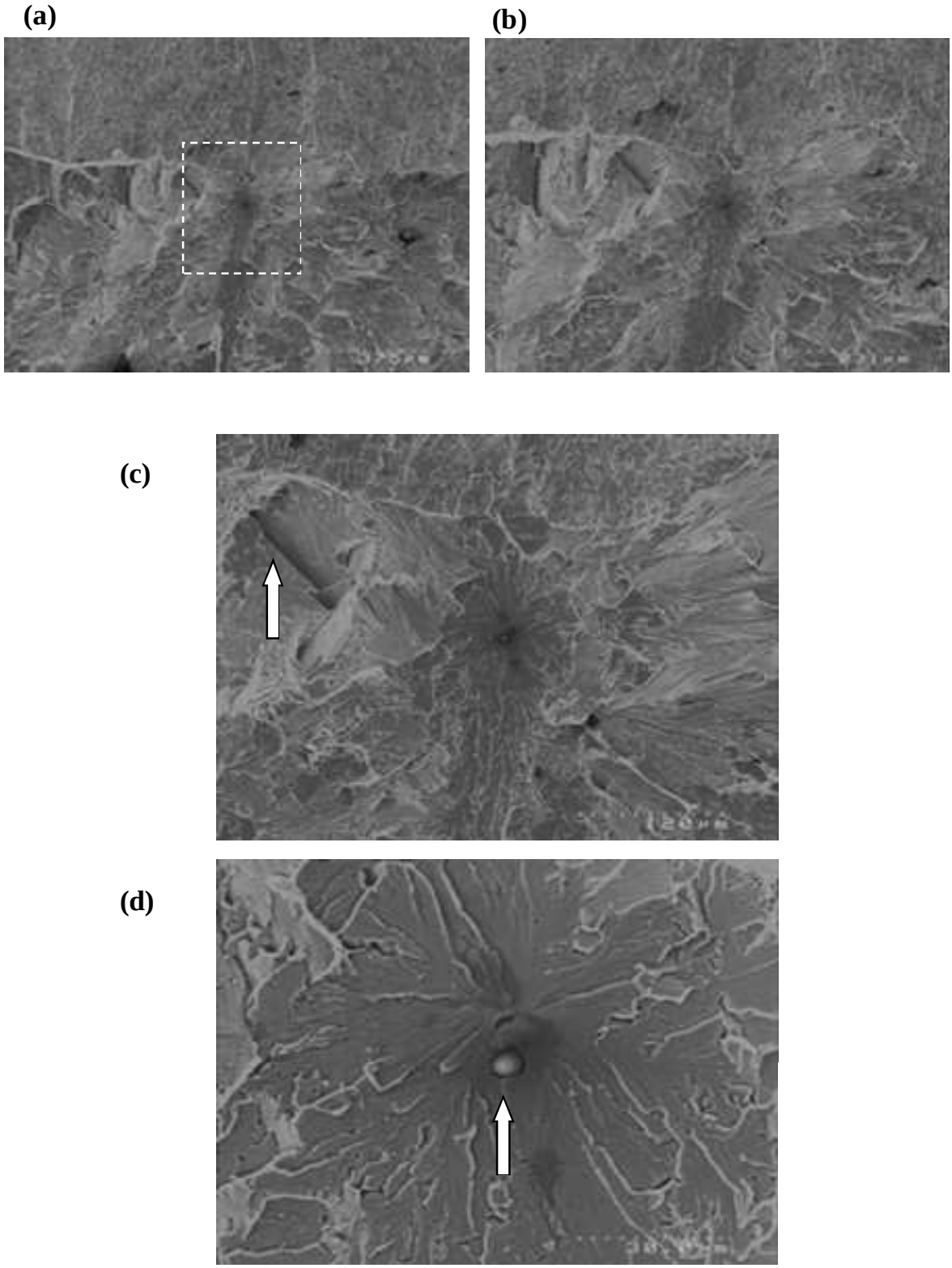

Figure 8.22 - Weld N^{o}1 Sample 6 RHAR, ductile crack growth; (a) overview of ductile crack growth, (b) magnification of (a), (c) magnification of inclusions in (b).

(a)

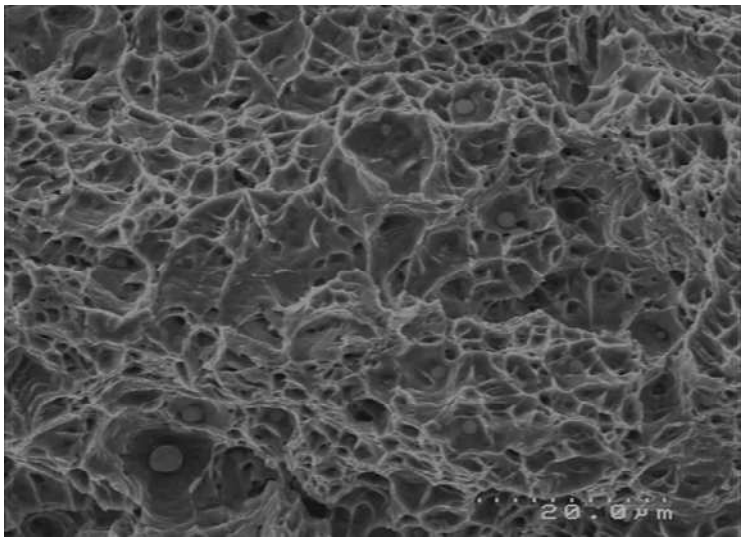

(b)

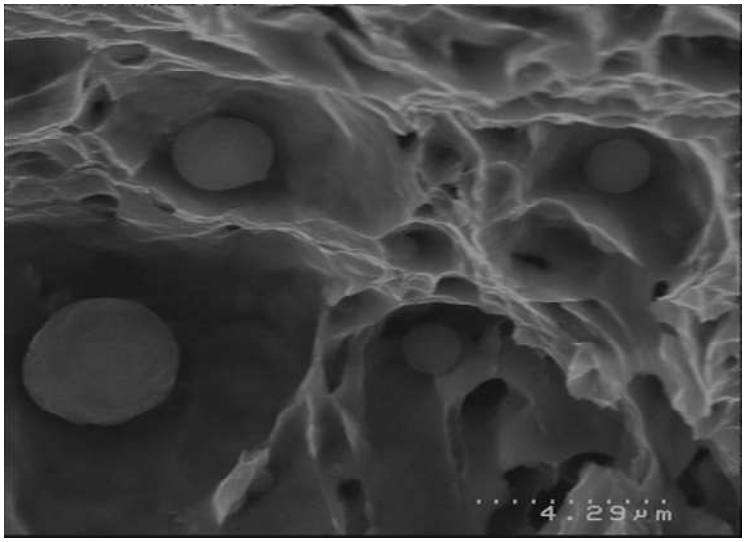

(c)

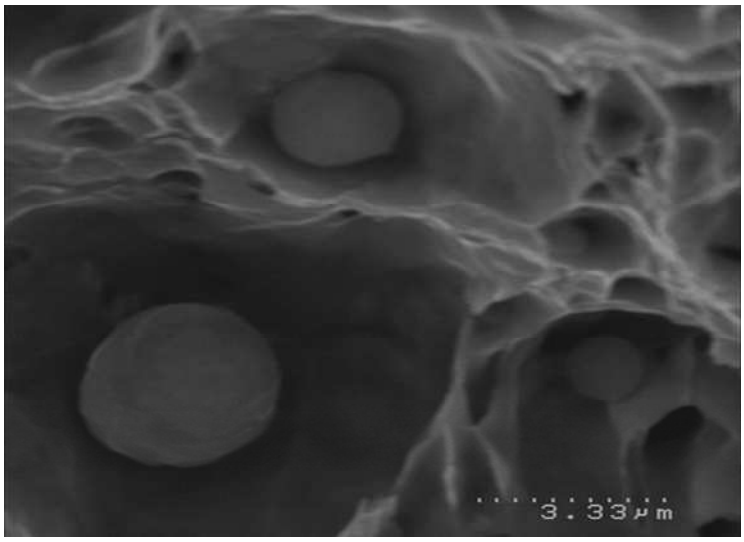

Figure 8.23 - Weld N^{o}1 Sample 31, ADAR; (a) general fracture surface, (b) magnification of framed area, (c) further magnification of the CIS. (d), (e) and (f) corresponding fracture face, (f) secondary cracking noted near CIS.

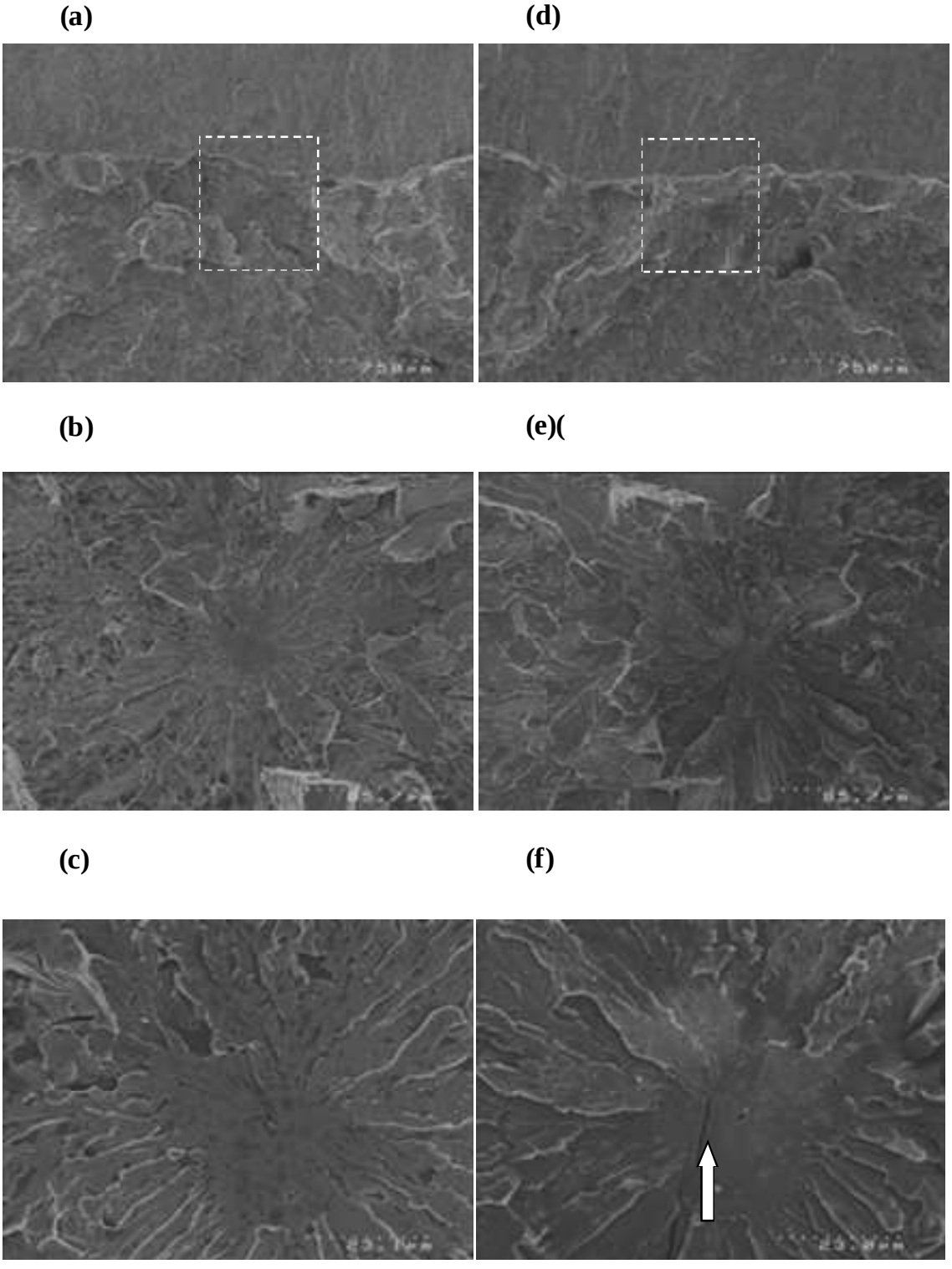

Figure 8.24 - Weld N^{o}2 Sample 1, RHAR; (a) general fracture surface, (b) magnification of framed area, (c) further magnification of CIS, with secondary cracking noted close to the site.

(a)

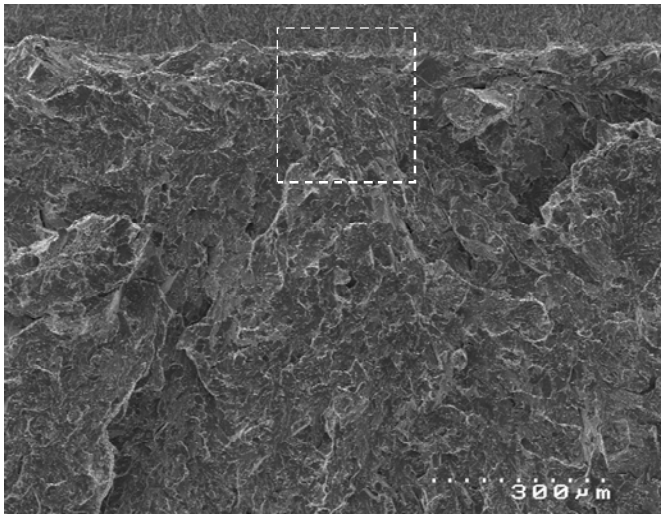

(b)

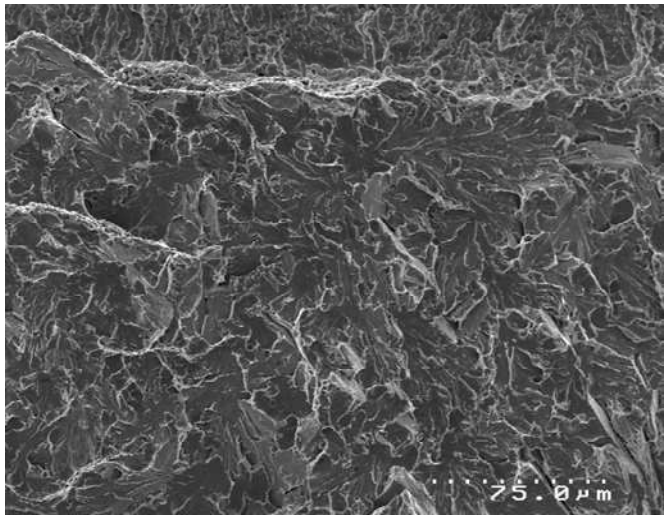

(c)

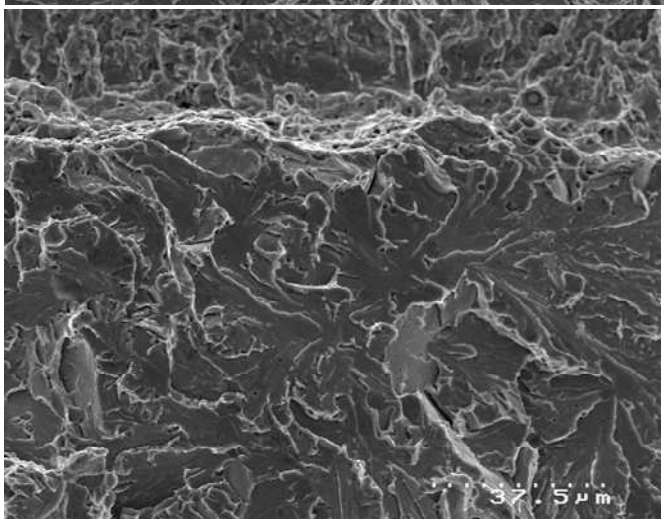

Figure 8.25 - Weld N^{o}2 Sample 2, RHAR; (a) general fracture surface, (b) magnification of framed area, (c) ductile tearing (arrowed) and cleavage steps (arrowed), (d) further magnification of CIS.

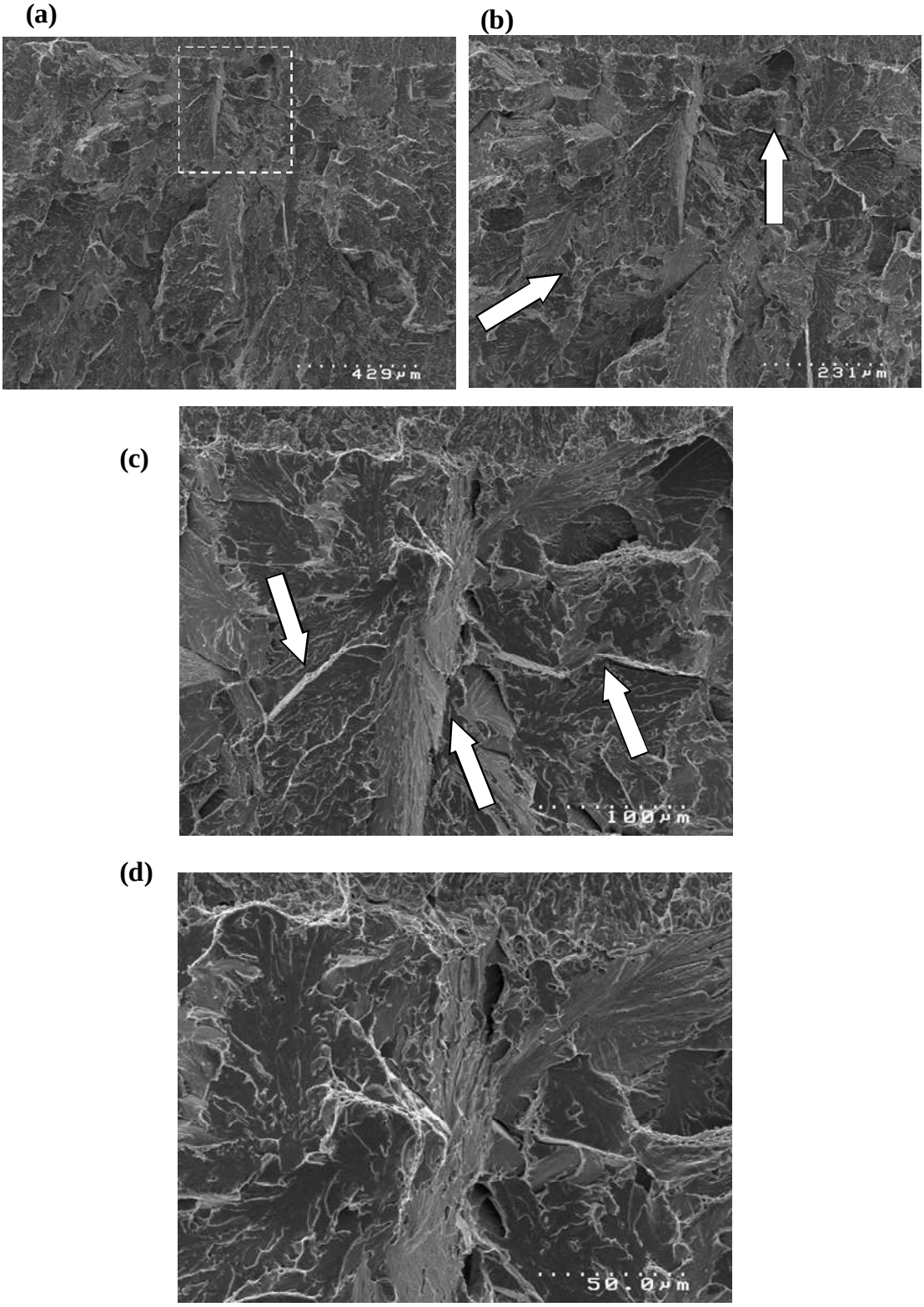

Figure 8.26 - Weld N^{o}2 Sample 5, ADAR; (a) general fracture surface, (b) magnification of framed area, (c) further magnification, noting the different sizes of inclusions and voids.

(a)

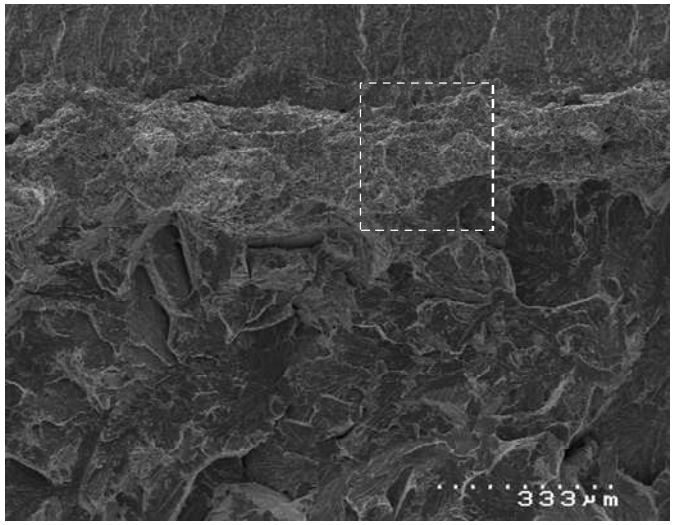

(b)

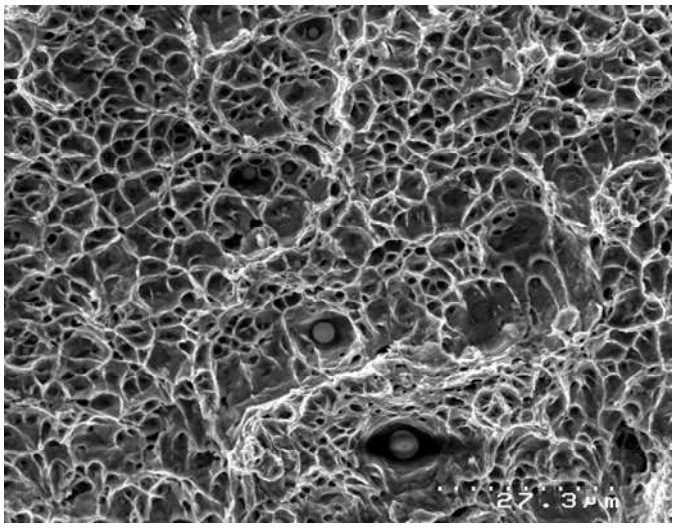

(c)

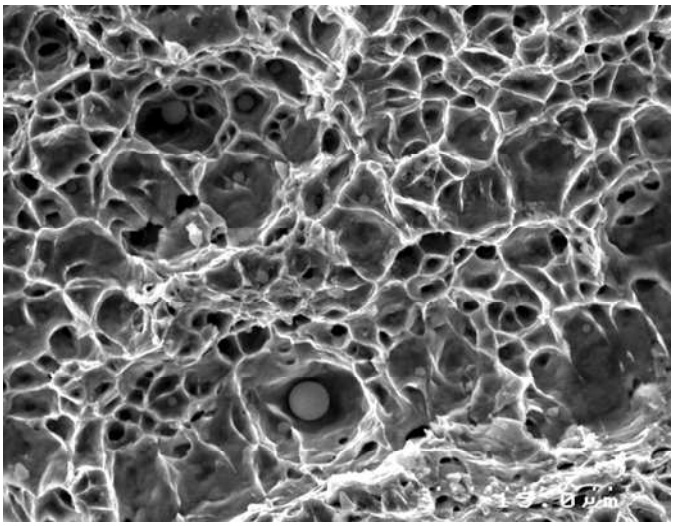

Figure 8.27 - Weld N^{o}2 Sample 11, ADAR; (a) general fracture surface, (b) magnification of framed area, (c) further magnification, noting the non-metallic inclusion at the CIS.

(a)

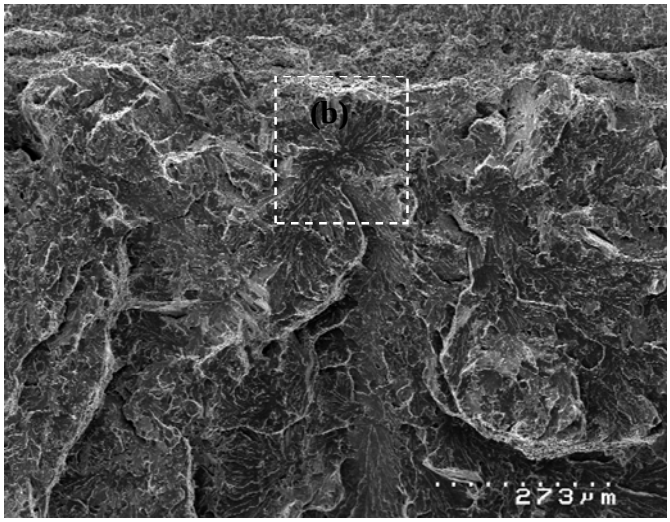

(b)

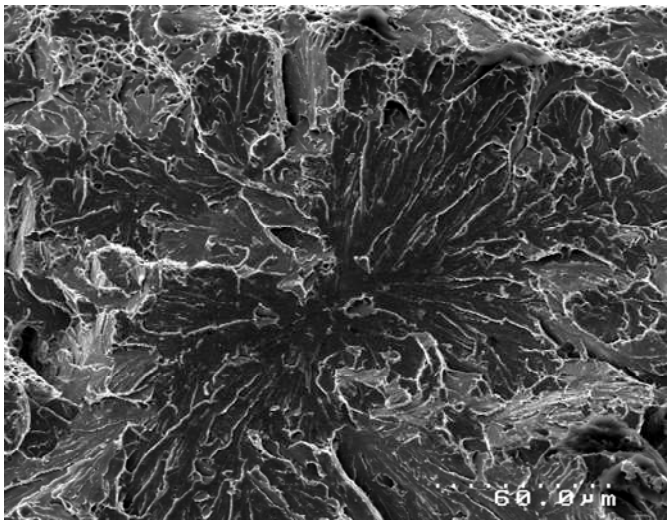

(c)

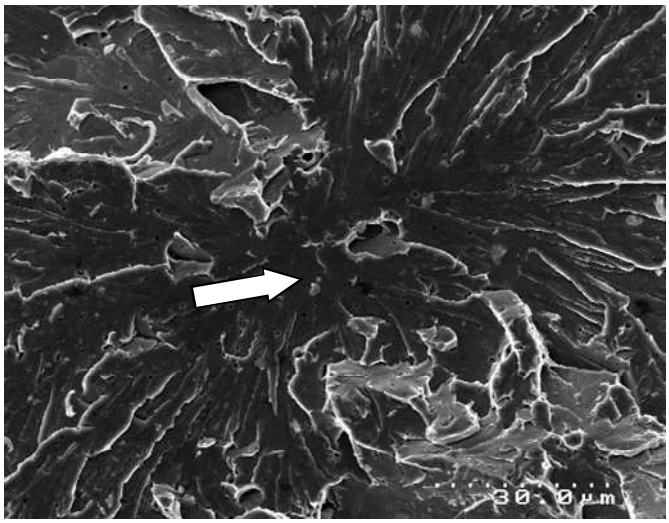

Figure 8.28 - Weld N^{o}2 Sample 12, RHAR; (a) general fracture surface, (b) magnification of framed area, fatigue precrack (arrowed), (c) further magnification, noting the CIS, the equiaxed grain structure is clearly seen, (d) magnification of CIS.

(a) **(b)**

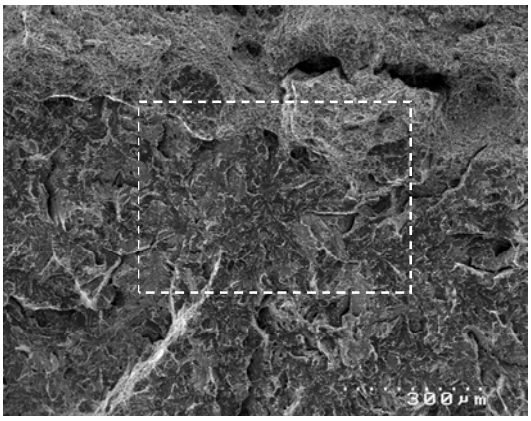

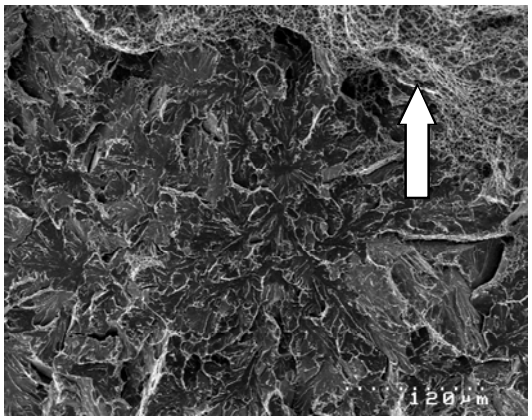

(c)

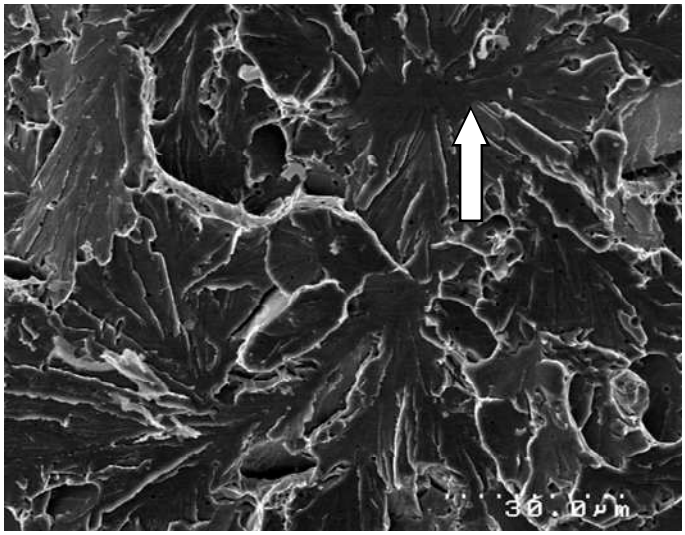

(d)

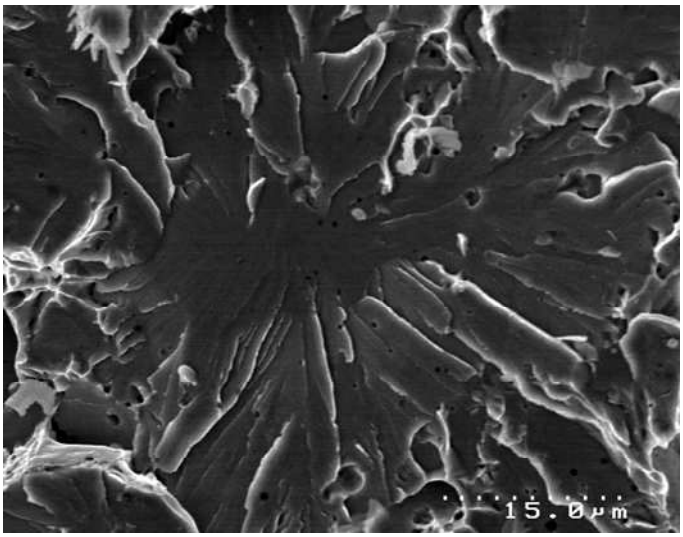

Figure 8.29 - Weld N^{o}2 Sample 33, ADAR; (a) general fracture surface, (b) magnification of framed area, (c) further magnification, noting the CIS.

(a)

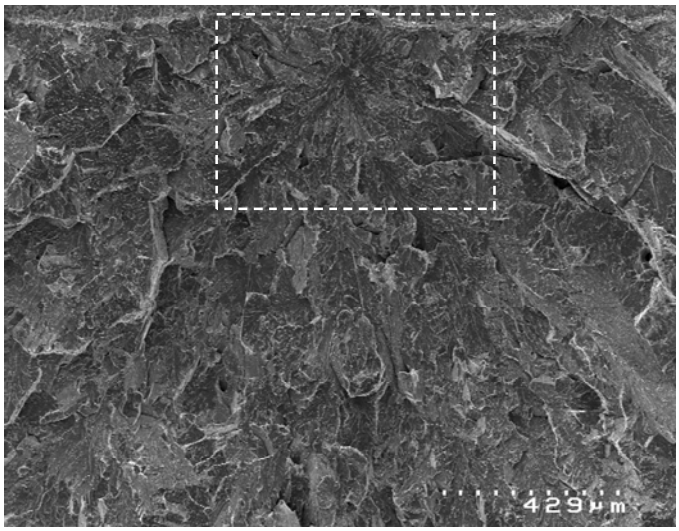

(b)

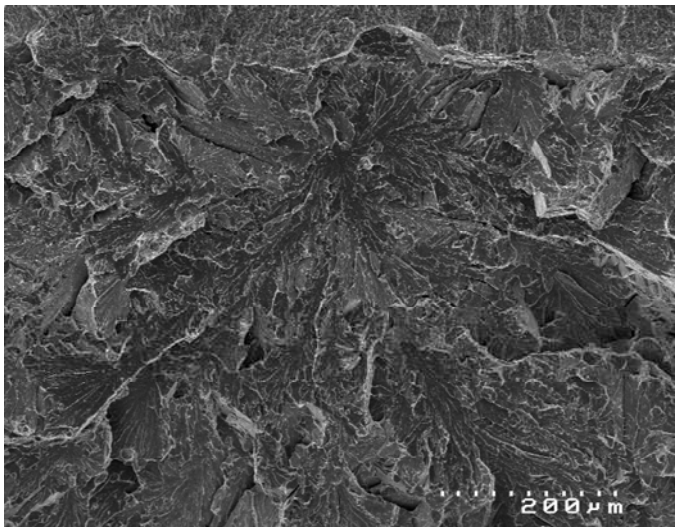

(c)

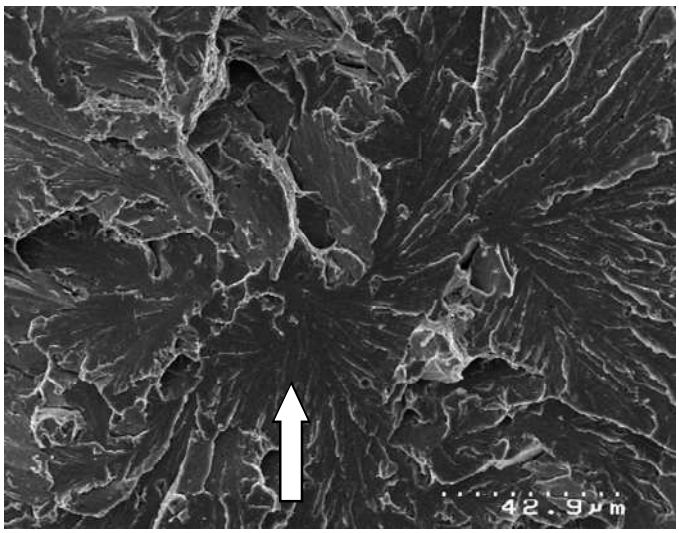

Figure 8.30 - Weld N^{o}2 Sample 5, RH5%SA; (a) general fracture surface, (b) magnification of framed area, (c) further magnification, noting the CIS, secondary cracking through the CIS.

(a)

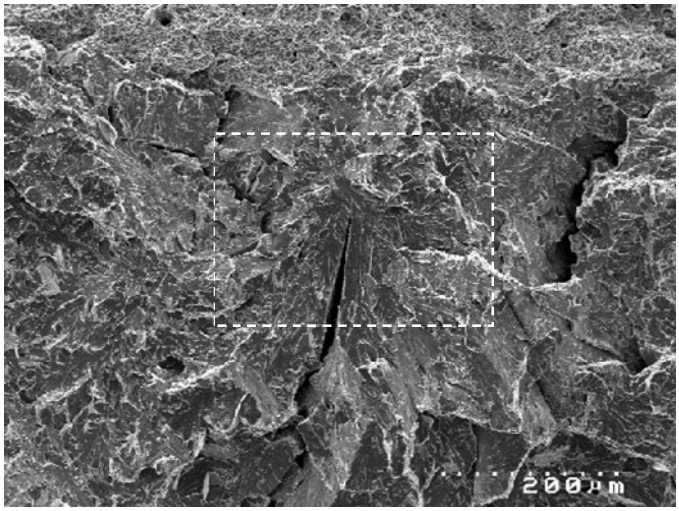

(b)

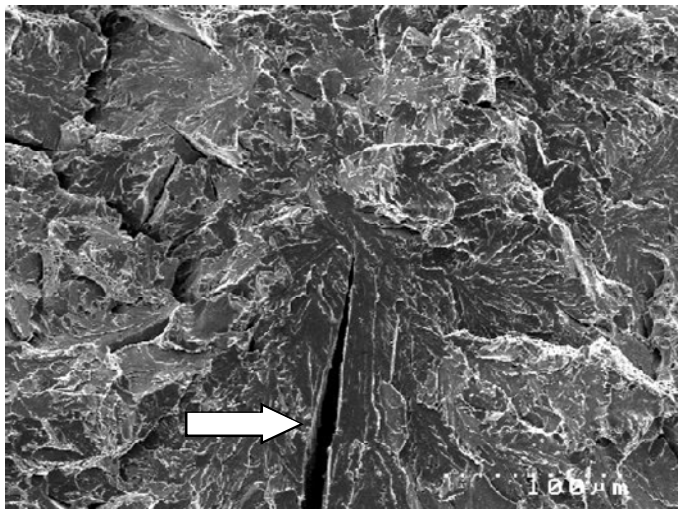

(c)

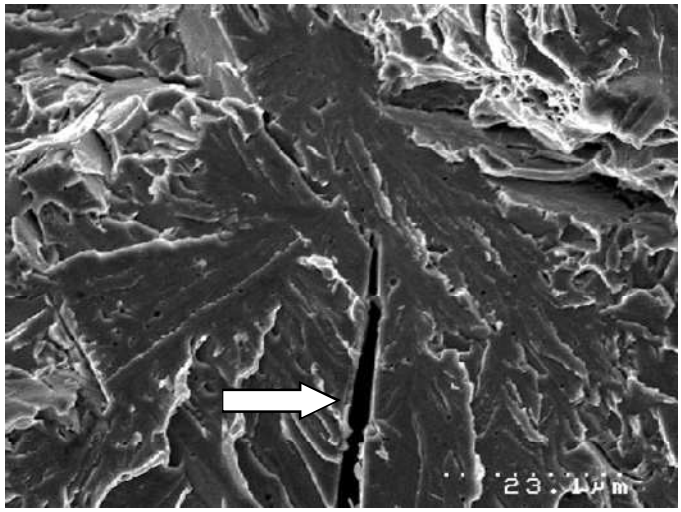

Figure 8.31 - Weld N^{o}2 Sample 6, AD5%SA; (a) general fracture surface, (b) magnification of framed area, (c) further magnification of stable crack growth.

(a)

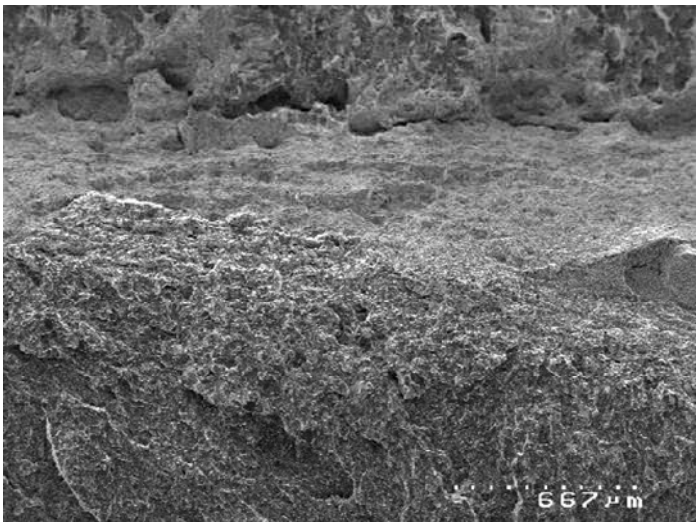

(b)

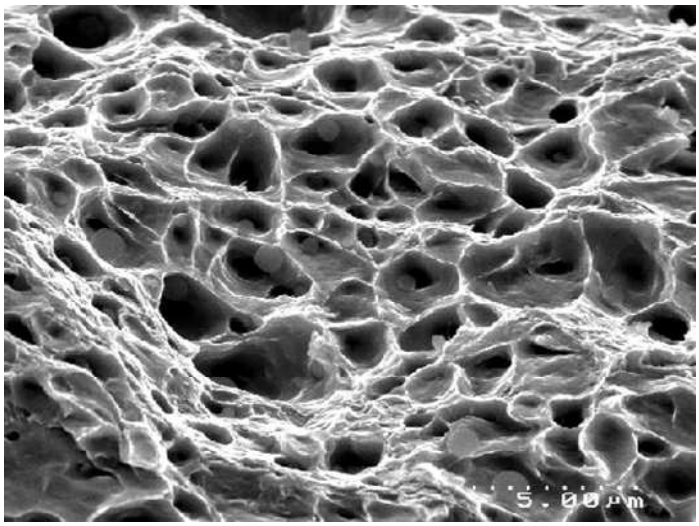

(c)

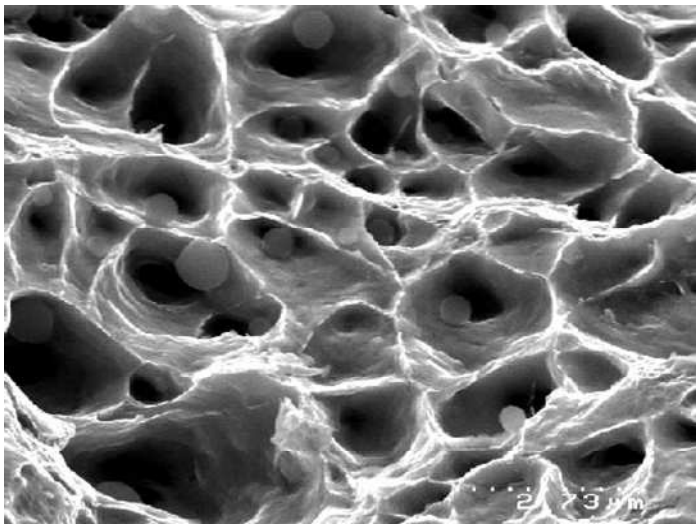

Figure 8.32 - Weld N^{o}2 Sample 9, RH5%SA; (a) general fracture surface, (b) magnification of framed area, (c) further magnification, noting the CIS, with extensive secondary cracking.

(a)

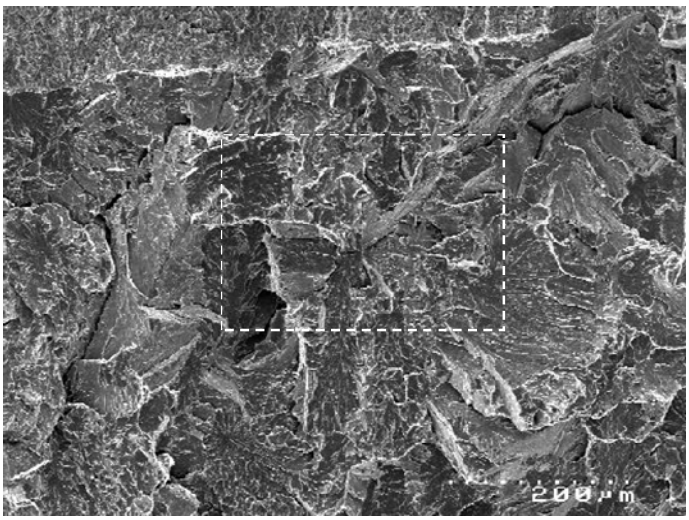

(b)

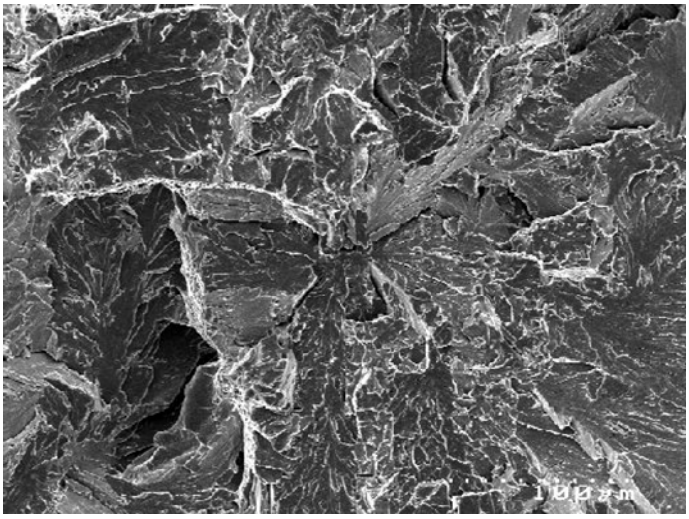

(c)

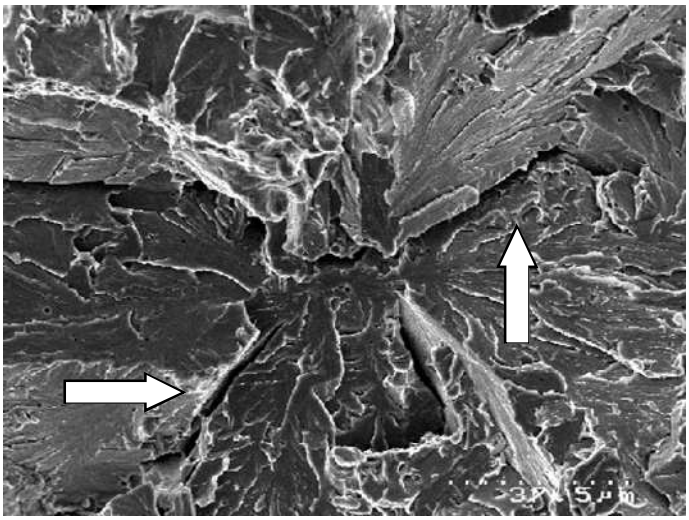

Figure 8.33 - Weld N^{o}2 Sample 22, AD5%SA; (a) general fracture surface, (b) magnification of framed area, (c) further magnification of stable crack growth.

(a)

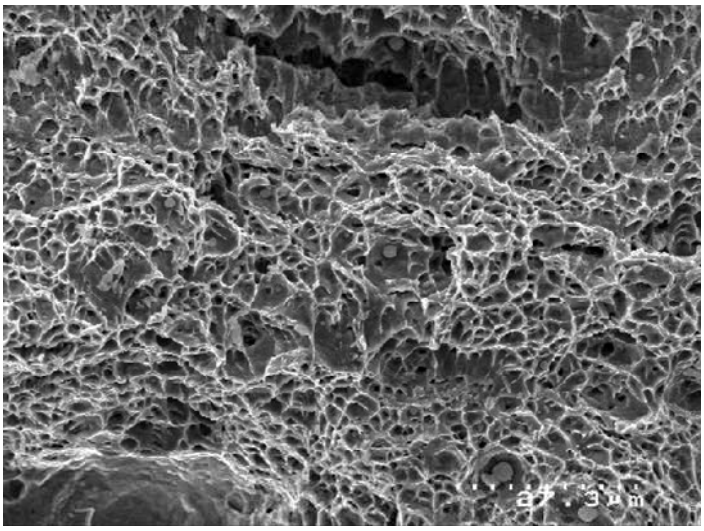

(b)

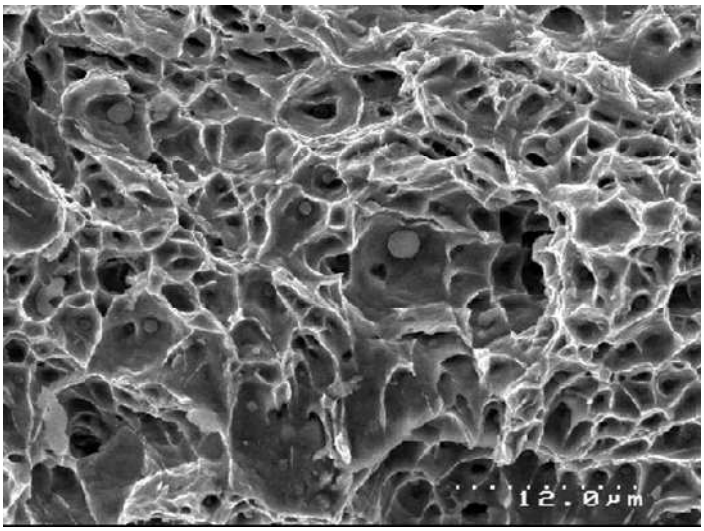

(c)

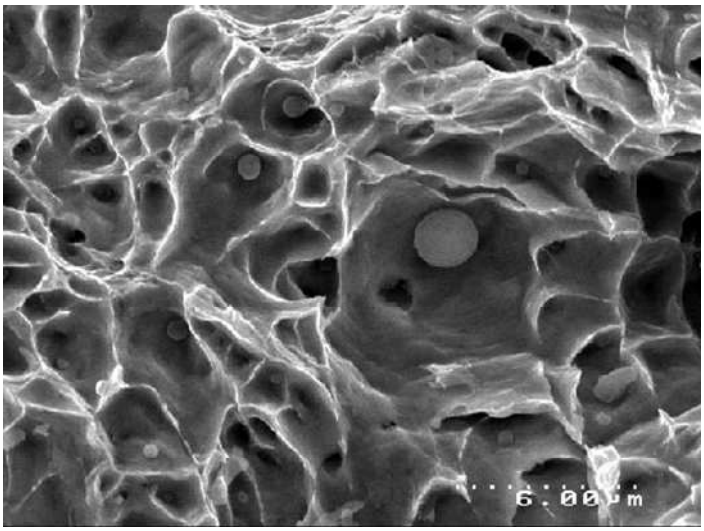

Figure 8.34 - Weld N^{o}2 Sample 14, AD5%SA; (a) general fracture surface, (b) magnification of framed area, (c) further magnification, noting the CIS.

(a)

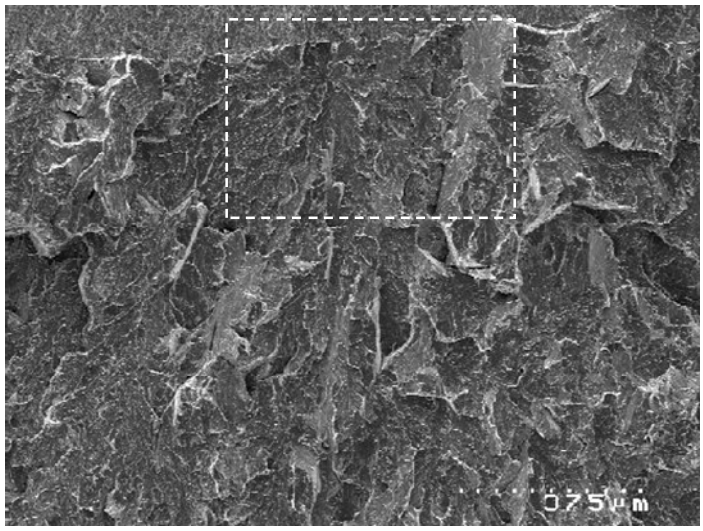

(b)

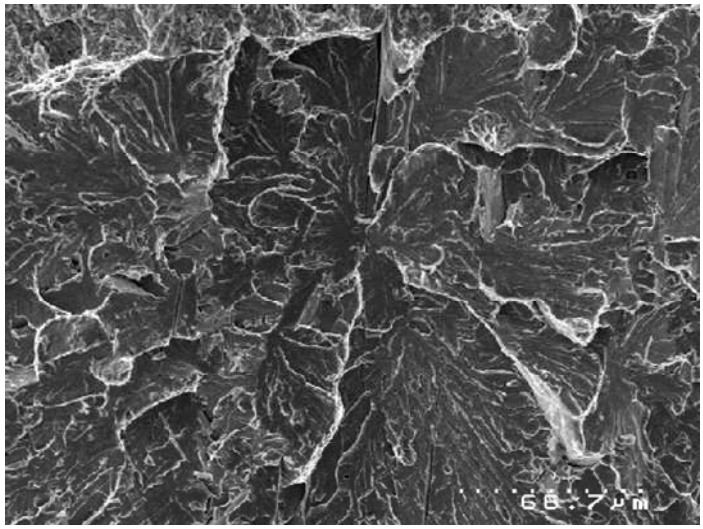

(c)

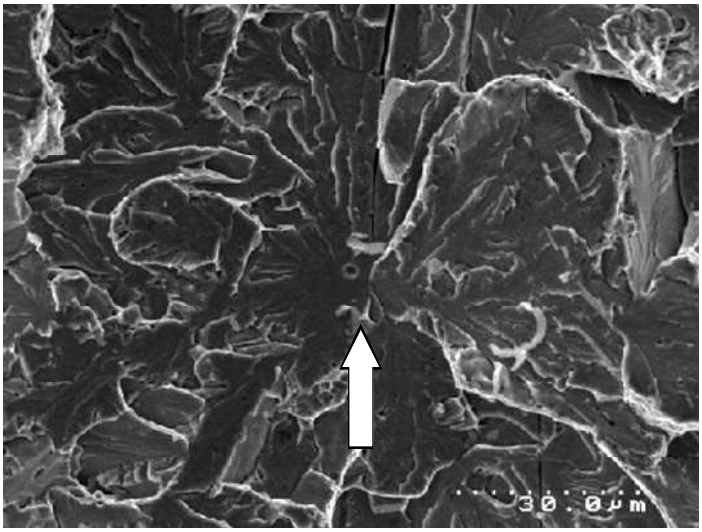

Figure 8.35 - Graph showing the McMeeking analysis and actual measurements for Weld N°1 plotted against temperature.

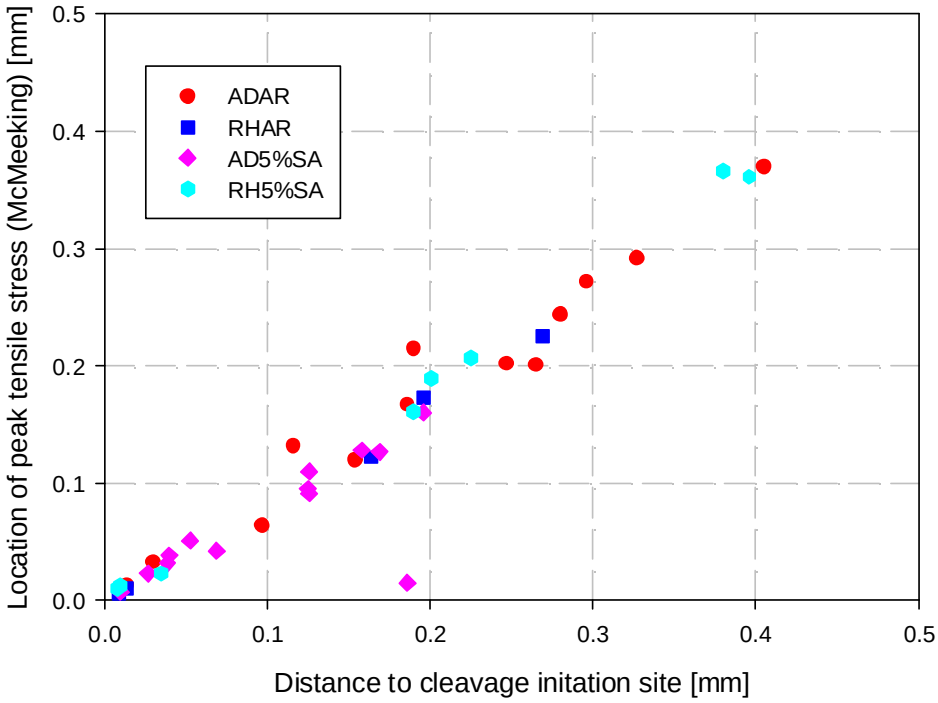

Figure 8.36 - Graph showing the McMeeking analysis and actual measurements for Weld N°2 plotted against temperature.

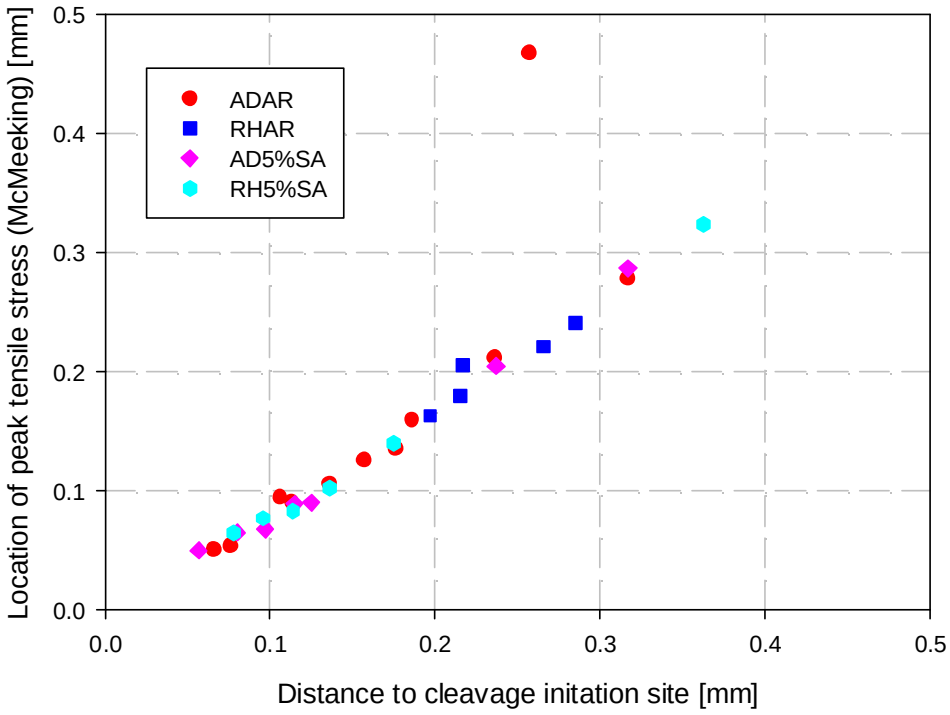

Figure 8.37 - Schematic drawing showing cleavage fracture initiation within second weld bead for the fracture toughness specimens, with the AD5%SA condition exhibiting brittle fracture.

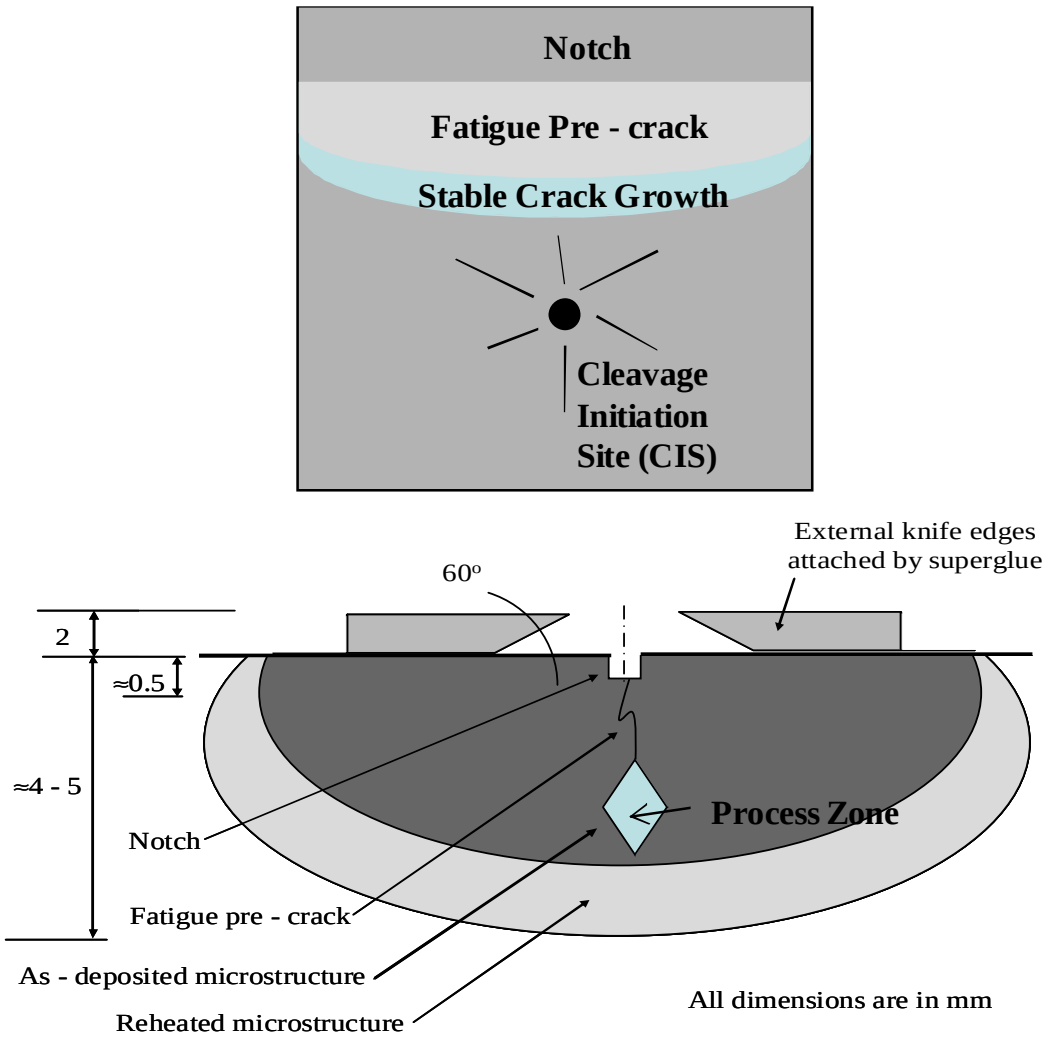

Figure 9.1 - Individual Charpy Impact curves for Weld N°1 and Weld N°2.

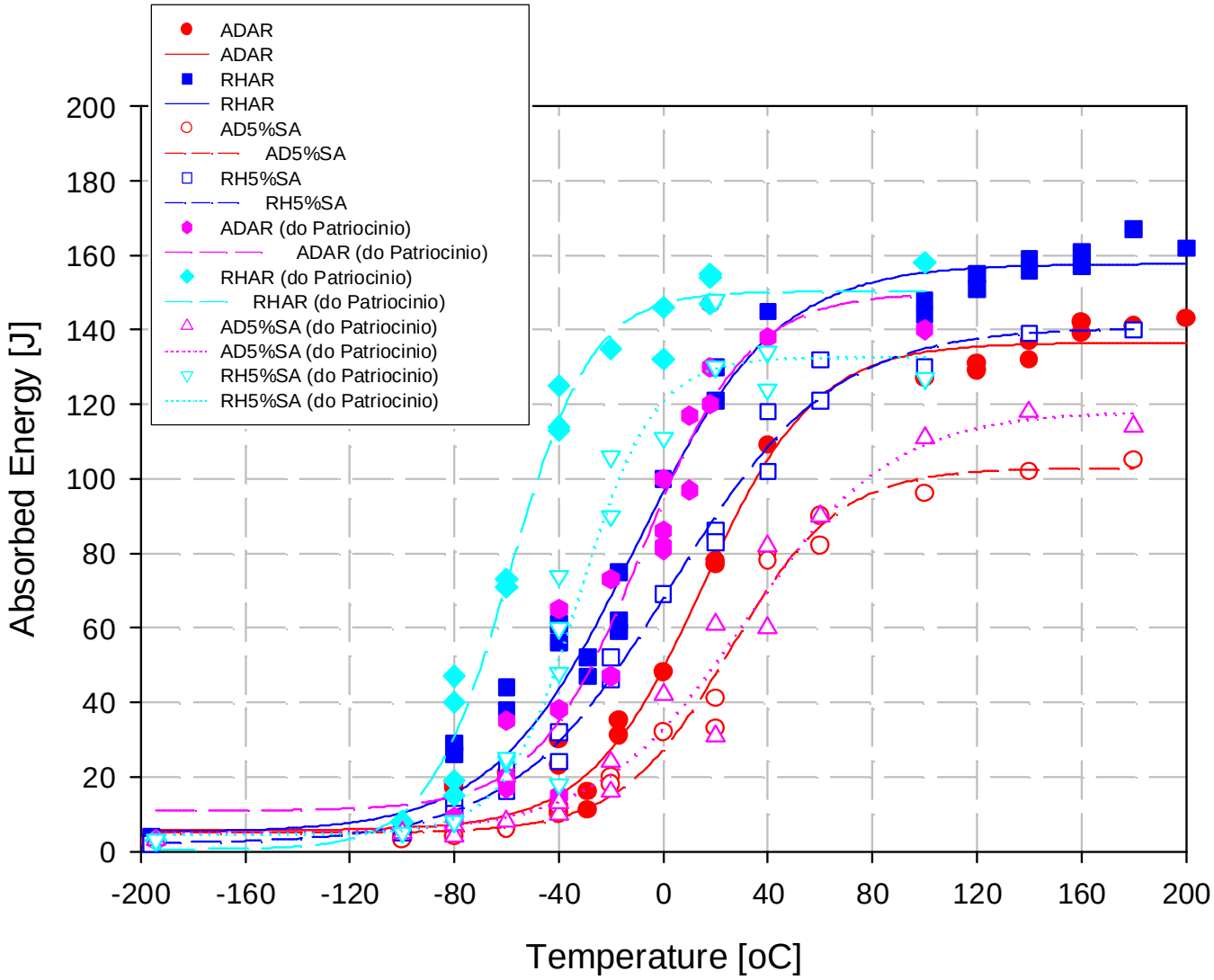

Figure 9.2 - Combined Charpy Impact curves for Weld N°1 and Weld N°2.

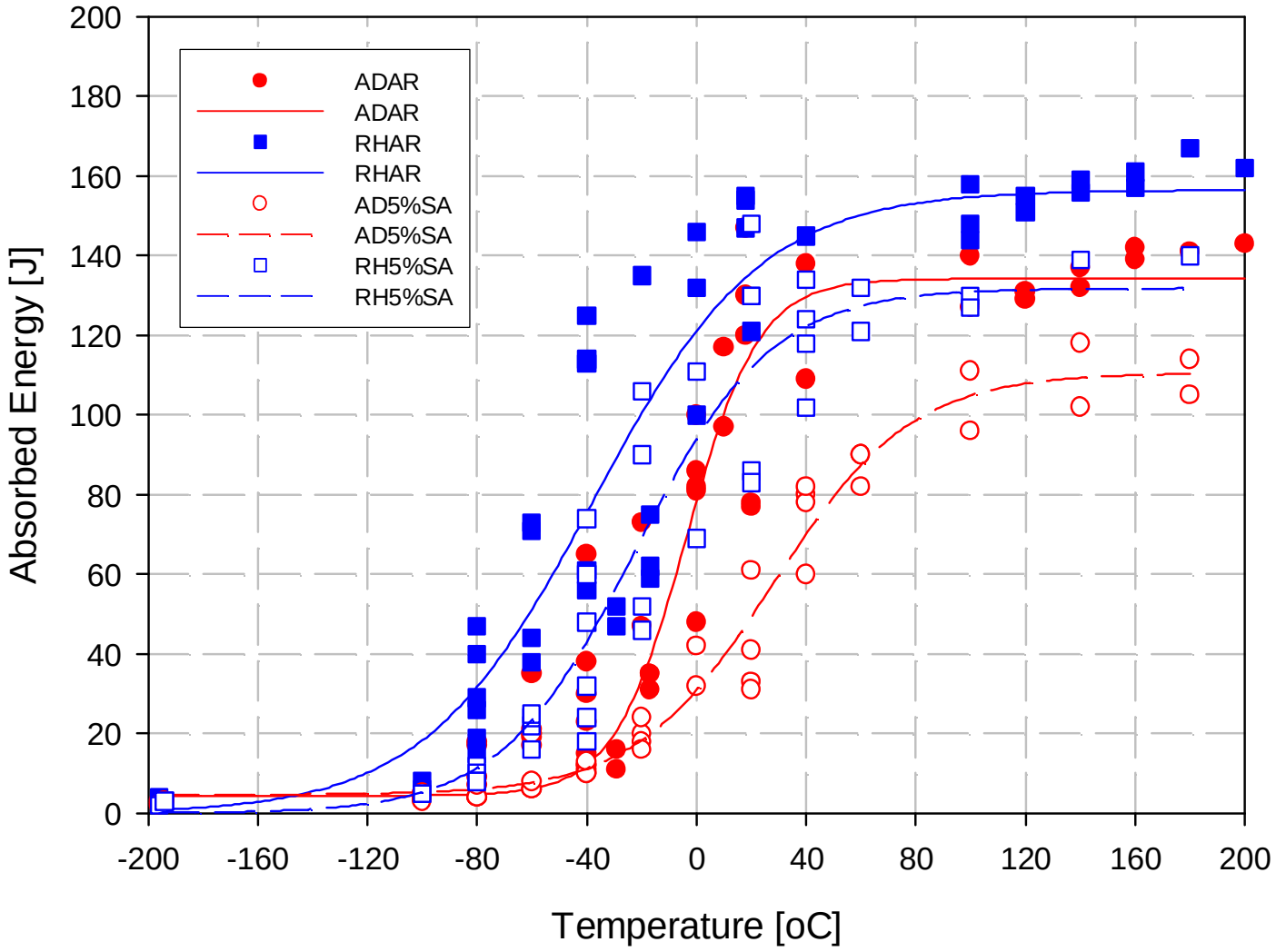

Figure 9.3 - Local cleavage fracture stress, σ_{X0}, for the AD and RH microstructural conditions in both the AR and 5%SA conditions for Weld N^{o}1 and Weld N^{o}2.

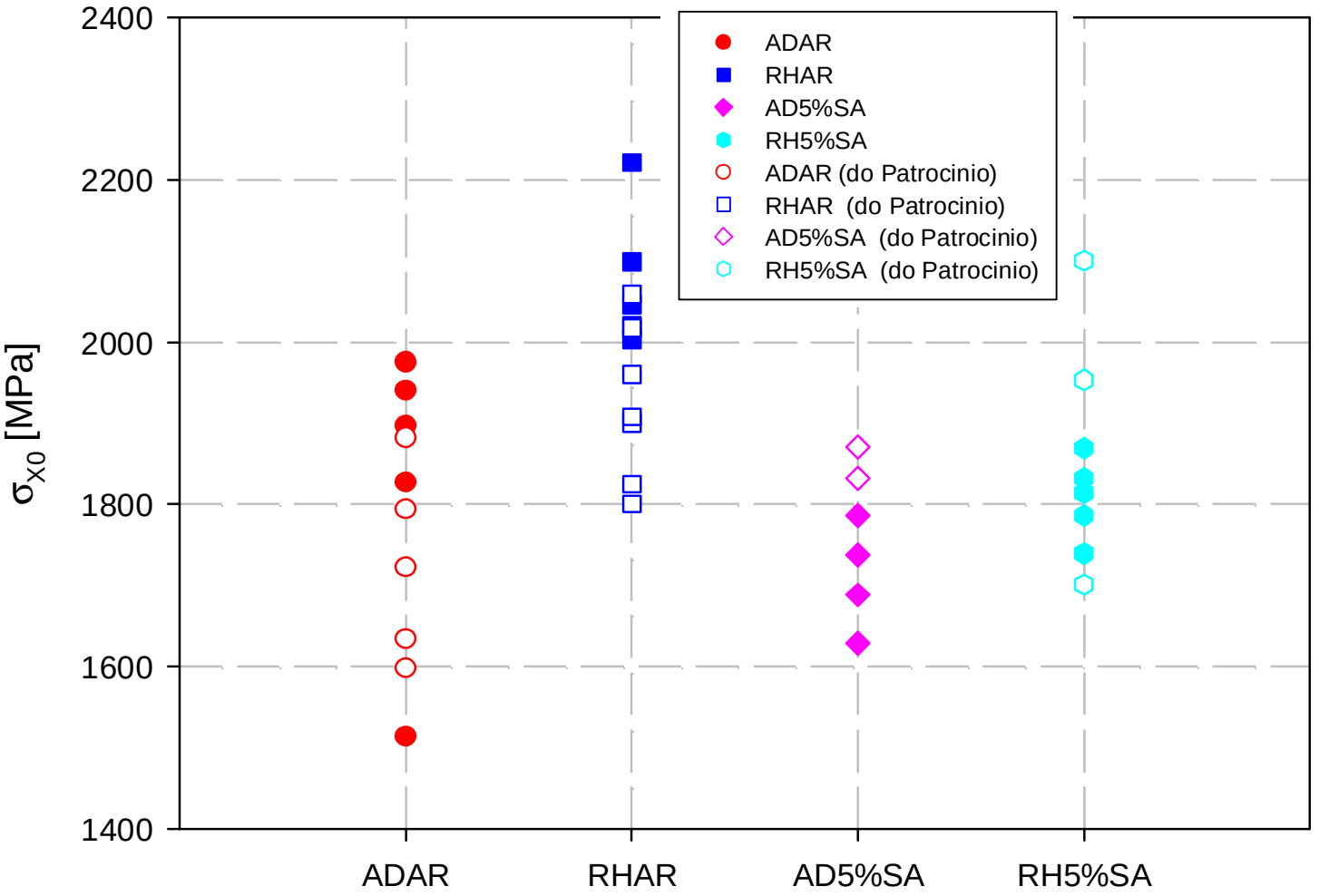

Figure 9.4 - Combined local cleavage fracture stress, σ_{X0}, for the as-deposited and reheated microstructural conditions in both the AR and 5%SA conditions.